ANALYTICAL METHODS FOR STUDYING INTRATUMORAL DRUG DELIVERY IN SOLID TUMORS

by

Darren L. Stirland

A dissertation submitted to the faculty of
The University of Utah
in partial fulfillment of the requirements for the degree of

Doctor of Philosophy

Department of Bioengineering

The University of Utah

August 2016

Copyright © Darren L. Stirland 2016

All Rights Reserved

The University of Utah Graduate School

STATEMENT OF DISSERTATION APPROVAL

The dissertation of **Darren L. Stirland**

has been approved by the following supervisory committee members:

You Han Bae	, Chair	**4/4/2016** Date Approved
Jindrich Kopecek	, Member	**4/4/2016** Date Approved
David Grainger	, Member	**4/4/2016** Date Approved
Hamidreza Ghandehari	, Member	**4/4/2016** Date Approved
Margit-Maria Janat-Amsbury	, Member	**4/5/2016** Date Approved

and by **Patrick Tresco** , Chair/Dean of

the Department/College/School of **Bioengineering**

and by David B. Kieda, Dean of The Graduate School.

ABSTRACT

The overall objective of this project is to develop methods that can help us to understand the movement of drugs and carriers along their routes inside solid tumors. The origins and current paradigm of targeted drug delivery offer a lot of promising strategies. However, the carriers often struggle with challenges in optimizing their own characteristics against that of the tumor's. Ultimately, they struggle with translation into the clinical setting. It is apparent that solid tumors pose a unique challenge in drug delivery. Many drug carrier characteristics are designed to take advantage of the pathophysiology of the tumor environment. However, this passive delivery and accumulation is constrained to partial distribution within the tumor. Many uncertainties remain regarding how nanoparticles enter and travel through the tumor environment. The barriers to intratumoral distribution are still currently being probed.

The research herein identified transport barriers using human fibroid tumors known to have impaired drug transport. After perfusing human uteri containing fibroids with stains, probe distribution was found to correlate with features of the pathophysiology such as blood vessel characteristics, tissue and collagen density, interstitial fluid pressure, and solid stress. Methods, including custom MATLAB code, were developed to analyze the spatiotemporal distribution of two uniquely fluorescent nanoparticle doses in xenograft mice. It shows how three-dimensional distance measurements of nanoparticles from nearest blood vessels are more precise than two-dimensional measurements. Colocalization analysis on the fluorescent signals showed the two different doses (administered hours apart from each other) did not accumulate in the same locations with the tumor. Furthermore, intravital imaging showed that some vessels of the tumor would only provide access to the first dose of nanoparticles.

Future work suggests further analysis of multidose interdependence and implementing these methods to screen strategies in the literature of modifying drug carriers and the tumor environment to improve intratumoral distribution of cancer drugs. The more understanding we have of the solid tumor environment and its barriers, the better we can navigate treatments to reach the tumor.

CONTENTS

LIST OF FIGURES

LIST OF TABLES

ACKNOWLEDGMENTS

Thanks above all to my wife Sherry for all the support she provided and for her patience when my estimates of finishing individual experiments or graduation requirements were underestimated. Thanks also to my family and friends for being eager to help. I would like to thank Joseph W. Nichols for being a sounding board for any ideas I had and for all the discussions we had on the topic of drug delivery in solid tumors. I also want to thank him for his help with experiments and editing of various documents. Thanks to all the other students in the lab: Hee Sook Hwang, Hongsuk Park, Sun Jin, and Li Tian for all the help they provided. Thanks to others (postdocs and visiting scholars) in the lab for being helpful colleagues whom I could turn to for questions: Tracey Denison, Jun Hu, Seiji Miura, and Hidenori Suzuki. Thanks to all other colleagues at the University of Utah who helped me. Likewise, thanks to the Department of Bioengineering and the Department of Pharmaceutics and Pharmaceutical Chemistry for their valuable coursework and student support. Special thanks to Karen Terry for her time in providing specific academic counseling to me. I want to thank the coauthors on the papers included in this dissertation. Their work was extremely valuable to each project. I want to thank Dr. Margit-Maria Janat-Amsbury for her supervision and crucial participation in the uterine perfusion project. Additionally, I want to thank OB/GYN department and research network, the various hospital staff, and especially the patients for volunteering to participate in the study. I would like to thank the entire supervisory committee: Dr. You Han Bae, Dr. Jindrich Kopecek, Dr. David Grainger, Dr. Hamid Ghandehari, and Dr. Margit-Maria Janat-Amsbury. I want to thank them for their time in reading and providing feedback on this dissertation. Also, I appreciate all of their help and advice in the included research projects as well. Special thanks to Dr. You Han Bae for giving me the opportunity to work in his lab. I want to thank him for his teachings, guidance, and support.

CHAPTER 1

INTRODUCTION AND LITERATURE REVIEW

Drug delivery strategies seek to increase the efficacy and reduce the toxicity of therapeutic drugs. Cancer drugs are in need of drug delivery innovations to overcome special challenges such as the toxicity or solubility of the drug and barriers presented by the disease. To improve drug delivery, many therapies under investigation implement advanced technologies that have specially designed characteristics to aid in distribution of the drug. These will be termed drug carriers as they carry or act as a drug. While advances have led to seemingly improved drug delivery over traditional chemotherapy, challenges remain in effectively treating solid tumors (Fig. 1.1).

This chapter will introduce the current paradigm on drug delivery and the challenges facing it. Challenges lie in the carrier design, the tumor environment, and in translation to

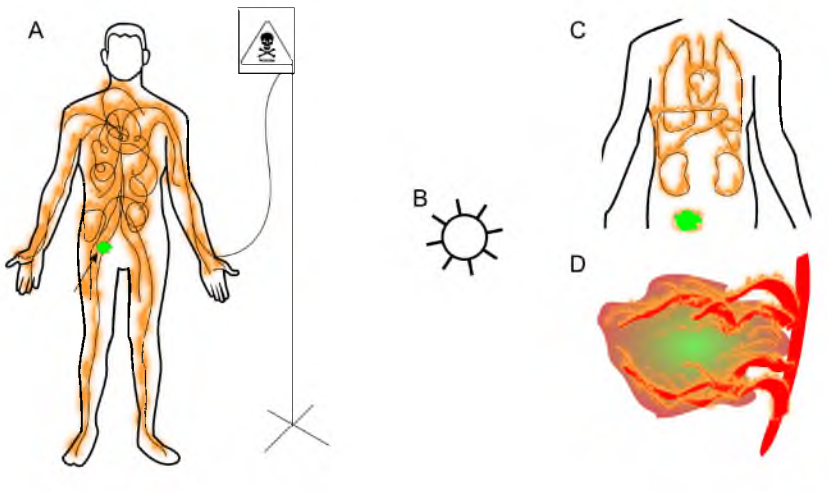

Figure 1.1. Distribution of cancer drugs. A) Traditional chemotherapy's toxicity (orange flames) spreads throughout the entire body in hopes of killing off the tumor (green with arrow). B) Drug carriers seek to be a magic bullet to direct toxicity to only the tumor, but iv administration still relies on passive delivery. While distribution is more selective and toxicity is often reduced (even clinically), it is still present in many major organs (C) and distribution throughout the tumor is limited (D).

the clinic. It is known that advanced strategies using drug carriers have a low success rate in the clinical setting [1]. While the literature boasts of miraculous efficacy in animal models, mediocre clinical results limit their approval or relegate them to secondary or combination treatments after traditional chemotherapy fails [2]. The review will show an interesting trend in approved targeted drug delivery therapies. A common denominator is access to the tumor, as solid tumors have special challenges to drug delivery. The included published work will provide tools and methods to understand intratumoral drug delivery that may help overcome access barriers that limit effective treatments in reaching the clinic.

1.1 Ideal Drug Delivery

Ideal drug delivery for these drug carriers targets all the toxicity at the tumor site and very little in normal tissues. Essentially, having control over distribution in the body and in the tumor is the goal of targeted drug delivery. Targeted drug delivery is an umbrella term where "targeted" may refer to a number of different functions. It may refer to passive targeting, active targeting, or loosely as a goal of the design.

Targeted drug delivery seeks to improve the therapeutic index (i.e., lower the toxicity but increase the efficacy) of a drug. Some designs try to minimize side effects and allow a higher dose to remain bioavailable longer for increased therapeutic effects (most passive carriers like liposomes). Other designs focus on increasing efficacy to require less drug that could cause side effects (might incorporate active targeting). The methods of targeted drug delivery often control both when and where the drug is effective. If the drug can be presented only to the disease in the body, then there will be no side effects and efficacy will be improved with high concentrations in the target area. Research has been ongoing for years to accumulate a significant amount of knowledge into the field and fill the literature with the seemingly subjective term "targeted drug delivery" (Fig 1.2).

Some have very aggressive claims regarding targeted drug delivery and others, perhaps more accurately, state a goal of improving targeted drug delivery [3, 4]. While clear delineations of what targeted drug delivery is and is not would help, there are challenges with the current state of targeted drug delivery that extend beyond defining the term. These challenges, which are present in both the carrier and the target, make translation into the clinic difficult. Carrier technology has improved greatly yet still has trouble delivering drug to the target. The target, solid tumors in the clinical setting, is still resisting treatment. The systems may be targeted by design, but they are not hitting the target thoroughly nor exclusively. The challenges associated with this problem need to be addressed in order to

Figure 1.2. What is effective targeting? Targeting strategies in drug delivery do not guarantee that drugs will be delivered exclusively to the target. Often, a spread distribution reaching other sites is unavoidable. Many targeted therapies are designed to be less effective outside the target (blunt tips). Nevertheless, these systems can fail.

move forward.

1.1.1 Origins in targeted drug delivery

The current paradigm of targeted drug delivery is linked to its origins, which are tied to chemotherapy and immunology. Paul Ehrlich was a pioneer in chemotherapy and is known for the metaphor of a magic bullet. The vision of the magic bullet was inspired from his ability to selectively stain bacteria cultures [5]. He reasoned a toxic molecule could be tied to the stains to selectively kill only that target. Targeted drug delivery has been guided by Paul Ehrlich's vision, particularly in the field of cancer therapy [6]. Targeting designs are usually incorporated in a variety of drug carriers such as lipid-based, polymer-based, protein-based, viral-based, and various other nanoparticles (Fig. 1.3).

Liposomes are composed of lipids that assemble into vesicles with a bilayer capable of carrying drug molecules. Gold and iron oxide nanoparticles are among the more popular

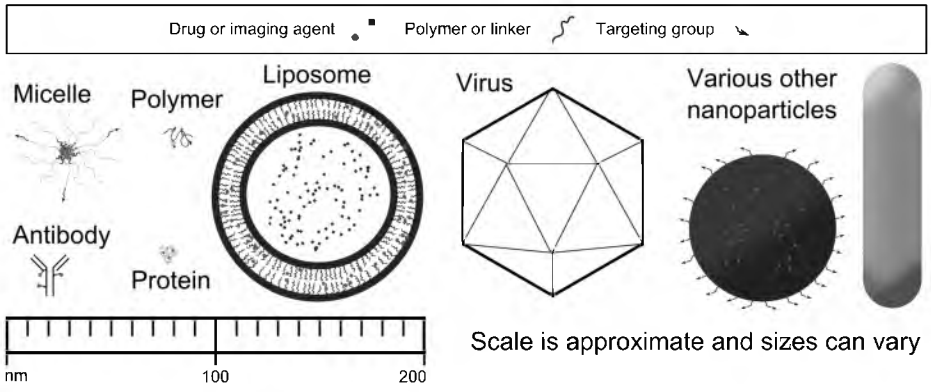

Figure 1.3. Various drug carrier types. Besides having specific targeting groups, sometimes the size or other characteristics provide targeting effects.

inorganic compositions used. Viral carriers, made by modifying existing viruses or by using certain aspects from them, have also been used in targeted drug delivery of therapeutics [7, 8].

Polymer chemistry is a major tool for drug carriers that seek to provide the properties of a magic bullet. Helmut Ringsdorf suggested a standard model that could be used to improve targeted drug delivery by suggesting that a biocompatible polymer can serve as a backbone to link drugs and targeting groups together [9]. The Ringsdorf model has been an inspiration for many polymer designs in drug delivery for cancer therapy [10]. It has led to a trend of polymer therapeutics with researchers devising various ways to give properties to polymers. The versatility in chemistry and molecular architecture is one of the advantages of polymers in targeted drug delivery. Often, other categories of drug carriers will have polymer components to furnish additional characteristics. With polymer therapeutics and the rapidly expanding field of nanotechnology, the possibilities are only limited by one's imagination.

"Affinity therapy" is a term used over 30 years ago to describe designs that involve forces between molecules that cause them to bind [11]. Besides polymer therapies, other categories such as inorganic nanoparticles have also included this type of active targeting into their design. These targeting groups with ligand-receptor binding are often referred to as targeting moieties. While various carriers have used ligand-receptor binding over the years, antibodies are one of the best forms of this. Advances in immunology and the advent of monoclonal antibodies have become an important part of pursuing the vision of a magic bullet.

All of these carrier types have dimensions on the scale of nanometers and can be described as nanoparticles. While colloidal chemistry and even targeted drug delivery have a long history, additional advances in nanotechnology and applications in drug delivery are quickly becoming popular topics. Review articles list various drug carriers that are approved or in clinical trials, the majority of which can be found in Table 1.1 [1, 12–18].

1.1.2 Current paradigm

The current paradigm associated with targeted drug delivery shapes the design of the drug carriers. However, even selectivity of the base drugs can help in localizing treatment to the tumor. Given a good base drug, there are additional carrier properties thought to maximize drug delivery to the tumor.

Table 1.1: Various drug carriers approved or in development.

Product Name	Category	Approval status
Abraxane	Protein	FDA approved
AD-70	Polymer	Phase I
Adcetris	Antibody	FDA approved
ADI-PEG20	Polymer	Phase I
ALN-VSP	Nanoparticle	Phase I
AP5280	Polymer	Phase I/II
Arzerra	Antibody	FDA approved
ASG-22ME	Antibody	Phase I
ASG-5ME	Antibody	Phase I
Atu027	Liposome	Phase I
Aurimune	Nanoparticle	Phase II
AuroLase	Nanoparticle	Phase I
Avastin	Antibody	FDA approved
Bexxar	Antibody	FDA approved
BIND-014	Micelle	Phase I
CALAA-01	Nanoparticle	Phase I
Campath	Antibody	FDA approved
Cea-scan	Antibody	FDA approved
Combidex	Nanoparticle	Phase III
CPX-1	Liposome	Phase II
CPX-351	Liposome	Phase I
CRLX101	Nanoparticle	Phase II
CT-2106	Protein	Phase I
C-VISA-BikDD	Liposome	Phase I (withdrawn)
Cyclosert	Nanoparticle	Phase I
DaunoXome	Liposome	FDA approved
DE-310	Polymer	Phase I
Depocyt	Liposome	FDA approved
Docetaxel-PNP	Nanoparticle	Phase I
Doxil	Liposome	FDA approved
Endorem	Nanoparticle	Europe
Erbitux	Antibody	FDA approved
EZN-2208	Polymer	Phase II
Feridex	Nanoparticle	FDA approved
Genexol-PM	Micelle	Several other countries
Herceptin	Antibody	FDA approved
INGN-401	Liposome	Phase I
Kadcyla	Antibody	FDA approved
Keytruda	Antibody	FDA approved
LE-SN38	Liposome	Phase II
MAG-CPT	Polymer	Phase I
Marqibo	Liposome	FDA approved

Table 1.1: (continued)

MBP-426	Liposome	Phase II
MCC-465	Liposome	Phase I
Mepact	Liposome	Europe
Mylotarg	Antibody	Withdrawn
Myocet	Liposome	Europe and Canada
NC-4016	Micelle	Phase I
NC-6004	Micelle	Phase I
NK-012	Micelle	Phase II
NK-105	Micelle	Phase II
NK-911	Micelle	Phase I
NKTR-102	Polymer	Phase III
NL CPT-11	Liposome	Phase I
Oncaspar	Polymer	FDA approved
Onivyde	Liposome	FDA approved
Ontak	Protein	FDA approved
Opaxio	Protein	Phase III
Opdivo	Antibody	FDA approved
OSI-211	Liposome	Phase II
OSI-7904L	Liposome	Phase II
Paclical	Micelle	Phase III
Pegamotecan	Polymer	Phase II
PegAsys	Polymer	Phase I/II
PegIntron	Polymer	Phase I/II
PEGPGA and DON	Polymer	Phase I/II
Perjeta	Antibody	FDA approved
PK1	Polymer	Phase II
PK2	Polymer	Phase I/II
PK3	Polymer	Phase I
PNU166945	Polymer	Phase I
ProLindac	Polymer	Phase II
Prostascint	Antibody	FDA approved
Prothecan	Polymer	Phase II
Resovist	Nanoparticle	Europe
Rexin-G	Viral	Philippines/FDA Phase III
Rituxan	Antibody	FDA approved
S-CKD602	Liposome	Phase I/II
SGN-75	Antibody	Phase I
SGN-CD19A	Antibody	Phase I
SGN-CD33A	Antibody	Phase I
SGT-53	Liposome	Phase I
SGT-94	Liposome	Phase I
SP1049C	Micelle	Phase II
SPI-077	Liposome	Phase II
Sylatron	Polymer	FDA approved

Table 1.1: (continued)

Thermodox	Liposome	Phase III
Vectibix	Antibody	FDA approved
Verluma	Antibody	FDA approved
XMT-1001	Polymer	Phase I
Yervoy	Antibody	FDA approved
Zevalin	Antibody	FDA approved
Zinostatin Stimalmer	Polymer	Japan

First, a stable carrier for the drug can help reduce side effects and increase the therapeutic effect. A stable carrier will mean that the drug is protected from the body and that normal (nontargeted) tissues are protected from the drug. Second, the carrier will accumulate into the tumor via the enhanced permeability and retention (EPR) effect. Third, the carrier can target the tumor with additional means based on environmental or cellular components.

Small molecule drugs can, by their mechanism of action, provide some targeted drug effect. It is often through targeting resources the cancer needs. Many anticancer drugs interfere with microtubules or DNA and affect cancer cells more because they divide more. The base drug in Oncaspar, asparaginase, can deplete asparagine levels that affect tumor cells more as they do not have the ability to synthesize asparagine like normal cells. These selective drugs can be augmented with stable drug carriers to increase their chances of reaching the tumor.

The first requirement of a stable carrier is simply the ability to carry the drug. The majority of anticancer drugs are hydrophobic and do not dissolve in aqueous solutions. As the carriers transport the drug, they need to form a stable barrier between the drug and the body. Protecting the body from the drug requires that the drug not interact with nontargeted cells, tissues, or organs. Protecting the drug from the body provides long circulation in the blood stream. To achieve long blood circulation, it needs to avoid interaction with the reticuloendothelial system (RES), also known as the mononuclear phagocyte system (MPS). Cell uptake by the MPS will decrease the efficacy of the treatment and can limit the chances of it reaching the target. There should be protection against blood-born proteins that would lead to inactivation, destabilization, or opsonization. The carrier should also be designed to limit accumulation into the kidney, liver, spleen, and other nontargeted organs. Administration of the chemotherapeutic agent Taxol® is a good example of the need for good carriers. Taxol consists of paclitaxel solubilized in Cremephor EL® (also known as Kolliphor EL®), which is a highly toxic mixture of ethoxylated castor oil. This excipient can cause hypersensitivity reactions in patients undergoing chemotherapy and can end up limiting their treatment [19]. Furthermore, the active pharmaceutical ingredient, paclitaxel, is known to cause dose-limiting neurotoxicity at high doses [20]. If stability and long circulation are achieved, it will be able to travel through the body long enough to reach the tumor site. Here, carrier technology can encourage preferential treatment to the tumor with designs tuned to target environmental characteristics or cellular components of the cancer.

The carrier can take advantage of environmental characteristics of the tumor. Some of the environmental characteristics provide a means for passive accumulation via the EPR effect. EPR is possible with two hallmarks of cancer: unchecked growth and continued angiogenesis [21]. Continuous growth of the tumor leads to a chaotic tumor environment with cells in hypoxic regions producing angiogenic factors that stimulate the production of new blood vessels. These new blood vessels are poorly formed and have gaps or fenestrations in the endothelium that allow passage of macromolecules into the tumor from the blood [22, 23]. Increased mass transport from the blood vessels is beneficial for a tumor that is starved for nutrients. Therapies can take advantage of this enhanced permeability (EP) that allows macromolecules to deposit into the tumor where this leakiness occurs. Furthermore, enhanced retention (ER) in the tumor is aided by the lack of functional lymphatics that would normally drain the tissue [24]. Thus, when the EP and ER allow the drug to accumulate in the tumor at a concentration higher than surrounding normal tissue, it can be said to have had an EPR effect.

The tumor environment allows for passive targeting via EPR, but it also has other characteristics that can be used to activate drug carriers when in the tumor environment. Some drug carriers use pH-sensitive groups to provide a triggered action in the acidic environment [25]. The low pH (from about pH 5.8 to pH 7.6) in solid tumors is a result of metabolism in hypoxic conditions [26, 27]. Consequently, hypoxic conditions can also be a trigger for targeted drug action [28]. It also might be possible to use the high concentration of matrix metalloproteinases (MMPs) in the extracellular matrix of tumors to convert the carrier into an active form [29].

Once in the tumor environment, ligand-receptor binding can provide preferential treatment via active targeting of specific molecules on cells [18]. Given access to the cancer cells, the drug is more likely to enter the cancer cell when a carrier with targeting moieties holds it in close proximity to the cell membrane. How quickly and by which route it enters is then dependent on the carrier properties [30]. Some cancer cell types overexpress certain surface markers. These markers are present in other cells, but can be much more abundant in some tumors. Overexpression of folate receptor and human epidermal growth factor receptor 2 (HER2) has been shown to be a predictor of poor prognosis of breast cancers [31,32]. These and other overexpressed proteins have become a target implemented into the designs of drug carrier technologies [33–35].

Thus, the current paradigm is to have the carrier transport the drug in a stable manner while circulating through the blood stream so that it can accumulate in the tumor where

a targeting mechanism will provide selective treatment. This paradigm has a plethora of opportunities for polymer therapeutics and nanotechnology. Designs can be custom tailored to fit certain aspects of the paradigm.

What often happens is a therapeutic approach will focus on one specific aspect of the paradigm to increase efficacy. Unfortunately, this can result in shortcomings in other areas. Overall, there is still a low rate of clinical success for drug carriers, especially those targeting solid tumors.

1.2 Challenges to Intratumoral Drug Delivery

Challenges to successful targeted drug delivery come from carrier-dependent factors and tumor-dependent factors. Biodistribution and EPR depend on carrier characteristics and these carriers are not always well characterized, stable, or biocompatible. On the other hand, the tumor is resisting treatment from the environmental to the cellular level. Furthermore, if good results with a drug carrier are seen in preclinical models, the success does not often translate into the clinical setting. Aspects of the paradigm need to be examined in order to see improvements. There have been critical examinations of targeted drug delivery for quite some time now and certain challenges are beginning to be understood more thoroughly [36, 37].

Table 1.2 shows some trends in 24 FDA approved drug carriers for cancer treatment. The table was inspired by a 2007 review article summarizing strategies to improve exposure to solid tumors [38]. While this table may quickly become outdated, additional and current information on drug carriers can be found surveying drugs@FDA or on their respective FDA labels [39]. Some insight might be gained from these drugs that had to prove they were safe and more efficacious than what is currently used in human patients.

The first thing noticed is that few of these are approved for primary treatment. For many, there is not enough evidence to risk jeopardizing patient care to these advanced carrier therapies. Sometimes, the clinical trials require the patients to first have treatments with a known track record fail before becoming eligible for the trial. Subsequently, the approved drug carriers are limited in showing that they could be a capable first line treatment. Though not listed here, even approved carrier-imaging agents (like Cea-scan, Prostascint, or Verluma) cannot be used alone for diagnosing a tumor. They must be confirmed by biopsy or other means.

Another predominant feature is that out of 24 approved drug carriers, 15 are antibodies. It shows the boon that monoclonal antibodies have been to anticancer therapy. Antibodies are on the lower range of drug carrier sizes at approximately 5-20 nm in diameter (depending

Table 1.2. Trends in approved drug carriers.

	Prior or combo treatment	Antibody	Passive targeting	Solid tumor	Blood/vessel cancer	Metastatic
Erbitux	+	+		+		+
Herceptin	+	+		+		+
Kadcyla	+	+		+		+
Perjeta	+	+		+		+
Vectibix	+	+		+		+
Avastin	+	+		+*		+
Adcetris	+	+			+	
Arzerra	+	+			+	
Bexxar	+	+			+	
Zevalin	+	+			+	
Doxil	+		+	+	+	
Onivyde	+		+	+		+
Abraxane	+		?	+		+
Sylatron	+		?	+*		
Oncaspar	+		?		+	
Marqibo	+		+		+	
DaunoXome			+		+	
DepoCyt			?		+	
Ontak			?		+	
Campath		+			+	
Rituxan		+			+	
Yervoy		+		+*		+
Keytruda	+	+		+*		+
Opdivo	+	+		+*		+

?: questions whether they are suited for EPR due to their characteristics or target.
*: indicated for solid tumor but has blood or vessel targets.

on the axis). They are made by cells resulting in uniform and biocompatible products. However, variation does exist due to metabolism/degradation, immune responses, organism of origin, drugs, and linkers. Still, there are more and more antibody therapies being approved by the FDA when compared to other targeted drug carriers. Preclinical studies are replete with polymers, liposomes, inorganic nanoparticles, etc., that contain multifunctional aspects, beyond just targeting moieties, that provide preferential treatment to the target

tissue; however, it seems relatively few of these enter clinical trials and they have yet to successfully navigate through clinical trials to market approval.

EPR is often repeated in the literature as a passive mechanism for delivering macromolecules to solid tumors in mice. It may be possible that some passive accumulation of antibodies also occurs due to their molecular weight of around 150 kDa. However, ideal sizes for taking advantage of EPR are often summarized as between 20 and 150 nm [40–43]. For 5 of the remaining 9 nonantibody carriers, EPR is likely not a dominant influence due to their size or target. Sylatron, at only 31 kDa, is smaller than most modern carriers designed to take advantage of EPR. Also, the attached interferon drug has active targeting through specific ligand-receptor binding. Abraxane is formulated into 130 nm nanoparticles [44]. However, the paclitaxel-bound albumin formulation likely dissolves in the blood stream into smaller molecules of approximately 7 nm in diameter. Ontak has a molecular weight similar to albumin at about 60 kDa and may benefit from some passive accumulation effects, but it is a fusion protein to direct action against cells expressing IL-2 receptor. Oncaspar has a molecular weight of around 300 kDa, but it also has a ligand target (asparagine) which circulates through the blood stream. DepoCyt is an exception in that 1) it is extremely large at 3–30 μm and 2) it has a unique target in lymphoma that has spread to the central nervous system. Doxil is the poster child for having characteristics (tuned size and PEG for long circulation) that take advantage of the EPR effect in solid tumors. Onivyde deserves some attention for similar reasons, even if it is indicated only for metastatic tumors. Marqibo and DaunoXome also solely rely on passive accumulation, but delivery is considerably easier in blood or vessel tumors.

While 13 carriers approved for solid tumors seems promising, 5 of those actually have either blood or vessel targets. Avastin is antiangiogenic and treats the blood vessels rather than the tumor. Sylatron differs in that it can only be used after surgical resection of melanoma. Thus, the target is no longer a large solid mass. While the FDA label states the mechanism of Sylatron is unknown, the interferon cytokine has been shown to help stimulate immune responses against tumors [45]. Yervoy, Keytruda, and Opdivo all interact with T cells. Discounting those exceptions, we see more drug carriers are approved for blood or vessel cancers (12) rather than solid tumors (8). Not excluded, but worth noting, is the large fraction of carriers for solid tumors that have an indication for metastatic cancer with cells circulating in the vessels. This trend is not surprising as blood or vessels targets are more accessible with fewer barriers to transport.

Bexxar is FDA approved, but it has been discontinued by the manufacturer as of

February 2014 due to limited use [46, 47]. Absent from the list of approved carriers is Mylotarg®, an antibody-drug conjugate that was approved for clinical use to treat leukemia. However, it has since been withdrawn due to poor results from a postapproval clinical trial and continued postmarketing surveillance reveals lack of improved efficacy and unacceptable side effects. The antibody has no trouble binding to its target antigen of CD33, but lack of antigen exclusivity to the cancer and accumulation in the liver doomed this product [48,49]. Its story will be discussed in more detail in the Appendix, but illustrates the challenge of designing exclusive targeting into the carrier.

1.2.1 Challenges present in the carrier

There are challenges in designing the carrier characteristics to be just right for targeting drug delivery to solid tumors. The carrier must be biocompatible in that it must be stable enough to perform its designed function in the body. This stability to its destination must not be left to chance, but should be verified with direct observations. A variety of targeting mechanisms can be use, but each have limitations or potential safety issues.

1.2.1.1 Stability and traceability

As mentioned earlier, a carrier needs to be stable and this will have an effect on safety and efficacy. The biocompatibility of the carrier is determined by the chemistry of the monomer and degradation products [50]. Viruses serve as effective carriers but have the risk of a severe immune response against pathogen-associated molecular patterns (PAMPs). Physicochemical characteristics also affect the carrier's biocompatibility and are often tuned to maximize EPR and blood circulation half-life. When the drug interacts with normal tissue because of the carrier's instability or is unable to reach targeted tissue because of insufficient circulation time, the targeted drug delivery has failed.

Carrier sizes are usually sought to be small enough to escape out of fenestrations in the tumor vasculature and avoid excessive liver accumulation, but large enough to avoid renal clearance [51–53]. Specifically, size ranges between 20 and 150 nm with a spherical shape are ideal for avoiding the lungs, liver, spleen, and kidneys [41]. Synthesized drug carriers will possess a size distribution as it is extremely difficult to avoid polydispersity. Moreover, many carriers become more polydisperse during storage or while circulating in the blood. Stability may be challenged upon dilution in the blood for some self-assembly-based carriers such as liposomes or micelles [54]. Polymer shells that give unique characteristics to inorganic nanoparticles can be lost in vivo [55]. Other potential problems that all carriers face when introduced into the blood include destabilization from high salt concentrations, adsorption

of proteins, interactions with lipids, opsonization, and phagocytosis from cells. Carriers with low hydrophobicity will quickly be cleared by the MPS and those with a positive charge are likely to be cytotoxic and taken up by the liver [40, 56]. Thus, a common technique to increase circulation time is to add extremely hydrophilic poly(ethylene glycol) (PEG) to oppose molecular interactions and to shield positive charges [57, 58]. PEG interacts with water to make it thermodynamically favorable for the PEG chains to extend and limit adsorption of proteins [59]. However, long circulation is only relative and there can still be some uptake by the MPS or other organs and eventual recognition from antibodies is also possible [60]. This is evident when PEG only increases the blood circulation half-life of liposomes in blood by just hours [61].

Essentially, only a fraction of the carriers may have the ideal characteristics for drug delivery. Furthermore, only a small percentage of the drug carrier's population will reach the tumor as it is a matter of probability on whether the drug carrier will happen to be on the right path to hit the narrow opening in the vascular structure or if it will have to make another pass through the body and risk uptake by other means. Uptake can occur in normal tissues that have vascular fenestrations that are in a similar ideal range of 40–80 nm or as big as 150 nm in the liver [62]. Any particles too large to pass through fenestrations in normal tissues can still be engulfed by resident macrophages.

Carrier properties also determine how different nanoparticles will move within the tumor environment. Generally, a smaller molecule can more easily extravasate and diffuse to penetrate into the tumor; however, it can also diffuse away more quickly. On the other hand, a larger particle will be retained more readily in the tumor environment, but has a slower rate of extravasation and likely will not penetrate into the tumor core.

The probability of any given nanoparticle reaching the tumor, extravasating, entering a cancer cell, and ultimately causing an effect within that cell is extremely difficult to gauge. Imaging and tracking techniques have become increasingly popular to study this issue leading to the growth of theranostics where diagnosis is combined with therapy. Fluorescence resonance energy transfer (FRET) may be particularly useful as it will help to determine whether self-assembly-based or other complexes have dissociated [63, 64]. Tracking the dissociation or aggregation of these drug carriers is important as it directly affects the polydispersity and biodistribution of these particles. Furthermore, Nomoto *et al.* developed a new imaging method to allow in vivo real-time observation of how PEGylation limits aggregation [65]. In situ tracking of these nanoparticles will provide more accurate confirmation of delivery than analyzing statistical distributions.

1.2.1.2 Targeting mechanisms

In Paul Ehrlich's day, a magic bullet seemed an appropriate analogy for the vision he had. Modern-day scientists sometimes present this analogy as something more akin to a homing missile [66]. To overcome some of the problems in targeted drug delivery products, the exaggerations promoting these magic bullets will have to be called out. Current targeting drug delivery designs are not target-seeking as they cannot sense the target from a distance and adjust their trajectory to home in on it. Furthermore, current designs are not capable of self-propulsion. Instead, they are stochastic in that they rely on being carried to the target by convective blood flow and diffusion through tissues. Thus, a more honest comparison for these inanimate objects might be magic rafts. These magic rafts may not have paddles, but they can have an anchor.

As stated before, designs can target molecules, cells, conditions, or resources the cancer needs. Some means of targeting are more exclusive than others. Antibodies are excellent tools for providing mechanisms of binding. They can be selected to have high specificity and affinity for their target ligand. However, care must be taken to select the correct ligand target. It is difficult to find binding targets that are unique to cancer cells. This is even more challenging when solid tumors have less specific antigens than hematologic cancers [67]. Often, therapies have to rely on overexpression of certain proteins by cancer cells. For example, eligibility for HER2 treatment involves checking the levels of overexpression of these surface proteins and assigning a score. However, for the highest score of 3+, the FDA needs only 10% of tumor cells to stain positively for HER2, while an updated scoring systems defines it as a uniform staining of more than 30% [68]. Additionally, it is sometimes difficult—yet very important—to find cell surface proteins that are exclusive to the cancer. There is circumstantial evidence that the HER2 antibody Trastuzumab could interfere with cardiac myocyte signaling and lead to cardiac dysfunction [69–71].

Targeting with monoclonal antibodies for HER2 has been show to increase tumor internalization [72]. On the other hand, it has also been shown that carriers with less specific ligand targeting are more limited in tumor penetration. It is assumed that these carriers experience a "binding site barrier" effect that inhibits penetration [73]. There remains some discord related to some of these cell binding and penetration strategies. With these cell targeting strategies, there is a need to find the correct balance of causing cell interaction to encourage uptake, yet still allow penetration throughout the rest of the tumor. Some carriers have been functionalized with peptides for improved penetration. The iRGD peptide is referred to as the tumor-penetrating peptide, but specificity is questioned with its ability

to bind with integrins beyond those on the tumor epithilium [74, 75]. The TAT peptide is sometimes referred to as a cell-penetrating peptide that targets the cell surface to increase cell uptake in a nonspecific way [76,77]. Similarly, the surface charge and shape of the carrier influences penetration as well. Positively charged particles may encourage internalization into the cells and penetration via transcytosis [64]. Furthermore, a modified albumin with a positive charge was shown to have better distribution in rat skin and skeletal muscle compared to native albumin with a negative charge. This exclusion to the negative probe was attributed to the fixed negative charge of the interstitium [78]. Shape also influence cell uptake profiles and could lead to different pathways in the cell [79, 80]. As mentioned in the stability section above, these charge and shape strategies could also have undesired effects of targeting the MPS [81].

Some fairly effective magic rafts have likely been made. While some may have failed because the design was flawed, others may have struggled with challenges that lie in tumor characteristics that make them difficult to target.

1.2.2 Challenges in the solid tumor environment

Once the particle extravasates, it is confronted with various obstacles in the tumor environment. While there is evidence explaining how EPR can benefit accumulation in tumors, there are also opposing influences from the tumor's pathophysiology [82]. Unfortunately, simplified descriptions of the EPR effect do not include the various challenges to drug delivery in the intratumoral environment (Fig. 1.4).

For solid tumors, additional barriers seem to hinder intratumoral distribution. Once the carrier reaches the tumor, it cannot be assumed that it will invariably reach and enter the

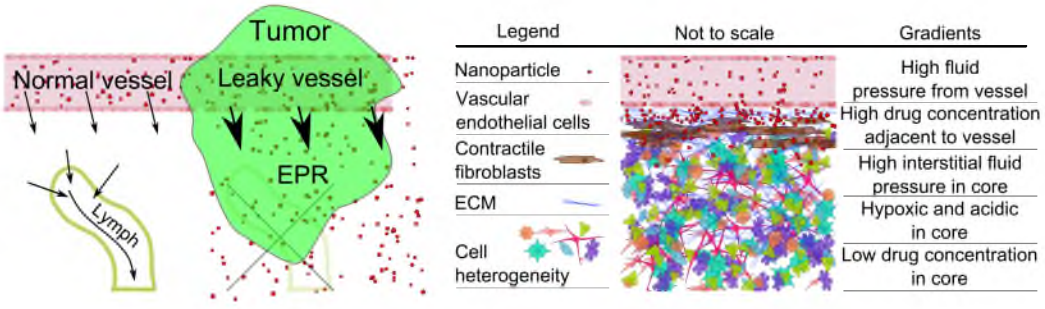

Figure 1.4. EPR is often over-simplified. Various forms of the illustration on the left have been used in research articles. They leave out important challenges in drug delivery to solid tumors. Even the depiction on the right cannot accurately represent all of the factors that impede passive targeting via EPR. Moreover, the pathophysiology is more complicated in clinical tumors where EPR is less reliable [83].

cancer cells. There are various factors that prevent the nanoparticle from penetrating into the tumor core [84]. Tumors grown in window chambers show heterogeneous permeation and the accumulation of nanoparticles adjacent to the blood vessel [85]. Other studies also show that the permeability varies and that liposomes do not diffuse far from blood vessels [86]. Distribution beyond the vicinity of blood vessels is a challenge even for viruses and free drug molecules [87, 88].

Besides the cancer cells themselves, the extracellular matrix (ECM) may be one of the biggest influencing factors for a solid tumor's progression. It can be thought of as the fertile soil for the developing tumor seed [89]. It supports the tumor in the form of survival signals, inhibition of the immune system, hindered diffusion of drug particles, and facilitation of cancer invasion and metastasis [90–93]. ECM in tumors is analogous to the biofilm that bacterial colonies will form for protection and continued growth. Under this protection, cancer cells can evolve, thrive, and multiply to a state of dense packing. The ECM has a higher stiffness and viscosity due to more fibronectin, collagen I, and cross-linking agents that can also limit diffusion [94, 95]. Finally, the ECM is one of multiple contributors to high interstitial fluid pressure (IFP) in solid tumors [96].

1.2.2.1 Tumor IFP

Elevated IFP is a feature often discussed as opposition to the enhanced permeability and retention of macromolecules that could otherwise be transported by bulk flow and penetrate into the core of solid tumors [97, 98]. In normal tissue, IFP is negative [99]. Thus, high IFP in tumors results in an outward convective flow preventing delivery and even promoting metastasis of detached cancer cells [100]. Interestingly, some of the same contributors to EPR (defective or permeable blood vessels along with dysfunctional lymph vessels) play a role in elevated IFP in tumors [101, 102]. The difficulty of accurately measuring all possible contributors to IFP prevents a comprehensive description of its etiology, but it has been verified in a variety of tumors [103, 104]. Explanations often say a combination of osmotic and hydrostatic pressures build up inside the tumor to nullify convective transport into the tumor [105]. Other possible contributing factors could be the ECM, contractile fibroblasts, or a high density of cells [106, 107]. Finally, Table 1.3 shows how additional factors may affect IFP in tumors.

In addition to small leaks from intercellular openings, fluid can spill out of poorly formed blood vessels, as evidenced by blood lakes observed in tumors [109]. Solutes in leaked fluids can flow into the interstitium from blood vessels and accumulate into the dense packing of matrix and cells to create an osmotic pressure. Furthermore, there is a significant metabolic

Table 1.3. Approaches for reducing IFP [107, 108].

VEGF antagonist	Normalize blood vessels, improve flow, and decrease permeability
PDGF antagonist	Decrease contraction and interaction of fibroblasts
TGFβ antagonist	Lower ECM content, inhibit macrophages, and normalize vessels
TNFα	Damage tumor vessels
Hyaluronidase	Degrade hyaluronan
Dexamethasone	Decreased vascular permeability and ECM content
Thalidomide	Anti-angiogenic
Bradykinin agonist	Improve blood flow
Nicotinamide	Decrease microvascular pressure
PGE_1	Decrease contractility of fibroblasts
Cytotoxins	Decrease cell packing and decompress vessels
Nicotinamide	Improve tumor blood flow
Pentoxifylline	Improves flow by reducing blood viscosity

contribution to the buildup of osmotic pressure when cells produce extra lactate in the hypoxic environment [100]. A combination of osmotic and hydrostatic pressures contribute to the Starling forces that drive fluid flow in tumor tissues [107]. These Starling forces are often placed in diagrams to describe the balances between the tumor tissue and the capillaries. If those were the only two compartments, an equilibrium should be reached fairly quickly at that interface. However, those simplified models restrict the tumor tissue to be a homogeneous compartment and exclude the surrounding normal tissue compartment. Fluid that is driven into interstitium from blood vessels percolates to areas of least resistance. This percolation is the convective flow in tissues. In normal tissues, the path of least resistance for the removal of any excess fluid would be the lymph vessels. However, these are not functional in tumors and the fluid must instead seep through dense networks of cells and ECM towards surrounding tissues [110]. There is evidence for this seepage in the literature showing carried cancer cell detritus and edema in tissues surrounding tumors [111, 112].

This seepage also helps explain how IFP is a continuous feature. There is a source of fluid into the tumor from the blood vessels; however, the flow rate through the tumor is limited because it must percolate through the less permeable tumor interstitium. Darcy's law can describe the flow rate (Q) of a fluid as being related to its viscosity (η) and the permeability (k) of the porous tumor interstitium [113]. Darcy's law can be equated to a simplified form of Poiseuille's law (where R is resistance to flow) to give the following [114]:

$$Q = \frac{k \times Area \times Pressure\ drop}{\eta \times Distance} = \frac{Pressure\ drop}{R}$$

Thus, the flow rate will be slower or the interstitial fluid pressure will need to be elevated

in order to overcome decreased permeability or increased resistance in the environment.

As an alternative, take the simplified example of filling a balloon. If water is constantly going into the balloon, there needs to be flow out of the balloon at the same rate or else pressure will build up. Of course, a normal balloon is elastic and will expand to relieve the pressure. Elasticity is the difference between high IFP in tumors and edema in normal tissue [115, 116]. The fluid accumulation with edema has also been studied for causes and treatments. Pulmonary edema is a significant topic in the literature as the health implications are serious. Furthermore, the lung is a more compliant tissue where large amounts of fluid can accumulate [117]. Causes of edema can be summarized in the following list: increased capillary pressure, decreased plasma proteins, increased capillary permeability, and blockage of lymph return [118, 119]. Tissue elasticity is related to ECM composition and its degradation can lead to edema [120, 121]. In comparison, stiffening of the ECM is a progressive feature of many solid tumors and explains why the wound healing process in this context results in high IFP instead of edema [94].

As the tumor has been labeled as a wound that will not stop healing, a comparison of relevant features found in wound healing may offer some insight. Fibroblasts play an important role in wound healing by helping to stiffen and pull together the wounded tissue [122, 123]. Fibroblasts can be differentiated to contractile fibroblasts (myofibroblasts) by growth factors present in wounded tissue and the tumor environment [124–126]. Performing as if in a wound, these differentiated fibroblasts in tumors can modulate the IFP through contraction and through production of ECM components [107, 127, 128].

Thus, we see multiple factors contribute to high IFP in tumors. However, if fluid can flow through tumors while maintaining an equilibrium of high IFP, other factors must prevent the even distribution of drug carriers within the tumors [98]. Results have shown that IFP is not sufficient for opposing penetration of antibodies [129]. The IFP had been lowered, but exclusion was assumed to be due to electrostatic opposition between the negatively charged antibodies and ECM [130].

Another contributor to uneven distribution is that convective flow of fluids and drug carriers in the tumors is likely through heterogeneously distributed rivulets in the tumor [131]. As stated previously, is should not be assumed that the tumor tissue is a homogeneous compartment. There will likely be some areas with high IFP and others with low IFP (i.e., paths of least resistance) within the tumor interstitium that allows for rivulets. Elevated IFP is often recorded by the wick-in-needle technique as homogeneous within the tumor and with a steep change at the periphery of the tumor [106]. As can be imagined, these are

not high-resolution measurements. Resolution is limited by the size of the probe needle tip and by the difficulty in knowing where the tip is at inside of the tissue. Table 1.4 shows how IFP can vary in different cancers and each cancer can have a wide range of IFP values across the sampled patients. For example, the IFP in cervical carcinomas has a range of nearly 100 mmHg between patients. While IFP is predominantly elevated, some recorded tumors show negative IFP values. Furthermore, the rivulets in the tumor or perfusion in the capillaries is in a state of flux [132,133]. This intermittent perfusion could be caused by elevated IFP impeding flow or by solid stress compressing vessels [134–136]. The variability of IFP in tumors brings us to another major challenge in treatment: heterogeneity.

1.2.2.2 Cancer is heterogeneous

There is both inter- and intratumoral heterogeneity with differences in the cancer type, environment, individual cells, and signaling. This heterogeneity can undermine the precise targeting mechanisms that were designed into the drug carriers. Heterogeneity in the tumor environment also explains how EPR is not equally present in all tumors.

Ovarian cancer is classified into different disease types by the type of cell from which it originates [137]. In neuroepithelial tissues, there are more than one hundred entities that have been discovered [138]. Similarly, cancer heterogeneity has been imaged in tissue specimens using antibody staining combined with quantum dots [139].

Low pH was discussed as a target before, but not all tumors possess a markedly low pH. It has been shown that a glucose infusion in nondiabetic patients can lower the pH in

Table 1.4. IFP (mm Hg) variability [111].

Tissue	n	Average IFP	Range
Normal skin	5	0.4	-1.0 to 3.0
Normal breast	8	0.0	-0.5 to 3.0
Metastatic melanomas	26	18.0	0.0 to 60.0
Breast carcinomas	21	23.7	4.0 to 53.0
Head and neck carcinoma	27	19.0	1.5 to 79.0
Cervical carcinomas	127	20.5	-2.8 to 94.0
Lung carcinomas	26	9.5	1.0 to 27.0
Brain tumors	28	4.6	-0.5 to 15.0
Rectal carcinoma	8	15.3	12.1 to 15.8
Colorectal liver metastasis	8	21.0	6.0 to 45.0
Lymphomas	7	4.5	1.0 to 12.5
Renal cell carcinoma	1	38.0	NA

Notes. Negative values imply flow into tissue. Positive values could indicate flow into surrounding tissue.

tumors [140]. However, this could have undesired consequences. It could cause elevated IFP through metabolic buildup and low flow in the tortuous tumor vessels [141]. It could also lead to increased angiogenesis and metastasis [142, 143].

Variability in the environment is apparent in the tumor's chaotic vasculature. Beyond shape, architecture, and density—tumors show differences in vascular permeability based on the type of tumor, location in the body, location in the tumor, hormone concentrations, and state of growth or regression of the tumor [144–146]. Differences in EP can exist for different types of tumors based on the characteristics of the capillaries: extravasation is limited in continuous capillaries, but possible in fenestrated or discontinuous capillaries. Passage can also be obtained via endothelial openings, transcytosis, or vesiculo-vacuolar organelles (VVOs) [62]. The different routes of extravasation might lead to the heterogenous distributions adjacent to tumor vessels [86]. Unfortunately, heterogeneity in tumor vasculature makes it difficult to know specific size cutoffs for carrier sizes targeting EP.

Variability in the density and rigidity of tumors will affect designs hoping to take advantage of ER in solid tumors. Many articles talk about the dense packing of tumors [147], but there is a lot of variability in the amount of interstitial space [97]. The process of transformation in the tumor environment is perhaps a contributor to this heterogeneity. Normal ECM is being broken down to make room for cancer cells that are secreting proteins for new ECM to support the growing tumor [148].

There is a diverse collection of cells, cancerous and noncancerous, in the tumor environment. Among the cancer cell population, there is a subdivision of cells that are cancer stem-like cells [149]. The properties of stem-like cancer cells make them a unique challenge in cancer therapy. They contribute to prosurvival signaling pathways, are able to differentiate into other cells, are more tumorigenic when injected into a new host, and imply increased metastatic potential [150–152]. Cancer stem-like cells seem to always be present and in equilibrium with other cancer cells [153]. While the source of these cells is debated (they may come from a mutated stem cell or a normal cancer cell mutates to become stem cell-like), the fact remains that they have characteristics that make them capable of resistance and renewal [154, 155]. Efforts to categorize and target cancer stem cells have been made by seeking after specific surface markers [156, 157]. However, it could be beneficial to use a magic shotgun that is selective toward more than just one target to effect a complete response in a heterogeneous population of cancer cells [158, 159]. Furthermore, multimarker therapies may reduce toxicity by giving cancer effectively a double-dose, but each drug will have nonoverlapping effects on normal tissue. The heterogeneity in the environment and

cell population results from the molecular biology of cancer. The differences in cellular phenotype and states of growth and quiescence are influenced by random variations of protein concentrations and interactions that lead to dynamics in molecular signaling, some of which originate from environmental cues [160]. Furthermore, genomic and epigenetic instability is characteristic of cancer cells [161]. These dynamic and heterogeneous characteristics play a role in how cancer is able to resist treatments [162].

1.2.2.3 Multidrug resistance

Tumor heterogeneity at the cellular level has a direct effect on multidrug resistance. Mutations cause diversity in cell characteristics and that diversity provides an opportunity to select for survival. Essentially, when a heterogeneous mixture of cells is treated with a drug, some will be able to resist the treatment. Furthermore, with treatment in solid tumors, cells at the periphery of the tumor often die off, leading to a smaller, yet more resistant, tumor mass. The apparent increase in resistance in the core could be due to conditioning from limited drug exposure, adaptations to survive in the already harsh environment, or the cells being more resistant inherently—as is the case with cancer stem-like cells.

Resistance comes from factors that range from the tumor environment down to cellular changes and mechanisms involving DNA. As stated before, only low amounts of drug are able to enter into the core of the tumor. Cancer cells are more easily able to adopt drug resistance to a low dose. This is apparent even in cultured cell lines as drug resistant lines are made by adding low doses of the drug into the growth medium [163, 164]. Furthermore, the core of the tumor is hypoxic and acidic and the cells have already adapted to survive in these harsh conditions. Some of these adaptations and cellular mechanisms for resistance are: detoxification via active efflux pumps, exocytosis, sequestration in acidic vesicles, DNA repair, compensation in chemical pathways, triggering of specific oncogenes, and even quiescence [165]. For example, it is easy for a cancer cell to resist the effects of doxorubicin or paclitaxel when it is not actively dividing.

As seen in Fig. 1.5, cancer cells that are able to survive will be prepared to resist future treatment, repopulate the tumor, and metastasize. If the cancer relapses, more aggressive cell types have been selected and the prognosis for the patient is poor. While the immune system provides a great example of targeted cancer therapy, cancer is still able to escape and continue growing [167, 168].

Immune evasion has become an emerging hallmark of cancer and is made possible by the heterogeneity inherent in cancer [169]. Understanding how cancer resists the immune system may lead to improved therapeutics in the future.

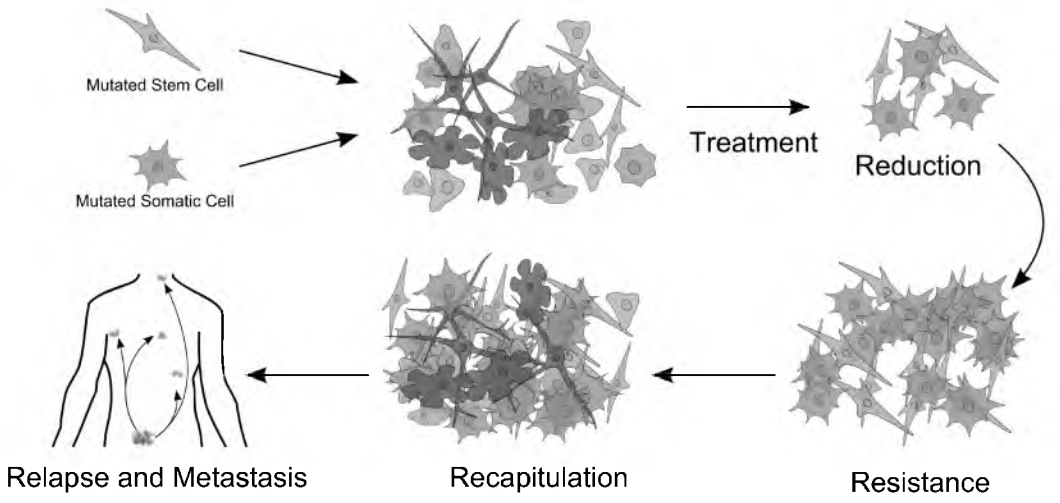

Figure 1.5. The 4 Rs of tumor treatment. Reduction, resistance, recapitulation, and relapse can occur when treating a heterogeneous collection of cancer cells. This process is similar to what occurs in immunosurveillance [166].

The process of immunoediting explains how the immune system can drive the progression of a tumor to a more resistant and aggressive state. Studies have shown that tumor formation is much more likely when the cancer cell line comes from a tumor grown in an immunocompetent mouse [170]. Tumors grown in immunodeficient mice are less aggressive than tumors that are grown in immunocompetent mice. Since most murine tumors are xenografts, they need to be placed in immunodeficient mice. Now we begin to see some shortcomings with the animal models in preclinical trials.

1.2.2.4 Model limitations

Modeling the tumor environment is difficult for some of the reasons related to heterogeneity mentioned above. There are a variety of models used in cancer research and each has its limitations. Animal models, specifically the mouse model, are routinely used to test the efficacy of new drug carriers. They have characteristics that make them easy to run the experiments in the lab and measure the results. These simplifications, of course, have shortcomings in their ability to provide accurate representations of clinical tumors.

Some of the disparity is present in the methods used to grow the tumors in animal models. As explained earlier, the environment plays a major role in cancer development. Unfortunately, mouse models are not always orthotopic. Breast cancer cells injected to grow a tumor in the hind quarters of a mouse will not accurately portray what a tumor in breast tissue will do. The rate and size of tumor growth in animal models is not representative of clinical cancers. Clinical tumors have many years to undergo genetic mutations, slow

growth, and evasion of the immune system [171]. Mouse models can be controlled to develop cancers in a random nature and a more representative timescale; however, for convenience and efficiency, many mouse models can form tumors approximately ten days following inoculation [172, 173]. Essentially, mice have a higher rate of metabolism that results in faster tumor growth and requires a more frequent dosing regimen for treatment. Additionally, the ratio of tumor to body weight is also much larger in mouse models compared to human patients. Having a large tumor mass may contribute to lower pH and increased EPR effect for mouse models. A good portion of targeting with drug carriers is passive and relies on the EPR effect. While EPR has a lot of evidence in animal models, it could be studied more extensively in human models as it can sometimes be notably absent [174]. An excellent study in human patients used scintigraphy to evaluate the effectiveness of EPR-based delivery and shows the difficulties of avoiding accumulation in normal tissues [175]. Study animals are generally sacrificed posttreatment to harvest tissues and accurately ascertain treatment efficacy. Tumor response is not always an accurate predictor of survival [176]. Furthermore, when the animal is sacrificed, there is no chance to check for tumor relapse. Overall, they simply do not provide as much of a challenge for treatment as clinical tumors. See the Appendix for an article comparing preclinical and clinical trial data for various drug carriers.

1.3 Included Work

The included work will address the limitations and challenges presented here by providing additional insights, models, and methods for analyzing intratumoral distribution. Specifically, it will provide a new model for drug distribution in the tumor environment, additional evidence for IFP as an inhibitor, real-time imaging to understand how nanoparticles distribute, tracking multiple doses and measuring their interdependence, and measuring distance traveled from blood vessels in three dimensions. The work uses surrogates for smaller sized drug carriers such as Abraxane (in Chapter 2) and for larger nanoparticles (in Chapter 3).

An explanted human organ model may compliment the mouse model to accurately represent barriers in a clinical tumor. Using uteri with naturally occurring benign fibroids as a model for solid tumors proved useful in understanding drug distribution in the tumor and surrounding tissue. It provides a clinically relevant model because the tissue is human, the complex structure is maintained, and the tumor to organ size ratios are appropriate. Fibroids have a slower, more natural growth rate than xenograft tumors and can average

around 9% growth in 9 months [177]. Furthermore, the observed lack of EPR in these tumors make it a good model for understanding distribution challenges in clinical tumors that do not show an EPR effect. The source is relatively plentiful, compared to other human tissues, due to the large number of hysterectomies performed each year. High collagen and hyaluronic acid content is already well established, but the research in this dissertation shows the tumor has transport barriers similar to other desmoplastic, malignant tumors. The research shows the following conditions within the fibroids: dense packing of cells and ECM, limited vasculature and transport, high IFP, and solid stress. An illustrative summary is provided in Fig. 1.6.

This work also takes a look at the distribution of multiple doses (each uniquely fluorescent) in xenograft tumors. It is acknowledged that xenograft tumors are a less than ideal model, but additional information can be gained from the new methods introduced and compared against the large collection of prior results obtained with that established model. Analyzing the distribution and interdependence of multiple doses is important as it fills a gap not prevalent in preclinical studies.

When patients undergo traditional chemotherapy or are treated with drug delivery technologies, multiple doses are required. Studies have not tested how multiple doses can interact with each other and possibly affect intratumoral distribution, even though dosing is clearly related to treatment efficacy. This work shows that distribution patterns of two different doses circulating in the blood stream at different times is influenced by the dynamics of the tumor environment. This information is relevant to therapies reliant on

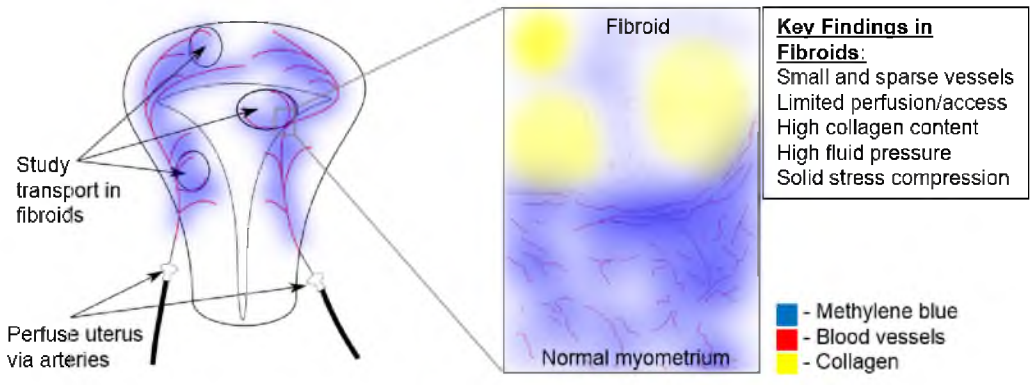

Figure 1.6. Chapter 2 illustrative summary. We perfused the uterus and studied distribution in the fibroids to understand transport barriers.

passive mechanisms for extravasating into the tumor environment. Better understanding these dynamics may influence planning of dosing schedules and combination treatment strategies. Furthermore, it identifies limitations in measuring the distribution of drug in the tumor (relative to blood vessels) in two dimensions versus three dimensions. Research that tracks multiple doses independently and how it relates to intratumoral distribution is important to guide clinical treatment strategies. An illustrative summary is provided in Fig. 1.7.

The National Institutes of Health has a desire to see quantitative measurements of how cancer therapies affect the tumor in clinical trial settings [NIH PAR-14-116]. This work uses quantitative analysis of imaging data on a new model that could become an additional precursor to clinical trials. The work also tracks multiple doses and has the potential to influence how dosing and other clinical decisions are made. It identifies additional barriers in the translation from the laboratory to the clinic by using fluorescent probes, in addition to other methods, to characterize delivery to the tumor with implications to therapy response [NIH PAR-13-185].

The research presented in this dissertation uses models and methods in new applications to help shed light on some of the intricacies of passive delivery to solid tumors. These additional methods for distribution analysis can be employed in future work that seeks to get past some of the barriers inherent in solid tumors.

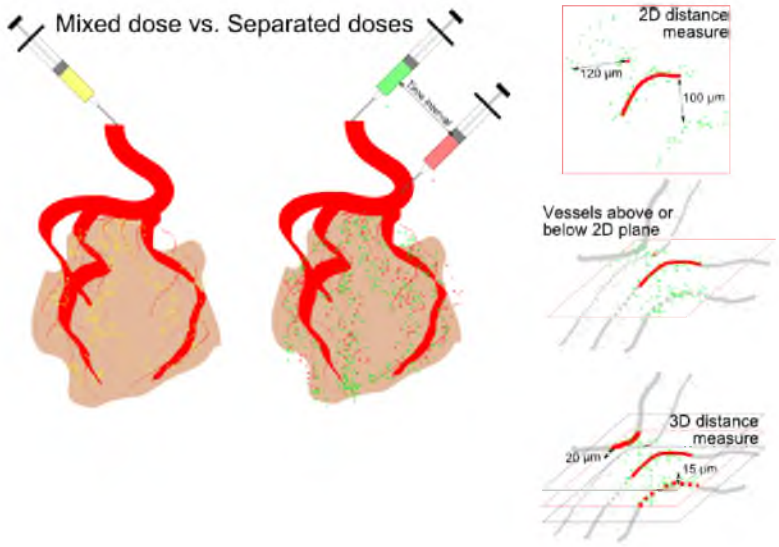

Figure 1.7. Chapter 3 illustrative summary. Spatiotemporal analysis of two uniquely fluorescent doses: administered as separate or mixed doses.

CHAPTER 2

UTERINE PERFUSION MODEL FOR ANALYZING BARRIERS TO TRANSPORT IN FIBROIDS

D. L. Stirland, J. W. Nichols, E. Jarboe, M. Adelman, M. Dassel, M.-M. Janát-Amsbury, and Y. H. Bae, Uterine perfusion model for analyzing barriers to transport in fibroids, J. Control. Release, vol. 214, pp. 8593, Sep. 2015. http://dx.doi.org/10.1016/j.jconrel.2015.07.006.
Included with kind permission of Elsevier and the coauthors.

Journal of Controlled Release 214 (2015) 85–93

Contents lists available at ScienceDirect

Journal of Controlled Release

journal homepage: www.elsevier.com/locate/jconrel

Uterine perfusion model for analyzing barriers to transport in fibroids

Darren L. Stirland [a], Joseph W. Nichols [a], Elke Jarboe [c,d], Marisa Adelman [c], Mark Dassel [c], Margit-Maria Janát-Amsbury [a,b,c,*], You Han Bae [b,e,**]

[a] Department of Bioengineering, University of Utah, United States
[b] Department of Pharmaceutics and Pharmaceutical Chemistry, University of Utah, United States
[c] Department of Obstetrics and Gynecology, University of Utah, United States
[d] Department of Pathology, University of Utah, United States
[e] Utah-Inha DDS and Advanced Therapeutics Research Center, Incheon, Korea

ARTICLE INFO

Article history:
Received 30 April 2015
Received in revised form 14 June 2015
Accepted 3 July 2015
Available online 13 July 2015

Keywords:
Uterine fibroid
Drug delivery
Intratumoral distribution
Interstitial fluid pressure
Ex vivo model
Clinical tumor model

ABSTRACT

This project uses an ex vivo human perfusion model for studying transport in benign, fibrous tumors. The uterine arteries were cannulated to perfuse the organ with a buffer solution containing blood vessel stain and methylene blue to analyze intratumoral transport. Gross examination revealed tissue expansion effects and a visual lack of methylene blue in the fibroids. Some fibroids exhibited regions with partial methylene blue penetration into the tumor environment. Histological analysis comparing representative sections of fibroids and normal myometrium showed a smaller number of vessels with decreased diameters within the fibroid. Imaging of fluorescently stained vessels exposed a stark contrast between fluorescence within the myometrium and relatively little within the fibroid tissues. Imaging at higher magnification revealed that fibroid blood vessels were indeed perfused and stained with the lipophilic membrane dye; however, the vessels were only the size of small capillaries and the blood vessel coverage was only 12% that of the normal myometrium. The majority of sampled fibroids had a strong negative correlation (Pearson's $r = -0.68$ or beyond) between collagen and methylene blue staining. As methylene blue was able to passively diffuse into fibroid tissue, the true barrier to transport in these fibroids is likely high interstitial fluid pressure, correlating with high collagen content and solid stress observed in the fibroid tissue. Fibroids had an average elevated interstitial fluid pressure of 4 mm Hg compared to −1 mm Hg in normal myometrium. Our findings signify relationships between drug distribution in fibroids and between vasculature characteristics, collagen levels, and interstitial fluid pressure. Understanding these barriers to transport can lead to developments in drug delivery for the treatment of uterine fibroids and tumors of similar composition.

© 2015 Published by Elsevier B.V.

1. Introduction

Uterine fibroids are desmoplastic, benign tumors—also known as leiomyomas—whose growth has been shown to be influenced by ovarian steroid hormones and mediated by growth factors [1]. Current treatments provide symptom control, and result in a short-term reduction in fibroid volume, but only hysterectomy can provide definitive treatment [2]. Approximately 600,000 hysterectomies are performed every year—200,000 of which are for uterine fibroids [3]. The prevalence of uterine fibroids and the frequency of hysterectomy provided an opportunity to study drug transport in solid tumors, while preserving the macro- and microenvironments.

We hypothesized that the pathophysiology of uterine fibroids contains various barriers, similar to many other solid tumors, which impede the transport of macromolecules. To test this, we perfused human uterine specimens ex vivo with stains and fluorescent probes. Methylene blue served to visualize drug transport in this study. We analyzed the distribution of methylene blue for correlation with any of the identified, inert pathophysiological tissue barriers. During the perfusion process we measured the interstitial fluid pressure (IFP) of the fibroids. Through gross examination, histological analysis, and fluorescent microscopy, we measured the nature of vessel perfusion, collagen density, and looked for relationships with inhibited methylene blue transport. The uterine perfusion model maintains the complexity of the target tissue, but offers more control by not involving the entire organism. It has previously been shown that fibroids have decreased and chaotic vasculature [4–7]. Additionally, intercapillary distances have been linked to

* Correspondence to: M.-M. Janát-Amsbury, Department of Obstetrics and Gynecology, University of Utah, Salt Lake City, UT 84132, USA.
** Correspondence to: Y.H. Bae, Department of Pharmaceutics and Pharmaceutical Chemistry, University of Utah, Salt Lake City, UT 84112, USA.
E-mail addresses: margit.janat-amsbury@hsc.utah.edu (M.-M. Janát-Amsbury), you.bae@utah.edu (Y.H. Bae).

http://dx.doi.org/10.1016/j.jconrel.2015.07.006
0168-3659/© 2015 Published by Elsevier B.V.

Table 1
Patient details.

Patient	Reason for hysterectomy/diagnosis	Fibroid characteristics		Other tissue features
		Location	Diameter	
1	Menorrhagia, fibroids	No fibroids		Endometrial polyp and adenomyosis
2	Abnormal uterine bleeding, dysmenorrhea, endometriosis	No fibroids		Endometrial polyp and adenomyosis
3	Pelvic pain, abnormal uterine bleeding (ovulatory dysfunction), tubal ligation ablation syndrome	Intramural	~1 cm	None
4	Postmenopausal bleeding, complex left adnexal mass, endometrial atrophy	Submucosal; intramural	~0.5 and 2 cm; ~1 and 1.5 cm	Mucinous cystadenoma
5	Abnormal uterine bleeding (ovulatory dysfunction)	Intramural	~1 cm	None
6	Dysmenorrhea, von Willebrand disease, fibroids	Dominant	8 cm	None
7	Hysterectomy with risk-reducing oophorectomy	Subserosal; intramural	~1 cm; ~0.5 cm	None
8	Menorrhagia, fibroid, urinary frequency, pain, pressure	Dominant; others	5 cm; multiple small	None
9	Pelvic pain/dyspareunia, high grade cervical dysplasia	No fibroids		None
10	Adenomyosis, pelvic pain	Intramural	~1 and < 1 cm	Adenomyosis
11	Dysmenorrhea, dyspareunia, high grade dysplasia	No fibroids		High grade dysplasia
12	Abnormal uterine bleeding (fibroids)	Submucosal	~8 cm	Endometrial polyp and adenomyosis
13	Dysmenorrhea, pelvic pain	No fibroids		None
14	Dysmenorrhea, menorrhagia	Intramural; submucosal; submucosal-pedunculated	~0.4, 0.8, 1.3, 1.3 cm; ~0.4 cm; ~2.1 cm	None

hypoxic conditions identified within these tumors [8]. Other uterine perfusion models have demonstrated successful perfusion of the tissue, while maintaining viability, as various study drugs were delivered to the specimen [9,10]. Further, polymer resins have been perfused into uterine specimens to provide information on the vascular architecture of uterine fibroids; however, the highly viscous resin may not have reached the smallest capillaries or the delicate casts may have become damaged [11,12]. Radio-opaque dyes have also been perfused, but resolution limits would make discerning of the smallest vessels challenging. This project expands on previously reported efforts with additional methods as well as shifting to a new purpose of investigating drug distribution in solid tumors (fibroids) that can exist in the uterus. For this purpose, we chose light microscopy with resolution limits near 1 μm, the ability to capture mosaics of entire tissue sections, and the ability to use multiple probes with different fluorescence simultaneously. We therefore probed, stained, and imaged the fibroid environment to investigate the distribution of molecules administered arterially.

A large body of research suggests that delivery to solid tumor environments is possible via the enhanced permeability and retention (EPR) effect. As some hemorrhagic leiomyomas may have leaky vessels [13], we sought to use this model to explore the existence and balance of the EPR effect and barriers that might oppose it [14]. Furthermore, intratumoral transport in solid tumors continues to be a relevant research topic for understanding why some treatments may fail in the clinical setting, especially because EPR does not seem to be evident throughout all various types of clinical tumors [15,16].

2. Materials/methods

Salts and reagents for the perfusate solution were obtained from Sigma-Aldrich (St. Louis, MO, USA). Masterflex silicone tubing was purchased from Cole-Parmer (Vernon Hills, IL, USA). The MicroLab FS-522 interface, thermistor, pH electrode, and redox probe were purchased from MicroLab, Inc. (Bozeman MT, USA). Insyte Autogaurd winged 24-gauge catheters (BD381512) were purchased from the University of Utah general store. The incubator was fashioned from a clear plastic dessicator and the manometer from a 25 mL plastic pipette. The Falcon 40 μm cell strainers were purchased from Fisher Scientific (352340, Pittsburg, PA, USA). 1,1′-Dioctadecyl-3,3,3′,3′-tetramethylindocarbocyanine perchlorate (DiI) was purchased from Santa Cruz Biotechnology, Inc. (sc-213424, Dallas, TX, USA). Collagen

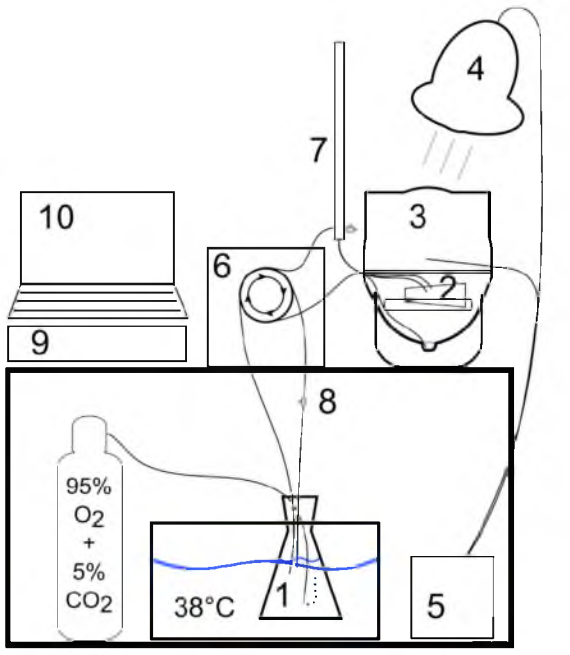

Fig. 1. A perfusion system to keep the uterus sample viable during experiments. The perfusate reservoir (1) is heated and bubbled with 95% oxygen. The uterus (2) is placed in a clear plastic incubator (3) heated with an infrared lamp (4) connected to a temperature regulator (5). A peristaltic pump (6) pushes perfusate through the tubing. The tubing passes through a bubble catcher (7) that also serves as a manometer and site for injections and sampling. Perfusate enters the organ by cannulating the two uterine arteries. The perfusate trickles out of the organ and into a small collection area and tubing returns the perfusate to the reservoir for recirculated flow. Samples can be taken from the venous side of the organ via a sampling port in the tubing (8). A MicroLab (9) connected to a laptop (10) records data such as pressure, pH, and pO_2 levels.

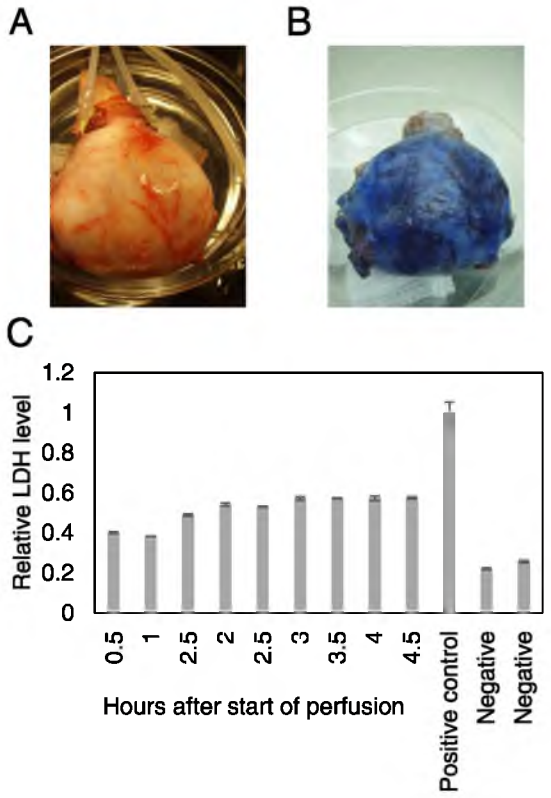

Fig. 2. Progressive perfusion of the ex vivo uterus. Perfusion is apparent in the clearing of blood and whitening of the tissue (A) and subsequent staining with methylene blue added to the perfusate (B). C) Assay checking lactate dehydrogenase (LDH) levels to quantify the amount of cell lysis present in the perfused organ. Our method of perfusing the organ was able to stabilize tissue viability as measured by LDH levels.

mimicking peptide (CMP) stain was generously given by Dr. Michael Yu in the Department of Bioengineering at the University of Utah.

2.1. Perfusion of uteri

Human uteri were obtained according to an Institutional Review Board approved protocol. All patients consented to procedures outlined and only patients who were already scheduled to undergo a surgical hysterectomy (based on various diagnoses listed in Table 1) through the Department of Obstetrics and Gynecology at the University of Utah Hospital were approached. Upon receipt, each specimen was weighed and measured prior to cannulation of the bilateral uterine arteries with catheters. The wings of the catheter were secured to the tissue and the cuff of the arterial stump was constricted around the catheter using suture to limit accidental removal and back flow. An initial flush of 10 mL of heparinized isotonic saline solution was used to ensure proper placement of catheters in the arteries. The uterus was then placed inside the incubator and connected to the perfusion system (Fig. 1) via the catheters. The perfusate was a modified Kreb–Henseleit (KH) buffer solution with a pH of 7.4 composed of: 118 mM NaCl, 4.7 mM KCl, 1.2 mM $MgSO_4$, 1.25 mM $CaCl_2$, 1.2 mM KH_2PO_4, 25 mM $NaHCO_3$ 11 mM glucose, 2.5 IU/mL heparin, 1 mM DTT, sacharose, glutathione, gentamicin, and a 100 IU insulin bolus. The initial flush volume was approximately 1–2 mL/g of tissue to clear the vasculature of remaining blood components and cellular debris. This preparatory procedure lasted for approximately 30 min or until the solution in the venous line flowed clear. Following this initial flush, the venous return line was directed into the main reservoir for isovolumetric perfusion. The volume for the recirculated perfusion was approximately 300 mL in the reservoir plus the volume contained in the tissue. Possible causes of vascular occlusion were detritus from cell or blood products and air bubbles. Occlusion was mitigated by designing the manometer in a way to catch air bubbles and by using the cell strainer to filter any aggregates present in the perfusate reservoir.

Methylene blue was added to the main reservoir to visually monitor effective perfusion and to mimic drug distribution. Perfusion was also monitored with the MicroLab data acquisition instrument. The instrument had probes to check the pH and pO_2 levels. It was further equipped with a pressure reading port, used to check the pressures in the arterial lines via the manometer site. A target pressure near 100 mm Hg was

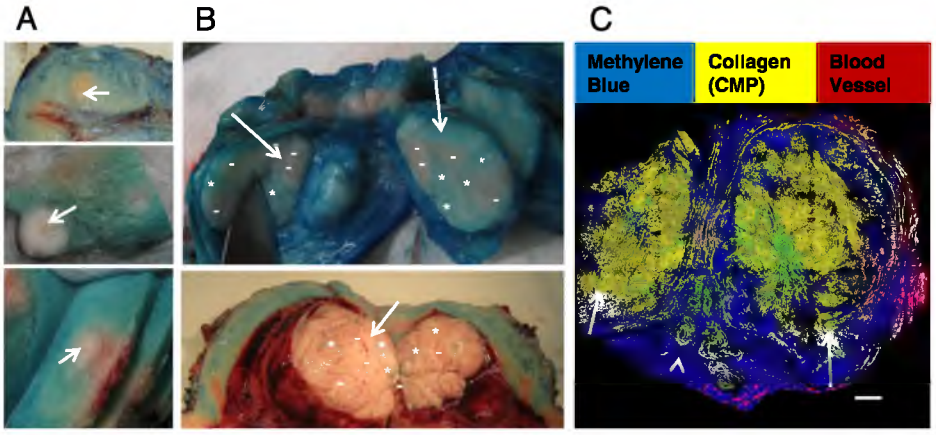

Fig. 3. A) Visible staining of methylene blue is limited in the fibroids (arrows). B) Some regions can be identified that have slight staining (*) compared to no staining (—). C) A high contrast binary image of tissue section captured with a fluorescent microscope and processed with Matlab reveals the same phenomenon of limited stain in the fibroid. The primary colors represent unique locations of fluorescence. Secondary colors are regions of overlap—e.g., green for overlap of methylene blue and collagen. Arrowhead points to myometrium (normal tissue) and arrows to fibroids. Scale bar is 1000 μm. (For interpretation of the references to color in this figure legend, the reader is referred to the web version of this article.)

obtained by adjusting the peristaltic flow rate and by adjusting the catheter as strain from the tubing can push the catheter tip against a bend in the torturous uterine artery, obstructing the flow. Every 30 min, samples of the perfusate buffer were taken from the venous line to run a lactate dehydrogenase (LDH) assay probing for tissue damage. For the final 30 min of perfusion, DiI—the lipophilic membrane staining dye—was added to the main reservoir to fluorescently stain the perfused vasculature [17]. The perfusion period would be terminated after a maximal duration of 8 h. Then the specimen was further processed by the Department of Pathology to ensure no interference with routine diagnostics.

2.2. Interstitial fluid pressure measurements

Interstitial fluid pressure measurements were taken during specimen perfusion with a 24-gauge needle manufactured with a side port. The needles fit snugly into capillary tubing. After priming the tubes with water, the needles were inserted into the tissue being perfused and the water lines were immediately marked with a marker and the tubes were erected vertically. The IFP was measured in fibroids that were palpable. At least 10 min passed before measuring the change in water level.

2.3. LDH assay

Reagents were purchased from Sigma-Aldrich (St. Louis, MO, USA). Perfusate samples were collected every 30 min and stored at 4 °C before adding to a 96-well plate containing the freshly prepared Tris buffered solution of lithium lactate, phenazine methosulfate, iodonitrotetrazolium chloride, and nicotinamide adenine dinucleotide. Following a 5 minute incubation at room temperature, the absorbance was read at 490 nm to measure the amount of cytosolic LDH released from lysed cells. Richter et al. performed uterine perfusions and found LDH levels elevated to about 600 IU/L in control groups that resulted in damaged tissue [10]. Lactate dehydrogenase at a concentration of 662 IU/L was used as the positive control and upper limit for acceptable cell lysis. Two negative controls of blank buffer with assay reagents and a perfusate sample without reagents were also used.

2.4. Biospecimen analysis

Any visible or palpable fibroids were noted and measured if possible. The organ was weighed again after the procedure to assess any fluid retention during perfusion. Upon completion of perfusion, the organ was grossly examined in collaboration with the Department of Pathology. Pictures were taken with a consumer-level digital camera for qualitative assessment of perfusion of the uterine myometrium, endometrium, and fibroids. At the pathology assistant's discretion, small excess tissue samples (approximately $1 \times 1 \times 0.5$ cm) were obtained, embedded in optimal cutting temperature (OCT) compound for flash freezing the fresh tissue, and stored at −80 °C until cryo-sectioning and further analysis. Following routine medical diagnostics, additional fixed tissue was obtained and stored at room temperature in formalin before taking samples for additional analysis and benchtop experiments. Fixed samples were also embedded in OCT, flash frozen and stored at −20 °C before sectioning. As the fluorescent DiI vessel stain and methylene blue were introduced during the perfusion stain, the samples could be quickly cryo-sectioned into 50 μm thick slices and mounted for imaging without further preparation. Representative tissue sections were additionally stained with the fluorescently-labeled CMP or with histological stains. The fixed tissue sections were stained for collagen by CMP as previously described by Li et al. [18]. A Nikon A1 confocal microscope imaged the CMP stain excited at a wavelength of 488 nm, DiI stain at 561 nm, and methylene blue at 638 nm. Formalin-fixed tissue was cut into 3 μm sections and stained with either hematoxylin and eosin (H&E) or Masson's trichrome in the histology division of the Department of Pathology at the University of Utah. When processed as part of routine diagnostics, it was paraffin embedded. If the tissue sample was from our collection and to be compared with fluorescently imaged sections, it was OCT embedded. OCT embedding was chosen to avoid washing away the fluorescent stains in the paraffin embedding process.

2.5. Experiments on isolated tissue chunks

Cylindrical tissue chunks (roughly 4 mm in diameter and 5 mm thick) were cut from representative parts of each fibroid and myometrium from a non-perfused control specimen. The tissue chunks were arranged in a

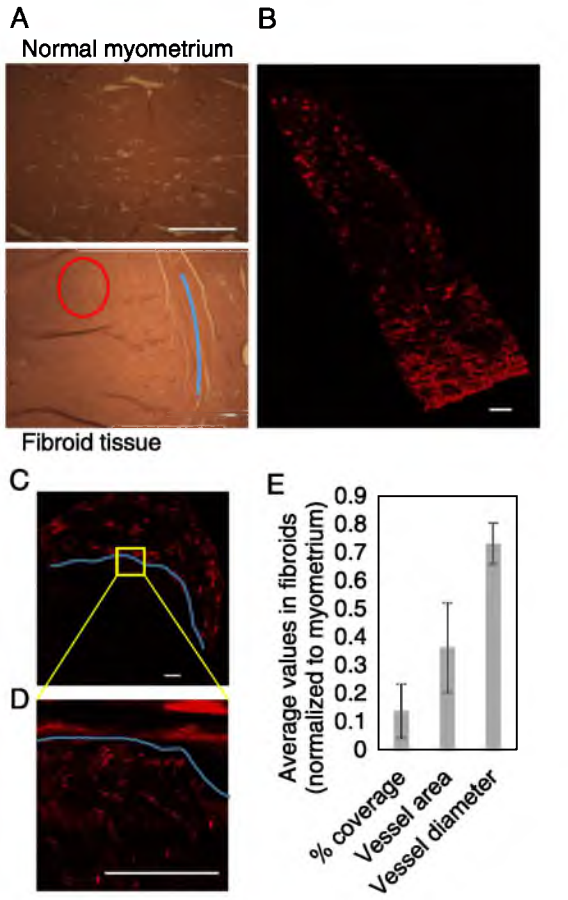

Fig. 4. Reduced vasculature in fibroids. All scale bars represent 1000 μm. A) A reduced number and average diameter of vessels in fibroids are seen in sections stained with H&E. The normal myometrium has large diameter vessels visible throughout tissue while only limited, small-diameter vessels are seen (red circles) in the fibroid (boundaries between normal and fibroid tissue marked by blue lines). Fluorescent staining of vasculature via perfusion is psuedocolored red (B–D). B) The perfusion stain of the vasculature reaches the entire thickness of the myometrium and increased vasculature is apparent in the endometrium. C) Stained vasculature is clearly seen in the myometrium tissue but appears lacking in the fibroid regions of the uterine tissue. D) Higher resolution imaging of the fibroid tissue shows that blood vessels do exist, albeit at smaller diameters. E) Data for the vasculature in the fibroids are presented after normalizing the values with respect to comparable normal tissue of the same organ. The averages for all three features of vessel measurement are significantly smaller in the fibroid tissue compared to normal tissue ($P < 0.05$). (For interpretation of the references to color in this figure legend, the reader is referred to the web version of this article.)

12-well plate and submerged in 2 mL of perfusate buffer with and without methylene blue for 2 h for the experiment testing passive diffusion of methylene blue through the tissue. Larger tissue chunks (approximately 10 × 10 × 5 mm) were used when testing the effect of fluid pressure on methylene blue distribution. Capillary tubing was passed through the tissue chunk by first impaling with a needle to guide the tube through the tissue. A water depth of 5 cm simulated IFP of approximately 3.7 mm Hg was sufficient to overcome the slight pressure of about 1.5 mm Hg exiting the fenestrae (made with a 30 gauge needle—approximately 310 μm in diameter) in the tubing wall. Thus, pressure into the tube was approximately 2 mm Hg, which was intentionally set to mimic the high interstitial pressure reported for other solid tumors [19].

2.6. Image analysis

ImageJ was used to analyze fluorescent microscopy images [20]. Images of the fluorescently stained vasculature were auto-thresholded to detect and analyze vessel objects providing average areas and Feret minimum diameters to estimate the vessel size (area), percent coverage (area fraction), and vessel diameters. The percent coverage was determined by dividing the total area of all vessels by the total area of the tissue analyzed. The Feret minimum diameter estimated the vessel diameter quickly and without user interference. Images of CMP and methylene blue fluorescence were combined into stacks and areas of interest were analyzed for average intensity values. Custom Matlab code was used to generate the high-contrast image showing unique colors for distinct and overlapping fluorescent signals.

2.7. Statistical analysis

Values were averaged from multiple measurements from the images. Error bars in graphs represent standard deviation. Statistical significance of Pearson's correlation values was determined with a critical value table for a One-Tailed test. All other instances of statistical significance were calculated with a One-Tailed Student's test.

3. Results

3.1. Stain does not pervade fibroid tissue despite thorough perfusion of organ

Qualitative assessments of perfusion quality showed that the tissue would whiten with the flush perfusion and turn blue upon the addition of methylene blue (Fig. 2A–B). Furthermore, the LDH assay showed acceptable tissue viability during our experiments lasting fewer than 8 h (Fig. 2C). The perfusion system allowed us to observe and maintain physiological conditions such as temperature, neutral pH, elevated pO_2 level, and arterial pressure near 100 mm Hg (data not shown). Even with thorough perfusion, the fibroid regions seemed unaffected by the perfusion and would not be stained like the surrounding normal myometrium. This was observed during gross examination and with fluorescent microscopy of the sectioned tissue (Fig. 3). The interface

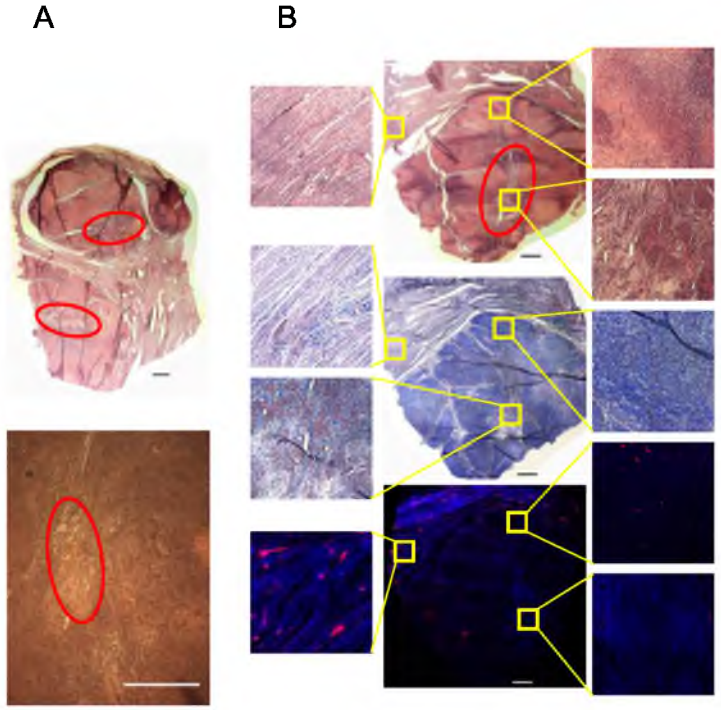

Fig. 5. A) Multiple fibroids had regions (marked with red circles in A and B) in their interior where the tissue density appeared similar to that of the myometrium. B) Shows successive sections of fibroid tissue stained with H&E, Masson's trichrome, and fluorescence introduced during perfusion. The tissue in those regions appeared to be less dense with less prominent staining for collagen and higher accumulation of methylene blue stain (psuedocolored blue) by fluorescent imaging. Fluorescence from blood vessels is psuedocolored red. (For interpretation of the references to color in this figure legend, the reader is referred to the web version of this article.)

between fibroid and normal myometrium was evident in microscopic images of the sections with compressed lines of displaced tissue at the periphery of the fibroid.

3.2. There is limited vasculature in fibroids

The vasculature also appeared to be compressed and limited in the fibroid tissue. H&E stains and fluorescent imaging of fibroid and myometrium sections showed that vessels in the fibroid are sparse and consist mainly of capillaries. Fig. 4 shows representative examples of imaged vasculature and quantifies the vessel areas, percent coverage, and minimum diameters compared to respective normal myometrium. The vasculature was measured using two main parameters: area and minimum diameter. The minimum diameter would estimate the vessel diameter while the vessel area measurement includes information about size and coverage. The average vessel diameter in the fibroids is only slightly smaller than that of the normal myometrium (approximately 9 μm compared to 14 μm, respectively). This is not surprising, as the normal tissue also includes capillaries with a large number of those affecting the average, being closer to the average vessel diameter found in the fibroid. On the other hand, the squared value of the vessel area likely accentuates the disparity between the two tissue types. The DiI was successful in fluorescently staining the perfused vessels. The highly visible stain throughout the myometrium extending into the endometrium indicates that the entire organ was sufficiently perfused. However, only at high magnification (20× or above) can small vessels in the fibroids be seen more clearly. This confirms that vascular perfusion is limited, yet still present, in the fibroids.

3.3. There is a negative relationship between collagen density and methylene blue distribution

Results from stained tissue sections showing intratumoral features of the fibroids are shown in Fig. 5. Comparing successive sections revealed relationships in different areas of tissue when comparing packing density, collagen density, and methylene blue distribution. The negative relationship between methylene blue distribution and collagen density was first observed qualitatively. By sampling different areas in fibroid and normal myometrium, it was found that areas with high methylene blue fluorescence had relatively low fluorescence for the CMP stain (Fig. 6). We further analyzed the relationship between the distribution of methylene blue and collagen density based on average fluorescence intensities and found a negative correlation between the two with the exception of one fibroid sample. The Pearson's correlation values (and significance) for 4 fibroids were −0.89 ($P < 0.01$), −0.92 ($P < 0.01$), −0.68 ($P < 0.1$), and an outlier of 0.70 ($P < 0.1$). The controls had weaker correlation and were not

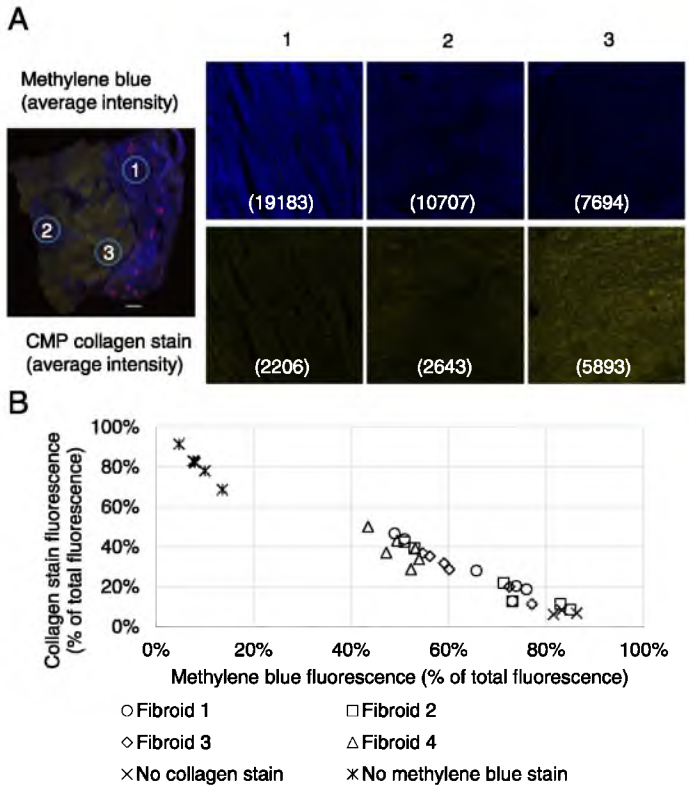

Fig. 6. Comparing fluorescence of the collagen stain and methylene blue for various regions of interest. A) Qualitatively shows how different regions show a negative relationship between collagen stain (psuedocolored yellow) and methylene blue (psuedocolored blue) according to the average fluorescence intensity. B) Fluorescence values of various areas for multiple fibroids (normalized as a percentage of total fluorescence to fit on one graph). Fibroids 1 through 3 have a negative correlation. Fibroid 4 does not show the same relationship. Two additional fibroids used as controls for collagen stain and methylene blue appear at the two ends of the spectrum. (For interpretation of the references to color in this figure legend, the reader is referred to the web version of this article.)

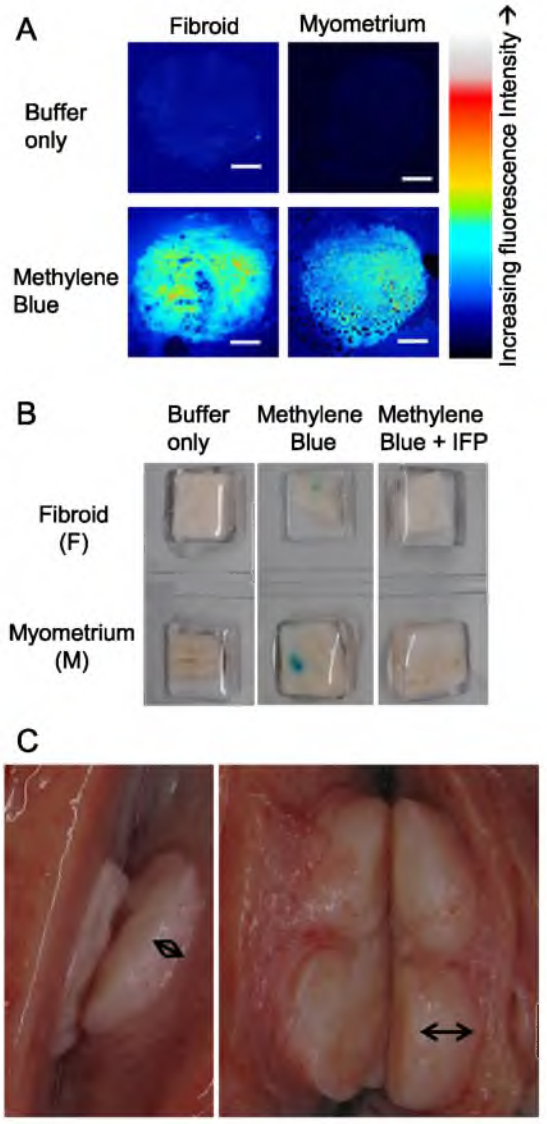

Fig. 7. A) High accumulation of stain via passive diffusion was evident after submerging fibroid tissue in a methylene blue buffer solution. The grayscale image was colorized using the royal lookup table. Scale bars are 1000 μm. B) Perfusing tissue chunks while controlling IFP confirmed that high pressure could prevent staining of the tissue. C) Evidence for solid stress in fibroids. The tissue was sliced during gross examination and tissue expansion (double arrows) was observed in the fibroids. (For interpretation of the references to color in this figure legend, the reader is referred to the web version of this article.)

statistically significant ($P > 0.1$). On a larger, macroscopic scale, the negative relationship is clear when comparing the collagen and methylene blue content between the fibroid tissue and the normal myometrium as a whole. Under the microscope, the interior of the fibroid tissue showed heterogeneous distributions of methylene blue and collagen content. Unsurprisingly, further heterogeneity existed amongst the different fibroid specimens. One fibroid in particular showed relatively low levels of collagen density in both the CMP and Masson's trichrome stain (data not shown). Perhaps for that reason, the sample was an exception to the correlation analysis in that it did not show a negative relationship between methylene blue staining and collagen content.

3.4. Hydrostatic pressure is a barrier to transport

Fig. 7 shows results from experiments probing how passive diffusion and interstitial fluid pressure affect methylene blue distribution inside fibroids. When testing passive diffusion of methylene blue through the fibroid and myometrium tissue, a high fluorescence intensity for methylene blue was found within the fibroid tissue. As suspected, the mere presence of collagen is not sufficient to prevent transport of the methylene blue. Methylene blue can permeate into fibroid tissue as easily as, or more so, into the normal tissue with the passive diffusion tests. It has already been shown that diffusivity is less hindered through some neoplastic tissues [21]. Still, methylene blue distribution seems inhibited in the fibroids when delivered via arterial perfusion. This is likely due to high IFP in the collagen rich areas of the fibroid acting as a barrier. To further confirm these findings, experiments perfusing isolated tissue chunks showed how pressure can overwhelm transport and therefore prevent staining of methylene blue into the tissue.

During the ex vivo perfusion of the organ, IFP measurements probing palpable fibroids saw an average hydrostatic pressure of about 4 mm Hg (net flow out of fibroid tissue) while normal myometrium tissue had an average pressure near −1 mm Hg (net flow into tissue). Probing the IFP in two different locations of one fibroid in particular resulted in distinct pressure values of 2 and 6 mm Hg, which also represent the maximum and minimum values recorded from various fibroids. Our needle probing data affirm secondary evidences suggesting existence of high IFP. Fibroid tissue exerts forces on and displaces surrounding tissue. The solid-stress-induced tissue expansion of the fibroid tissue was observed during gross examination after the tissue was sliced cleanly and evenly. This built-up solid stress could be growth induced or due to the compressive nature of the myometrium tissue and correlates with high IFP in the tumor [22]. Similar to lesional edema, the collagen content in fibroids can increase filtration and restrict the volume from expanding to equilibrate the high IFP [23,24]. IFP has been shown to be almost uniformly high and a transport barrier in other solid tumors [19,25,26]. The challenge of teasing out heterogeneous IFP within the tumor could be due to the imprecise nature of the needle probing method with resolution limited by the size of the needle tip. Non-image guided introduction and positioning of the needle within a fibroid tumor proved challenging in our experiments. While we found two distinct pressure values in one fibroid, there was considerable variation amongst pressure values across all examined fibroids. This variation precludes statistical significance between the averages for normal and fibroid tissue; however, the pressure differences seemed meaningful in that all pressure measurements from the normal myometrium were at 0 mm Hg or below and all fibroid pressures were positive. These positive pressures found inside fibroids could inhibit convective flow into interstitium and create a barrier to the intratumoral transport of molecules. Granted, failure to attribute a neutral or negative pressure to any undetected fibroid—assuming needles ended up being positioned within normal, non-fibroid myometrium—could not be excluded. While technologies mapping the intratumoral IFP in high resolution are unknown to the authors at this point, our imaging data suggests rivulets of transport inside fibroids and is consistent with previously published research [27,28]. Such rivulets depend on areas of high and low pressure to dictate paths of least resistance out towards the normal tissue containing functional lymphatics.

4. Discussion

Poor penetration of visible stains, dense environments evident in histological sections, fewer vessels with decreased diameters seen in

fluorescent microscopy, and higher IFP measured by needle probes confirm barriers to transport in these fibrotic tumors. The distribution of the methylene blue within fibroids is likely dominated by pressure gradients and not solely by collagen packing or even vasculature. These results may help to explain the pathophysiology of and improve treatment strategies for uterine fibroids as well as for other desmoplastic tumors.

Given an annual health care cost exceeding $2.1 billion and the invasiveness of the procedure, hysterectomy may not be an ideal solution for the treatment of fibroids [2,29]. Furthermore, hysterectomy is not a compatible option for women of reproductive age who have not completed childbearing, as well as for patients suffering from other comorbidities, making them poor surgical candidates. Hormone therapy (gonadotropin-releasing hormone agonists) can show drastic effects by shrinking the fibroids after 3 months of treatment, but the fibroids can quickly return to pretreatment size when treatment is discontinued [30]. Furthermore, hormone therapy longer than 6 to 12 months is avoided to prevent bone loss [31]. Hormone therapy is able to function despite the barriers found in this research because the medications do not need to be delivered directly to the fibroid. Rather, they function by changing the hormonal balance of the environment that feeds the fibroids. It has been shown that fibroids within the same uterus can respond differently to their hormonal environment, with some shrinking and others growing in size [32]. This may be due to the presence of additional growth factors present within the fibroid tissue, which can influence their progression [33–35]. Thus, drug or gene therapies targeting growth factors that mediate fibroid growth may be a viable treatment alternative benefiting from this research on access and distribution barriers.

These results also describe some physiological features that relate to the clinical strategy of embolization. First, blood vessels inside fibroids appear to be very small and prone to embolization. Second, the normal myometrium contains larger vessels that are not as easily obstructed. If embolization occurs in the myometrium, anastomosis is a characteristic of uterine tissue and will allow collateral vessels to compensate for the blocked vessels [36]. Likewise, redundancy can exist in the blood supply to the fibroids and can result in failure of the embolization treatment [37].

As similarly reported by a group pioneering ex vivo uterine perfusion, we found that some uteri were more difficult to perfuse than others [38]. Physiologically occurring variations in uterine vasculature could make it difficult to locate the main arteries supplying the uterus. In some cases, anastomosis allowed the entire organ to be perfused even when some vessels were cauterized or otherwise occluded. The uteri that did not perfuse well, as indicated by lack of blood clearing and blue staining, were not included in the correlation analysis of methylene blue distribution. At times, specimen numbers were limited by the availability of tissue following routine medical diagnostics. However, some specimens contained multiple fibroids, each providing an independent sample. Despite the challenges in the model, the ability to study transport in human tissue containing naturally occurring benign tumors provided valuable and clinically relevant insights into factors that affect drug distribution.

The results from this research expand on our current understanding of transport barriers in desmoplastic tumors within their intact macro- and microenvironments. Jain et al. investigated the effects of reducing collagen content to reduce interstitial fluid pressure and improve perfusion in dense fibrotic tumors such as adenocarcinomas [39,40]. Collagenase and hyaluronidase have also been shown to improve transport of monoclonal antibodies and liposomes in human osteosarcoma xenografts [41,42]. Some tumors are more fibrotic than others and therefore our results and methods may be cautiously relevant to malignant tumors such as leiomyosarcomas, malignant fibrous histiocytomas, mesotheliomas, pancreatic adenocarcinomas, and desmoplastic small round cell tumors—all desmoplastic, solid tumors where drug delivery is limited by similar physiological barriers.

Our focus in this study was to better characterize the access a potential drug can have throughout tissues harboring tumorous growths. However, this model does have potential to study the efficacy of some treatment strategies. Testing some of the slower-acting treatment methods for overcoming transport barriers, such as ECM degradation by enzymes or inhibition of collagen synthesis by drugs such as Losartan in uterine fibroids, ex vivo perfusion might be required to reach a point where tissue viability can be maintained longer than 48 h. In vivo preoperative testing may be possible, but is limited by patient safety concerns. Additional alternatives could include hyperthermia treatment (to increase diffusivity), elevated vascular pressure (to overcome IFP), or penetrating peptides (to increase permeability)—all of which can be readily administered and observed within our model.

5. Conclusion

The ex vivo uterine perfusion model allowed us to perfuse entire, intact human organs with solid benign tumors present. Furthermore, this strategy enabled us to observe barriers to transport of staining molecules introduced via the vasculature and assess the tumor's macro- and microenvironments. Our findings include: limited staining inside the fibroid, limited intratumoral vasculature, high levels of intratumoral collagen, solid stress, and elevated IFP. These observations are considered clinically relevant to better understand why some similar solid tumors may have an ability to inertly impede drug therapy treatments. Limited access to and decreased diffusion inside solid tumors are difficult challenges currently hampering clinical treatment outcomes that need to be better understood for improved drug delivery. We plan to investigate treatment strategies seeking to overcome access barriers (currently being studied in other desmoplastic tumors) by applying them to the uterine perfusion model.

Acknowledgments

The authors would like to acknowledge the assistance from all in the Obstetrics and Gynecology Research Network at the University of Utah with special thanks to Marie Gibson (IRB, Compliance Manager). Additionally we would like to thank the Department of Pathology for their services in the gross room (Christian Horrocks in coordinating specimen retrieval and help from various pathologist's assistants in gross anatomical tissue examination) and histological staining of tissue sections (Biorepository and Molecular Pathology Shared Resource). We would also like to thank Dr. Yang Li for guidance in applying the CMP staining protocol to the uterine tissue sections and Dr. Michael Yu for the kind gift of the CMP stain. The project described in this article made use of REDCap—supported by the National Center for Research Resources and the National Center for Advancing Translational Sciences (National Institutes of Health) through grant 8UL1TR000105 (formerly UL1RR025764). Imaging was performed at the Fluorescence Microscopy Core Facility, a part of the Health Sciences Cores at the University of Utah. Microscopy equipment was obtained using a NCRR Shared Equipment Grant # 1S10RR024761-01. The project was also supported with resources from the University of Utah's Department of Obstetrics and Gynecology, Vice President of Research Office, and grants from the National Institutes of Health (CA101850 and CA122356) and the National Institute of Child Health and Human Development (F32HD085685).

References

[1] G.P. Flake, J. Andersen, D. Dixon, Etiology and pathogenesis of uterine leiomyomas: a review, Environ. Health Perspect. 111 (2003) 1037–1054 (http://www.pubmedcentral.nih.gov/articlerender.fcgi?artid=1241553&tool=pmcentrez&rendertype=abstract (accessed May 9, 2014)).
[2] NIH Fact Sheets — Uterine Fibroids, (2013). http://report.nih.gov/nihfactsheets/viewfactsheet.aspx?csid=50 (accessed March 5, 2015).
[3] L.A. Lepine, S.D. Hillis, P.A. Marchbanks, L.M. Koonin, B. Morrow, B.A. Kieke, et al., Hysterectomy surveillance—United States, 1980–1993, MMWR CDC Surveill.

Summ. 46 (1997) 1–15 (http://europepmc.org/abstract/MED/9259214 (accessed January 23, 2015)).
[4] R.L. Faulkner, The blood vessels of the myomatous uterus, Am. J. Obstet. Gynecol. 47 (1944) 185–197, http://dx.doi.org/10.5555/uri:pii:S000293784490253X.
[5] G. Farrer-Brown, J.O.W. Beilby, M.H. Tarbit, The vascular patterns in myomatous uteri, BJOG An Int. J. Obstet. Gynaecol. 77 (1970) 967–975, http://dx.doi.org/10.1111/j.1471-0528.1970.tb03439.x.
[6] A.G. Society, Transactions of the American Gynecological Society, http://books.google.com/books?id=hh04AQAAMAAJ1911.
[7] R. Casey, An immunohistochemical analysis of fibroid vasculature, Hum. Reprod. 15 (2000) 1469–1475 (http://humrep.oxfordjournals.org/cgi/content/abstract/15/7/1469 (accessed August 10, 2012)).
[8] A. Mayer, M. Höckel, A. Wree, C. Leo, L.-C. Horn, P. Vaupel, Lack of hypoxic response in uterine leiomyomas despite severe tissue hypoxia, Cancer Res. 68 (2008) 4719–4726, http://dx.doi.org/10.1158/0008-5472.CAN-07-6339.
[9] C. Bulletti, V.M. Jasonni, S. Lubicz, C. Flamigni, E. Gurpide, Extracorporeal perfusion of the human uterus, Am. J. Obstet. Gynecol. 154 (1986) 683–688 (http://www.ncbi.nlm.nih.gov/pubmed/3953718 (accessed February 26, 2013)).
[10] O. Richter, E. Wardelmann, F. Dombrowski, C. Schneider, R. Kiel, K. Wilhelm, et al., Extracorporeal perfusion of the human uterus as an experimental model in gynaecology and reproductive medicine, Hum. Reprod. 15 (2000) 1235–1240, http://dx.doi.org/10.1093/humrep/15.6.1235.
[11] J.A. Walocha, Vascular system of intramural leiomyomata revealed by corrosion casting and scanning electron microscopy, Hum. Reprod. 18 (2003) 1088–1093 (http://humrep.oxfordjournals.org/cgi/content/abstract/18/5/1088 (accessed August 13, 2012)).
[12] F.E. Hossler, J.E. Douglas, Vascular corrosion casting: review of advantages and limitations in the application of some simple quantitative methods, Microsc. Microanal. 7 (2001) 253–264, http://dx.doi.org/10.1017/S1431927601010261.
[13] E. Murase, E.S. Siegelman, E.K. Outwater, L.A. Perez-Jaffe, R.W. Tureck, Uterine leiomyomas: histopathologic features, MR imaging findings, differential diagnosis, and treatment, Radiographics 19 (1999) 1179–1197, http://dx.doi.org/10.1148/radiographics.19.5.g99se131179.
[14] J.W. Nichols, Y.H. Bae, EPR: evidence and fallacy, J. Control. Release (2014)http://dx.doi.org/10.1016/j.jconrel.2014.03.057.
[15] M.N. Wente, J. Kleeff, M.W. Büchler, J. Wanders, P. Cheverton, S. Langman, et al., DE-310, a macromolecular prodrug of the topoisomerase-I-inhibitor exatecan (DX-8951), in patients with operable solid tumors, Investig. New Drugs 23 (2005) 339–347 (http://www.ncbi.nlm.nih.gov/pubmed/16012793).
[16] D.L. Stirland, J.W. Nichols, S. Miura, Y.H. Bae, Mind the gap: a survey of how cancer drug carriers are susceptible to the gap between research and practice, J. Control. Release 172 (2013) 1045–1064.
[17] Y. Li, Y. Song, L. Zhao, G. Gaidosh, A.M. Laties, R. Wen, Direct labeling and visualization of blood vessels with lipophilic carbocyanine dye DiI, Nat. Protoc. 3 (2008) 1703–1708, http://dx.doi.org/10.1038/nprot.2008.172.
[18] Y. Li, D. Ho, H. Meng, T.R. Chan, B. An, H. Yu, et al., Direct detection of collagenous proteins by fluorescently labeled collagen mimetic peptides, Bioconjug. Chem. 24 (2013) 9–16, http://dx.doi.org/10.1021/bc3005842.
[19] C.-H. Heldin, K. Rubin, K. Pietras, A. Ostman, High interstitial fluid pressure — an obstacle in cancer therapy, Nat. Rev. Cancer 4 (2004) 806–813, http://dx.doi.org/10.1038/nrc1456.
[20] C.A. Schneider, W.S. Rasband, K.W. Eliceiri, NIH Image to ImageJ: 25 years of image analysis, Nat. Methods 9 (2012) 671–675, http://dx.doi.org/10.1038/nmeth.2089.
[21] L.J. Nugent, R.K. Jain, Extravascular diffusion in normal and neoplastic tissues, Cancer Res. 44 (1984) 238–244 (http://cancerres.aacrjournals.org/content/44/1/238.short (accessed February 19, 2015)).
[22] T. Stylianopoulos, J.D. Martin, M. Snuderl, F. Mpekris, S.R. Jain, R.K. Jain, Coevolution of solid stress and interstitial fluid pressure in tumors during progression: implications for vascular collapse, Cancer Res. 73 (2013) 3833–3841, http://dx.doi.org/10.1158/0008-5472.CAN-12-4521.
[23] G. Miserocchi, D. Negrini, A. Passi, G. De Luca, Development of lung edema: interstitial fluid dynamics and molecular structure, News Physiol. Sci. 16 (2001) 66–71 (http://physiologyonline.physiology.org/content/16/2/66 (accessed July 30, 2014)).
[24] R. Rogers, J. Norian, M. Malik, G. Christman, M. Abu-Asab, F. Chen, et al., Mechanical homeostasis is altered in uterine leiomyoma, Am. J. Obstet. Gynecol. 198 (474) (2008) e1–e11, http://dx.doi.org/10.1016/j.ajog.2007.11.057.
[25] M. Heine, B. Freund, P. Nielsen, C. Jung, R. Reimer, H. Hohenberg, et al., High interstitial fluid pressure is associated with low tumour penetration of diagnostic monoclonal antibodies applied for molecular imaging purposes, PLoS One 7 (2012) e36258, http://dx.doi.org/10.1371/journal.pone.0036258.
[26] Y. Boucher, L.T. Baxter, R.K. Jain, Interstitial pressure gradients in tissue-isolated and subcutaneous tumors: implications for therapy, Cancer Res. 50 (1990) 4478–4484 (http://cancerres.aacrjournals.org/content/50/15/4478.short (accessed July 29, 2014)).
[27] R.K. Jain, Transport of molecules in the tumor interstitium: a review, Cancer Res. 47 (1987) 3039–3051 (http://cancerres.aacrjournals.org/content/47/12/3039.short (accessed June 21, 2014)).
[28] L.T. Baxter, R.K. Jain, Transport of fluid and macromolecules in tumors. I. Role of interstitial pressure and convection, Microvasc. Res. 37 (1989) 77–104, http://dx.doi.org/10.1016/0026-2862(89)90074-5.
[29] C.L. Walker, E.A. Stewart, Uterine fibroids: the elephant in the room, Science 308 (2005) 1589–1592, http://dx.doi.org/10.1126/science.1112063.
[30] A.J. Friedman, D. Harrison-Atlas, R.L. Barbieri, B. Benacerraf, R. Gleason, I. Schiff, A randomized, placebo-controlled, double-blind study evaluating the efficacy of leuprolide acetate depot in the treatment of uterine leiomyomata, Fertil. Steril. 51 (1989) 251–256 (http://europepmc.org/abstract/med/2492232 (accessed February 8, 2015)).
[31] J.E. Compston, K. Yamaguchi, P.I. Croucher, N.J. Garrahan, P.C. Lindsay, R.W. Shaw, The effects of gonadotrophin-releasing hormone agonists on iliac crest cancellous bone structure in women with endometriosis, Bone 16 (1995) 261–267, http://dx.doi.org/10.1016/8756-3282(94)00038-2.
[32] S.D. Peddada, S.K. Laughlin, K. Miner, J.-P. Guyon, K. Haneke, H.L. Vahdat, et al., Growth of uterine leiomyomata among premenopausal black and white women, Proc. Natl. Acad. Sci. U. S. A. 105 (2008) 19887–19892, http://dx.doi.org/10.1073/pnas.0808188105.
[33] R. Tal, J.H. Segars, The role of angiogenic factors in fibroid pathogenesis: potential implications for future therapy, Hum. Reprod. Update 20 (2014) 194–216, http://dx.doi.org/10.1093/humupd/dmt042.
[34] S. Hague, L. Zhang, M.K. Oehler, S. Manek, I.Z. MacKenzie, R. Bicknell, et al., Expression of the hypoxically regulated angiogenic factor adrenomedullin correlates with uterine leiomyoma vascular density, Clin. Cancer Res. 6 (2000) 2808–2814 (http://clincancerres.aacrjournals.org/content/6/7/2808.abstract).
[35] R.S. Mangrulkar, Isolation and characterization of heparin-binding growth factors in human leiomyomas and normal myometrium, Biol. Reprod. 53 (1995) 636–646, http://dx.doi.org/10.1095/biolreprod53.3.636.
[36] J.P. Pelage, O. Le Dref, P. Soyer, D. Jacob, M. Kardache, H. Dahan, et al., Arterial anatomy of the female genital tract: variations and relevance to transcatheter embolization of the uterus, AJR Am. J. Roentgenol. 172 (1999) 989–994, http://dx.doi.org/10.2214/ajr.172.4.10587133.
[37] J.-P. Pelage, J. Cazejust, E. Pluot, O. Le Dref, A. Laurent, J.B. Spies, et al., Uterine fibroid vascularization and clinical relevance to uterine fibroid embolization, Radiographics 25 (Suppl. 1) (2005) S99–S117, http://dx.doi.org/10.1148/rg.25si055510.
[38] C. Bulletti, V.M. Jasonni, G. Martinelli, E. Govoni, S. Tabanelli, P.M. Ciotti, et al., A 48-hour preservation of an isolated human uterus: endometrial responses to sex steroids, Fertil. Steril. 47 (1987) 122–129 (http://www.ncbi.nlm.nih.gov/pubmed/3792566 (accessed January 17, 2013)).
[39] V.P. Chauhan, J.D. Martin, H. Liu, D.A. Lacorre, S.R. Jain, S.V. Kozin, et al., Angiotensin inhibition enhances drug delivery and potentiates chemotherapy by decompressing tumour blood vessels, Nat. Commun. 4 (2013) 2516, http://dx.doi.org/10.1038/ncomms3516.
[40] M.A. Jacobetz, D.S. Chan, A. Neesse, T.E. Bapiro, N. Cook, K.K. Frese, et al., Hyaluronan impairs vascular function and drug delivery in a mouse model of pancreatic cancer, Gut 62 (2013) 112–120, http://dx.doi.org/10.1136/gutjnl-2012-302529.
[41] L. Eikenes, Ø.S. Bruland, C. Brekken, C. de L. Davies, Collagenase increases the transcapillary pressure gradient and improves the uptake and distribution of monoclonal antibodies in human osteosarcoma xenografts, Cancer Res. 64 (2004) 4768–4773, http://dx.doi.org/10.1158/0008-5472.CAN-03-1472.
[42] L. Eikenes, M. Tari, I. Tufto, O.S. Bruland, C. de Lange Davies, Hyaluronidase induces a transcapillary pressure gradient and improves the distribution and uptake of liposomal doxorubicin (Caelyx) in human osteosarcoma xenografts, Br. J. Cancer 93 (2005) 81–88, http://dx.doi.org/10.1038/sj.bjc.6602626.

2.7 Supplementary Information

2.7.1 Image Resolution

The resolution defined in Fig. 2.4 applies to all figures in Chapter 2. Essentially, all scale bars in all figures and widths of images in call-outs (Fig. 2.5 B and Fig. 2.6 A) are 1000 μm. There is no defined scale for images taken with a hand-held digital camera (Fig. 2.2 A and B, Fig. 2.3 A and B, and Fig. 2.7 B and C).

2.7.2 Clarifications on methods

The needles used for IFP measurements were taken from the Insyte Autogaurd winged 24-gauge catheters (BD381512) used for cannulation. These needles have a side port (a notch cut on the side of needle near the tip) that can interface with the tissue in case the tip of the needle is clogged upon insertion. The tissue chunks (or excised tissue samples) were placed at the bottom of a cylinder with a water height of 5 cm to simulate an IFP that could prevent transport. A diagram for this is provided in Fig. 2.8.

2.7.3 Other corrections

Various instances of "psuedocolored" should be spelled "pseudocolored".

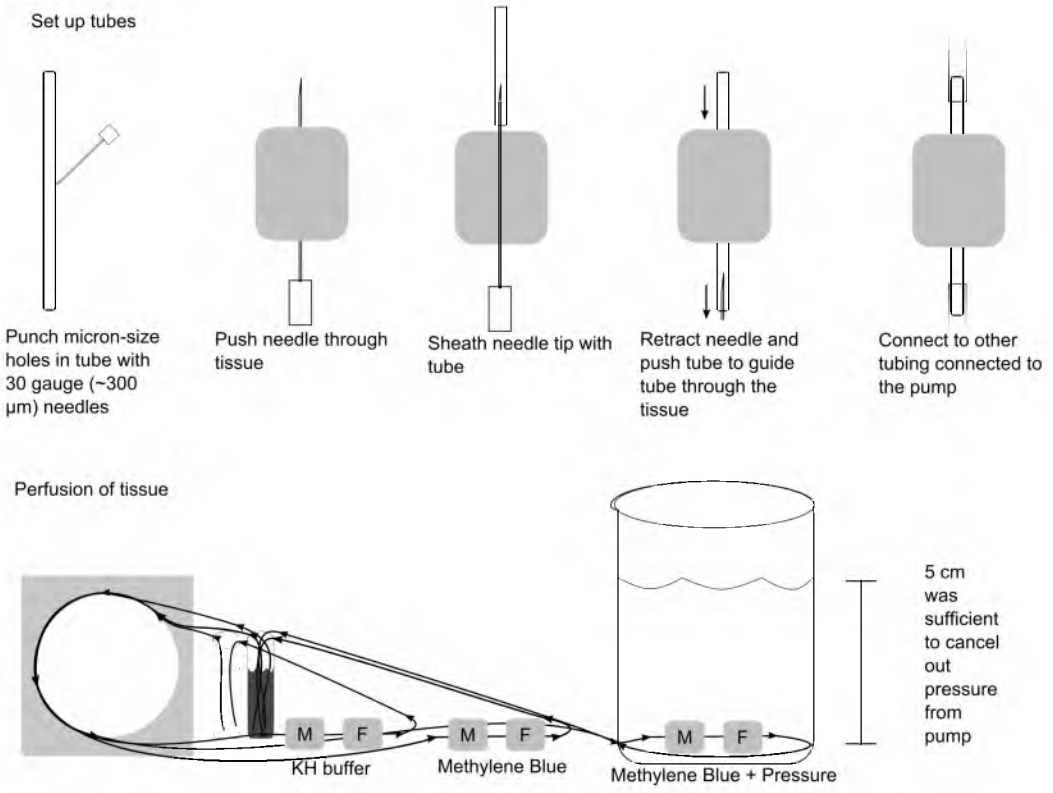

Figure 2.8. Supplementary: Diagram of methods for Fig. 2.7 B. The tubing was perforated to simulate extravasation potential. Staining of tissue via perfusion in an artificial environment of elevated IFP was observed and compared against buffer without stain and stain without pressure. "M" stands for myometrium tissue and "F" stands for fibroid tissue.

CHAPTER 3

ANALYZING SPATIOTEMPORAL DISTRIBUTION OF UNIQUELY FLUORESCENT NANOPARTICLES IN XENOGRAFT TUMORS

D. L. Stirland, Y. Matsumoto, K. Toh, K. Kataoka, and Y. H. Bae, Analyzing spatiotemporal distribution of uniquely fluorescent nanoparticles in xenograft tumors, J. Control. Release, vol. 227, pp. 3844, Apr. 2016. http://dx.doi.org/10.1016/j.jconrel.2016.02.016. Included with kind permission of Elsevier and the coauthors.

Journal of Controlled Release 227 (2016) 38–44

Contents lists available at ScienceDirect

Journal of Controlled Release

journal homepage: www.elsevier.com/locate/jconrel

Analyzing spatiotemporal distribution of uniquely fluorescent nanoparticles in xenograft tumors

Darren L. Stirland [a], Yu Matsumoto [b,c], Kazuko Toh [b], Kazunori Kataoka [d], You Han Bae [e,f,*]

[a] Department of Bioengineering, The University of Utah, United States
[b] Division of Clinical Biotechnology, Center for Disease Biology and Integrative Medicine, Graduate School of Medicine, The University of Tokyo, Japan
[c] Department of Otorhinolaryngology and Head and Neck Surgery, Graduate School of Medicine and Faculty of Medicine, The University of Tokyo, Japan
[d] Department of Bioengineering, Graduate School of Engineering, The University of Tokyo, Japan
[e] Department of Pharmaceutics and Pharmaceutical Chemistry, The University of Utah, United States
[f] Utah-Inha DDS and Advanced Therapeutics Research Center, Incheon, Republic of Korea

ARTICLE INFO

Article history:
Received 22 October 2015
Received in revised form 12 January 2016
Accepted 6 February 2016
Available online 9 February 2016

Keywords:
Solid tumors
Nanoparticles
Perfusion
Extravasation
Dynamic drug delivery

ABSTRACT

A dose circulating through the blood at one time will have different opportunities to access the tumor compared to a dose circulating hours later. Methods to test this hypothesis allowed us to differentiate two uniquely fluorescent doses of nanoparticles (administered as a mixture or sequentially) and to measure the distribution and correlation of these nanoparticle doses in three dimensions. Multiple colocalization analyses confirm that silica nanoparticles separated into different dose administrations will not accumulate in the same location. Decreased colocalization between separate doses implies dynamic extravasation events on the scale of microns. Further, the perfusion state of different blood vessels can change across the dosing period. Lastly, analyzing the distance traveled by these silica nanoparticles in two dimensions can be an overestimation when compared with three-dimensional distance analysis. Better understanding intratumoral distribution of delivered drugs will be crucial to overcoming the various barriers to transport in solid tumors.

© 2016 Elsevier B.V. All rights reserved.

1. Introduction

In the past few decades, nanoparticles have become popular tools to make inroads into treating cancerous tumors. Traditional chemotherapy causes widespread toxicity to the entire body in order to treat the cancer. Drug delivery via nanoparticles seeks to be a magic bullet that limits toxicity to the cancer. However, nanoparticles still must rely on passive delivery mechanisms. There are numerous barriers that stand in their way of treating the tumor. They pass through the blood circulation and encounter other organs or tissues where they may become sequestered by the mononuclear phagocyte system (MPS). Even when they encounter the tumor there are still more barriers that inhibit transport and delivery.

This research focuses on understanding distribution in the intratumoral environment. Many nanoparticle based treatments rely on the enhanced permeability and retention (EPR) of macromolecules in solid tumors, but more research needs to be done to test some of the assumptions. The way to access an inoperable solid tumor is via the vasculature. Often the vasculature of the tumor does not cover the entire tumor volume evenly. That limits access to certain parts of the tumor. Studies show that solid tumors often prevent the penetration of macromolecules far beyond the proximity of blood vessels [1–3]. Furthermore, the distribution of these extravasation locations appears to be heterogeneous within the tumor environment [3]. This is likely due to the remodeling of the vascular networks in a nutrient hungry tumor with increased angiogenesis.

The details of intratumoral distribution are still uncertain. Beyond the assumptions made related to accumulation via the EPR, it is difficult to predict how the drug dose will be distributed inside of the tumor environment. This research builds on research seeking to quantify drug distribution in the intratumoral environment. This research tests the hypothesis that these extravasation events are not only heterogeneous in location, but also dynamic in time. Specifically, we sought to explore how the drug distribution may change over time by differentiating an earlier dose from a later dose. Furthermore, we sought to glean additional information by observing the distribution of the two uniquely fluorescent doses in real-time with intravital microscopy. Finally, we hypothesized that calculating the distance to the nearest blood vessels would be different for two dimensions (2D) and three dimensions (3D).

As an analogy for the value of understanding accessibility changes over time, modern online maps with navigation suggestions allow us to select a day and time to see typical traffic patterns for the given conditions. It provides information on which routes are going to be blocked and which routes have access. If similar predictions for access to a tumor could be offered, this would be valuable information when delivering

* Corresponding author at: Department of Pharmaceutics and Pharmaceutical Chemistry, College of Pharmacy, University of Utah, Rm 2972, Skaggs Pharmacy Institute, 30S 2000E, Salt Lake City, Utah 84112, USA.
E-mail address: you.bae@utah.edu (Y.H. Bae).

http://dx.doi.org/10.1016/j.jconrel.2016.02.016
0168-3659/© 2016 Elsevier B.V. All rights reserved.

drug to a tumor given certain conditions. As we currently treat clinical tumors, the tumor mass can be reduced with delivered drugs; however, partially due to the limited delivery of drug to the entire tumor, the tumor will eventually resist treatment and grow back in a more aggressive state.

This research will help characterize EPR as it exists in the majority of tumors used in preclinical studies. For that reason, a xenograft mouse model is used. Perhaps by understanding EPR in this model, we might discover some flaws that explain why results do not always translate to the clinical setting.

2. Materials/methods

Red and green fluorescent silica nanoparticles were purchased from micromod (40-00-701 and 42-00-701, Rostock, Germany) and their sizes and surface charges were verified with dynamic light scattering and zeta potential measurements using a Malvern Zetasizer. Athymic nude mice (Simonsen Labs, Gilroy, CA) were injected subcutaneously with a 100 μL PBS solution (20% FBS) containing HeLa cells (7.5×10^6 cells) or HT29 cells (1.25×10^6 cells) in the rear flank to initiate tumor growth. When the tumor volume reached approximately 100 mm^3, the mice would receive tail vein injections of silica nanoparticle solutions at a concentration of 20 mg/kg for each dose. The red and green silica nanoparticles were either administered as a mixed solution or separately with varying intervals, ranging from 30 min to 12 h. Unless otherwise stated (two groups in SF3 and one mouse in Fig. 3C), the green silica nanoparticles were injected as the first dose followed by red silica nanoparticles as the second dose. Three hours after the final dose, the mice were sacrificed and 1,1′-Dioctadecyl-3,3,3′,3′-tetramethylindodicarbocyanine iodide (DiD) (84903, Anaspec, Fremont, CA) was introduced by cardiac perfusion to fluorescently stain the blood vessels. This vessel staining protocol was previously found to be adequate in staining even the small vessels of densely packed human fibroid tissue [4]. Following perfusion, the liver and tumor tissues were collected and placed in Optimal Cutting Temperature compound for at least 5 min before flash freezing with isopentane in a metal beaker cooled by liquid nitrogen. Samples were stored at −80 °C until sectioning with a cryotome at a thickness of 100 μm for mounting on microscopy slides. As all probes and stains were introduced before harvesting tissues, no further staining was required and this also facilitated acquisition for 3D image stacks. A Nikon A1 confocal microscope with a motorized stage automated the process of acquiring 3D Z stacks and stitched mosaics of the entire tissue section. Sequential imaging was performed to isolate each fluorescent signal: green silica nanoparticles were excited at 488 nm, red silica nanoparticles at 561 nm, and the DiD stain at 638 nm. The acquired images were then processed in batches with custom MATLAB code to determine the distribution and colocalization of the multiple doses.

Binary images were created by applying a threshold to the images. A distance map was created from the binary blood vessel image. The pixel values in the distance map gave the Euclidean distance from that pixel to the nearest blood vessel (in 2D or 3D). This distance map was multiplied by the binary image for the nanoparticle signal to assign distance values for each pixel representing nanoparticles. The code also assigned primary colors and unique values to each binary channel to facilitate qualitative observation and quantitative summation of overlapped or unique pixels.

The percent overlap provides the simplest and most intuitive measure for colocalization of the two signals by showing the overlap of detected signal objects relative to the total signal from either the first or second dose of silica nanoparticles.

$$1\text{st Dose } \% \text{ overlap} = \frac{\sum \text{Rt} \cap \text{Gt}}{\sum \text{Gt}} \times 100$$

$$2\text{nd Dose } \% \text{ overlap} = \frac{\sum \text{Rt} \cap \text{Gt}}{\sum \text{Rt}} \times 100$$

where *Gt* and *Rt* represent the thresholded binary values of signal coming from the green and red silica nanoparticles, respectively, for each pixel. The intravital images were only analyzed for percent overlap to simply show whether or not the signal was there and overlapping.

The end-point analysis of extravasated silica nanoparticles used Pearson's and Mander's coefficient values to look at more than just binary presence of the signal, but also at the intensity (or concentration) correlation which was present. The colocalization analysis by these means was more robust even if the signal was dim or had background noise [5,6]. These further colocalization analyses were performed by first creating a mask or region of interest based on the thresholded silica nanoparticle images. With the region of interest defined, the original, non-thresholded images were used to calculate the correlation between green and red signals. Defining a region of interest for colocalization analysis eliminated the large areas of background containing common blackness or random signal noise which could erroneously increase or decrease, respectively, the correlation value.

The Mander's value describes the fraction of overlap from the two signals' intensities.

$$\text{Mander's} = \frac{\sum_i \text{R}_i \cdot \text{G}_i}{\sum_i \text{Ri}^2 \cdot \sum_i \text{Gi}^2}$$

where *Ri* and *Gi* represent the intensities for red and green signal, respectively, in each pixel. The equation for Pearson's value subtracts the average value for red or green (R_{avg} or G_{avg}) and provides information on the covariance of the two signals: if the two signals tend to increase together the value is closer to 1.

$$\text{Pearson's} = \frac{\sum_i \left(\left(\text{R}_i - \text{R}_{avg}\right) \left(\text{G}_i - \text{G}_{avg}\right) \right)}{\sqrt{\sum_i \left(\text{R}_i - \text{R}_{avg}\right)^2 \cdot \sum_i \left(\text{G}_i - \text{G}_{avg}\right)^2}}$$

Furthermore, this subtraction allows for a value as low as −1 which indicates that one signal tends to increase while the other decreases.

Multiple areas from numerous Z stacks were analyzed for correlation between the nanoparticle signals. A p value was produced by the built in MATLAB corrcoef function to represent the chances of getting the same correlation by random chance. Only images with a p value less than 0.05 were included in the averages. The MATLAB code generated both Pearson's and Mander's values describing the colocalization of the two silica nanoparticle signals. Finally, these values were averaged for the groups of mice and statistical significance of the separately dosed mice having a lower value was calculated with a Student's t-test.

Intravital imaging was performed using a Nikon A1R confocal laser scanning microscope system attached to an upright ECLIPSE Ni-E equipped with a CFI Plan Apo Lambda 20× objective. The blood circulation half-lives of the two colors of silica nanoparticles were determined by checking the fluorescence intensity in the blood vessels of the earlobe of mice using the microscopy methods described in previously published work [7]. To prepare the tumor bearing mice, 6–8 week old female BALB/c nu/nu mice (Charles River Laboratories Japan, Inc., Kanagawa, Japan) were subcutaneously inoculated with murine colon carcinoma C26 cells (American Type Culture Collection, Manassas, VA, USA). Mice were anesthetized and maintained with 1.0–1.5% isoflurane onto a stage-top temperature-controlled pad calibrated at 37 °C. The tumor was imaged as 6 dimensions composed of XY Large Scan (using a motorized stage), Z stack (10 μm thickness, three slices), Time-Lapse (10 min interval), and 2 Channels (green and red). Two mice were administered with green silica nanoparticles 10 min after the imaging

was initiated. After 2 h, the red silica nanoparticles were administered. The order was switched for one mouse as a control.

3. Results/discussion

The silica nanoparticle batches of different colors were characterized and it was confirmed that both have a hydrodynamic diameter of about 73 nm, a strong negative surface charge, and half-life in the blood of about 30 min (SF1).

We chose simple, inorganic, fluorescent nanoparticles because the characteristics could be controlled and verified to be nearly identical. Although it is anticipated that protein adhesion and aggregation will occur upon entering the body (like any nanoparticle), degradation into smaller particles was not a concern as the in vivo experiments lasted no longer than a day and significant degradation of non-porous silica nanoparticles takes longer than a week [8,9].

Two uniquely fluorescent doses of silica nanoparticles were administered either as a mixed dose or separately at varying intervals for temporal analysis. When the two uniquely fluorescent silica nanoparticles are administered separately, the two colors can be distinguished with some non-overlapping signal. Fig. 1 shows qualitative and quantitative differences in colocalization between mixed and separate doses for representative images in liver and tumor tissue.

The two fluorescent signals were analyzed for colocalization in the tumor environment and compared with values from the liver as a positive control. The liver was chosen as it has more reliable silica nanoparticle accumulation and a better signal/noise ratio. The better signal to noise ratio, the more consistent the correlation was. This accumulation in the liver is characteristic of hepatic circulation from tail vein administration [10]. Notoriously leaky vessels in the sinusoids allow for high accumulation of nanoparticles and the Kupffer cells in the liver could phagocytose the nanoparticles into concentrated, bright bundles. As a comparison for showing dynamic events, the phagocytosis is clearly not a static event and the dynamic leakiness of liver sinusoids has been summarized in a review article [11]. When the two doses were mixed together and then administered, there was a high percentage of signal overlap in both the tumor and liver tissue. However, the lower percentages of signal overlap for separately administered doses suggest dynamics in both the liver and tumor environments.

The overlap analysis in Fig. 2A merely shows a trend supporting the hypothesis that separate doses will have decreased colocalization. Unlike Fig. 1, the data in Fig. 2 only includes images of tumor tissue where the signal was weaker and not as consistent. Simple overlap analysis is not as robust for the weak nanoparticle signal outside of the blood vessel in the tumor tissue where there is also more background noise. A noteworthy difference is that the 2nd dose signal had a better signal to noise ratio and the data was significant. In contrast, the 1st dose appeared more diffuse and weak. Quantifying the colocalization with additional, more sophisticated, colocalization techniques found a statistical difference when comparing the Pearson's and Mander's values for mixed and separate doses in the tumor (Fig. 2B).

Correlation analysis for various dosing intervals sought to identify a spectrum of temporal dynamics in the tumor environment. Unfortunately, we were not able to discern significant differences between the various dosing intervals, but merely the difference between mixed and separate doses. The analysis may result in false negatives for dynamic extravasation or false positives for colocalization (it is unable to resolve two different nanoparticles that are spaced only 100 nm apart). The point spread function for the Nikon A1 microscope used for these experiments gives a theoretical resolution of 147 nm along the X and Y axis and 368 nm along the Z axis in ideal conditions. Furthermore, the 3D image acquisition with certain step sizes effectively set the resolution as low as 5 μm along the Z axis. Other processing techniques, such as thresholding for distance or object overlap analysis, further reduced the resolution. Explorative calculations based on regions of interest determined by thresholds generally only varied by 10 μm. Thus, the figures of merit for this approach put our resolution near 5 to 10 μm. This allows for detection of dynamic extravasation events from blood vessels (as a result of remodeling) that are at least 50 μm (length of endothelial cell) apart from each other. Thus, we could still determine whether dynamic extravasation events occurred in intratumoral drug delivery. To observe dynamics on a larger scale, intravital microscopy was performed with a purpose of verifying and teasing out additional results.

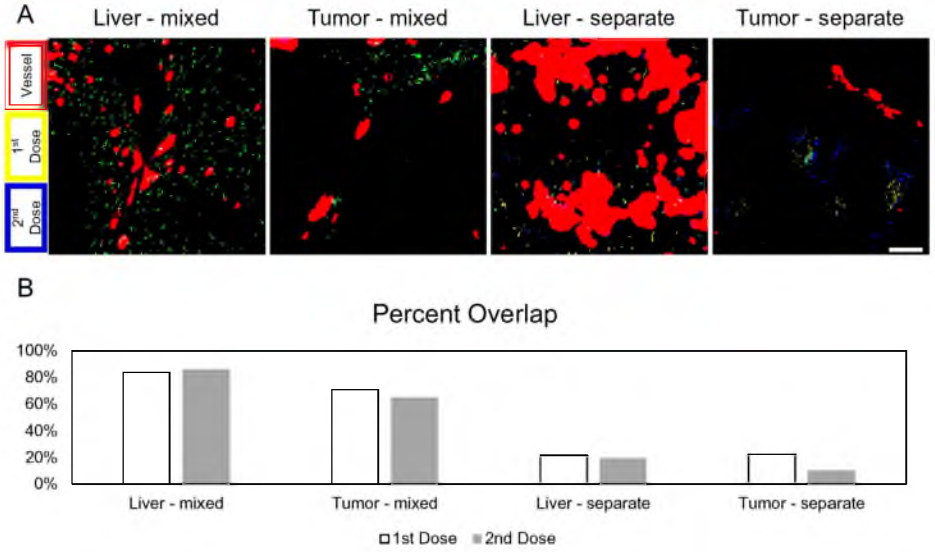

Fig. 1. Representative images of the fluorescent signals from two silica nanoparticle doses in liver and tumor tissues. A) The example images are thresholded to show high-contrast images of the signals for blood vessel (red), 1st dose (yellow), and 2nd dose (blue). Furthermore, secondary colors represent overlapping signal (e.g., green for overlap of the two dose signals). Scale bar is 100 μm and applies to all images. B) The example images were quantified for the percent overlap of each dose. (For interpretation of the references to color in this figure legend, the reader is referred to the online version of this chapter.)

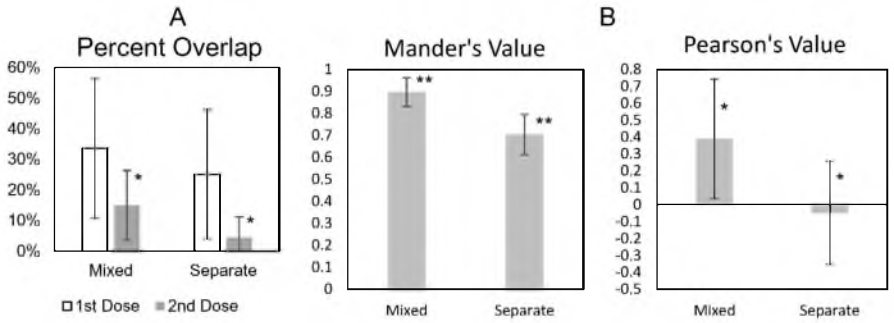

Fig. 2. Colocalization analysis of silica nanoparticle doses in tumor tissues. Error bars are standard deviation. * $p < 0.05$. ** $p < 0.01$. A) Average values for percent overlap analysis for a larger data set of 10 different mice: 4 with mixed doses and 6 with separate doses. B) Average Mander's and Pearson's values for 24 different mice: 4 with a mixed dose and 20 separately dosed.

Real-time intravital microscopy showed strong signals for the fluorescent nanoparticles in the blood vessels (Fig. 3). Analysis of the fluorescent signals through the perfused vessels suggests dynamics in entire blood vessels within the tumors. Overlap analysis demonstrates that a dose can have as much as 98% or as little as 34% of its perfusion overlapped with the other dose. Some vessels maintained high signal levels for both doses and showed high overlap. Other vessels showed strong signals, only to fade with blood clearance of the nanoparticles. Finally, some vessels appeared to only show signal for one of the two doses (often the first dose). Averaging the 3 mice, the first dose had more unique signal locations and the second dose had a higher percentage of signal overlap. Image C of Fig. 3 appears to be an exception to this, but further inspection reveals that the two doses perfuse through many of the same vessels (Fig. 4). Due to the blood circulation half-life being shorter than the administration interval, the overlap of signal in these vessels was low. This implies that the majority of dynamics (on this time scale) results in blood vessels closing off and preventing access for the second dose. The trend of high overlap for the second dose was not observed in the end-point analysis of extravasation into the tumor tissue. In that case, the second dose can continue to have low overlap due to dynamic extravasation events beyond dynamic perfusion events. Dynamic extravasation and perfusion events are each on a different spatial scale which greatly affects determination of colocalization.

The spatial analysis (presented qualitatively and quantitatively in Fig. 5) found that measuring the distance of extravasated nanoparticles from the blood vessel in only 2D often overestimates the distance traveled. This can be seen qualitatively when comparing the 2D and 3D distance maps. The 3D distance map shows a similar pattern for all slices of the Z stack because blood vessels in one slice influence the distance map in slices above or below. For our collection of images, we found that the average overestimation of distance traveled by 2D measurements compared to 3D was about 25 μm. The distance measurements in 2D had a large spread of values when comparing the different Z stacks of a given tissue volume. If investigators were to analyze a 2D slice from region 4 in Fig. 5C, there is the potential to overestimate the distance by about 150 μm in that case. Three regions of negative control result in very low distances as would be expected when no nanoparticles are administered, but one had some speckles of background noise or non-specific staining that was included in the distance analysis. Other regions had low distance values simply because some tumor regions had stronger signal from silica nanoparticles than others.

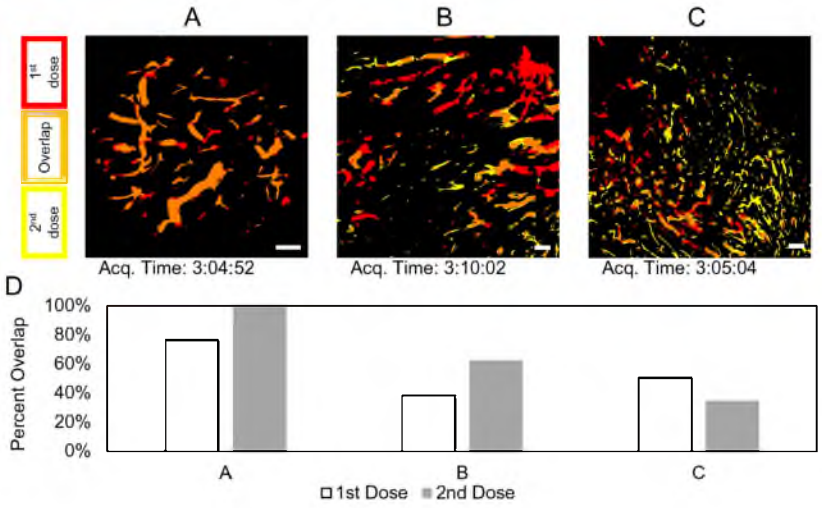

Fig. 3. Thresholded images from intravital microscopy for three different mice (A, B, C) showing blood vessels perfused with silica nanoparticles. For (A and B), the green silica nanoparticles were administered first; then after 2 h, the red silica nanoparticles were administered. The order of administration was reversed for (C). Scale bars are each 200 μm. D) Overlap analysis of the respective images. (For interpretation of the references to color in this figure legend, the reader is referred to the online version of this chapter.)

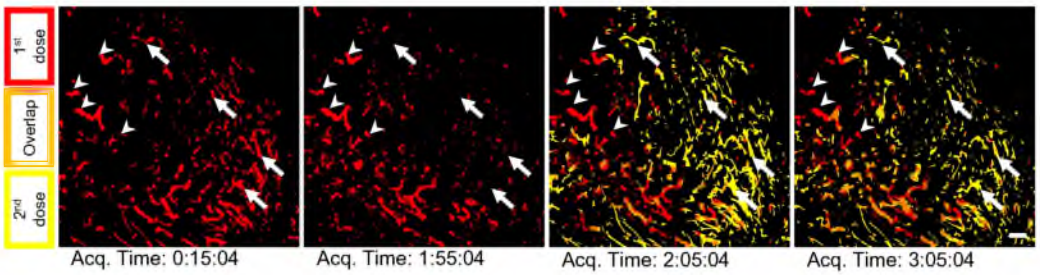

Fig. 4. Additional images for Fig. 3C: right after the first dose, right before and after the second dose, and near the end of the perfusion period. Some regions (a selection marked with arrows) appear to be unique perfusion events, but instead they are just transient perfusion events for both doses such that there is little to no overlap at a given time. In other words, the areas designated by the arrows are reached by both doses but not at the same time. Other areas (a selection marked with arrowheads) appear to be only accessed by a single dose for the entire perfusion period. Scale bar is 200 μm.

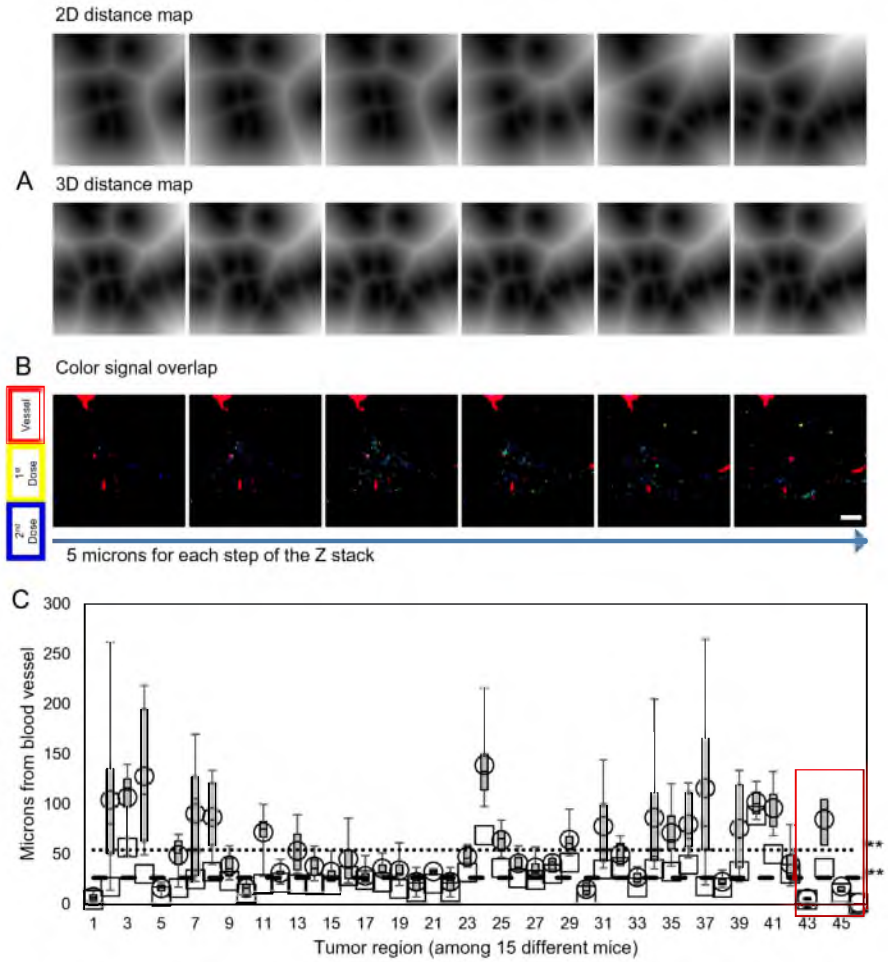

Fig. 5. Overestimation of distance traveled by 2D measurements. A) Comparison of MATLAB generated distance maps for 2D and 3D analysis. Increased brightness signifies increased distance from the blood vessel. B) Image slices are thresholded to show high-contrast images of the signals for blood vessel (red), 1st dose (yellow), and 2nd dose (blue). Secondary colors represent overlapping signal. Scale bar is 100 μm and applies to all images. C) Selection of different tumor regions (and different mice) showing how the distance traveled is overestimated when measuring in 2D versus 3D. The box plots represent the spread of 2D distance values for each tumor region. Clearly, there can be multiple 2D distance values (one for each 2D image slice through the volume of each tumor region). The open circles represent the average of all the 2D distance values for each region. The open squares represent the 3D distance values for each region. The dotted and dashed line represent the average 2D and 3D, respectively, distance value for all the different tumor regions. The red rectangle encloses the data points from negative controls. ** $p < 0.01$. (For interpretation of the references to color in this figure legend, the reader is referred to the online version of this chapter.)

The overestimation in distance traveled occurs as most 2D methods cannot include any possible vessels above or below the frame of interest. However, even with imaging tissue sections in 3D, there is still the chance for slight overestimation of distance traveled as there may be a vessel just beyond the tissue section being imaged. It is possible to image all sections of the entire tumor; however, the increase in accuracy is likely not proportional to the increase in required resources. Similarly, some meaningful trends can still be observed with 2D distance analysis. Still, given the ease of obtaining 3D stacks with confocal microscopes, we recommend distance measurements be performed in 3D when possible for increased accuracy.

Calculating distance between vessel and nanoparticle objects identified by thresholding relies heavily on the threshold value chosen. Thresholding can shift the mean distance from the nearest blood vessel, but two things will remain: the 2D distance measurement will be greater than the 3D measurement and the 2D measurement will have greater variability. Finally, it is possible that the DiD stain introduced via cardiac perfusion may not stain all blood vessels. The high interstitial fluid pressure may cause some blood vessels to collapse or have limited perfusion. We chose to measure distances from perfused vessels because we were not interested in measuring distances from occluded vessels, from which the particles likely did not extravasate from. With our results confirming dynamic perfusion of blood vessels, it becomes more challenging to know from which blood vessels you should measure the distance traveled.

Researchers are looking into the effect of size and shape on extravasation and penetration into the tumor environment [12–14]. Generally, the smaller particles have higher permeability and diffuse more rapidly in tumors [15]. Future experiments could investigate whether different sizes could be susceptible to different extravasation events (from the cellular level with fenestrae and intercellular gaps to larger events resulting in blood lakes or when vessels change their perfusion state) and thus be sensitive to different dynamics relating to colocalization [16]. Analyzing different sizes is also relatable to determining how aggregated particles are influenced by the dynamics. We have already built computer models to understand how extravasation events occur [17]. We will continue to develop these and other numerical models to test various parameters. Future experiments will also need to test the effects of pro or anti-angiogenic factors on the dynamic leakiness of these tumor blood vessels. These experiments should determine the cause of the dynamics at the different levels and whether the multiple doses have a direct effect on each other via saturation or blocking effects. It is possible that vessels could become embolized from aggregated nanoparticles and new perfusion events could occur from sprouting vessels. On the other hand, solid stress inside the tumor could play a role in the opening and closing of vessels. It is known that tumors can cause lymph and blood vessels to collapse, but treatments can reverse this and increase the number of patent vessels [18,19]. Even without therapeutic intervention, Debbage et al. previously showed dynamic perfusion using lectin stains [20]. The results herein confirm that phenomenon using fluorescent nanoparticles in the blood circulation. We further showed how dynamics influence the extravasation of the doses to different locations in the interstitial space. Understanding these dynamics will educate how access to the tumor via the vasculature can be in an open or closed state.

Knowing how access to the tumor may change over time may influence planning of dosing schedules and combinatorial strategies in the clinical setting. With a lower fraction of unique perfusion for the second dose 2 h after the first, long circulation may not be beneficial in all aspects. A relevant clinical trial showed that filtering liposomal doxorubicin 24 h after administration reduced side effects yet did not discern a change in efficacy [21]. The authors speculate that the tumor tissue had become saturated and all other drug particles circulating were likely to cause toxicity in healthy tissue. This is backed up by the fact that the non-PEGylated version of Doxil (Myocet) has a lower occurrence of palmar plantar erythrodysesthesia syndrome [22,23]. Clinical dosing schedules are often around 2 weeks apart. The dosing schedule is primary limited by the toxicity of treatment, but this is much longer than the half-life of the drugs administered. Thus, each dosing may have different access to the tumor. Many first line cancer therapies involve combinations of drugs to improve efficacy and limit resistance. The efficacy of concurrent versus sequential administrations has been studied in cells, xenografts in mice, and even in patients. Though not conclusive, concurrent therapy tends to be more favorable than sequential [24–28]. In addition to cell cycles, dynamics in vascular access may be a contributing factor in these studies. Concurrent therapy is more likely to deliver the combinatorial drugs to the same location in the tumor and allow synergistic benefits. Newer drug carrier formulations are considering whether it is better to combine two drugs into one carrier as opposed to having each drug in separate carriers [29]. Some clinicians may prefer the control afforded by having each drug in separate carriers. This would allow different release rates for each carrier and the ability to modify drug ratios by adjusting the carrier weight ratios. However, until more details on dynamic extravasation events over time and dynamic perfusion events of vessel segments within the tumor can be elucidated, a single carrier housing both drugs best ensures they reach the same locations (at the ratios intended) in the tumor.

4. Conclusion

While dynamic perfusion and extravasation events have been shown in animal tumors that grow faster with chaotic vasculature, similar experiments need to probe clinical tumors for similar dynamics. Targeting the tumor environment through EPR is passive delivery and relying on passive delivery in the complex tumor environment appears to be inconsistent—especially in clinical applications [30]. Perhaps nanoparticle characteristics can be tuned to provide a way to mitigate the dynamic events observed in the chaotic tumor environment. Alternatively, methods of altering the tumor environment (via the vasculature or other contributors to pressure) may prove to be necessary to return the tumor environment to a more predictable and consistent state for delivering multiple doses.

Acknowledgments

End-point microscopy imaging was performed at the University of Utah's Fluorescence Microscopy Core Facility, a part of the Health Sciences Cores at the University of Utah. Microscopy equipment was obtained using a NCRR Shared Equipment Grant # 1S10RR024761-01. The project was also supported with grants from the National Institutes of Health: CA101850 and CA122356.

Intravital microscopy imaging was performed at the University of Tokyo. The equipment was obtained and supported using the CREST and COI Program from Japan Science and Technology, the FIRST Program from the Japan Society for the Promotion of Science, and KAKENHI Grant Numbers 2379004 (YM), 15K06871 (KT), and 25000006 (KK) from the Japanese Ministry of Education, Culture, Sports, Science and Technology.

Appendix A. Supplementary data

Supplementary material in a PowerPoint file is provided for additional figures and video. The figures show data characterizing the silica nanoparticles, the original (non-thresholded) versions of the example images shown in Fig. 1, more comprehensive graphs for Mander's and Pearson's values showing the different experimental groups (varying intervals for separately dosed administrations), and an additional set of images from different time points for Fig. 3B analyzing transiently overlapped and unique perfusion events. The videos are the intravital imaging data. This material is available via the Internet. Supplementary

data associated with this article can be found in the online version, at http://dx.doi.org/10.1016/j.jconrel.2016.02.016.

References

[1] M.R. Dreher, W. Liu, C.R. Michelich, M.W. Dewhirst, F. Yuan, A. Chilkoti, Tumor vascular permeability, accumulation, and penetration of macromolecular drug carriers, J. Natl. Cancer Inst. 98 (2006) 335–344.

[2] A.J. Primeau, A. Rendon, D. Hedley, L. Lilge, I.F. Tannock, The distribution of the anticancer drug Doxorubicin in relation to blood vessels in solid tumors, Clin. Cancer Res. 11 (2005) 8782–8788, http://dx.doi.org/10.1158/1078-0432.CCR-05-1664.

[3] F. Yuan, M. Leunig, S.K. Huang, D.A. Berk, D. Papahadjopoulos, R.K. Jain, Microvascular permeability and interstitial penetration of sterically stabilized (stealth) liposomes in a human tumor xenograft, Cancer Res. 54 (1994) 3352–3356.

[4] D.L. Stirland, J.W. Nichols, E. Jarboe, M. Adelman, M. Dassel, M.-M. Janát-Amsbury, et al., Uterine perfusion model for analyzing barriers to transport in fibroids, J. Control. Release 214 (2015) 85–93, http://dx.doi.org/10.1016/j.jconrel.2015.07.006.

[5] K.W. Dunn, M.M. Kamocka, J.H. McDonald, A practical guide to evaluating colocalization in biological microscopy, AJP Cell Physiol. 300 (2011) C723–C742, http://dx.doi.org/10.1152/ajpcell.00462.2010.

[6] E.M.M. Manders, F.J. Verbeek, J.A. Aten, Measurement of co-localization of objects in dual-colour confocal images, J. Microsc. 169 (1993) 375–382, http://dx.doi.org/10.1111/j.1365-2818.1993.tb03313.x.

[7] T. Nomoto, Y. Matsumoto, K. Miyata, M. Oba, S. Fukushima, N. Nishiyama, et al., In situ quantitative monitoring of polyplexes and polyplex micelles in the blood circulation using intravital real-time confocal laser scanning microscopy, J. Control. Release 151 (2011) 104–109, http://dx.doi.org/10.1016/j.jconrel.2011.02.011.

[8] H. Yamada, C. Urata, Y. Aoyama, S. Osada, Y. Yamauchi, K. Kuroda, Preparation of colloidal mesoporous silica nanoparticles with different diameters and their unique degradation behavior in static aqueous systems, Chem. Mater. 24 (2012) 1462–1471, http://dx.doi.org/10.1021/cm3001688.

[9] J.-H. Park, L. Gu, G. von Maltzahn, E. Ruoslahti, S.N. Bhatia, M.J. Sailor, Biodegradable luminescent porous silicon nanoparticles for in vivo applications, Nat. Mater. 8 (2009) 331–336, http://dx.doi.org/10.1038/nmat2398.

[10] L. Yildirimer, N.T.K. Thanh, M. Loizidou, A.M. Seifalian, Toxicology and clinical potential of nanoparticles, Nano Today 6 (2011) 585–607, http://dx.doi.org/10.1016/j.nantod.2011.10.001.

[11] F. Braet, E. Wisse, Structural and functional aspects of liver sinusoidal endothelial cell fenestrae: a review, Comp. Hepatol. 1 (2002) 1 (http://www.pubmedcentral.nih.gov/articlerender.fcgi?artid=131011&tool=pmcentrez&rendertype=abstract (accessed October 30, 2013)).

[12] B.R. Smith, P. Kempen, D. Bouley, A. Xu, Z. Liu, N. Melosh, et al., Shape matters: intravital microscopy reveals surprising geometrical dependence for nanoparticles in tumor models of extravasation, Nano Lett. 12 (2012) 3369–3377, http://dx.doi.org/10.1021/nl204175t (accessed August 16, 2012).

[13] H. Cabral, Y. Matsumoto, K. Mizuno, Q. Chen, M. Murakami, M. Kimura, et al., Accumulation of sub-100 nm polymeric micelles in poorly permeable tumours depends on size, Nat. Nanotechnol. 6 (2011) 815–823, http://dx.doi.org/10.1038/nnano.2011.166.

[14] S.D. Perrault, C. Walkey, T. Jennings, H.C. Fischer, W.C.W. Chan, Mediating tumor targeting efficiency of nanoparticles through design, Nano Lett. 9 (2009) 1909–1915, http://dx.doi.org/10.1021/nl900031y.

[15] R.K. Jain, T. Stylianopoulos, Delivering nanomedicine to solid tumors, Nat. Rev. Clin. Oncol. 7 (2010) 653–664, http://dx.doi.org/10.1038/nrclinonc.2010.139.

[16] H. Hashizume, P. Baluk, S. Morikawa, J.W. McLean, G. Thurston, S. Roberge, et al., Openings between defective endothelial cells explain tumor vessel leakiness, Am. J. Pathol. 156 (2000) 1363–1380.

[17] Y. Matsumoto, J. Nichols, K. Toh, T. Nomoto, H. Cabral, Y. Miura, et al., Vascular bursts enhance permeability of tumour blood vessels and improve nanoparticle delivery, Nat. Nanotechnol. http://dx.doi.org/10.1038/nnano.2015.342 (in press).

[18] T.P. Padera, B.R. Stoll, J.B. Tooredman, D. Capen, E. di Tomaso, R.K. Jain, Pathology: cancer cells compress intratumour vessels, Nat. Commun. 427 (2004) 695.

[19] V.P. Chauhan, J.D. Martin, H. Liu, D.A. Lacorre, S.R. Jain, S.V. Kozin, et al., Angiotensin inhibition enhances drug delivery and potentiates chemotherapy by decompressing tumour blood vessels, Nat. Commun. 4 (2013) 2516, http://dx.doi.org/10.1038/ncomms3516.

[20] P.L. Debbage, J. Griebel, M. Ried, T. Gneiting, A. DeVries, P. Hutzler, Lectin intravital perfusion studies in tumor-bearing mice: micrometer-resolution, wide-area mapping of microvascular labeling, distinguishing efficiently and inefficiently perfused microregions in the tumor, J. Histochem. Cytochem. 46 (1998) 627–639, http://dx.doi.org/10.1177/002215549804600508.

[21] J. Eckes, O. Schmah, J.W. Siebers, U. Groh, S. Zschiedrich, B. Rautenberg, et al., Kinetic targeting of pegylated liposomal doxorubicin: a new approach to reduce toxicity during chemotherapy (CARL-trial), BMC Cancer 11 (2011) 337 (http://www.biomedcentral.com/1471-2407/11/337 (accessed August 10, 2012)).

[22] C.E. Swenson, L.E. Bolcsak, G. Batist, T.H.J. Guthrie, K.H. Tkaczuk, H. Boxenbaum, et al., Pharmacokinetics of doxorubicin administered i.v. as Myocet (TLC D-99; liposome-encapsulated doxorubicin citrate) compared with conventional doxorubicin when given in combination with cyclophosphamide in patients with metastatic breast cancer, Anticancer. Drugs 14 (2003) (http://journals.lww.com/anti-cancerdrugs/Fulltext/2003/03000/Pharmacokinetics_of_doxorubicin_administered_i_v_.8.aspx).

[23] G. Batist, Cardiac safety of liposomal anthracyclines, Cardiovasc. Toxicol. 7 (2007) 72–74, http://dx.doi.org/10.1007/s12012-007-0014-4.

[24] F. Cavalli, M. Beer, G. Martz, W.F. Jungi, P. Alberto, J.P. Obrecht, et al., Concurrent or sequential use of cytotoxic chemotherapy and hormone treatment in advanced breast cancer: report of the Swiss Group for Clinical Cancer Research, BMJ 286 (1983) 5–8, http://dx.doi.org/10.1136/bmj.286.6358.5.

[25] P. Francis, J. Crown, A. Di Leo, M. Buyse, A. Balil, M. Andersson, et al., Adjuvant chemotherapy with sequential or concurrent anthracycline and docetaxel: Breast International Group 02-98 randomized trial, J. Natl. Cancer Inst. 100 (2008) 121–133, http://dx.doi.org/10.1093/jnci/djm287.

[26] A.S. Fung, L. Wu, I.F. Tannock, Concurrent and sequential administration of chemotherapy and the Mammalian target of rapamycin inhibitor temsirolimus in human cancer cells and xenografts, Clin. Cancer Res. 15 (2009) 5389–5395, http://dx.doi.org/10.1158/1078-0432.CCR-08-3007.

[27] M.L. Citron, D.A. Berry, C. Cirrincione, C. Hudis, E.P. Winer, W.J. Gradishar, et al., Randomized trial of dose-dense versus conventionally scheduled and sequential versus concurrent combination chemotherapy as postoperative adjuvant treatment of node-positive primary breast cancer: first report of Intergroup Trial C9741/Cancer and Leukemia, J. Clin. Oncol. 21 (2003) 1431–1439, http://dx.doi.org/10.1200/JCO.2003.09.081.

[28] P. Fournel, G. Robinet, P. Thomas, P.-J. Souquet, H. Léna, A. Vergnenègre, et al., Randomized phase III trial of sequential chemoradiotherapy compared with concurrent chemoradiotherapy in locally advanced non-small-cell lung cancer: Groupe Lyon-Saint-Etienne d'Oncologie Thoracique-Groupe Français de Pneumo-Cancérologie NPC 95-01 Study, J. Clin. Oncol. 23 (2005) 5910–5917, http://dx.doi.org/10.1200/JCO.2005.03.070.

[29] Y. Bae, T.A. Diezi, A. Zhao, G.S. Kwon, Mixed polymeric micelles for combination cancer chemotherapy through the concurrent delivery of multiple chemotherapeutic agents, J. Control. Release 122 (2007) 324–330, http://dx.doi.org/10.1016/j.jconrel.2007.05.038.

[30] D.L. Stirland, J.W. Nichols, S. Miura, Y.H. Bae, Mind the gap: a survey of how cancer drug carriers are susceptible to the gap between research and practice, J. Control. Release 172 (2013) 1045–1064.

CHAPTER 4

CONCLUSIONS AND FUTURE WORK: STRATEGIES TO IMPROVE DISTRIBUTION

4.1 Summary of Included Work

As evidenced by limited success in the clinic and known challenges studied in the literature, intratumoral distribution in solid tumors requires special considerations. This work used a novel application of the uterine perfusion model to analyze distribution in solid tumors. We also sought to bring further understanding to knowledge gained with xenograft models by developing and applying methods of analyzing the distribution of multiple doses with respect to each other and the blood vessels.

In Chapter 2, the uterine fibroid model using human tissue was shown to have resistance to drug delivery correlated to characteristics within the tumor environment. These results are directly relevant to drug delivery problems that limit uterine fibroid treatment options. However, it also suggests the uterine fibroid model could be a valuable tool for studying barriers to drug distribution in solid tumors within their original macro- and microenvironment. The fibroids most closely mimic desmoplastic tumors (pancreatic cancer, desmoplastic small round cell tumors, mesotheliomas, etc.).

Of course, no one model will completely replicate the conditions of every clinical tumor. As the statistician George E. P. Box said, "... all models are wrong, but some are useful" [178]. The uterine fibroid model may supplement other models to provide a collection of data to better guide treatment against tumors in patients. For example, genetically engineered mouse models (GEMMs) are emerging as an advanced model to study tumors [179]. GEMMs have the distinction of including the entire organism where the ex vivo uterine model is limited to only the organ. Including the entire organism would be an advantage when interested in interactions with other parts of the body. However, it may be a disadvantage when seeking more simplicity and control at the organ of interest.

Additionally, potential treatments can be given to the human explant organ and thoroughly analyzed without the risk of causing harm to the organism.

Currently, the duration of the ex vivo uterine perfusion is limited and it cannot test the efficacy of treatments. Considerable methods optimization is needed to perfuse the organ for longer than 72 h without compromising the tissue. Also, we do not know for sure if stain patterns in tumors are indicative of flow patterns (from heterogeneous IFP within tumors). It could be possible that flow seeps through a larger portion of the tissue but only stains select portions due to other interactions: stained areas could be rich in albumin or a similar molecule to which the methylene blue stain can easily bind. Future research could elucidate the binding tendencies of methylene blue. More importantly, it should include various, well-defined probes to better understand how carriers are distributed in this model for desmoplastic, solid tumors.

With the work presented in Chapter 3, we analyzed the spatiotemporal distribution of multiple doses. Xenograft models have chaotic, heterogeneous, and dynamic natures that affect drug delivery transport. Nanoparticles, compared to small molecules drugs, are slow to diffuse away from the blood vessel. Thus, accurate means of measuring the distance from the blood vessels in three dimensions is a useful tool for researchers seeking to design penetrating drug carriers. In the end point colocalization analysis, separately administered doses were less likely to colocalize. However, we do not know how these doses affect each other. Still, the intravital data show the second dose had a larger percentage of signal overlap. With these data, we hypothesize that the first dose has more access to the tumor and the second dose may reach and collide with the accumulated concentration gradient of the first dose, inhibiting further penetration to new frontiers in the tumor environment. Future work can test this hypothesis with slight adjustments to the current methodology.

The xenograft models we used have limitations as previously stated. However, the point of this work was to gain additional understanding surrounding already established data found using xenograft models and to test additional tools that would also work in other models. The spatial and temporal extravasation dynamics observed may be bad news in the clinical setting by being unable to provide a consistent dose to the tumor or it could be good news by spreading the dose around eventually. Further research analyzing dependency between multiple doses should be performed.

Included work did not explore variability in carriers (challenges present in the carrier). Furthermore, there are treatment strategies that have been developed to overcome some of the barriers discovered in this work. We can test these strategies, such as making

changes to the nanoparticle and the tumor environment, side-by-side while using additional experimental methods included in this work. Better understanding will also come from a new model of distribution in a human tumor that continues to resist current drug therapy. The information from these items of focus will provide valuable insight into the problems of intratumoral distribution of anticancer drugs and it will help other researchers design better drug therapies for solid tumors.

4.2 Future Work

There are two specific areas that may be interesting to pursue further. The first is specific analysis on the interdependence of multiple doses. More specifically, it will determine if the second dose is limited in distribution by the prior dose acting as a roadblock. The second area will use the models and methods developed thus far to test different nanoparticles characteristics or environmental treatments that seek to improve drug distribution in solid tumors. Both of these areas could benefit from computational models that could test or verify certain parameters for nanoparticles or tumors, but that will not be discussed herein [180].

4.2.1 Roadblock effect

Ours and other published data show that drug extravasation is heterogeneous, limited to certain regions of the tumor, and not penetrating far from blood vessels [85–87]. The majority of nanoparticle drug delivery data show high concentrations built up immediately adjacent to the tumor vessels [25, 105, 181]. Once this accumulation has taken place, the resulting decreased concentration gradient could hinder or serve as a roadblock to subsequent nanoparticle extravasations into the tumor.

As mentioned in Chapter 3, there was a clinical study that removed excess Doxil from blood two days after administration. The authors hypothesized further extravasation was limited. The excess drug particles were removed from blood circulation so as not to enter other organs. The small trial showed that toxicity was reduced and efficacy was not affected [182]. On the other hand, a preclinical study showed that the liver could become saturated and lead to increased accumulation of Doxil in the tumor [183]. However, saturating normal liver tissue with drug is unacceptable for human patients. The same author later showed the need for adjustments in subsequent doses to minimize toxicity [184].

To explore the plausibility of a roadblock effect by previous doses, some accessible volumes were calculated through meta-analysis as a proof of concept. While many published imaging data show intense pockets of extravasation localized near the blood vessel, it is

not known whether the signals are coming from particles located in void empty spaces (where there might be small rivulets or vesicles of free fluid), from those stuck in the ECM, or whether they are being taken up into cells. Some estimates of void spaces were calculated from SEM images of a pancreatic tumor [185]. However, some inaccuracy may be present due to shrinking or other artifacts from sample preparation for SEM. Exploratory calculations were made with particles ranging from 100 nm to 1 μm (aggregation in the blood stream is highly possible) to fill void spaces represented by spheres with diameters ranging from 800 nm to 8.5 μm. It was found only 1×10^{-4}% to 1×10^{-10}% of an injected dose (50 mg/kg) would be needed to fill up some of the void spaces, making it a relevant investigation.

While the work in Chapter 3 was not able to quantitatively measure a roadblock effect, the intravital data showed the first dose penetrating into more unique areas than the second dose. Additional experiments are recommended to investigate the possibility of a roadblock effect. Simply administering two nanoparticle doses and comparing their unique fluorescence will not be sufficient to distinguish a diminished signal from any blocking effect versus a diminished signal from the later dose not having as much time to accumulate a strong signal. Instead, distributions will be well defined with reliable signals for a nanoparticle dose. Those distributions will be compared between groups with and without a prior blocking dose administered. The blocking dose of nanoparticles need not be fluorescent, but labeling would confirm the presence of the blocking dose and allow for further colocalization analysis. In situ real-time imaging would be beneficial to more easily detect any blocking effect as the entire administration period can be observed for individual blocking events (rather than just the accumulated events present at the end point).

4.2.2 Nanoparticle and environmental changes

The majority of research on biocompatibility and biodistribution of nanoparticles has been done with spherical nanoparticles [40, 41]. This work adds some new methods for studying distribution, but is still limited only to spherical shapes. Additional work should be done with different shapes and surface properties.

New knowledge can be obtained by applying known methods that have been developed to improve intratumoral distribution. Of course these strategies have been studied before, but not in this human tumor model that is resistant to carrier penetration and not while being able to look at how multiple doses might distribute in relation to each other in three dimensions.

Specifically, methods that improve intratumoral distribution in solid tumors by affecting

the extravasation and diffusivity of nanoparticles can be screened. Numerous researchers have investigated how different geometries and surface modifications affect intratumoral distribution [72,73,186,187]. Furthermore, a tumor's environment plays a role in its ability to resist treatments. As not all solid tumors have the same characteristics, it will be necessary to learn how to change the tumor environment to be more favorable to drug carriers.

Table 4.1 shows the different strategies that will be implemented to screen methods that improve intratumoral distribution. The variables tested will be changes in the characteristics of silica nanoparticles and the tumor environment. Specifically, changes to the size, shape, and surface chemistry of silica nanoparticles will be explored to see changes in penetration or diffusion rates. Changes to environmental characteristics will be effected with coadministration of iRGD, high arterial pressure, hyperthermia, paclitaxel, and collagenase. The analysis and controls will be simplified such that only one treatment strategy is either present or absent. For example, 30 nm, negatively charged, silica nanoparticles with a red fluorescent tag will be compared against 80 nm, negatively charged, silica nanoparticles with a green fluorescent tag. Appropriate controls should be considered to ensure the fluorescent intensity is compensated and comparable for the nanoparticles with different sizes. For simplicity of testing maximum possible effect, combination treatments, such as collagenase and hyaluronidase, would be administered together for one group and compared with mice that receive neither.

Silica nanoparticles will serve as the probe nanoparticles as they are relatively inexpensive and easy to make batches with low polydispersity. A modified Stöber synthesis will be used where tetraethoxysilane (TEOS) is added to a mixture of water and ammonium hydroxide in an ethanol solution and stirred for at least 6 h [194]. During this time, the TEOS will undergo hydrolysis and condense at nucleation sites to form the silica nanoparticles.

Table 4.1. Select strategies to improve distribution.

Effect	Treatment/Formulation		Model
Increase diffusivity	Modified nanoparticles	Smaller size	Mouse/Fibroid
		Surface	Mouse/Fibroid
		Rods	Mouse/Fibroid
	Collagenase and hyaluronidase		Mouse/Fibroid
Increase Extravasation	iRGD		Mouse/Fibroid
	Hyperthermia and high arterial pressure		Fibroid
Increase accessible area	Paclitaxel priming		Mouse

References: [101,187–193]

The characteristics of silica nanoparticles can also be easily modified and verified. Size can be controlled by choosing methanol or ethanol for the alcohol solvent and by adjusting molar ratios of ammonium hydroxide, water, and TEOS. Providing primary amine groups on the surface of the silica nanoparticles via condensation (3-aminopropyl)triethoxysilane (APTES) will give a positively charged surface and could even allow further functionalization (such as linking RITC and FITC via their isothiocyanate groups). Silica nanorods can be synthesized through the use of the surfactant cetyl trimethylammonium bromide (CTAB) [195]. The resulting mesoporous silica nanorods will be complimented with mesoporous spheres as a control for any effects due to porosity.

These are suggested methods of extending the current work by providing additional carriers characteristics for testing. These are still not representative of all possible carriers characteristics. Any type of carrier could be administered to the perfusate buffer for the uterine perfusion model. The spatiotemporal analysis methods are compatible with any drug carriers that provide unique signals for multiple doses.

From a different perspective, cancer can be considered as an organ with its own ecosystem where disturbing the ecology may be an effective treatment method [126, 196, 197]. There is increased interest in causing a therapeutic effect or improving intratumoral distribution by changing the tumor environment [108]. These methods of changing the environment, along with some combination therapy, will be screened in the context of the included work.

It may be possible to try to increase permeability in the tumor with hyperthermia or with iRGD peptides, the latter having been classified as tumor penetrating peptides [190, 191]. To test whether iRGD peptides can help extravasation, two typical examples (CRGDK and RPARPAR) will be examined [74]. A peptide concentration of 2 μM will be administered at the same time as the nanoparticles [190]. It also may help to artificially increase the vascular pressure to slightly improve tumor extravasation [192, 198]. Increasing the arterial pressure to 180 mmHg, to compensate for the high IFP, will be done by increasing the flow speed of the perfusion. Hyperthermia will be easily applied by adjusting the temperature of the incubator in which the uterus is perfused. Investigation will begin with the temperature of 42 °C for a period of 1 hour. In order to reduce cell packing and allow more accessible area for extravasation and diffusion, the mice will be treated with a priming agent, paclitaxel, at a concentration of 40 mg/kg for a period of 24 h [193]. After 4 h, the probe nanoparticles will be administered via tail vein injection and after another 4 h the mice will be sacrificed and tumors harvested to ascertain the priming effect. Validation of sufficient perfusion of oxygen and nutrients will be of increased importance to verify cell death is a result of only paclitaxel

treatment. Alternatively, other cytotoxic drugs may be tested that have a faster effect on clearing the accessible area for extravasation and diffusion of nanoparticles. Administration of hyaluronidase (30 kU/kg) and collagenase (2 mg/kg) will also help to clear a path for improved distribution of nanoparticles [188, 189]. However, in using hyaluronidase and collagenase, there are concerns that this treatment may increase the metastatic potential of a given cancer. The perfusate can be checked for any cellular components that may suggest the potential for migration.

Again, these are not novel treatment strategies related to improving distribution in the tumor environment. Rather, the purpose is to test already established strategies in combination with methods from the included work. How will these strategies fare in a clinical tumor dense in cells and fibrous content? Alternatively, do these treatment strategies affect the extravasation dynamics and possible interdependence of multiple doses discovered in this work? Answers to these questions will also help explain why distribution in solid tumors is so challenging.

It is anticipated that the presence of some treatment methods will increase drug concentration adjacent to the tumor vasculature while other methods will aid distribution throughout the tumor. If extravasation and distribution can be improved in dense fibroids, that represent a severe case of drug delivery resistance, we suspect that many other desmoplastic, clinical tumors will also respond positively.

Some methods for improving intratumoral distribution are questionable in terms of safety. Environmental treatments like high arterial pressure, collagenase/hyaluronidase, and hyperthermia could not be tested for efficacy in humans without a proven safety record. As mentioned previously, the ex vivo uterine perfusion model has an advantage to be able to test aggressive strategies without concern for toxicity or pain caused to a living organism. This model will not be able to show if a method is safe as it excludes many other organs that can be affected by treatments. It can, however, show if it is unsafe. Still, the focus of this project would be testing these methods for efficacy (in terms of drug distribution), not safety. If the methods are shown to be effective, further studies with other models can investigate means to ensure or improve their safety. The methods and models in this project are meant to supplement existing strategies to bring a more complete vetting process of therapies before testing in human patients.

4.3 Revolution: A Thought-Provoking Detour

A lot has been discovered and accomplished with nanotechnology research as applied to cancer therapies. However, right now we are at an asymptote or an inflection point and we

may need a paradigm shift to ensure progress in the positive direction.

In 1962, Thomas Kuhn wrote a book about paradigms and scientific revolution [199]. Right now we are in a state of collecting knowledge with only slow improvements in targeted drug delivery occurring. It is possible that a shift of paradigm can be a catalyst for a massive leap forward in targeted drug delivery.

It is true that there are new targeting moieties and new technologies, but progress is in a seemingly slow evolution and the fight against cancer needs a revolution. This is not discrediting the value of basic science; useful tools will find meaningful applications. Nanotechnology is an incredibly useful and versatile tool. For example, there are more polymeric therapeutics approved for various other diseases [200, 201]. However, it has not proven to be a pancea for cancer treatment—that would be extremely unlikely for this collection of diverse diseases.

As an observer, the conclusion drawn is that passive delivery to solid tumors have a challenge in thoroughly treating solid tumors. They can do better than standard chemotherapy (or else they would not be approved), but they still have limitations. The limitations also apply to carriers that have active targeting groups. If their target is within the solid tumor, passive carriers will have difficulties in exclusively and thoroughly hitting it. Thus, a change of paradigm is needed for nanomedicine: to recognized its weaknesses and take advantage of them. For example, they accumulate in the periphery and are often taken up by the MPS. These two characteristics, initially perceived as weaknesses, can become strengths in drug carrier design. They will have more success reaching targets in or near the blood vessels. Furthermore, it is suggested that activating T cells in the blood stream will be easier to access and they can act more like a magic bullet that can move about, detect, and ensure destruction.

4.3.1 Target the periphery

The market success of drug carriers has occurred mostly when designs have targets in the blood or vessels. This concept relates to the included work in that hormone therapies work well in the dense fibroids because they do not have to enter the tumor, they only have to reach action sites upstream that influence the growth of the fibroids. Chances for success may be improved by designing carriers that only have to reach the tumor periphery to be effective. In this position, the therapy can still alter resources feeding tumor growth, change the tumor's environment, or recruit some of the body's natural defense mechanisms.

The most prevalent example of targeting the environment is through the use of antiangiogenic therapies to starve the tumor of needed resources. Further evidence for the idea

of targeting the environment comes in a study using aromatase inhibitors in combination with a biophosphonate drug that inhibits bone loss and reduces the risk of metastasis in the bone [202]. The biophosphonate drug leads to bone or environment remodeling while the aromatase inhibitor starves the breast cancer cells of the estrogen needed for growth.

A physical attack such as hyperthermia can also modify the tumor environment. As an example, G. von Maltzahn *et al.* used one nanoparticle system to prepare the tumor environment for a second nanoparticle system [203]. They called this influence communication between the two nanoparticle systems. Essentially, they use one system to modify the tumor environment such that the second system can recognize it. They first confirmed that they can localize PEGylated gold nanorods to the tumor. They then used near infrared radiation to stimulate the gold nanoparticles and cause hypothermia and vascular damage in the tumor area. They were able to show tumor localization of nanoparticle by fluorescence and confirmed this using a temperature map showing hyperthermia only in the tumor area. They then showed that this vascular damage led to coagulation in the area of the tumor. They used staining to show increased levels of fibrinogen in heat treated tumors. The second nanoparticle system had receptors for fibrin or factor XIII. This communication between the nanoparticle systems increases accumulation in the tumor environment [203].

This method could also communicate with the immune system. Attacking the environment has the potential to not only disrupt the normally supportive tumor ecology, but also attract the immune system. Furthermore, damage done in the environment will also produce some damage-associated molecular pattern (DAMP) molecules. These DAMPs are cytokines that can help trigger an immune response. Activation of platelets, the coagulation cascade, and the complement cascade can respectively lead to cytokine release, fibrin, and both C3a and C5a, which all play a role in recruiting the immune system [204]. Inflammation and scarring through a foreign body response can prevent cancer in some situations [205].

From one perspective, it is considered a failure when intravenous injections of a therapeutic agent do not reach the entirety of the tumor and only accumulate at the periphery. However, from another perspective, this localization at the periphery of the tumor is the perfect location to attract the immune system to the tumor. It may be possible to cause a chain of events that will make it easier for the immune system to be able to detect and follow the trail that leads it to attack the cancer.

4.3.2 Activate the immune system

Inanimate carriers of drug are unreliable when they rely on passive delivery. They are at the whim of the forces that act upon them and cannot truly home in on tumor targets. The

most representative magic bullet is found in the body's own immune system. Paul Ehrlich himself stated that cancer would be more prevalent if not for the immune system [206]. It has both mobility and specificity. Immune cells can follow chemical gradients and have specificity with antibodies and cell receptors.

The immune system is a revolution in the fight against cancer, a leap forward in technology, and a highly evolved weapon for pathogen rejection. It is important to have a therapy incorporate the natural and robust immune defenses of the body as they are specialized yet versatile. Furthermore, it will take many years before a nanoparticle synthesized in the laboratory equals the sophistication of a lymphocyte. Lymphocytes are able to multiply, migrate into tissues, produce their own toxic agents, and have other qualities that make them superior to nanoparticles in killing cancer cells. Even when cancer has been able to escape the immune system, therapies that intervene and boost the immune system have had success in causing tumor rejection.

One of the hallmarks of tumor escape from the immune system is its ability to supress the immune system. CD25 positive regulatory T cells can be reprogrammed to create tolerance for cancer, thereby allowing tumor growth. IL-2 has been shown to stop Treg immunosuppression and leads to cancer rejection [207]. Onizuka *et al.* showed that administration and binding of monoclonal antibodies to the IL-2 receptor α on these cells would prevent clonal expansion and reduce the number of regulatory T cells that support the cancer growth [208]. They found there was a time frame within which the monoclonal antibody had to be administered to result in tumor rejection by the immune system. They also performed controls by checking the effects of monoclonal antibodies for CD4+ and CD8+ T cells. When the CD8+ T cells were also prevented from expanding, the tumors were not rejected. They also tested the secondary response of treated mice. After successful immune rejection of the tumor following anti-CD25 monoclonal antibody administration, they transplanted more cancer cells and saw that they had acquired cancer resistance [208].

Immunobioengineering is a relatively new term to describe the engineering of biomaterials to interact with the immune system. Initially, biomaterials started out as simply the medical application of metals and other materials that were not designed to go into the body. It evolved to a need for biocompatibility to where the material is designed to be inert so it will have an acceptable host response and still be able to function. This is done by carefully selecting the material and by changing the bulk chemistry and surface properties at the interface with the body. It is now evolving to where the material should no longer be inert but interact with the biology and should cause a beneficial response to

boost function [209]. Drug therapies have undergone a similar evolution. As mentioned in Chapter 1, Cremephor EL is an unsophisticated drug excipient used to solubilize paclitaxel that often results in unacceptable host responses. To address that issue, many drug carriers have been designed to offer stealth delivery of the drug. With recent progress, there are also carrier therapies that interact with the immune system and cause a beneficial response rather than trying to hide from the body [210].

Looking at the success of Keytruda, Opdivo, and Yervoy shows we can directly interact with the immune cells to promote tumor rejection. The difference between CTLA-4 and PD-1 antibodies is that the CTLA-4 blockade activates proliferation of T cells while PD-1 primarily blocks the adaptive immune resistance developed by the tumor [211,212]. Thus, PD-1 antibodies make the T cells more effective in the intratumoral environment rather than boosting general T cell proliferation and antigen-specific immunity. PD-1 also results in higher response rates and reduced toxicity [213]. These antibody therapies work so well because they do not have to physically distribute into the tumor mass, but they act on immune cells that can migrate.

Beyond antibodies (a major component of the immune system), it has been shown that polymers can interact with the immune response when present in the tumor environment [214]. N-(2-Hydroxypropyl)methacrylamide (HPMA) can cause immunostimulation to the point of reaching cancer resistance. Mrkvan *et al.* treated mice with tumors using HPMA-doxorubicin conjugates. Any mice that survived were saved and showed resistance to another inoculation of cancer cells that would otherwise be lethal [215]. Polymers have also been expressly designed to interact with dendritic cells to aid in activating T cells [216]. Nanoparticles and polymers can prime the immune system as they interact with it by containing Tumor Associated Antigens (TAAs) [217–219]. By involving the immune system in fighting the tumor, it brings a component capable of adapting and seeking after evasive cancer cells. However, care must be taken to thoroughly analyze the interactions with the immune system to avoid unintended immunosuppressive effects that have been shown to actually promote tumor growth [220–223].

4.3.3 Challenges

To achieve tumor rejection by focusing treatment on the environment and immune system, there are certain challenges this approach must test. There must be a change in the environment by physical placement of therapeutics or by actions that cause a host response. There must be a recruitment of cellular components of the immune system and a reversal of immunosuppression. This tumor rejection must occur in an immunocompetent

model where the tumor has been immunoedited.

The perception of a patient's quality of life has changed over the decades with advanced treatments, but toleration still requires mustered courage [224, 225]. Sometimes, cancer drugs can only temporarily relieve the pain and other symptoms of the tumor and do so at the cost of other side effects (including pain). Current anticancer treatments are used because it balances the risk to benefit ratio. A minimally effective treatment is allowed because it does not increase the likelihood of death. In this perspective, some chemotherapies could be reminiscent of the abandoned neurological procedure of lobotomies: the body is damaged in an attempt to destroy the disease.

However, immunotherapy has the same challenge of balancing the risk to benefit ratio. Immunotherapy (such as CAR T cell therapy) can have impressive clinical outcomes, but that potency carries over to cases of severe toxicity [226, 227]. Thus, it may be helpful to design fail-safe mechanisms into any type of immunotherapy [67].

Treatment focused on both the environment and immune system is a recommended paradigm shift. Some drug carrier technologies have been found to cause biocompatibility problems that could be beneficial if controlled and localized in the tumor environment. Furthermore, most chemotherapeutic drugs reduce the white blood cell count when it would be more beneficial to boost the activity of the immune system against the cancer (and also prevent any other opportunistic disease).

4.4 Conclusion

This project uses new tools to explore the role of the tumor environment in drug distribution. The environment may block or divert different doses of drug particles to limited areas of the tumor. Understanding these transport barriers is crucial to translating targeted therapies from the research bench to the patient—new models will need to be developed to make up for the shortcomings of the mouse model. The uterine fibroid model provides a challenging model for drug delivery and can be helpful in investigating the barriers to drug transport in solid tumors. There is risk for failure in developing new models, but the potential reward is substantial as it might change the way cancer medicines are vetted before entering clinical trials. The spatiotemporal analysis brings additional information by including two more dimensions: the third axis in space and the dimension of time. While this research builds upon previous work investigating drug transport in tumors, it brings a new perspective looking at dynamics between multiple doses. If some of the barriers cannot be fully overcome, better characterizing the factors that influence distribution will be helpful for predicting successful drug delivery for certain tumor types. Furthermore,

we may be able to adapt and have more success hitting peripheral targets that can have downstream effects on cancer.

APPENDIX

CHALLENGES IN TRANSLATION

D. L. Stirland, J. W. Nichols, S. Miura, and Y. H. Bae, Mind the gap: A survey of how cancer drug carriers are susceptible to the gap between research and practice, J. Control. Release, vol. 172, no. 3, pp. 10451064, 2013. http://dx.doi.org/10.1016/j.jconrel.2013.09.026. Included with kind permission of Elsevier and the coauthors.

A.1 Preamble

To better understand the translational difficulties of these drug carriers, a small selection of drug carriers designed to improve drug delivery is surveyed in the included article. These carriers do not represent the latest advances in technology. Older or established carriers were chosen because it often takes years for clinical data to be released [228]. While limited in scope, it shows some of the challenges that drug carriers face when trying to achieve active targeting. It also shows that antibody therapeutics are not immune to these challenges. The safety and efficacy data from preclinical studies are explored and compared with any available clinical data in an attempt to determine what may influence successful treatment of clinical tumors.

Journal of Controlled Release 172 (2013) 1045–1064

Contents lists available at ScienceDirect

Journal of Controlled Release

journal homepage: www.elsevier.com/locate/jconrel

Perspective review

Mind the gap: A survey of how cancer drug carriers are susceptible to the gap between research and practice

Darren Lars Stirland [a,1], Joseph W. Nichols [a,1], Seiji Miura [b,c,1], You Han Bae [c,*]

[a] University of Utah, Department of Bioengineering, College of Engineering, Salt Lake City, 84112, USA
[b] Fuji Research Laboratories, Pharmaceutical Division, Kowa Co. Ltd., 332-1 Ohnoshinden, Fuji Shizuoka, Japan
[c] University of Utah, Department of Pharmaceutics and Pharmaceutical Chemistry, College of Pharmacy, Salt Lake City, 84112, USA

ARTICLE INFO

Article history:
Received 14 August 2013
Accepted 25 September 2013
Available online 2 October 2013

Keywords:
Cancer therapy
Drug carrier
Nanomedicine
Drug delivery
Clinical translation

ABSTRACT

With countless research papers using preclinical models and showing the superiority of nanoparticle design over current drug therapies used to treat cancers, it is surprising how deficient the translation of these nano-sized drug carriers into the clinical setting is. This review article seeks to compare the preclinical and clinical results for Doxil®, PK1, Abraxane®, Genexol-PM®, Xyotax™, NC-6004, Mylotarg®, PK2, and CALAA-01. While not comprehensive, it covers nano-sized drug carriers designed to improve the efficacy of common drugs used in chemotherapy. While not always available or comparable, effort was made to compare the pharmacokinetics, toxicity, and efficacy between the animal and human studies. Discussion is provided to suggest what might be causing the gap. Finally, suggestions and encouragement are dispensed for the potential that nano-sized drug carriers hold.
© 2013 Elsevier B.V. All rights reserved.

Contents

* Corresponding author at: Department of Pharmaceutics and Pharmaceutical Chemistry, College of Pharmacy, University of Utah, Rm 2972, Skaggs Pharmacy Institute, 30S 2000E, Salt Lake City, Utah 84112, USA. Tel.: +1 801 585 1518.
E-mail address: you.bae@utah.edu (Y.H. Bae).
[1] The authors equally contributed to this article.

0168-3659/$ – see front matter © 2013 Elsevier B.V. All rights reserved.
http://dx.doi.org/10.1016/j.jconrel.2013.09.026

1. Introduction

Nanotechnology is a remarkable example of human achievement. In only a few decades of concerted effort, our knowledge of the laws of physics and chemistry has expanded to the point that we are able to manipulate matter at nearly the atomic scale to create complex structures with unique and potentially revolutionary functions. Nanotechnology describes the ability to manipulate matter at the scale of 1–100 nm in order to create and use structures with new, unique and useful properties [1]. This technology has far-reaching implications for improving the human condition, including more compact and powerful microchips and processors, more robust agriculture, cleaner, more efficient fuels, and better health. With this promise in mind, billions of dollars have been invested in nanotechnology research, and in some fields the return of that investment is starting to be realized [2]. However, as with most new technologies, progress has been uneven and the nature of future advancements uncertain.

Nanomedicine is the application of nanotechnology to improve the health of individuals through better diagnoses and treatments. However, nanomedicine is a very broad term, including applications in sensors, tissue engineering, imaging agents and other diagnostics, lab-on-a-chip devices, therapeutic agents, and drug carriers. Its usefulness has been diluted by a degree of irrational exuberance that has permeated the discussion of nanotechnology over the last few decades [2–12]. Furthermore, certain technologies such as liposomes, polymer therapeutics, and protein therapeutics have existed long before "nanotechnology" was introduced. Thus, when considering drug delivery technology, particularly for anti-cancer therapeutics, it may be useful to abandon the term nanomedicine and instead adopt less loaded descriptors. This review will refer to these technologies as nano-sized drug carriers or simply drug carriers which are injectable into the blood stream, and focus on those drug carriers which were designed to provide better efficacy and lower toxicity for cancer therapeutics. The impact of drug carriers has in some ways been difficult to judge; they can be quite versatile, allowing researchers the flexibility to design delivery strategies specific to environmental challenges posed by the body. On the other hand, the more complex designs have thus far had little impact on clinical therapies beyond merely adding the rhetoric of targeted drug delivery to somewhat conventional therapies.

Cancer has been an area of particular interest for nano-sized drug carriers due to the enhanced permeability and retention (EPR) effect which is thought to provide them with significant therapeutic advantages over small molecule chemotherapy drugs [13,14]. EPR refers to the tendency for nanoparticles and macromolecules to accumulate in tumors more, in comparison with the control solution formulations, due to the disorganized and ill-formed blood vessels that contain large fenestrae through which these large molecules can pass. Retention is increased by the dysfunctional lymph vessels which significantly hinder drainage from the tumor interstitial space. EPR was first discovered in the 1980s by Dr. Hiroshi Maeda and has subsequently become a key concept in the field of cancer drug delivery [15,16]. According to the EPR hypothesis, nano-sized drug carriers should enjoy a natural advantage over traditional therapies as the increased drug concentration within a tumor should provide improved efficacy, and shielding of the drug from the rest of the body can provide reduced toxicity. This has generally been the case in the animal models used for preclinical studies [17–20], but the improved efficacy promised by the EPR effect has often failed to materialize in clinical settings [21,22].

The apparent gap between preclinical animal models and the clinical tumors encountered by clinicians is of great interest if drug carriers are to make a significant impact at the core of cancer therapy rather than just at the margins. Oncology drugs (including drug carrier technologies) suffer a 95% failure rate after entering human trials. Most of these failures occur in the efficacy phases and can cost hundreds of millions of dollars. A better understanding of the shortcomings of commonly used models could thus potentially save billions of dollars in wasted effort.

This review presents a cross section of some of the most important formulation strategies being pursued by researchers including liposomal formulations, micelles, linear polymers and protein carriers. Each of these formulations is unique in the way it changes the interactions between the drug and body. Some are designed with a half-life of several days, leaving a portion to circulate for weeks in the blood, with the intent to slowly accumulate in the tumor *via* EPR. Others simply attempt to improve the solubility of the drug cargo without harmful effects. Still others seek to actively target tumors by attaching groups that participate in ligand binding events with either cancer cell surface proteins or other targets of interest. Most of these formulations drastically impact how the drug and body interact, including starkly different pharmacokinetic parameters such as half-life, area under the curve, distribution, and clearance. Curiously, however, the impact of these formulations on efficacy is rarely significant outside the laboratory (Fig. 1).

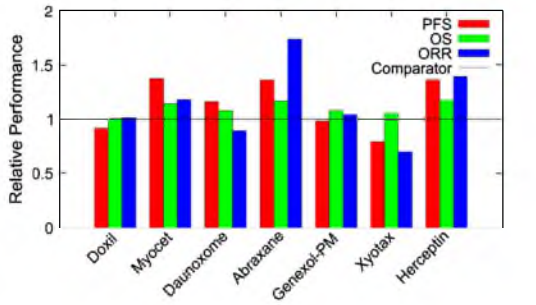

Fig. 1. Summary of phase III performance of selected drug carrier therapies compared to standard treatment. PFS: progression free survival; OS: overall survival; ORR: overall response rate. Data gathered from phase III trials [21,22,69,106,119,122,183–185].

Comparing human tumors to animal models can be a difficult game. In addition to the obvious differences in size, lifespan, physiology and metabolism between humans and mice which most commonly serve as models, the cancers themselves are significantly different from their naturally derived counterparts. Model cancers are grown artificially, from single cell lines, and in a matter of weeks, whereas human tumors emerge from complex tissues under immune surveillance over years. To make matters worse, preclinical and clinical studies rarely use the same benchmarks or endpoints. Preclinical studies often make use of measurements not available to the clinician, such as tumor diameter. Phase III efficacy studies generally use the best available therapy as a comparator, which often includes combinational therapies. Preclinical studies, on the other hand, do not always use the best available therapies as comparators but rather single compound formulations of the same drug contained in the carrier.

Given these differences, it may be reasonable to ask what can realistically be expected from human trials after successful animal trials, and are new drug formulations to treat human patients or mice being designed? Some of these discrepancies are beyond our control, but others can be ameliorated by concerted effort and greater global communication between the research and clinical communities as well as relevant regulatory agencies. Following the history of these drugs from the benchtop to the bedside provides some insight into where the shortcomings are, whether in the models used or in the discussions about them.

2. Doxorubicin

Doxorubicin is an anthracycline topoisomerase inhibitor. It was first isolated from culture medium of *Streptomyces peucetius* var. *caesius* by F. Arcamone from Farmitalia Research Laboratories in 1967 [23]. The anticancer activity of doxorubicin is given by multiple mechanisms [24,25]. Doxorubicin intercalates between base pairs in the DNA helix, and inhibits the binding of DNA and RNA polymerase, resulting in the prevention of DNA replication and protein synthesis. Specifically, DNA intercalated with doxorubicin stabilizes the topoisomerase II-DNA complex during DNA replication, and prevents the ligation of the nucleotide strand after double-strand breakage. Since its approval, doxorubicin has been widely used to treat various malignancies (acute lymphoblastic leukemia, acute myelogenous leukemia, breast cancer, gastric cancer, Hodgkin's lymphoma, neuroblastoma, non-Hodgkin's lymphoma, ovarian cancer, small cell lung cancer, soft tissue and bone sarcomas, thyroid cancer, transitional cell bladder cancer, Wilms' tumor and others) [26–28]. However, the use of doxorubicin has been limited by toxicities such as hematopoietic suppression, nausea, vomiting, apoplexy, alopecia and especially cardiotoxicity, which is a fatal adverse effect. Cardiotoxicity is characterized by a broad spectrum of symptoms ranging from asymptomatic electrocardiography (ECG)-changes, to pericarditis and decompensated cardiomyopathy. The probability of developing cardiotoxicity is largely dose-dependent. The usual dosage of doxorubicin is 60–75 mg/m^2 every 3 weeks. Cardiomyopathy and congestive heart failure occur most frequently above a cumulative dose of 450–550 mg/m^2 doxorubicin [29]. The most common cause of doxorubicin-related cardiotoxicity is oxidative stress. Doxorubicin produces oxygen free radical resulting in lipid peroxidation of cell membrane lipids [30–33]. The specificity of the oxidative stress to the cardiac cells could be due to relatively low levels of antioxidant enzymes in heart [34].

2.1. Doxil®/Caelyx®

Doxil® [US], or Caelyx® [outside US], was the first FDA-approved nano-sized drug carrier formulation [35]. As seen in (Fig. 2), the doxorubicin molecules are encapsulated in a bilayer vesicle of lipids known as a liposome. This liposome is coated by a layer of poly(ethylene glycol) (PEG) to limit uptake by the mononuclear phagocyte system (MPS). Doxil® was developed as pegylated liposomal doxorubicin (PLD) to enhance efficacy and decrease toxicity of doxorubicin by virtue of its size (80–90 nm), pegylated surface, and stability in the blood, which allow prolonged blood circulation time considered necessary for high accumulation of doxorubicin in tumors [36].

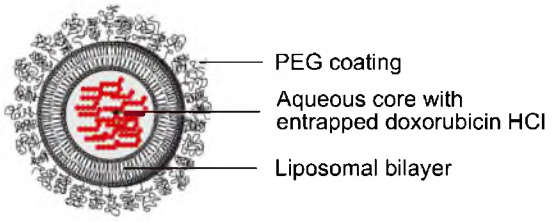

Fig. 2. Pegylated liposomal doxorubicin (Doxil®/Caelyx®). Particle size is 80–90 nm. Developed by Johnson and Johnson and approved in 1995 for treating AIDS-related Kaposi's sarcoma. So far, the indications have been extended to ovarian cancer and multiple myeloma. Illustration modified from FDA label.

2.1.1. Preclinical studies

Doxorubicin shows biphasic curves of plasma concentration after intravenous (i.v.) injection. First phase accounts for rapid distribution with a half-life of 5–10 min and second phase is an elimination with a half-life of 30 ± 8 h [37]. In contrast to the rapid elimination of free doxorubicin from blood circulation, Doxil maintains a significantly higher blood concentration than free doxorubicin for several days in various animals (rabbit, rat, and dog) [38–42]. The area under the plasma concentration-time curve (AUC) of doxorubicin in animals treated with Doxil is at least 60 times greater than that treated with free doxorubicin. The distribution volume of Doxil is close to the blood volume in the body. Clearance curves of total doxorubicin and doxorubicin entrapped in pegylated liposomes are superimposable [38,43]. This indicates that the leakage of doxorubicin from pegylated liposomes while circulating is negligibly small.

A number of studies have investigated the tissue distribution of doxorubicin after i.v. injection of Doxil. Doxil treatment shows more accumulation of doxorubicin in various xenograft tumors (*e.g.*, J6456 lymphoma [44], PC-3 human prostate adenocarcinoma [45], A375 human melanoma [46], N87 human gastric carcinoma [46], and C26 murine colon carcinoma [38]) than free doxorubicin treatment. Doxorubicin accumulation in the liver and spleen by Doxil is also increased [45,46].

The most important advantage of PLD is that doxorubicin accumulation in the heart was drastically reduced compared to free doxorubicin [47]. Comparative studies in rats, rabbits and dogs demonstrated the decrease in cardiotoxicity [37,48].

Several efficacy studies using various tumor xenograft mice (*e.g.*, C-26 murine colon carcinoma [49], PC-3 human prostate carcinoma [45], AsPC-1 human pancreatic carcinoma [50], HEY Human Ovarian Carcinoma [51], 3LL Human Lewis lung, carcinoma, [52], BT474 breast carcinoma [52] and MCF-7 breast adenocarcinoma [52]) revealed significant efficacy gains of Doxil over free doxorubicin [53,54]. Studies using Lewis lung xenografts and breast cancer xenografts showed that the efficacy of Doxil at 2 mg/kg was approximately equivalent to that of doxorubicin at 4–9 mg/kg [52], indicating a 2 to 4.5-fold increase in potency of Doxil compared with free doxorubicin.

2.1.2. Clinical studies

The first clinical trial of Doxil in patients with broad types of cancer (breast cancer, non-small cell lung cancer, ovarian cancer, mesothelioma, soft tissue sarcoma, and pancreatic cancer) was conducted from 1991 to 1994 in Jerusalem, and showed first proof of passive targeting based on the EPR effect in humans after intravenous administration [55]. Since then, a huge number of clinical studies have been conducted in various cancers: mainly AIDS-related Kaposi's sarcoma (ARKS), ovarian cancer, breast cancer, multiple myeloma and soft tissue sarcoma.

Pharmacokinetic results are summarized in a review article by Gabizon et al. [39]. Doxil has significantly longer half-life than that of free doxorubicin. Surprisingly, the half-life found in clinical studies of ~45 h is even longer than that found in rodents and dogs of ~20 h and ~30 h, respectively.

Tissue distribution has also been studied from the first clinical trials. All results reveal that Doxil had a higher accumulation in the tumor compared to the adjacent, normal tissues as well as the tumor treated with free doxorubicin [55–58]. There is a tissue distribution study based on the use of ^{111}In-DTPA labeled, drug free, pegylated liposomes of identical lipid composition to Doxil [36]. Tumors were visualized in fifteen of seventeen patients with breast, head and neck, bronchus, glioma and cervix cancer by gamma camera. Various normalized levels of accumulation (33% of injected dose/kg (ID/kg) in head and neck cancer, 18.3% ID/kg in lung cancer and 5.3% ID/kg in breast cancer) were detected. However, less than 5% ID was in a tumor as a whole due to small sizes of the solid tumors while a significant accumulation in other organs (liver, spleen and bone marrow) was detected.

Doxil shows a vastly different adverse-effect profile from that of free doxorubicin. These profiles are well summarized in review articles [59,60]. While many toxicities induced by doxorubicin, as represented by cardiotoxicity, were dramatically decreased [61,62], overall mucocutaneous toxicity was increased. Palmer-planter erythrodysesthesia (PPE) is particularly recognized as dose limiting toxicity.

The efficacy of Doxil has been extensively summarized in many articles and book chapters [63,64]. Doxil showed better efficacy than conventional single or combinatory therapies in several cancers: bleomycin and vincristine [65,66], paclitaxel [67] and highly active antiretroviral therapy [68] in ARKS, as well as topotecan in recurrent ovarian cancer [69,70]. On the other hand, Doxil showed equivalent efficacy with reduced toxicity to free doxorubicin in metastatic breast cancer [22] and multiple myeloma [71], despite prolonged blood circulating time and improved accumulation in tumors (see Table 1).

In summary, Doxil improved the toxicity profile owing to its different pharmacokinetics and biodistribution from those of free doxorubicin; however, Doxil introduced other toxicities like PPE. Unlike preclinical results, Doxil has yet to show improvement in efficacy when compared with free doxorubicin. For the patient, Doxil absolutely has an advantage compared with conventional therapy due to reduced toxicity. Still, there seems to be an unknown gap in efficacy between preclinical and clinical studies.

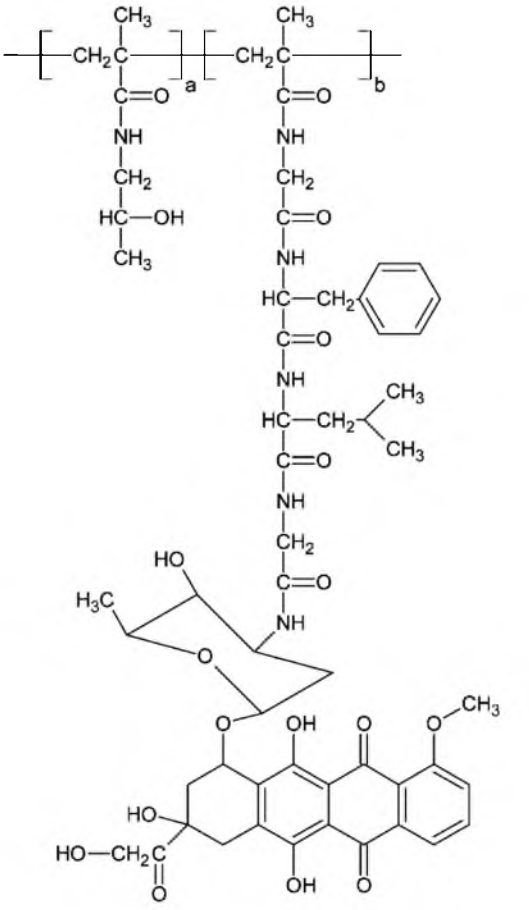

Fig. 3. PK1/FCE 28068. a = 96.1%, b = 3.9%. Particle size is around 8 nm. Developed by Pharmacia which merged with Pfizer [88].

2.2. PK1/FCE 28068

PK1 (FCE 28068) (Fig. 3) was the first drug-polymer conjugate to enter clinical trials. Doxorubicin is conjugated with a synthetic N-(2-hydroxypropyl)methacrylamide (HPMA) copolymer *via* Gly-Phe-Leu-Gly peptidyl linker designed to degrade by thiol-dependent lysosomal protease [72,73] and forms a unimolecular micelle in aqueous solution

Table 1
Summary of clinical efficacy.

Cancer type	ARKS		ARKS		ARKS		ARKS		Recurrent ovarian cancer		Metastatic breast cancer		Multiple myeloma	
Characteristics	PLD1	BV	PLD1	BV	PLD1	PTX	PLD1	HAART	PLD2	TPN	PLD2	DOX	DVd	VAd
No. of patients	121	120	133	125	37	36	13	15	239	235	254	255	97	95
CR (%)	6.0	1.0	1.0	0.0	5.0	8.0	31.0	13.0	3.8	4.7	–	–	3.1	0.0
PR (%)	53.0	22.0	45.0	25.0	41.0	47.0	46.0	7.0	15.9	12.3	–	–	41.3	41.1
OR (CR + PR, %)	59.0	23.0	46.0	25.0	46.0	55.0	–	–	19.7	17.0	33.0	38.0	44.4	41.1
Stable (%)	38.0	68.0	53.0	67.0	32.0	25.0	–	–	32.2	40.4	25.0	25.0	39.2	48.4
Progressive (%)	0.0	4.0	2.0	8.0	3.0	3.0	–	–	48.1	42.6	18.0	11.0	2.1	0.0
Not assessable (%)	3.0	5.0	0.0	0.0	24.0	17.0	–	–	–	–	18.0	21.0	14.4	10.5
PFS (months)	–	–	–	–	12.2	17.5	–	–	3.8	4.0	6.9	7.8	78%*	76%*
OS (months)	5.3	5.3	–	–	–	53.6	–	–	14.0	13.2	21.0	22.0	88%*	85%*
Ref.	[64]		[63]		[65]		[66]		[67]		[20]		[69]	

CR: Complete response; PR: Partial response; OR: Overall response; PFS: Progression free survival; OS: Overall survival; ARKS: AIDS-related Kaposi's sarcoma; PLD1: Pegylated liposomal doxorubicin (20 mg/m^2); PLD2: Pegylated liposomal doxorubicin (50 mg/m^2); BV: bleomycin (15 IU/m^2) and vincristine (2 mg); ABV: doxorubicin (20 mg/m^2), bleomycin (10 mg/m^2) and vincristine (1 mg); PTX: Paclitaxel (100 mg/m^2); HAART: highly active antiretroviral therapy; TPN: Topotecan (1.5 mg/m^2); DOX: Doxorubicin (60 mg/m^2); DVd: pegylated liposomal doxorubicin (40 mg/m^2), vincristine (1.4 mg/m^2; maximum, 2.0 mg) and reduced-dose dexamethasone (40 mg); VAd: vincristine (0.4 mg) doxorubicin (9 mg/m^2) and reduced-dose dexamethasone (40 mg); '–'not available; '*' 1 year PFS or OS rate [22,65–69,71].

with a diameter of around 8 nm [74,75]. HPMA is non-biodegradable and essentially nontoxic in the rat, even at doses of 30 g/kg [72]. Its hydrophobicity limits MPS sequestration and its relatively high molecular weight (~20–30 kDa) allows it to avoid renal elimination [74]. These features allow prolonged blood circulation time resulting in high accumulation in tumors. Furthermore, the high molecular weight prevents diffusion across the membrane, restricting cellular uptake to endocytic pathways and facilitates the cleavage of the linker and the release of doxorubicin in endosomes. Additionally, PK1 has been developed to overcome the resistance due to P-glycoprotein overexpression based on contributions of the endocytic (pinocytic) cellular uptake and the controlled release in the endosome. The *in vitro* results using A2780 resistant human ovarian carcinoma cell line showed no induction of *MDR1 gene* by PK1 and indicates that PK1 can avoid excretion by P-glycoprotein [76–78].

2.2.1. Preclinical studies

Since doxorubicin is conjugated with HPMA, free doxorubicin is not detected in plasma and tissues after administration of PK1. The pharmacokinetics study of PK1 using mice showed the half-life of PK1 was approximately 15 times longer than that of the free drug in mice [79].

Consistent with prolonged blood circulation time, several studies reveal relatively high accumulation of PK1 in xenograft tumors in mice [80–85]. PK1 showed 17–77 times higher accumulation in B16FIO melanomas in mice compared with free doxorubicin [80]. The correlation between molecular weight of HPMA and tumor accumulation was studied as well [82,83]. Higher molecular weight allows longer blood circulating time and higher accumulation in the tumor, liver and spleen. The molecular weight of PK1 is correlated with high tumor accumulation and low accumulation in other tissues. In a study using A2780 human ovarian carcinoma in mice, PK1 showed 45–250 times higher accumulation in the tumor than that in the other tissues (liver, kidney, lung, spleen, and heart) [81]. Remarkably, the accumulation of PK1 in normal tissues was 6–50 times lower than that of free doxorubicin over 30 days.

Due to decreased distribution of PK1 in normal tissues, PK1 significantly improves the doxorubicin toxicity profile [85,86]. Regarding cardiotoxicity, rat models given free doxorubicin or the mixture of free doxorubicin and HPMA showed decreased cardiac output and heart rate, while rats given PK1 showed no significant change even in histological examination [85].

The efficacy studies of PK1 have been conducted using various ascites tumor models: (L1210 murine lymphocytic leukemia, B16F10 murine melanoma, Walker sarcoma, P388 murine leukemia, M5076 murine reticulum cell sarcoma, LS174T human colon adenocarcinoma, and A2780 multidrug resistant human ovarian carcinoma [19,72,81,84]). In all models, PK1 demonstrated greater efficacy compared to free doxorubicin. Moreover, PK1 was effective in both the sensitive and drug resistant A2780 xenograft models, decreasing the tumor size to 3.5 and 5.6% of the initial size, whereas free doxorubicin was effective in only the sensitive model and decreased tumor size by about 33.3% [81,84]. In addition to avoiding excretion by P-glycoprotein, the result was partially accounted for by decreasing the permeability of blood vessels and creating a more homogeneous drug distribution. Generally, doxorubicin increases the permeability of blood vessels by up-regulation of the VEGF gene and enhances the accumulation in the same location. This results in heterogeneous distribution of doxorubicin in a tumor. In contrast, PK1 decreases the permeability of blood vessels by down-regulation of VEGF gene and prevents excess accumulation in dead cells. This resulted in a more homogeneous distribution of nanoparticles in murine tumors [81,84].

2.2.2. Clinical studies

Phase I and II clinical studies were conducted in thirty-six and sixty-two patients with non-small cell lung cancer (NSCLC), colorectal cancer, and breast cancer in the United Kingdom [87,88].

Pharmacokinetic results showed a profile similar to that of preclinical studies. Blood circulating time was prolonged in PK1; the distribution half-life was 1.8–3.0 h while free doxorubicin was only several minutes.

Tissue distribution was also examined using the ^{131}I-labeled analog for gamma camera imaging. Minimal accumulation of PK1 in the liver, kidney, and tumor was observed after 24 h. Only six patients showed accumulation in the tumor in phase I studies [87] and there was no evidence of tumor accumulation in phase II studies [88].

PK1 showed no polymer-related toxicity and a significant decrease in dose-limiting toxicity caused by doxorubicin. Cardiotoxicity was not observed even when a cumulative dose of PK1 reached 1680 mg/m^2 (doxorubicin equivalent), despite a cumulative dose of doxorubicin which most frequently causes cardiotoxicity is 450–550 mg/m^2 [87].

Regarding efficacy, PK1 demonstrated only two partial and two minor responses in thirty-six patients with NSCLC, colorectal cancer and breast cancer in phase I studies [87]. However, it is notable that PK1 showed activity in the cancer considered resistant/refractory to conventional chemotherapy and can be interpreted as a proof of concept that drug-polymer conjugations may be advantageous in resistant cancers. In contrast, PK1 demonstrated 6 partial responses in forty patients with NSCLC or breast cancer in Phase II studies, but all patients that responded were anthracycline-naive or chemotherapy-naive patients [88]. Moreover, PK1 showed no activity in patients with colorectal cancer.

The pharmacokinetic results of PK1 of preclinical and clinical studies correlated. However, there seems to be a gap between preclinical and clinical studies on tissue distribution and efficacy.

3. Paclitaxel

Taxanes were discovered in the early 1960's as part of an NCI initiative to screen synthetic and natural compounds for anti-cancer activity. It was initially collected from the bark of the rare and highly noxious Pacific yew tree [89]. The clinical utility of the drug was limited until the 1990's due to both environmental concerns and the difficulty in formulating the highly insoluble compounds [90]. However, by the late 80's clinical trials for paclitaxel and a slightly more soluble taxane, docetaxel, were being conducted in earnest, and new methods for synthesizing the drug from the more common varieties of the yew plant brought the drug into common use [91]. Once brought to the market, taxanes had a significant impact on clinical therapies and were used as a first or second line therapy for numerous cancer types including lung, breast and ovarian cancers.

These drugs work by binding the beta-tubulin subunit and stabilizing the microtubules within the cell cytoplasm [92]. This prevents the microtubules from disassembling, even in the presence of signals normally causing catastrophe. The stabilized microtubules are unable to separate from the centromeres during mitosis which arrests the cell cycle and triggers apoptosis. Microtubules are capable of polymerizing stable microtubules even in the absence of guanosine triphosphate (GTP) [92].

Formulating paclitaxel and its counterpart for systemic administration proved to be a very difficult challenge. The drug contains a high number of fused rings and is very hydrophobic. To solubilize the drug, researchers turned to Cremophor® EL, an emulsifying compound closely related to Castor oil [93]. This formulation is marketed as Taxol®. Taxol sufficiently solubilized paclitaxel for systemic delivery and finally allowed paclitaxel to come to the market and provide a new standard of care for many cancer patients. This solubilizing agent, however, could be highly toxic causing many patients to have acute hypersensitivity reactions and limiting the allowable dosage for the patient [94]. Acute toxicities associated with the Cremophor EL formulation are managed by premedication in current practice. The limiting toxicity for paclitaxel therapies is generally neutropenia, which is managed by giving the patient granulocyte stimulating factor before treatment in an effort to prevent crashing neutrophil levels [95]. Docetaxel is a slightly more soluble member of the taxane family and has been somewhat useful in reducing this toxicity [96,97].

The current standard formulation of paclitaxel using Cremophor EL provides a low-hanging fruit for drug carrier technologies. Reformulating the drug in a less toxic carrier allows more of the drug to be used with less risk to the patient and improve outcomes without relying on EPR, targeted delivery or other characteristics of cancer drug delivery.

3.1. Abraxane®

Among the most successful second generation paclitaxel formulations is Abraxane®. Abraxane (Fig. 4) is indicated for metastatic breast cancer, non-small cell lung cancer, and has recently shown promise as a tool against pancreatic cancer [98–100]. It generated $385.9 million in 2011, which is expected to rise to $2 billion if Abraxane becomes standard care for pancreatic cancer [101]. Tens of thousands of patients have been treated with this formulation.

3.1.1. Preclinical studies

Preclinical evidence has suggested that albumin accumulates preferentially in tumors in comparison with surrounding tissue [102]. Multiple potential mechanisms have been invoked to explain the phenomena, including EPR and tumor protein targeting. However, the extent of albumin accumulation in clinical practice is still unknown and may or may not contribute to enhanced drug efficacy.

Fig. 5 shows the comparison of Abraxane and Taxol treatments in animal models [103]. For xenograft ovarian and breast tumors, the difference between the two is indeed remarkable, showing p-values of 0.004 and 0.0001, respectively, with impressive numbers of mice surviving tumor free for the duration of the study. The pharmacokinetic advantages were also significant though not dramatic compared with the pharmacokinetic changes in other drugs. The Abraxane formulation shows an approximately 50% reduction in AUC and a dramatic drop in maximum concentration (C_{max}). Interestingly, the volume of distribution and clearance rate significantly increased, indicating that Abraxane behaves more like a small molecule drug than Taxol [104].

3.1.2. Clinical studies

Abraxane utilizes the serum protein albumin to solubilize and carry the drug in circulation, the formulation is Cremophor free and clinical trials indeed indicated a reduction in acute toxicity in patients (Table 2) [98,105]. The reduction in toxicity allows Abraxane to be more aggressively dosed than Taxol. The recommended paclitaxel dosing for Taxol is 175 mg/m^2, compared to 260 mg/m^2 for Abraxane, though this leads to a total exposure AUC only 17% higher than Taxol

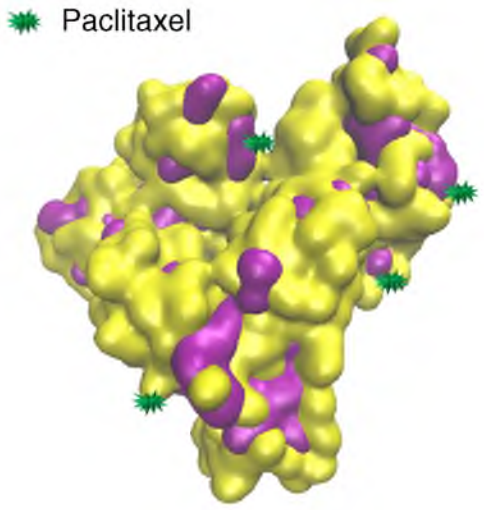

Fig. 4. Albumin-bound paclitaxel (Abraxane). Purple represents hydrophobic regions. Particle size 7 nm or 67 kDa (size of albumin protein). FDA approval 2005 for treating advanced metastatic breast cancer. Recommended dose is 260 mg/m^2 every 3 weeks while tolerated [186].

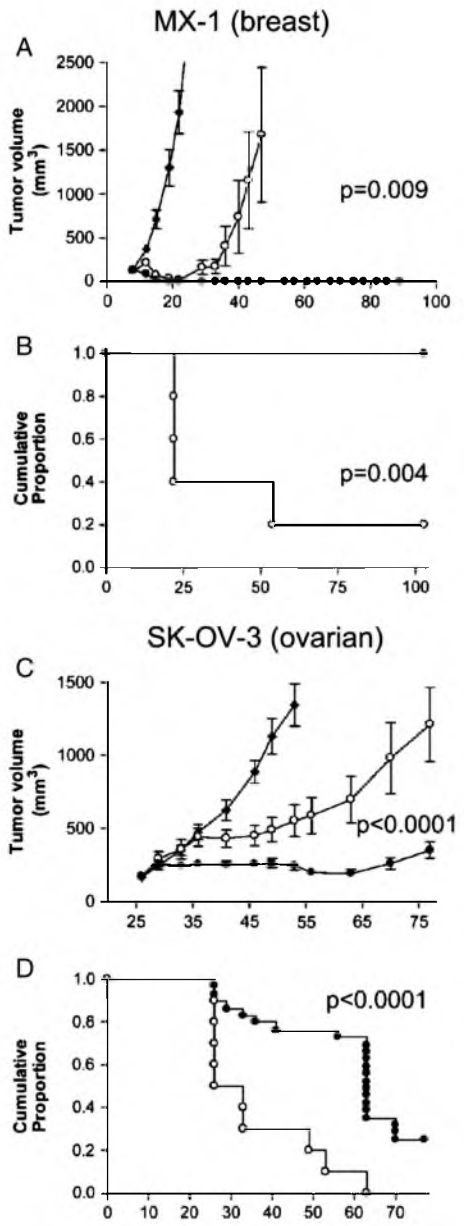

Fig. 5. Tumor volume and Kaplan–Meier analysis of tumors in two xenograft mouse tumor models treated with Abraxane (closed circles), Taxol (open circles), and untreated controls (closed diamonds). A & B MX-1 (breast tumor xenograft); C & D SK-OV (ovarian tumor xenograft).
Reprinted with permission from Desai *et al*: Increased antitumor activity, intratumor paclitaxel concentrations, and endothelial cell transport of cremophor-free, albumin-bound paclitaxel, ABI-007, compared with cremophor-based paclitaxel. Clin Cancer Res 12:1317-1324, 2006. Copyright 2006 by the American Association for Cancer Research [103].

Table 2
Summary of toxicities for various paclitaxel-based cancer treatments.

Drug	Taxol [104]		Abraxane [97]		NK105 [105]		Xyotax [106]		Genexol-PM [107]	
Paclitaxel dose	175 mg/m2		260 mg/m2		150 mg/m2		210 mg/m2		300 mg/m2	
	All	Severe	All	Severe	All	Severe	All	Severe	All	Severe
Neutropenia	82	22	80	9	91	65	21	14	71	46
Anemia	–	–	33	1	54	12	17	5	19	3
Platelet	3	1	2	1	28	0	7	2	2	0
Nausea	22	1	30	3	28	0	33	4	70	3
Vomiting	10	1	18	4	–	–	19	2	52	3
Diarrhea	15	1	26	1	23	0	16	1	25	2
Fatigue	39	3	47	8	58	4	27	6	7	3
Arthralgia	49	4	44	8	46	2	12	<1	29	7
Myalgia	49	4	44	8	60	0	–	–	54	6
Neuropathy	56	2	71	10	65	2	50	19	71	13
Alopecia	94	N/A	90	N/A	88	N/A	9	N/A	81	N/A
AST	32	N/A	36	N/A	32	N/A	–	–	–	–
Hypersensitivity	12	2	4	0	–	–	–	–	7	4

[106]. Directly comparing these numbers can be difficult, however, because the ratio of free to bound paclitaxel will be different for each formulation. Lower toxicity also allows Abraxane to be administered in a fraction of the time that Taxol is (30 min *vs.* 3 h) and without premedication to mitigate acute side effects [105].

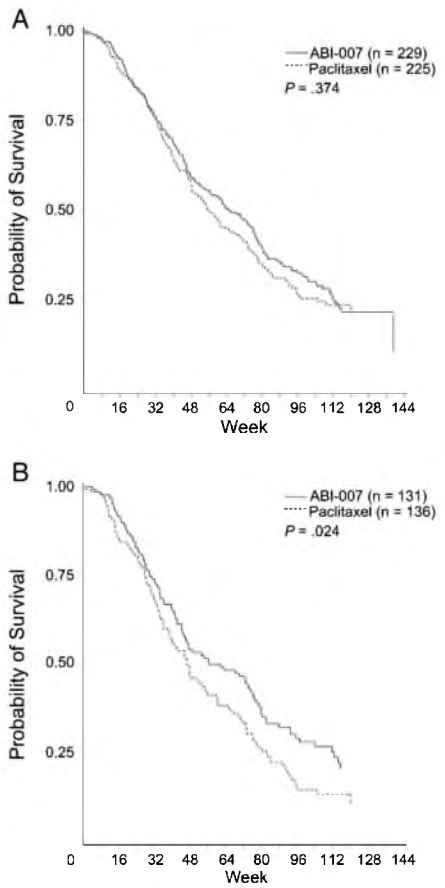

Fig. 6. (A) Patient survival over time. (B) Patient survival over time in patients who received second-line or greater therapy. P values from log-rank test. Survival indicates time from first dose of study drug to date of death.
Reprinted with permission. © 2005 American Society of Clinical Oncology. All rights reserved. Gradishar, W. *et al*: J Clin Oncol 23(31) 2005: 7794-7803.

Abraxane does seem to have clear efficacy gains compared to Taxol. On average, the median time to disease progression was approximately five weeks longer for Abraxane treatment than Taxol ($p = 0.006$), while quality of life (QOL) measurements were basically steady. Overall survival did not differ significantly between Taxol and Abraxane (Fig. 1) as a front line therapy, though as a second line therapy Abraxane appeared to extend life by nearly ten weeks ($p = 0.024$) [106]. Toxicity also did not differ significantly (Table 2).

While extending life five to ten weeks may seem paltry in terms of the overall tragedy of cancer, seeing any improvement over standard care does provide hope. It cannot be construed, however, as anything more than an incremental gain or as a revolutionary technology. Especially in light of the tremendous promise Abraxane showed in preclinical studies.

Clinical and preclinical studies both indicate that albumin-conjugated paclitaxel enjoys an efficacy advantage over the Taxol formulation (see Figs. 5 and 6). This improvement is credited both to the higher dosage allowed by the elimination of the highly toxic Cremophor EL solubilizing agent and to tumor specific targeting *via* EPR and receptor-ligand targeting [107]. SPARC (secreted protein acidic and rich in cysteine) is a protein that appears to be up-regulated in many tumors. It is capable of interacting with albumin and potentially capable of increasing the retention of albumin bound drugs in the tumor [102]. Combined with EPR from a tumor's pathological vasculature, SPARC binding may help explain some of the improved efficacy of Abraxane, especially in preclinical studies. However, the relatively minor efficacy improvement in human patients may not require any more explanation than the increased paclitaxel dosage and availability compared to Taxol. Still, Abraxane showed greater efficacy gains than any other drug carrier for which phase III were available. Interestingly, paclitaxel would likely be bound to albumin when administered as a free drug. The Cremophor EL emulsion that is used in Taxol, however, may act as a micelle nanocarrier that can significantly alter the drug concentration compared to a non-formulated state [108,109]. Thus the improved efficacy of the Abraxane formulation over the Taxol in humans may be a result of Abraxane more closely approximating the free drug state than Taxol.

3.2. NK105

NK 105 (Fig. 7) is a micellar formulation of paclitaxel currently making its way through clinical trials in the United States. The micelles are formed using a diblock copolymer of PEG (hydrophilic) and polyaspartate (hydrophobic) modified to convert half the carboxylic groups to phenyl-1-butanol to create a more stable, hydrophobic core. Paclitaxel

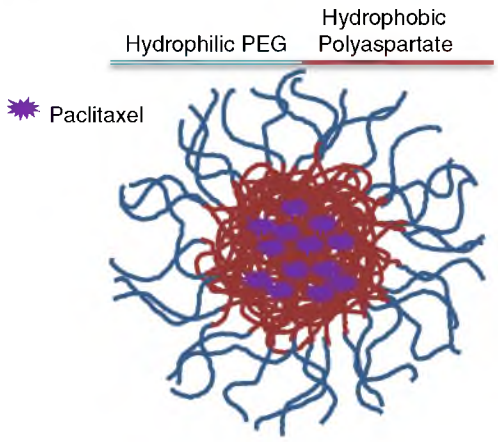

Fig. 7. NK105, micellar paclitaxel. Size range 20–430 nm, average size 85 nm. Not FDA approved but previously tested for use as second-line therapy for recurrent metastatic gastric cancer. Recommended dose is 150 mg/m^2.

loads into the core by hydrophobic interactions. The process is well controlled and creates micelles with an average diameter of 85 nm [110].

3.2.1. Preclinical studies

The PEG coating of the NK105 micelle radically alters the pharmacokinetics of the drug cargo. Preclinical studies indicated the paclitaxel AUC was 25 times higher for NK105 than for paclitaxel, with 4–6 times longer half-life and 3 times higher maximum concentration. Perhaps most impressive were the differences in intratumoral concentrations which were more than 100 times greater than paclitaxel after 72 h [110].

Preclinical trials showed remarkable promise for the NK105 paclitaxel formulation. In a one month study performed by Hamaguchi et al., escalating equivalent paclitaxel doses were administered using the NK105 and Taxol formulations. At every dose point tested, NK105 performed significantly better than free paclitaxel and at doses above 100 mg/kg, all mouse models receiving NK105 were completely cured (Fig. 8). Toxicity indicators did not appear significantly different between the two treatments, though neurotoxicity as measured by demyelination of nerve fibers was significantly less ($p < 0.001$) [110].

3.2.2. Clinical studies

Clinical trials indicated a ninefold increase in the AUC though a lower paclitaxel dose was used (150 mg/kg *vs.* 210 mg/kg) [111]. In spite of

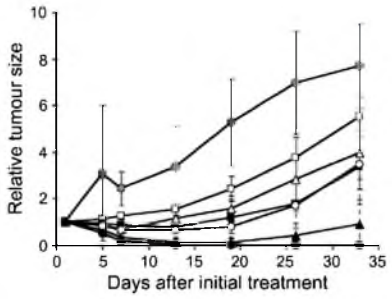

Fig. 8. Relative changes in HT-29 tumor growth rates in nude mice. (A) Effects of PTX (open symbols) and NK105 (closed symbols). PTX and NK105 were injected i.v. once weekly for 3 weeks at PTX-equivalent doses of 25 mg/kg (squares), 50 mg/kg (triangles), and 100 mg/kg (circles), respectively. Saline was injected to control animals (shaded circles). Reprinted by permission from Macmillan Publishers Ltd on behalf of Cancer Research UK: British Journal of Cancer [110], copyright 2005.

the large increase in overall drug exposure as measured by the AUC, neutropenia, the primary toxicity of paclitaxel, was slightly changed from the Taxol formulation. Other hematological toxicities also changed little from Taxol. Hypersensitivity reactions were markedly reduced as well.

At the time of writing, NK105 was being recruited for phase III trials, leaving only limited clinical efficacy data from the phase II trial. In the phase II study for NK105, as a second-line therapy for gastric cancer, the overall response rate (ORR) was 25% with the 95% confidence intervals between 14.4% and 38.4%. Other indicators were progression-free survival (PFS) and overall survival (OS) which came in at 3.0 months and 14.4 months, respectively. Though the phase II study did not use a comparator, we may consider trials of other drugs and drug combinations to give a rough idea of how these values compare to existing treatments. Other trials using paclitaxel alone have yielded ORRs of 17–23% [112]. The recommended frontline treatment for gastric cancer is a combinational therapy using epirubicin, cisplatin and continuous infusion of 5-FU (ECF) [112]. Studies of previously untreated advanced gastric cancers have yielded ORRs as high as 71%, but generally above 40% [113–115]. If frontline treatment fails there are still numerous other combinational therapies from which to choose to treat the recurrent cancer [112,116].

While upcoming phase III trials may show greater efficacy gains of NK105 over paclitaxel or currently available combinatory therapies against recurrent cancer, early evidence indicates that the ORR of the drug is unrelated to the orders-of-magnitude improvement in intratumoral drug accumulation seen in preclinical studies.

3.3. Genexol-PM®

Genexol-PM® is a polymeric micelle composed of a diblock copolymer of monomethoxy PEG-*block*-poly(D,L-lactide) (mPEG-PDLLA) (Fig. 9). The micelles are formed by the solid dispersion technique and form stable structures ranging from 20 to 50 nm in diameter [117]. The formulation is in numerous clinical trials including a phase IV trial for metastatic breast cancer.

3.3.1. Preclinical studies

Preclinical pharmacokinetic studies showed a unique drug distribution pattern. In a preclinical study, the paclitaxel dosage for the Cremophor EL formulation was 20 mg/kg and the micelle formulation

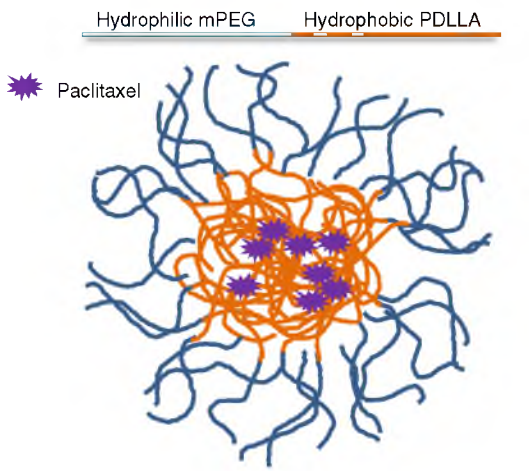

Fig. 9. Genexol-PM. Size range 20–50 nm. In phase III trials as second-line therapy for recurrent metastatic breast cancer. Recommended dose 300 mg/m^2 paclitaxel equivalent.

was dosed at 50 mg/kg. In spite of the lower dosage of the Taxol and the pegylation of the micelle, the AUC of the Genexol-PM formulation was nearly 30% lower than Taxol. In spite of the lower AUC, the drug accumulation was higher in all sampled tissues including a nearly 100% increase in tumor accumulation. At equivalent doses the AUC could be an order of magnitude lower yet still more than double tissue concentrations [117]. The unique pharmacokinetics of the Genexol PM formulation may simply be a result of the relatively unstable nature of the mPEG-b-PDLLA copolymer micelle, which appears to substantially release the drug into the bloodstream very soon after administration. This allows the drug to be cleared much more rapidly, but the higher overall dose allowed for greater tissue accumulation. When equivalent paclitaxel doses were administered, the tissue exposure remained the same in spite of the fact that the AUC of the Genexol-PM formulation was an order of magnitude lower.

Preclinical studies proved Genexol-PM to be remarkably capable at producing complete tumor remission in mouse models. One study done on athymic mice bearing MX-1 human breast tumor xenograft showed Genexol-PM administered at the maximum tolerated dose (MTD) of 60 mg/kg was able to produce complete remission in all tumors while Taxol at 20 mg/kg was only able to delay tumor growth for approximately 14 days, after which growth resumed as quickly as without treatment. The authors indicated that the increased efficacy is likely due to the significantly lower toxicity, allowing a dose three times higher than could be achieved with Taxol. A similar protocol with a SKOV-3 human ovarian cell line xenograft tumor also showed a marked improvement over Taxol. While Taxol was only able to slow tumor growth, Genexol-PM significantly reduced the tumor mass and caused complete remission in some mice, giving an overall delay in tumor progression of nearly six weeks (Fig. 10) [117].

3.3.2. Clinical studies

As in the preclinical trials, early clinical studies showed that the AUC of Genexol-PM was consistently lower than Taxol. Reduced toxicity allowed a much higher dose of paclitaxel to be administered than was possible for Taxol (300 mg/m^2). In clinical studies the AUC and plasma half-life of Genexol PM remained well below that of Taxol [118]. This can be explained by the instability of the PEG-PDLLA micelles, which can break up soon after administration, allowing the paclitaxel to be carried in the blood as a small molecule drug.

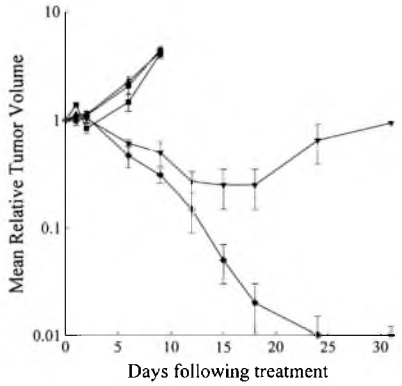

Fig. 10. Antitumor efficacy of Genexol®-PM and Taxol® on Tac:Cr:(NCr)-nu athymic mice bearing MX-1 human breast tumor xenograft. Tumors were allowed to establish and mice were treated on 3 consecutive days with saline (•), Taxol® vehicle (■), Genexol®-PM vehicle (▲), Taxol® 20 mg/kg (▼) or Genexol®-PM 60 mg/kg (♦). Each point represents a mean ± S.D. Reprinted from J. Control. Release 72 (1-3) S. W. C. Kim, D. W. Kim, Y. H. Shim, J. S. Bang, H. S. Oh, and M. H. Seo, In vivo evaluation of polymeric micellar paclitaxel formulation: toxicity and efficacy, 191–202, Copyright 2001 with permission from Elsevier.

Samyang has conducted or is currently conducting numerous clinical trials for Genexol-PM covering multiple indications and often in combination with small molecule drugs. The toxicity profile of the drug from phase II studies is generally in line with the paclitaxel formulations previously discussed, though at a much higher dose (Table 2). A phase IIb study of Genexol PM in combination with cisplatin to treat non small cell lung cancer was able to show only non-inferiority providing progression free survival and overall survival curves that were nearly identical to the paclitaxel + cisplatin controls (Fig. 11). Toxicity was also substantially similar for both treatments, though neutropenia was greater in the Genexol-PM + paclitaxel formulation. Progression free survival for the Genexol PM + cisplatin formulation was 5.4 months compared to 5.5 months for free paclitaxel + cisplatin and overall survival was one month longer for the former [119].

Genexol-PM seems to provide another case of a seemingly revolutionary drug becoming rather ordinary during clinical trials. The formulation allows a much higher paclitaxel dose to be administered without increasing the toxicity, but the higher dose apparently fails to provide greater efficacy. Samyang is still pursuing FDA approval for the drug, which may be granted on the same basis as Doxil, based on an altered toxicity profile making it more suitable for a subset of patients.

3.4. Xyotax™

Xyotax™ (Fig. 12), paclitaxel poliglumex (PPX) was among the most promising of the second generation paclitaxel formulations. The formulation grafts paclitaxel in a comb-like pattern to a linear polymer of L-glutamic acid using a degradable linker. The link between the paclitaxel and the polymer backbone effectively disables the active site of the taxane drug rendering it inert until it is released from the conjugate. Because the link is relatively stable, drug release tends to happen slowly. The total size of the conjugated system is approximately 48 kDa, of which more than a third is the paclitaxel drug.

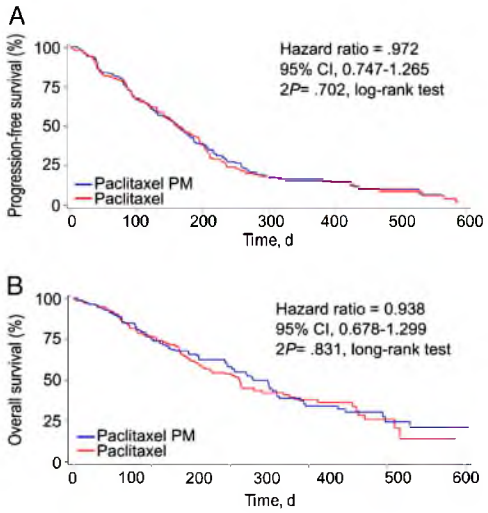

Fig. 11. PFS and OS among the study patients. (A) Kaplan–Meier curves for PFS in the Intent-to-Treat (ITT) Population (2P = .70). (B) OS in the ITT Population (2P = .83). Blue represents Genexol-PM + cisplatin and red represents paclitaxel + cisplatin.
Reprinted from Clin. Lung Cancer 14(3), S. Y. Lee, H. S. Park, K. H. K. Y. Lee, H. J. Kim, Y. J. Jeon, T. W. Jang, Y. C. Kim, K. S. Kim, I. J. Oh, and S. Y. Kim, Paclitaxel-loaded polymeric micelle (230 mg/m(2)) and cisplatin (60 mg/m(2)) vs. paclitaxel (175 mg/m(2)) and cisplatin (60 mg/m(2)) in advanced non-small-cell lung cancer: a multicenter randomized phase IIB trial, 275-282, Copyright 2013, with permission from Elsevier. (For interpretation of the references to color in this figure legend, the reader is referred to the web version of this article.)

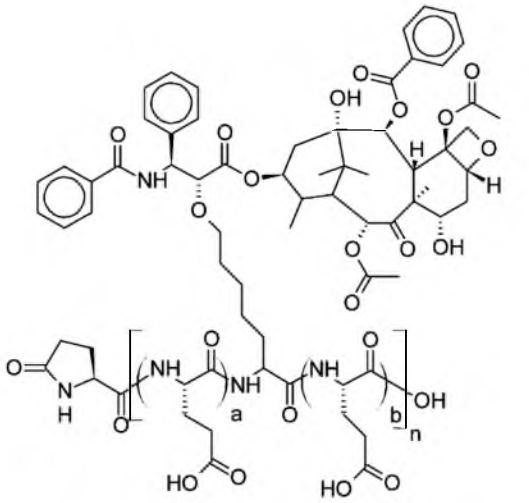

Fig. 12. Paclitaxel poliglumex (PPX; Xyotax). Size range 40–50 kDa. Not FDA approved. Under investigation to treat NSCLC. Recommended dose 210 mg/m^2 paclitaxel equivalent.

3.4.1. Preclinical studies

As with other drug carriers, the poliglumex formulation can drastically alter the pharmacokinetic profile of the drug. Due to the stable binding of paclitaxel to the polymer backbone, the patient exposure to the bioactive drug can be quite low even when the total paclitaxel dose becomes very high. Preclinical pharmacokinetic studies using equivalent paclitaxel doses in mice showed that even with a twelvefold increase in total AUC for poliglumex in comparison with Taxol (due to slower clearance), the plasma exposure to active taxane was more than sixteenfold less. Intratumoral exposure to active drug, on the other hand, was nearly double that of the Taxol formulation. On the surface, this result shows great potential for improving efficacy while drastically reducing systemic drug exposure and toxicity, but the slow release of the drug into surrounding tissue could drive high drug concentrations in tissues other than the tumor by a similar mechanism.

Early preclinical studies showed great promise for the PPX formulation to improve anti-tumor efficacy of paclitaxel for some cell lines. In one study by Li et al., PPX at a dose of 40 mg/kg effected complete regression in OCA-1 ovarian and 13762F breast cancer tumors in mice, whereas free paclitaxel was only able to suppress growth for approximately ten days after which growth resumed [120]. The formulation did not appear to be so successful in all cell lines. HCa-1 hepatocarcinoma tumors were only marginally slowed by PPX at a dose of 80 mg/kg, though a statistically significant gain was seen over free paclitaxel administered at 800 mg/kg. Efficacy gains against FSa-II fibrosarcoma tumors were similarly modest [121].

3.4.2. Clinical studies

Phase I clinical studies determined the MTD for PPX to be 233 mg/m^2 given in three week doses. At that level, the AUC of bound taxane was 1583 mg·h/L with a half-life of approximately 120 h. Exposure to free paclitaxel was significantly less, only 27.8 mg·h/L, a nearly sixtyfold decrease between total dose and available paclitaxel. This result proved similar to the preclinical results which also showed a large increase in total AUC, even while exposure to the active drug declined.

The success of PPX in eradicating some types of tumors in preclinical studies helped fuel a large number of clinical trials, many of which progressed to phase III [21,122–125]. Xyotax generally shows less toxicity than other paclitaxel formulations; neutropenia and alopecia, in particular, showed marked improvement with the poliglumex formulation. Neuropathy on the other hand, was increased in comparison with the docetaxel standard used in the study [21].

At least six phase III clinical trials were launched with Xyotax, based on enthusiasm from preclinical and early clinical results. A few trials were based on administering PPX alone, and several others tested PPX in combination with other drugs. A large portion of these studies were completed in 2008 leaving a wealth of efficacy data. Almost all of this data indicates that PPX is no more efficacious than the comparative treatment. A phase III study comparing either PPX or paclitaxel in combination with carboplatin against NSCLC. This study failed to show any benefit of PPX over paclitaxel; overall median survival for the PPX group was 7.9 months and 8 months for the paclitaxel group, similarly the time to progression was 3.9 months and 4.6 months, respectively. Neither of these differences was statistically significant. Toxicities differed somewhat between the two treatments, with patients receiving PPX experiencing less cardiac toxicity, alopecia and muscle toxicity, but more nausea and vomiting [124].

Another trial for treating NSCLC using PPX alone and comparing with single agent docetaxel yielded similar results, the docetaxel treatment is ostensibly better than the PPX. Overall median survival for both was 6.9 months, though median time to progression was 2.6 months for docetaxel and 2.0 months for PPX. Again, toxicities differed only slightly with neutropenia being more common in patients receiving docetaxel and neuropathy being more common in patients receiving PPX [21]. A third trial published in 2008 comparing single agent PPX with single agent control (gemcitabine or vinorelbine) for treating NSCLC yet again tells the same story. The study showed similar overall median survival times between the experimental and control groups (7.3 months *vs.* 6.6 months), similar time to progression (2.9 months *vs.* 3.6 months), and slightly different toxicities (improved hematological and gastrointestinal effects but worsened neuropathy) [122].

Xyotax is a fairly simple drug carrier that packages paclitaxel in a slow releasing formulation. The goal is to allow the nanoparticle form of the drug to accumulate in a tumor *via* EPR then slowly release the drug in the tumor while sparing the rest of the body drug exposure. The approach was largely successful in preclinical trials, causing complete remission of some tumors in mice, though success was limited in other cell lines. As with other drug formulations, clinical trials did not bear out the promise of preclinical studies. All three clinical trials reported show no significant difference in efficacy, in spite of the radically different pharmacokinetic profile of the formulation.

4. Cisplatin

Cisplatin, cis-diamminedichloroplatinum (II), cis-[$PtCl_2(NH_3)_2$] (CDDP) is the first anti-cancer drug containing inorganic platinum and one of the most widely used anti-cancer drugs. In the 1960s, Barnett Rosenberg unexpectedly discovered the inhibition of cell division by platinum salts from "inert" platinum electrodes [126–128] and its potent anti-cancer activity was revealed in sarcoma 180 and leukemia L1210 in mice [129,130].

The anti-cancer activity of cisplatin is given by crosslinking DNA [131]. Cisplatin forms highly reactive and charged platinum complexes which bind to nucleophilic groups, such as guanine and cytosine in DNA and form intrastrand and interstrand DNA cross-links, as well as DNA-protein crosslinks. These cross-links result in apoptosis and cell growth inhibition. Since approved for use in testicular and ovarian cancers by the FDA in 1978, cisplatin is widely used to treat various malignancies (bladder cancer, cervical cancer, malignant mesothelioma, non-small cell lung cancer, ovarian cancer, squamous cell carcinoma of the head and neck, and testicular cancer) [132]. However, the major toxicity of cisplatin therapy is irreversible nephrotoxicity, which has been recognized in rats as early as 1971 [133]. Cisplatin accumulates in proximal tubular epithelial cells by both active and passive uptake. The active uptake is mediated by organic cation transporter (OCT2) and is especially recognized as a critical pathway for accumulation in proximal tubules

[134]. Nephrotoxicity was a serious obstacle during clinical trials and remains a major dose-limiting toxicity. To reduce nephrotoxicity, patients are hydrated excessively pre- and post-treatment and associated inconveniences can decreases their quality of life (QOL) [135]. Cisplatin therapy also causes neurotoxicity, gastrointestinal toxicity (nausea and vomiting), hematological toxicity and ototoxicity [136]. Ototoxicity is usually bilateral, irreversible, and cumulative. Audiological studies have indicated that up to 90% of the patients treated with cisplatin experience significant hearing loss, especially at high frequencies [137,138]. Various types of cisplatin analogs (carboplatin, oxaliplatin, satraplatin, and picoplatin) have been developed to reduce these toxicities [139–141]. Furthermore, its anti-tumor activity is limited by various types of resistance such as increased efflux, inactivation by sulfhydryl molecules (*e.g.*, glutathione), and increased DNA repair [142].

4.1. NC-6004

As early as 1996, cisplatin-incorporated polymeric micelles using PEG-poly amino acid block copolymer has been developed to decrease cisplatin's toxicity [143–146]. NC-6004 (Fig. 13) was first introduced in 2003 [147] and is currently undergoing phase II clinical trials. NC-6004 consists of the block copolymer, PEG which constitutes the outer shell and poly(glutamic acid) which constitutes the inner core. The cisplatin drug forms a complex with the carboxyl group of poly(glutamic acid) in this formulation. NC-6004 is clearly distinguished from typical micelles consisting of an amphiphilic polymer. The micelle formation is driven by the ligand substitution of platinum (II) from chloride to carboxyl groups of glutamine. The molar ratio of cisplatin to the carboxyl groups in the copolymers was 0.71. The size is around 30 nm with a narrow distribution. NC-6004 is remarkably stable in distilled water and it dissociates into unimers accompanied by cisplatin release in chloride-rich solutions. The high stability is assumed to be allowed by the rigid structure stabilized by interpolymer cross-linking by Pt(II) atom.

4.1.1. Preclinical studies

NC-6004 shows significantly prolonged blood circulating time compared with cisplatin in rats [148,149]. Using frameless atomic absorption spectrophotometer (FAAS) to detect elemental platinum, it was found that free cisplatin was detected in plasma only up to 4 h after i.v. injection while cisplatin delivered by NC-6004 was detected up to 48 h after i.v. injection. The AUC and C_{max} of elemental platinum in the rat treated with NC-6004 are 65 times and 8 times greater, respectively, compared with cisplatin treatment. Furthermore, total body clearance and volume at steady state of NC-6004 are significantly lower than that of cisplatin. These findings are accounted for by the "stealth effect" seen in pegylated nanoparticles.

As mentioned in the introduction of cisplatin, it accumulates in the kidney within 1 h after i.v. injection in the rat. In contrast, NC-6004 shows relatively high accumulation in the liver and the spleen instead of the kidney, and highest accumulation is seen at 48 h after i.v. injection [148,149]. The maximum concentration of platinum in the kidney is 3.8-fold lower for NC-6004 than for cisplatin. Tumor accumulation was examined using a xenograft model of MKN-45 human gastric carcinoma in mice. Although C_{max} is observed 10 min after i.v. injection of cisplatin, NC-6004 shows 3.6 fold higher C_{max} than cisplatin at 48 h after i.v. injection. These results are consistent with the prolonged blood circulating time in pharmacokinetics results.

Nephrotoxicity (dose limiting toxicity) and neurotoxicity were mainly studied using rats [148–150]. Seven days after injection of cisplatin or NC-6004, the concentration of blood urea nitrogen (BUN) and creatinine, assessors of kidney function, was increased only in rats treated with cisplatin. Moreover, 4 of 12 rats treated with cisplatin died while no deaths were observed in the rats treated with NC-6004. Histological studies using TUNEL assay also revealed the significant decrease of nephrotoxicity of NC-6004 compared with cisplatin [150].

Neurotoxicity was examined by electrophysiological methods. There was no delay of sensory nerve conduction velocities observed in the rats treated with NC-6004 although a significant delay was observed in the rats treated with cisplatin. Additionally, NC-6004 shows significantly

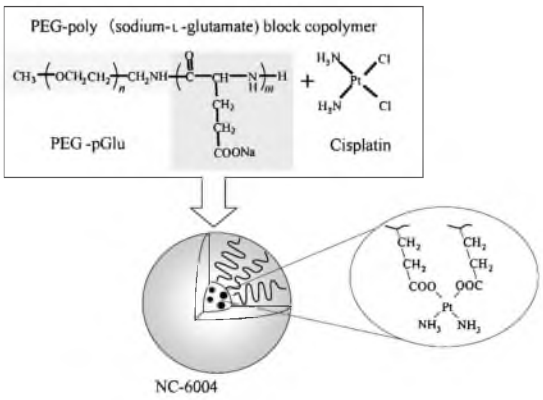

Fig. 13. Cisplatin incorporated polymeric micelle (NC-6004). Particle size is around 50 nm. Developed by Nanocarrier. Yasuhiro Matsumura, Polymeric Micellar Delivery Systems in Oncology, Japanese Journal of Clinical Oncology, 2008, 38, 12, 793–802, by permission of Oxford University Press [187].

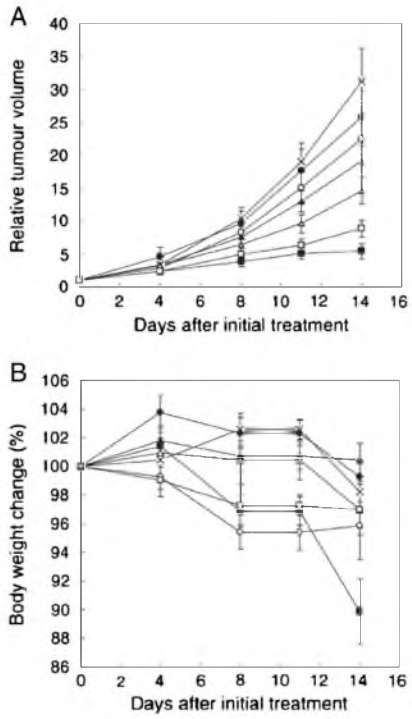

Fig. 14. Relative changes in MKN-45 tumor growth rates in nude mice. (A) Cisplatin and NC-6004 were injected i.v. every 3 days, three administrations in total, at CDDP-equivalent doses of 0.5 mg/kg (●, ○), 2.5 mg/kg (▲, △), and 5 mg/kg (■, □), respectively. Glucose (5%) was injected in the control mice (×). (B) Changes in relative body weight. Data were derived from the same mice as those used in the present study. Values are expressed as the mean ± S.E.
Reprinted by permission from Macmillan Publishers Ltd on behalf of Cancer Research UK: British Journal of Cancer [148], copyright (2005).

lower accumulation of platinum in the sciatic nerve compared with cisplatin in histological examination. These results clearly revealed NC-6004's improved toxicity compared to cisplatin.

Recently another serious toxicity, ototoxicity, was studied in guinea pigs [151]. Auditory brainstem responses to sound stimulation of various frequencies were examined before and after treatment with NC-6004 or cisplatin. Although cisplatin induced a threshold shift of auditory brainstem response, particularly at high frequency, NC-6004 showed no apparent threshold shifts.

NC-6004 significantly inhibits the xenograft tumor growth of MKN-45 human gastric carcinoma in mice [148] and OSC-19 oral squamous cell carcinoma in mice [150], but there was no significant difference from the cisplatin at the same dosage. Additionally, significant weight loss was observed in the mice treated with cisplatin. On the other hand, the mice treated with NC-6004 did not show as much weight loss as the mice treated with cisplatin which is accounted for by the difference of toxicity profile between the two formulations (Fig. 14).

4.1.2. Clinical studies

A phase I study was conducted with seventeen patients that had various advanced solid tumors (lung, colon, hepatic cell, mesothelioma, esophagus, pancreas, melanoma, and renal cell) in the UK starting in the year 2000 [152]. NC-6004 was administered intravenously every 3 weeks. The dose escalation started at 10 mg/m^2 and reached 120 mg/m^2.

The pharmacokinetics was examined at 120 mg/m^2. The C_{max} and AUC of total platinum in plasma were 11-fold higher than those of cisplatin, and 88% of those were due to intact micelle form. Therefore, C_{max} and AUC of active species of platinum in plasma are 35-fold smaller and 8.5-fold larger compared with the values of cisplatin from other clinical trials [153]. Consistent with these results, NC-6004 generally shows less severe and less frequent toxicities compared with cisplatin. No significant myelosuppression, ototoxicity, emesis, or neurotoxicity was observed. Although nephrotoxicity was mitigated, it was still observed in patients who received 120 mg/m^2 even with a pre- and post-treatment hydration regimen. Cisplatin therapy generally requires 8 h of hydration both before and after the cisplatin treatment to reduce nephrotoxicity. Therefore, low nephrotoxicity of NC-6004 is clearly advantageous over cisplatin due to increased QOL. On the other hand, unanticipated hypersensitivity was frequently observed and was related to all dose interruptions. The mechanism of hypersensitivity has not been determined yet. As for efficacy, seven out of seventeen patients showed stable disease status and the median progression free survival time was 49 days. However, neither complete nor partial responses were seen.

Remarkably, these clinical results generally correspond to preclinical results despite unpredicted toxicities such as hypersensitivity. It could be accounted for by the sustained release of platinum from NC-6004 which is promoted by chloride replacement unlike the designs of other drug carriers. It might prevent a significant increase of plasma concentration of active platinum that in turn decreases the toxicity. Still, released free active platinum in plasma could be functioning in the same manner as cisplatin.

5. Targeting moieties

One of the ways that drug carriers may improve cancer therapy is by targeted therapy. While many drug carriers claim targeting based on improved distribution profiles, this section will focus on drug carriers that have specific groups added to provide receptor-specific targeting functionality. Obviously, these targeted therapies cannot sense their target from a distance nor do they have any control over their own trajectory. Drug carriers that are designed to be targeted must rely on circulation in the blood stream and must rely on access to the cancer cells. Given access to the target, interactions between the drug and the cancer cell can be increased with targeting moieties. Targeting moieties present on the drug carrier can be antibodies that bind to a specific antigen or they can be various biological molecules that have been shown to interact with receptors on certain cell types. Essentially, enabling receptor-ligand binding between the drug and the target increases the likelihood of the drug being in the presence of the desired target. The most common and most successful (in terms of FDA approval) method of receptor-ligand binding involves the use of antibodies. Some of these antibodies act as a drug when binding their ligand (antigen), others are linked to a drug such as with antibody-drug conjugates. Antibodies are excellent tools for providing mechanisms of binding. They can be selected to have high specificity and affinity for their target ligand. However, care must be taken to select the correct ligand target. It is difficult to find binding targets that are unique to cancer cells. Often, therapies have to rely on overexpression of certain proteins by cancer cells. Care must also be taken in the selection of an appropriate linker to conjugate the drug to the drug carrier/targeting moiety. Beyond antibodies, there are numerous preclinical studies showing how adding targeting moieties to drug carriers such as polymers, liposomes, micelles, *etc.* will improve efficacy — many have even made it to clinical trials. However, they have yet to make a presence in the field of clinically approved drug carriers for targeted cancer treatment.

5.1. Mylotarg®

Mylotarg (Fig. 15) is the product name for gemtuzumab ozogamicin which is a humanized monoclonal antibody (hP67.6) against the CD33 antigen that is linked to a derivative of calicheamicin, an antibiotic that is toxic due to its ability to damage DNA [154,155]. Approximately 50% of the antibodies have about four to six drug molecules per antibody (the remainder of the antibodies are unconjugated). CD33 was chosen as a target because approximately 90% of AML patients have CD33+ leukemia cells and because it is internalized upon binding [156,157]. Following encouraging phase II trials, it gained accelerated approval to address an unmet medical need for relapsed AML [154,155].

5.1.1. Preclinical studies

In vitro and *in vivo* studies tested various linkers joining the P67.6 antibody (not yet humanized for preclinical studies) with the calicheamicin drug derivative. The *in vivo* studies used HL-60 human

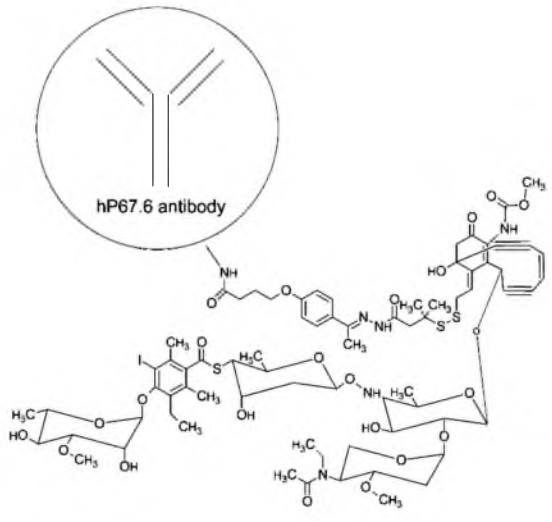

Fig. 15. Mylotarg/gemtuzumab ozogamicin. Size range: 5–20 nm or 151–153 kDa. Binding site: CD33. FDA approved in 2000 and withdrawn in 2010. Indicated for CD33 positive acute myeloid leukemia. Recommended dose is 9 mg/m^2 i.v. over 4 h and repeated in 14 days. Company: Pfizer.

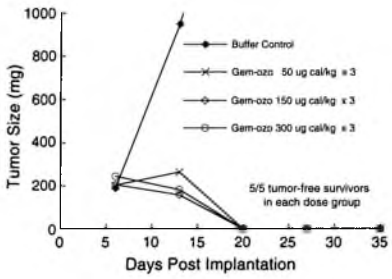

Fig. 16. Complete cure rates in mice for various dose strengths of Mylotarg. Reprinted with permission from Bioconjug. Chem. 13(1) Hamann P. et al. 47-58, 2002. Copyright 2002 American Chemical Society.

promyelocytic leukemia cells implanted subcutaneously into athymic mice and found a formulation that showed a complete inhibition of tumor growth but was only compared to a buffer control. Unfortunately, that formulation was abandoned due to an unexpected problem with sensitivity to periodate oxidation after humanizing the P67.6 antibody [158]. A new formulation with a bifunctional linker was chosen and named gemtuzumab ozogamicin. *In vivo* studies found the formulation to be effective with complete inhibition of HL-60 xenografts in mice when tested at various doses (Fig. 16) [159].

A summary of preclinical trials boasts selective *in vitro* activity against a CD33+ cell line when treatment was compared in cells not expressing the CD33 antigen. When administering 6 weekly doses up to 7.2 mg/m^2 in mice and 22 mg/m^2 in monkeys, myelotoxicity and toxicity in the liver, kidney, and testes were present, though not lethal. Preclinical studies also showed that Mylotarg distributed preferentially to the liver and the major excretion pathway was biliary [154].

5.1.2. Clinical studies

Phase I trials used a dosing interval of 2 weeks, as the half-life of the drug is over 3 days. It was found that three biweekly doses caused myelosuppression, thus, most received only two doses. The major toxicity found in phase I trials was myelosuppression (neutropenia and thrombocytopenia) because CD33 is expressed on myeloid progenitor cells [154]. The dose limiting toxicity was stated to be neutropenia. Other complications were fever, nausea, chills, leukopenia, vomiting, rash, and pain. Furthermore, some patients developed antibodies against Mylotarg after 2–3 doses. While testing the safety of various doses in the phase I trial, two out of forty-one patients (one dosed at 1 mg/m^2 and the other at 4 mg/m^2) achieved a complete response (CR) defined by transfusion independence and clearance of leukemic blasts as well as a recovery of hemoglobin, neutrophils, and platelets. Seven patients (dosed at 5, 6, and 9 mg/m^2) had clearance of leukemic blasts but not a recovery of their platelet count and were designated as a partial response (PR). The approval summary for phase I trials states that the hepatobiliary excretion pathway was not included in the pharmacokinetic studies and no mention was made of liver toxicity, despite evidence in preclinical studies. As only 50% of the antibodies are actually linked to the calicheamicin, the methods used to characterize the pharmacokinetics of Mylotarg may be questionable. The data simply do not provide much information when the half-life of a 9 mg/m^2 dose of antibody varied greatly from 67 ± 37 h to 88 ± 58 h for the first and second doses, respectively. The AUCs for the antibody were also quite varied-ranging from 132 ± 136 to 243 ± 198 mg·h/L for the first and second doses. For comparison, the total calicheamicin half-life was found to be 39 ± 25 h for the first dose and 63 ± 63 h for the second dose. Finally, the AUC of total calicheamicin was 2.1 ± 1.8 mg·h/L for the first dose and 4.7 ± 4.1 mg·h/L for the second dose. Following the Phase I trial, the recommended phase II dose was 9 mg/m^2 i.v. over 2 h for two doses [154].

Table 3
Colony formation of patient-derived leukemic marrow cells in the presence of gemtuzumab ozogamicin [159].

	Concentration (ng/mL)[a]	Total no. samples	0–25% inhib	25–60% inhib	60–90% inhib	>90% inhib
Adult samples	2	27	17	6	3	1
	10	27	12	3	6	6
Pediatric samples	2	15	2	5	3	5
	10	5	0	1	1	3

[a] Concentration of N-acetyl-gamma calicheamicin dimethyl hydrazide. Antibody concentration is 40-fold greater.

The phase II trials consisted of 142 patients between three study groups labeled 201, 202, and 203. They used the recommended dose of 9 mg/m^2 and all 142 patients received at least one dose while 109 received two doses and 5 received 3 doses. The phase II studies saw 16% with a CR and 13% with a PR. The CR and PR were summed to 30% and termed as the overall response (OR) rate. Among these responders, the CR group had a relapse-free survival (RFS) of 7.2 months and the PR group had a RFS of 4.4 months, thus averaging 6.8 months for the OR group. Treatment was generally well tolerated except for cases of infusion related symptoms, fever, chills, hypotension, hypoxia, difficulty breathing, and bleeding. However, treatment caused tumor lysis syndrome in four cases with one resulting in death. Furthermore, in the phase II clinical trials the hepatotoxicity was evident with hepatic function abnormalities, bilirubin elevations, and transaminase elevations. Most cases were treatable, but one patient died of hepatic failure. However, by combining the CR and PR to form an impressive OR rate, there was enough evidence for efficacy and to gain a fast track approval [154].

5.1.3. Postmarketing data

The postmarketing data revealed some severe adverse events such as hypersensitivity reactions, pulmonary toxicity, and hepatotoxicity-especially veno-occlusive disease (VOD). A post-market phase III trial from 2004 to 2009 at the Southwest Oncology Group showed a poor response rate and adverse effects of Mylotarg plus various chemotherapies compared to traditional chemotherapies alone [160]. Not long after, on June 21, 2010, there was a FDA news release announcing that Pfizer voluntarily withdrew Mylotarg from the U.S. market [161]. A recent study completed in Germany showed a similar lack of improved efficacy. The CR rate for gemtuzumab ozogamicin therapy was 31% while standard care had a CR rate of 32%. While there may be some slight advantage in the relapse free survival, due to the improvements in preventing relapse, there is very little difference between the overall survival percentages. Unfortunately, this study also showed serious toxicities associated with the gemtuzumab ozogamicin therapy. There were eight induction deaths in the gemtuzumab ozogamicin group and three in the standard care and two of the induction deaths from the GO group had severe VOD as an underlying complication [162]. Another large randomized open-label trial in the UK produced results of lack of superiority in efficacy for those patients receiving gemtuzumab ozogamicin therapy. The survival percentage and relapse free survival percentages are shown in Fig. 17. It was only by separating patients with favorable cytogenics or prognostic index that benefits could be seen [163]. The gap present could be a matter of choice for the target. Inconsistent expression is much more prevalent in clinical cancers with a varied human population. Prior results from *ex vivo* studies on inhibition of colony formation were less than impressive compared to the *in vivo* studies on tumor growth suppression in mice (Table 3) [159]. Furthermore, liver toxicity was an issue and it is likely that Mylotarg was passively targeting the liver by targeting CD33+ cells of myeloid lineage (leukemia and others) in the liver sinusoids [164].

5.2. PK2

PK2 is an HPMA drug-polymer conjugate very similar to PK1 except that it has a galactosamine moiety added to target the liver (Fig. 18). The galactosamine moiety is a biomimetic ligand for the asialoglycoprotein

receptor found on differentiated hepatocytes; thus, this receptor is not uniquely expressed by hepatomas. Furthermore, depending on the state of differentiation of the cancer cells, expression can even exist at lower levels than healthy liver tissue [165]. Still, the hope was to induce more accumulation of the drug into the liver to treat hepatomas which is aided by the fact that liver physiology is conducive to accumulation of nanoparticles that rely on the EPR effect.

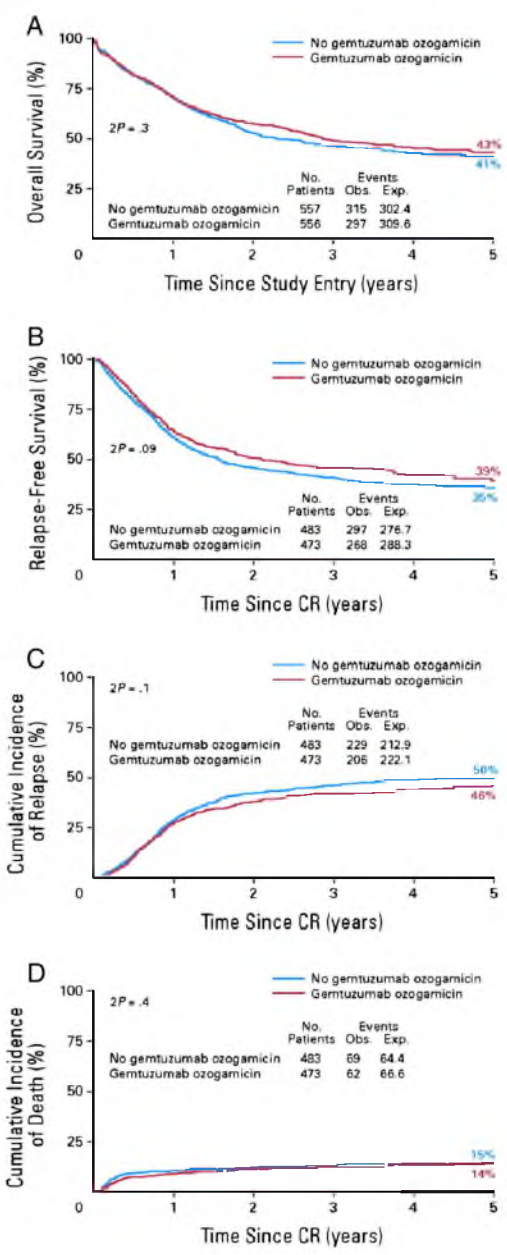

Fig. 17. An open-label trial involving 1113 patients that were randomly assigned whether or not to include gemtuzumab ozogamicin as part of their induction therapy. Broadly, there were only slight differences in overall survival (A), relapse-free survival (B), cumulative incidence of relapse (C), and cumulative incidence of death (D).
Reprinted with permission. © 2011 American Society of Clinical Oncology. All rights reserved.
Burnett, A. et al. J Clin Oncol 29(4) 2011 369-377.

5.2.1. Preclinical studies

Preclinical studies in mice have shown drastically faster blood clearance and higher liver uptake in formulations containing higher galactosamine content (4 mol% compared to 1 mol%). These studies showed formulations with greater than 80% of the ^{125}I-labeled dose accumulated in the liver [166]. Another preclinical study grew human colon carcinomas in the livers of nude mice. As the colon carcinoma does not have asialoglycoprotein receptors, radio labeled HPMA copolymer–doxorubicin–galactosamine conjugates were absent in tumor areas in the liver as shown by Fig. 19 [167].

5.2.2. Clinical studies

In the preliminary clinical study where a formulation of 1.0 mol% of galactosamine for PK2 was chosen, only 30% of the dose accumulated in the liver when scanned at 24 h following administration [168]. In the phase I clinical study they chose 1.5 mol% galactosamine for the PK2 formulation. However, this same study compared PK2 with PK1 (almost identical, save it has no galactosamine moiety) and planar gamma-camera imaging showed PK2 preferentially accumulating in the liver while PK1 was not [165]. Unfortunately, while it was accumulating in the liver, SPECT imaging showed it accumulating to a lesser degree in the cancerous regions of the liver likely lacking asialoglycoprotein receptors—where the treatment needs to go—and possibly explains why no efficacy gains were reported in clinical studies.

The AUC (from 0 to 192 h) at 120 mg/m^2 reached as high as 296 mg·h/L when administered by a 24 h infusion [165,168]. The MTD was found to be 160 mg/m^2 due to doxorubicin associated toxicity of myelosuppression, mucositis, and fatigue. The recommended dose for phase II trials was 120 mg/m^2. For comparison, the MTD of PK1 was higher at 320 mg/m^2 [87,165].

Some dated review articles state that PK1 is in phase I/II clinical trials; however, it is notably absent in lists of more recent review articles and government databases of clinical trials [13,169–171]. It may be safe to assume it has "quietly disappeared" after not performing as well in clinical studies.

5.3. CALAA-01

Another example of a targeted drug carrier uses siRNA as the delivered drug. The product name is CALAA-01 (Fig. 20) and the nanoparticle is the delivery vehicle Rondel™. It is composed of a linear polycationic polymer containing cyclodextrin and imidazole groups [172]. The imidazole groups are added to enhance unpacking and delivery of siRNA [173]. The cyclodextrin groups form a complex with hydrophobic adamantane (Ad) groups where each are conjugated to PEG alone or with a human transferrin (Tf) protein for targeting. The PEG is to help stabilize and minimize unwanted interactions (such as aggregation, protein binding, or macrophage uptake). They conjecture that these nanoparticles are able to take advantage of the tumor physiology to aid in intended tissue targeting [172]. Additionally, the Tf groups bind to Tf receptors that are found in a wide variety of malignant tissues [174,175]. Using siRNA to inhibit the expression of RRM2 results in an antiproliferative effect that could potentially treat a wide range of tumors [176].

5.3.1. Preclinical studies

In non-human primate studies, they tested the safety of the nanoparticles at doses of 3, 9, and 27 mg siRNA/kg. There was concern about the possibility of the PEG component causing hypersensitivity reactions, activating complement, or accelerating clearance from the blood. The results showed that there was some antibody formation only at the highest dosage, but that it was formed against the Tf protein on the drug carrier. Regardless of the dose, the majority of nanoparticles and siRNA had been cleared from plasma within 2 h. While ELISA

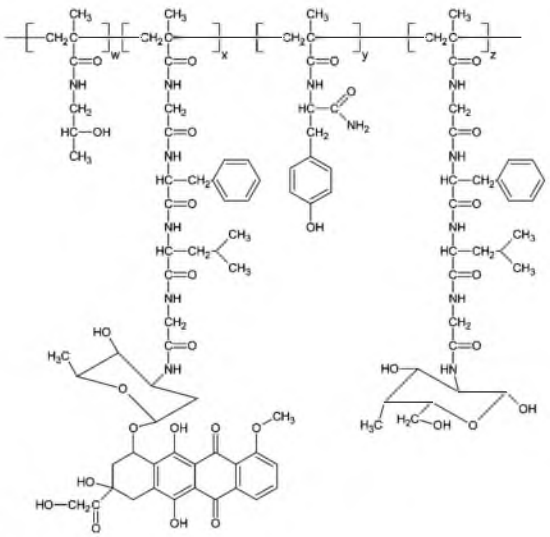

Fig. 18. PK2/FCE 28069. Size: about 27,100 Da. Binding site: Asialoglycoprotein receptor. Review articles state phase I/II FDA trials, though not currently found on clinicaltrials.gov. Indicated for hepatocellular carcinoma. The recommended dose is a 4 mg/kg loading dose with 2 mg/kg weekly doses or an 8 mg/kg loading dose with a 6 mg/kg dose every 3 weeks. Developed by Pharmacia which merged with Pfizer.

studies showed an increase in cytokine levels for IL-6, IL-12 and IFN-gamma, they saw no salient physiological signs of toxicity. However, the highest dose saw an increase in blood urea nitrogen and creatinine significant enough to indicate kidney toxicity. Researchers doubted the toxicity was due to siRNA; unfortunately, they did not test a formulation without siRNA as a control. Still, they suggested there was a large therapeutic index by reasoning that the equivalent effective dose found in mice was near 0.5–1.0 mg/kg and well below the 27 mg/kg that had some indicated toxicities [177].

In vivo studies in mice using ^{64}Cu-DOTA-siRNA delivered by Tf-targeted and non-targeted nanoparticles showed similar tissue distribution, blood clearance, and tumor accumulation. The authors state that their methodology does not differentiate between the different states of ^{64}Cu-DOTA-siRNA [178].

The majority of the preclinical efficacy data focuses on protein expression levels and cell growth inhibition. A/J mice using siR2B + 5 had the best results in blocking protein expression *in vivo*. Also, Fig. 21 shows tumor volume progressed slower when treated with the targeted and pegylated nanoparticle formulation containing siR2B + 5 (which was eventually chosen for the CALAA-01 formulations) as well as an improvement in cumulative survival [179,180]. Unfortunately, an improvement of 20 days for cumulative survival in mice may not be predictive of how CALAA-01 will prolong life for humans. On the other hand, mathematical models were employed to elucidate the mechanisms affecting the threshold and duration of the knockdown in order to improve treatment design [180].

5.3.2. Clinical studies

CALAA-01 is only in phase I of clinical trials. Thus, clinical data is limited for comparison against preclinical data. As the best performer in preclinical trials, siR2B + 5 was selected for the siRNA component of CALAA-01 to be used for clinical trials and is termed C05C. Research is ongoing, but a review article states that there is fast clearance and an acute elevation of cytokines as seen in preclinical trials [172].

Fifteen patients were enrolled where the average age was 62. Dosing was tested at escalating doses of 3, 9, 18, 24, and 30 mg/m^2 for 30 min i.v. on days 1, 3, 8, and 10 of 21 day cycles. There were no dosage limiting toxicity issues and the most common adverse events were fatigue, fever/chills, allergic reactions, constipation, and nausea/vomiting. One patient had anemia and two patients had thrombocytopenia. One patient had sinus bradycardia [181]. While the purpose of the phase I trial was safety, they reported on some aspects of efficacy. One patient at the highest dose saw their metastatic melanoma change course and become stable for 4 months. Furthermore, a total of four patients with melanoma had biopsies that showed nanoparticles internalized in cells. At the highest dose, RRM2 knockdown had occurred at the mRNA and protein level [179,181].

Still, it remains to be seen what kind of response will be seen in the clinical setting. In the clinical trial report, the researchers saw no tumor responses in any of the patients. While the improvements of CALAA-01 in tumor growth deceleration and cumulative survival rates in preclinical studies are promising, early reports from phase I trials indicate that it may not have as much efficacy in clinical tumors. The targeted binding site of CALAA-01, transferrin receptors, is also found on some normal tissues and could be a potential pitfall in its clinical progression [174]. However, delivery of a less toxic siRNA that is antiproliferative—rather than a toxic small molecule drug—could abrogate some of the dangers from lack of specificity in their chosen target.

5.4. Discussion—Targeted formulations

There are general factors that make some of the products from this section unfit for market approval. Some of these targeted drug carriers suffered from similar problems as non-targeted drug carriers: unacceptable toxicity and insufficient efficacy in the clinical setting (*e.g.*, Mylotarg). Sometimes, targeted drug carriers appear to have issues due to their implementation of targeting and they may have performed better without targeting (*e.g.*, PK2). At times, the issues become apparent only after conducting clinical trials. Essentially, the selection of appropriate receptor-ligand binding is a key to its success in practice. There were two examples of how poorly chosen targeting groups likely caused problems in clinical trials and the third targets receptors known to be found on some normal tissues. Unfortunately, one of the difficulties with cancer in the clinical setting is its inherent heterogeneity and similarity to 'self', thus making it difficult to choose a ligand that will be universally expressed by cancer cells yet not expressed by healthy tissue. This is not as much of an issue in preclinical studies that use more homogeneous cancer cell lines and could explain the disparity in results when translating to the clinical setting.

The limited market success in drug carriers with targeting groups has occurred mostly with antibody therapies. A simple search on the FDA drug database, Drugs@FDA, for the suffix "mab" will return numerous FDA approved antibodies (a considerable fraction is for cancer treatment). Some are antibody-drug conjugates such as Adcetris® and

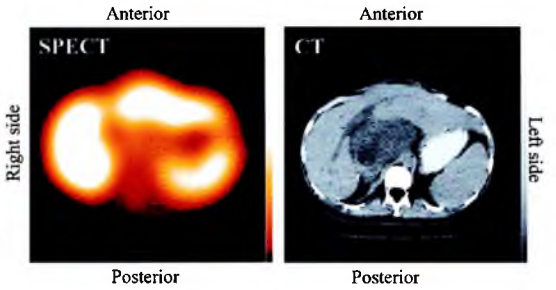

Fig. 19. SPECT and CT imaging of a patient treated with PK2 showing decreased accumulation of targeted nanoparticles in the tumor region. The SPECT shows accumulation of PK2 in the liver except in the central region. The tumor is visible in the CT image as the dark mass in the central region.
Reprinted with permission. © 2002 American Society of Clinical Oncology. All rights reserved.
Seymour, L. et al. J Clin Oncol 20(6) 2002 1668-1676.

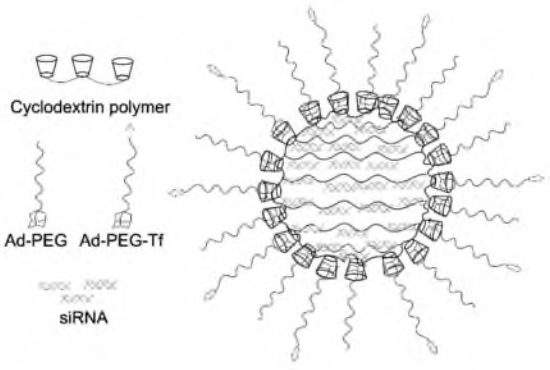

Fig. 20. CALAA-01. Size: about 70 nm. Binding site: Transferrin receptor. Currently in phase I of FDA clinical trials. Seeking indication for solid tumors. The recommended dose is 18–30 mg siRNA/m^2. Developed by Calando Pharmaceuticals, Inc.

Kadcyla®, while others act as a drug simply by binding to the ligand, such as Herceptin® and Erbitux®. Antibodies are on the lower range of drug carrier sizes at approximately 5–20 nm in diameter (depending on the axis). They are made by cells resulting in uniform and biocompatible products. However, variation does exist due to metabolism/degradation, immune responses, organism of origin, drugs, and linkers. Still, there are more and more antibody therapies being approved by the FDA when compared to other targeted drug carriers such as polymers,

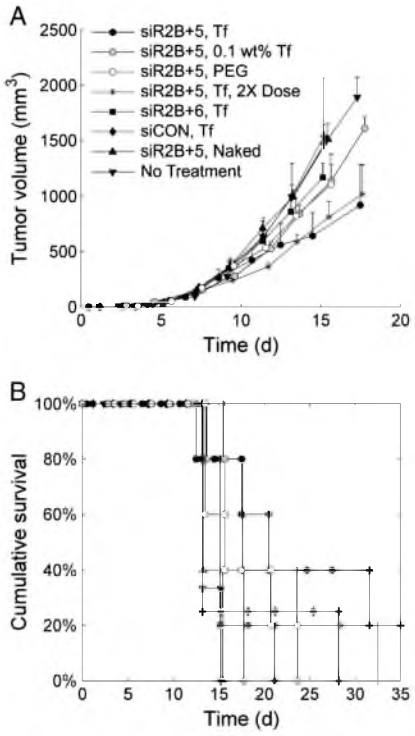

Fig. 21. The targeted and pegylated formulation containing the RRM2 sequence denoted as siR2B + 5 performed the best in tumor growth inhibition. (A) Tumor growth rates and (B) Kaplan–Meier survival curves.
From Derek W. Bartlett,Mark E. Davis, Biotechnology & Bioengineering [180] Copyright © 2000 by John Wiley Sons, Inc. Reprinted by permission of John Wiley & Sons, Inc.

colloids, or microemulsions. Preclinical studies are replete with polymers, micelles, liposomes, *etc.*, that contain multifunctional aspects, beyond just targeting moieties, that provide preferential treatment to the target tissue; however, it seems relatively few of these enter clinical trials and they have yet to successfully navigate through clinical trials to market approval. Apparently, the simplest designs have the best hope for causing positive effects in the complex clinical cancer setting.

6. Conclusion

This survey is meant to be a broad, though not comprehensive, review of intravenously injectable cancer drug carriers that have undergone some clinical testing. The formulation strategies used vary widely from compound to compound. Drugs can be covalently bonded to proteins or polymers, loaded into micellar or liposomal structures by hydrophobic interactions, bound to the nanoparticle surface by ionic bonds, or sterically trapped within a structure. The drug carriers have a drastic effect on the dosing of the drug either by frequency or MTD. Comparable doses ranged from slightly lower to many-fold higher drug equivalents than their free-drug counterparts. Pharmacokinetic properties were also substantially altered with circulation half-life in some cases extended from hours to days or even weeks; drug exposure as measured by the AUC often increased as well. In some of these cases, these increases in half-life and AUC compared to the free drug occurred in both preclinical and clinical trials. Unfortunately, these improvements in dosing or pharmacokinetics and this focus on comparing against a free drug do not coincide with the gap between preclinical and clinical results. Comparing the half-life, AUC, C_{max}, and other pharmacokinetic values between preclinical and clinical data is often not possible for the drug carriers as they are either not comparable or missing from the literature.

The efficacy in preclinical studies can be incredible; an HPMA-drug conjugate [81], Abraxane [103], NK105 [110], Genexol-PM [117], Xyotax [120], and gemtuzumab ozogamicin [159] were able to completely cure all mice of specific tumors (*i.e.*, show tumor regression and complete growth inhibition for the remainder of the study). In spite of the tremendous advantages in efficacy the drug carriers seem to enjoy in preclinical studies, the difference seems to collapse to nearly zero in human tumors. The question of why the nanoparticle should perform in clinical trials, essentially the same as the free drug, may be an important one for understanding how to best proceed with new drug carrier therapies. Furthermore, one must understand the differences that are present in the preclinical and clinical studies. Some of the differences are obvious and the known shortcomings in using animal models for human cancer therapy testing are accepted because the murine model is the most widely used model in preclinical studies and has been invaluable in providing information and saving human lives. Still we must acknowledge the differences with regard to immunocompetency, metabolism, biological rhythms, hormone cycles, and heterogeneity-among others-and how these can affect the rate and nature of tumor growth.

The clinical environment also differs in attitudes, goals, training, protocols, and sample population characteristics. Due to an increased level of complexity, successful clinical trials are highly dependent on the proper design of the experiments. There is heterogeneity not only from patient to patient, but clinical tumors are more heterogeneous in terms of environmental and cellular composition. Depending on the nature of the cancer and the patient, the results can be drastically different. It is not suggested that chaos theory rules supreme in clinical trials, but it does help to explain the difficulty in reproducing results. The butterfly effect suggests the importance of consistency in initial conditions. For example, a ball may come to rest in entirely different locations at the bottom of a hill based on where it is placed at the crest. Imagine now, the topography of that hill can change as cancer is different from patient from patient and the resulting path of treatment can be different. In reality, heterogeneity in clinical cancers (including genetic, epigenetic, and environmental differences) is considered to play a major role in failed treatments.

There are some promising strategies to navigate and bridge the gap between research and clinical practice. These include advancements in personalized medicine and theranostics which would both address the issue of adapting to the unique circumstances of an individual patient. There are also increased efforts in modifying the tumor environment, which could perhaps serve as a way to make the disease population more uniform and treatable. As a means of stimulating discussion and creativity in bridging the gap, a short list of suggestions is being submitted that might help. Initially, consistent protocols for specific experiments could be developed that would serve as a prerequisite for clinical trials. Similar experiments would then be required, and must be reported on, in clinical trials. This would, hopefully, improve reproducibility and allow for comparisons to be made between preclinical and clinical trials. This could be an opportunity to provide more transparent reporting of pharmacokinetic and efficacy results, even if the results are negative. As reporting negative results is perceivably not as rewarding, they are a lot more difficult to find in publications and sometimes get summarized in conference meetings. However, the Declaration of Helsinki states that authors have an ethical duty to publish all results from clinical trials-whether positive, negative, or inconclusive [182]. While there are provisions in section 801 of the Food and Drug Administration Amendments Act that require a summary of results, there seem to be loopholes in the system that allow for some negative results from clinical trials to avoid being published. If made publicly available, the negative data could be extremely useful to understand the faults of the drug, model, or protocols and to learn from such mistakes. A journal, forum, or collection could be created where all results will be made publicly available as a requirement in taking part in clinical trials. Finally, a simple suggestion for a continued effort of scientific criticism and skepticism is recommended. In more than one of the drugs presented in this paper, negative results were found in clinical studies that were also present (and should have been addressed) in the preclinical studies. It would be wise to trust the bad news and be skeptical of the good. Still, one must acknowledge that great progress has indeed occurred in the fight against cancer and that many drug carriers have been approved with good reasons and have saved or improved the quality of countless lives.

Acknowledgment

This work was supported by NIH CA101850 and 140348.

References

[1] M.C. Roco, Nanotechnology: convergence with modern biology and medicine, Curr. Opin. Biotechnol. 14 (2003) 337–346.
[2] V. Wagner, A. Dullaart, A.-K. Bock, A. Zweck, The emerging nanomedicine landscape, Nat. Biotechnol. 24 (2006) 1211–1217.
[3] N. Nasongkla, E. Bey, J. Ren, H. Ai, C. Khemtong, J.S. Guthi, et al., Multifunctional polymeric micelles as cancer-targeted, MRI-ultrasensitive drug delivery systems, Nano Lett. 6 (2006) 2427–2430.
[4] J.C. Pickup, Z. Zhi, F. Khan, T. Saxl, D.J.S. Birch, Nanomedicine and its potential in diabetes research and practice, Diabetes Metab. Res. Rev. 24 (2008) 604–610.
[5] S. Gelperina, K. Kisich, M.D. Iseman, L. Heifets, The potential advantages of nanoparticle drug delivery systems in chemotherapy of tuberculosis, Am. J. Respir. Crit. Care Med. 172 (2005) 1487–1490.
[6] U. Pison, T. Welte, M. Giersig, D.A. Groneberg, Nanomedicine for respiratory diseases, Eur. J. Pharmacol. 533 (2006) 341–350.
[7] A.V. Kabanov, H.E. Gendelman, Nanomedicine in the diagnosis and therapy of neurodegenerative disorders, Prog. Polym. Sci. 32 (2007) 1054–1082.
[8] R. Yatuv, M. Robinson, I. Dayan-Tarshish, M. Baru, The use of PEGylated liposomes in the development of drug delivery applications for the treatment of hemophilia, Int. J. Nanomedicine 5 (2010) 581–591.
[9] M. Vallet-Regí, Nanostructured mesoporous silica matrices in nanomedicine, J. Intern. Med. 267 (2010) 22–43.
[10] B.-B.S. Zhou, H. Zhang, M. Damelin, K.G. Geles, J.C. Grindley, P.B. Dirks, Tumour-initiating cells: challenges and opportunities for anticancer drug discovery, Nat. Rev. Drug Discov. 8 (2009) 806–823.
[11] B.Y.S. Kim, J.T. Rutka, W.C.W. Chan, Nanomedicine, N. Engl. J. Med. 363 (2010) 2434–2443.
[12] K. Riehemann, S.W. Schneider, T.A. Luger, B. Godin, M. Ferrari, H. Fuchs, Nanomedicine—challenge and perspectives, Angew. Chem. Int. Ed. 48 (2009) 872–897(in English).
[13] T. Lammers, F. Kiessling, W.E. Hennink, G. Storm, Drug targeting to tumors: principles, pitfalls and (pre-) clinical progress, J. Control. Release 161 (2012) 175–187.
[14] P.P. Adiseshaiah, J.B. Hall, S.E. McNeil, Nanomaterial standards for efficacy and toxicity assessment, Wiley Interdiscip. Rev. Nanomed. Nanobiotechnol. 2 (2009) 99–112.
[15] Y. Matsumura, H. Maeda, A new concept for macromolecular therapeutics in cancer chemotherapy: mechanism of tumoritropic accumulation of proteins and the antitumor agent smancs, Cancer Res. 46 (1986) 6387–6392.
[16] J. Fang, H. Nakamura, H. Maeda, The EPR effect: unique features of tumor blood vessels for drug delivery, factors involved, and limitations and augmentation of the effect, Adv. Drug Deliv. Rev. 63 (2011) 136–151.
[17] Y. Matsumura, K. Kataoka, Preclinical and clinical studies of anticancer agent-incorporating polymer micelles, Cancer Sci. 100 (2009) 572–579.
[18] A. Sparreboom, C.D. Scripture, V. Trieu, P.J. Williams, T. De, A. Yang, et al., Comparative preclinical and clinical pharmacokinetics of a cremophor-free, nanoparticle albumin-bound paclitaxel (ABI-007) and paclitaxel formulated in Cremophor (Taxol), Clin. Cancer Res. 11 (2005) 4136–4143.
[19] R. Duncan, L.W. Seymour, K.B. O'Hare, P.A. Flanagan, S. Wedge, I.C. Hume, et al., Preclinical evaluation of polymer-bound doxorubicin, J. Control. Release 19 (1992) 331–346.
[20] Z. Xu, W. Gu, J. Huang, H. Sui, Z. Zhou, Y. Yang, et al., *In vitro* and *in vivo* evaluation of actively targetable nanoparticles for paclitaxel delivery, Int. J. Pharm. 288 (2005) 361–368.
[21] L. Paz-Ares, H. Ross, M. O'Brien, A. Riviere, U. Gatzemeier, J. Von Pawel, et al., Phase III trial comparing paclitaxel poliglumex vs docetaxel in the second-line treatment of non-small-cell lung cancer, Br. J. Cancer 98 (2008) 1608–1613.
[22] M.E.R. O'Brien, N. Wigler, M. Inbar, R. Rosso, E. Grischke, A. Santoro, et al., Reduced cardiotoxicity and comparable efficacy in a phase III trial of pegylated liposomal doxorubicin HCl (CAELYX™/Doxil®) versus conventional doxorubicin for first-line treatment of metastatic breast cancer, Ann. Oncol. 15 (2004) 440–449.
[23] S.K. Carter, A. Di Marco, I.H. Krakoff, International Symposium on Adriamycin: Milan, 9th–10th September, 1971, Softcover, Springer, London, 2012, (Limited).
[24] A. Di Marco, Adriamycin (NSC-123127): mode and mechanism of action, Cancer Chemother. Rep. 3 6 (1975) 91–106.
[25] M. Potmesil, Y.H. Hsiang, L.F. Liu, B. Bank, H. Grossberg, S. Kirschenbaum, et al., Resistance of human leukemic and normal lymphocytes to drug-induced DNA cleavage and low levels of DNA topoisomerase II, Cancer Res. 48 (1988) 3537–3543.
[26] R.B. Weiss, The anthracyclines: will we ever find a better doxorubicin? Semin. Oncol. 19 (1992) 670–686.
[27] M.A. Jordan, Mechanism of action of antitumor drugs that interact with microtubules and tubulin, Curr. Med. Chem. Anticancer Agents 2 (2002) 1–17.
[28] Cancer Drug Information - Doxorubicin Hydrochloride, *National Cancer Institute*, [Online]. Available at: http://www.cancer.gov/cancertopics/druginfo/doxorubicinhydrochloride (Accessed: 08-Aug-2013).
[29] D.D. Von Hoff, M.W. Layard, P. Basa, H.L. Davis, A.L. Von Hoff, M. Rozencweig, et al., Risk factors for doxorubicin-induced congestive heart failure, Ann. Intern. Med. 91 (1979) 710–717.
[30] P.M. Alderton, J. Gross, M.D. Green, Comparative study of doxorubicin, mitoxantrone, and epirubicin in combination with ICRF-187 (ADR-529) in a chronic cardiotoxicity animal model, Cancer Res. 52 (1992) 194–201.
[31] F. Rossi, W. Filippelli, S. Russo, A. Filippelli, L. Berrino, Cardiotoxicity of doxorubicin: effects of drugs inhibiting the release of vasoactive substances, Pharmacol. Toxicol. 75 (1994) 99–107.
[32] J. Vásquez-Vivar, P. Martasek, N. Hogg, B.S. Masters, K.A. Pritchard, B. Kalyanaraman, Endothelial nitric oxide synthase-dependent superoxide generation from adriamycin, Biochemistry 36 (1997) 11293–11297.
[33] S. Rajagopalan, P.M. Politi, B.K. Sinha, C.E. Myers, Adriamycin-induced free radical formation in the perfused rat heart: implications for cardiotoxicity, Cancer Res. 48 (1988) 4766–4769.
[34] J.H. Doroshow, G.Y. Locker, C.E. Myers, Enzymatic defenses of the mouse heart against reactive oxygen metabolites: alterations produced by doxorubicin, J. Clin. Invest. 65 (1980) 128–135.
[35] Y. Barenholz, Doxil®—the first FDA-approved nano-drug: lessons learned, J. Control Release 160 (2012) 117–134.
[36] K.J. Harrington, S. Mohammadtaghi, P.S. Uster, D. Glass, A.M. Peters, R.G. Vile, et al., Effective targeting of solid tumors in patients with locally advanced cancers by radiolabeled pegylated liposomes, Clin. Cancer Res. 7 (2001) 243–254.
[37] P.K. Working, A.D. Dayan, Pharmacological–toxicological expert report. CAELYX. (Stealth liposomal doxorubicin HCl), Hum. Exp. Toxicol. 15 (1996) 751–785.
[38] D.M. Vail, M.A. Amantea, G.T. Colbern, F.J. Martin, R.A. Hilger, P.K. Working, Pegylated liposomal doxorubicin: proof of principle using preclinical animal models and pharmacokinetic studies, Semin. Oncol. 31 (2004) 16–35.
[39] A. Gabizon, H. Shmeeda, Y. Barenholz, Pharmacokinetics of pegylated liposomal Doxorubicin: review of animal and human studies, Clin. Pharmacokinet. 42 (2003) 419–436.
[40] T. Siegal, A. Horowitz, A. Gabizon, Doxorubicin encapsulated in sterically stabilized liposomes for the treatment of a brain tumor model: biodistribution and therapeutic efficacy, J. Neurosurg. 83 (1995) 1029–1037.
[41] A.A. Gabizon, Y. Barenholz, M. Bialer, Prolongation of the circulation time of doxorubicin encapsulated in liposomes containing a polyethylene glycol-derivatized phospholipid: pharmacokinetic studies in rodents and dogs, Pharm. Res. 10 (1993) 703–708.
[42] M. Amantea, M.S. Newman, T.M. Sullivan, A. Forrest, P.K. Working, Relationship of dose intensity to the induction of palmar-plantar erythrodysesthia by pegylated liposomal doxorubicin in dogs, Hum. Exp. Toxicol. 18 (1999) 17–26.

[43] A.A. Gabizon, O. Pappo, D. Goren, M. Chemla, D. Tzemach, A.T. Horowitz, Preclinical Studies with Doxorubicin Encapsulated in Polyethyleneglycol-Coated Liposomes, 2008.

[44] A.A. Gabizon, Selective tumor localization and improved therapeutic index of anthracyclines encapsulated in long-circulating liposomes, Cancer Res. 52 (1992) 891–896.

[45] J. Vaage, E. Barbera-Guillem, R. Abra, A. Huang, P. Working, Tissue distribution and therapeutic effect of intravenous free or encapsulated liposomal doxorubicin on human prostate carcinoma xenografts, Cancer 73 (1994) 1478–1484.

[46] A. Gabizon, D. Goren, A.T. Horowitz, D. Tzemach, A. Lossos, T. Siegal, Long-circulating liposomes for drug delivery in cancer therapy: a review of biodistribution studies in tumor-bearing animals, Adv. Drug Deliv. Rev. 24 (1997) 337–344.

[47] D. Papahadjopoulos, T.M. Allen, A. Gabizon, E. Mayhew, K. Matthay, S.K. Huang, et al., Sterically stabilized liposomes: improvements in pharmacokinetics and antitumor therapeutic efficacy, Proc. Natl. Acad. Sci. U. S. A. 88 (1991) 11460–11464.

[48] P.K. Working, M.S. Newman, T. Sullivan, J. Yarrington, Reduction of the cardiotoxicity of doxorubicin in rabbits and dogs by encapsulation in long-circulating, pegylated liposomes, J. Pharmacol. Exp. Ther. 289 (1999) 1128–1133.

[49] S.K. Huang, E. Mayhew, S. Gilani, D.D. Lasic, F.J. Martin, D. Papahadjopoulos, Pharmacokinetics and therapeutics of sterically stabilized liposomes in mice bearing C-26 colon carcinoma, Cancer Res. 52 (1992) 6774–6781.

[50] J. Vaage, D. Donovan, P. Uster, P. Working, Tumour uptake of doxorubicin in polyethylene glycol-coated liposomes and therapeutic effect against a xenografted human pancreatic carcinoma, Br. J. Cancer 75 (1997) 482–486.

[51] J. Vaage, D. Donovan, E. Mayhew, R. Abra, A. Huang, Therapy of human ovarian carcinoma xenografts using doxorubicin encapsulated in sterically stabilized liposomes, Cancer 72 (1993) 3671–3675.

[52] G.T. Colbern, A.J. Hiller, R.S. Musterer, E. Pegg, I.C. Henderson, P.K. Working, Significant increase in antitumor potency of Doxorubicin Hc1 by its encapsulation in pegylated liposomes, J. Liposome Res. 9 (1999) 523–538.

[53] A. Gabizon, F. Martin, Polyethylene glycol-coated (pegylated) liposomal doxorubicin, Drugs 54 (1997) 15–21.

[54] P.K. Working, M.S. Newman, S.K. Huang, E. Mayhew, J. Vaage, D.D. Lasic, Pharmacokinetics, biodistribution and therapeutic efficacy of doxorubicin encapsulated in Stealth® Liposomes (Doxil®), J. Liposome Res. 4 (1994) 667–687.

[55] A. Gabizon, R. Catane, B. Uziely, B. Kaufman, T. Safra, R. Cohen, et al., Prolonged circulation time and enhanced accumulation in malignant exudates of doxorubicin encapsulated in polyethylene–glycol coated liposomes, Cancer Res. 54 (1994) 987–992.

[56] D.W. Northfelt, F.J. Martin, P. Working, P.A. Volberding, J. Russell, M. Newman, et al., Doxorubicin encapsulated in liposomes containing surface-bound polyethylene glycol: pharmacokinetics, tumor localization, and safety in patients with AIDS-related Kaposi's sarcoma, J. Clin. Pharmacol. 36 (1996) 55–63.

[57] D.W. Northfelt, Liposomal anthracycline chemotherapy in the treatment of AIDS-related Kaposi's sarcoma, Oncology 11 (1997) 21–32.

[58] Z. Symon, A. Peyser, D. Tzemach, O. Lyass, E. Sucher, E. Shezen, et al., Selective delivery of doxorubicin to patients with breast carcinoma metastases by stealth liposomes, Cancer 86 (1999) 72–78.

[59] D.S. Alberts, F.M. Muggia, J. Carmichael, E.P. Winer, M. Jahanzeb, A.P. Venook, et al., Efficacy and safety of liposomal anthracyclines in phase I/II clinical trials, Semin. Oncol. 31 (2004) 53–90.

[60] R. Soloman, A.A. Gabizon, Clinical pharmacology of liposomal anthracyclines: focus on pegylated liposomal Doxorubicin, Clin. Lymphoma Myeloma 8 (2008) 21–32.

[61] T. Safra, F. Muggia, S. Jeffers, D.D. Tsao-Wei, S. Groshen, O. Lyass, et al., Pegylated liposomal doxorubicin (doxil): reduced clinical cardiotoxicity in patients reaching or exceeding cumulative doses of 500 mg/m2, Ann. Oncol. 11 (2000) 1029–1033.

[62] M.S. Ewer, F.J. Martin, C. Henderson, C.L. Shapiro, R.S. Benjamin, A.A. Gabizon, Cardiac safety of liposomal anthracyclines, Semin. Oncol. 31 (2004) 161–181.

[63] A. Gabizon, H. Shmeeda, T. Grenader, Pharmacological basis of pegylated liposomal doxorubicin: impact on cancer therapy, Eur. J. Pharm. Sci. 45 (2012) 388–398.

[64] A. Udhrain, K.M. Skubitz, D.W. Northfelt, Pegylated liposomal doxorubicin in the treatment of AIDS-related Kaposi's sarcoma, Int. J. Nanomedicine 2 (2007) 345–352.

[65] D.W. Northfelt, B.J. Dezube, J.A. Thommes, B.J. Miller, M.A. Fischl, A. Friedman-Kien, et al., Pegylated-liposomal doxorubicin versus doxorubicin, bleomycin, and vincristine in the treatment of AIDS-related Kaposi's sarcoma: results of a randomized phase III clinical trial, J. Clin. Oncol. 16 (1998) 2445–2451.

[66] S. Stewart, H. Jablonowski, F.D. Goebel, K. Arasteh, M. Spittle, A. Rios, et al., Randomized comparative trial of pegylated liposomal doxorubicin versus bleomycin and vincristine in the treatment of AIDS-related Kaposi's sarcoma. International Pegylated Liposomal Doxorubicin Study Group, J. Clin. Oncol. 16 (1998) 683–691.

[67] M. Cianfrocca, S. Lee, J. Von Roenn, A. Tulpule, B.J. Dezube, D.M. Aboulafia, et al., Randomized trial of paclitaxel versus pegylated liposomal doxorubicin for advanced human immunodeficiency virus-associated Kaposi sarcoma: evidence of symptom palliation from chemotherapy, Cancer 116 (2010) 3969–3977.

[68] L. Martin-Carbonero, A. Barrios, P. Saballs, G. Sirera, J. Santos, R. Palacios, et al., Pegylated liposomal doxorubicin plus highly active antiretroviral therapy versus highly active antiretroviral therapy alone in HIV patients with Kaposi's sarcoma, AIDS 18 (2004) 1737–1740.

[69] A.N. Gordon, J.T. Fleagle, D. Guthrie, D.E. Parkin, M.E. Gore, A.J. Lacave, Recurrent epithelial ovarian carcinoma: a randomized phase III study of pegylated liposomal doxorubicin versus topotecan, J. Clin. Oncol. 19 (2001) 3312–3322.

[70] A.N. Gordon, M. Tonda, S. Sun, W. Rackoff, Long-term survival advantage for women treated with pegylated liposomal doxorubicin compared with topotecan in a phase 3 randomized study of recurrent and refractory epithelial ovarian cancer, Gynecol. Oncol. 95 (2004) 1–8.

[71] R.M. Rifkin, S.A. Gregory, A. Mohrbacher, M.A. Hussein, Pegylated liposomal doxorubicin, vincristine, and dexamethasone provide significant reduction in toxicity compared with doxorubicin, vincristine, and dexamethasone in patients with newly diagnosed multiple myeloma: a Phase III multicenter randomized trial, Cancer 106 (2006) 848–858.

[72] R. Duncan, Drug-polymer conjugates: potential for improved chemotherapy, Anti-cancer Drugs 3 (1992) 175–210.

[73] F.M. Muggia, Doxorubicin–polymer conjugates: further demonstration of the concept of enhanced permeability and retention, Clin. Cancer Res. 5 (1999) 7–8.

[74] R. Duncan, Development of HPMA copolymer–anticancer conjugates: clinical experience and lessons learnt, Adv. Drug Deliv. Rev. 61 (2009) 1131–1148.

[75] A. Paul, M.J. Vicent, R. Duncan, Using small-angle neutron scattering to study the solution conformation of N-(2-hydroxypropyl)methacrylamide copolymer–doxorubicin conjugates, Biomacromolecules 8 (2007) 1573–1579.

[76] T. Minko, P. Kopeckova, V. Pozharov, J. Kopecek, HPMA copolymer bound adriamycin overcomes MDR1 gene encoded resistance in a human ovarian carcinoma cell line, J. Control Release 54 (1998) 223–233.

[77] T. Minko, P. Kopeckova, J. Kopecek, Comparison of the anticancer effect of free and HPMA copolymer-bound adriamycin in human ovarian carcinoma cells, Pharm. Res. 16 (1999) 986–996.

[78] T. Minko, P. Kopeckova, J. Kopecek, Chronic exposure to HPMA copolymer-bound adriamycin does not induce multidrug resistance in a human ovarian carcinoma cell line, J. Control. Release 59 (1999) 133–148.

[79] L.W. Seymour, K. Ulbrich, J. Strohalm, J. Kopecek, R. Duncan, The pharmacokinetics of polymer-bound adriamycin, Biochem. Pharmacol. 39 (1990) 1125–1131.

[80] L.W. Seymour, K. Ulbrich, P.S. Steyger, M. Brereton, V. Subr, J. Strohalm, et al., Tumour tropism and anti-cancer efficacy of polymer-based doxorubicin prodrugs in the treatment of subcutaneous murine B16F10 melanoma, Br. J. Cancer 70 (1994) 636–641.

[81] T. Minko, P. Kopeckova, J. Kopecek, Efficacy of the chemotherapeutic action of HPMA copolymer-bound doxorubicin in a solid tumor model of ovarian carcinoma, Int. J. Cancer 86 (2000) 108–117.

[82] L.W. Seymour, Y. Miyamoto, H. Maeda, M. Brereton, J. Strohalm, K. Ulbrich, et al., Influence of molecular weight on passive tumour accumulation of a soluble macromolecular drug carrier, Eur. J. Cancer 31A (1995) 766–770.

[83] Y. Noguchi, J. Wu, R. Duncan, J. Strohalm, K. Ulbrich, T. Akaike, et al., Early phase tumor accumulation of macromolecules: a great difference in clearance rate between tumor and normal tissues, Cancer Sci. 89 (1998) 307–314.

[84] T. Minko, P. Kopeckova, V. Pozharov, K.D. Jensen, J. Kopecek, The influence of cytotoxicity of macromolecules and of VEGF gene modulated vascular permeability on the enhanced permeability and retention effect in resistant solid tumors, Pharm. Res. 17 (2000) 505–514.

[85] T.K. Yeung, J.W. Hopewell, R.H. Simmonds, L.W. Seymour, R. Duncan, O. Bellini, et al., Reduced cardiotoxicity of doxorubicin given in the form of N-(2-hydroxypropyl)methacrylamide conjugates: and experimental study in the rat, Cancer Chemother. Pharmacol. 29 (1991) 105–111.

[86] B. Rihova, M. Bilej, V. Vetvicka, K. Ulbrich, J. Strohalm, J. Kopecek, et al., Biocompatibility of N-(2-hydroxypropyl) methacrylamide copolymers containing adriamycin. Immunogenicity, and effect on haematopoietic stem cells in bone marrow *in vivo* and mouse splenocytes and human peripheral blood lymphocytes *in vitro*, Biomaterials 10 (1989) 335–342.

[87] P.A. Vasey, S.B. Kaye, R. Morrison, C. Twelves, P. Wilson, R. Duncan, et al., Phase I clinical and pharmacokinetic study of PK1 [N-(2-hydroxypropyl)methacrylamide copolymer doxorubicin]: first member of a new class of chemotherapeutic agents–drug-polymer conjugates, Clin. Cancer Res. 5 (1999) 83–94.

[88] L.W. Seymour, D.R. Ferry, D.J. Kerr, D. Rea, M. Whitlock, R. Poyner, et al., Phase II studies of polymer-doxorubicin (PK1, FCE28068) in the treatment of breast, lung and colorectal cancer, Int. J. Oncol. 34 (2009) 1629–1636.

[89] D. Guenard, F. Gueritte-Voegelein, P. Potier, Taxol and taxotere: discovery, chemistry, and structure-activity relationships, Acc. Chem. Res. 26 (1993) 160–167.

[90] A. Stierle, G. Strobel, D. Stierle, P. Grothaus, G. Bignami, The search for a taxol-producing microorganism among the endophytic fungi of the Pacific Yew, *Taxus brevifolia*, J. Nat. Prod. 58 (1995) 1315–1324.

[91] B. Ganem, R.R. Franke, Paclitaxel from primary taxanes: a perspective on creative invention in organozirconium chemistry, J. Org. Chem. 72 (2007) 3981–3987.

[92] S.B. Horwitz, Taxol (paclitaxel): mechanisms of action, Ann. Oncol. 5 (Suppl. 6) (1994) S3–S6.

[93] F. Dosio, P. Brusa, P. Crosasso, S. Arpicco, L. Cattel, Preparation, characterization and properties *in vitro* and *in vivo* of a paclitaxel–albumin conjugate, J. Control. Release 47 (1997) 293–304.

[94] J. Szebeni, F.M. Muggia, C.R. Alving, Complement activation by Cremophor EL as a possible contributor to hypersensitivity to paclitaxel: an *in vitro* study, J. Natl. Cancer Inst. 90 (1998) 300–306.

[95] E.K. Rowinsky, E.A. Eisenhauer, V. Chaudhry, S.G. Arbuck, R.C. Donehower, Clinical toxicities encountered with paclitaxel (Taxol), Semin. Oncol. 20 (1993) 1–15.

[96] E.K. Rowinsky, N. Onetto, R.M. Canetta, S.G. Arbuck, Taxol: the first of the taxanes, an important new class of antitumor agents, Semin. Oncol. 19 (1992) 646–662.

[97] S.E. Jones, J. Erban, B. Overmoyer, G.T. Budd, L. Hutchins, E. Lower, et al., Randomized phase III study of docetaxel compared with paclitaxel in metastatic breast cancer, J. Clin. Oncol. 23 (2005) 5542–5551.

[98] A. Moreno-Aspitia, E.A. Perez, Nanoparticle albumin-bound paclitaxel (ABI-007): a newer taxane alternative in breast cancer, Future Oncol. 1 (2005) 755–762.

[99] M.R. Green, G.M. Manikhas, S. Orlov, B. Afanasyev, A.M. Makhson, P. Bhar, et al., Abraxane, a novel Cremophor-free, albumin-bound particle form of paclitaxel for the treatment of advanced non-small-cell lung cancer, Ann. Oncol. 17 (2006) 1263–1268.

[100] D.D. Von Hoff, R.K. Ramanathan, M.J. Borad, D.A. Laheru, L.S. Smith, T.E. Wood, et al., Gemcitabine plus nab-paclitaxel is an active regimen in patients with advanced pancreatic cancer: a phase I/II trial, J. Clin. Oncol. 29 (2011) 4548–4554.
[101] M. Tirrell, Celgene Rises as Abraxane Meets Pancreatic Cancer Goals, Bloomberg, 2012.
[102] N. Desai, V. Trieu, B. Damascelli, P. Soon-Shiong, SPARC expression correlates with tumor response to albumin-bound paclitaxel in head and neck cancer patients, Transl. Oncol. 2 (2009) 59–64.
[103] N. Desai, V. Trieu, Z. Yao, L. Louie, S. Ci, A. Yang, et al., Increased antitumor activity, intratumor paclitaxel concentrations, and endothelial cell transport of cremophor-free, albumin-bound paclitaxel, ABI-007, compared with cremophor-based paclitaxel, Clin. Cancer Res. 12 (2006) 1317–1324.
[104] A. Sparreboom, C.D. Scripture, V. Trieu, P.J. Williams, T. De, A. Yang, et al., Comparative preclinical and clinical pharmacokinetics of a cremophor-free, nanoparticle albumin-bound paclitaxel (ABI-007) and paclitaxel formulated in Cremophor (Taxol), Clin. Cancer Res. 11 (2005) 4136–4143.
[105] T.E. Stinchcombe, M.A. Socinski, C.M. Walko, B.H. O'Neil, F.A. Collichio, A. Ivanova, et al., Phase I and pharmacokinetic trial of carboplatin and albumin-bound paclitaxel, ABI-007 (Abraxane) on three treatment schedules in patients with solid tumors, Cancer Chemother. Pharmacol. 60 (2007) 759–766.
[106] W.J. Gradishar, S. Tjulandin, N. Davidson, H. Shaw, N. Desai, P. Bhar, et al., Phase III trial of nanoparticle albumin-bound paclitaxel compared with polyethylated castor oil-based paclitaxel in women with breast cancer, J. Clin. Oncol. 23 (2005) 7794–7803.
[107] E. Miele, G.P. Spinelli, E. Miele, F. Tomao, S. Tomao, Albumin-bound formulation of paclitaxel (Abraxane ABI-007) in the treatment of breast cancer, Int. J. Nanomedicine 4 (2009) 99–105.
[108] A. Sparreboom, L. van Zuylen, E. Brouwer, W.J. Loos, P. de Bruijn, H. Gelderblom, et al., Cremophor EL-mediated alteration of paclitaxel distribution in human blood: clinical pharmacokinetic implications, Cancer Res. 59 (1999) 1454–1457.
[109] A.J. ten Tije, J. Verweij, W.J. Loos, A. Sparreboom, Pharmacological effects of formulation vehicles, Clin. Pharmacokinet. 42 (2003) 665–685.
[110] T. Hamaguchi, Y. Matsumura, M. Suzuki, K. Shimizu, R. Goda, I. Nakamura, et al., NK105, a paclitaxel-incorporating micellar nanoparticle formulation, can extend *in vivo* antitumour activity and reduce the neurotoxicity of paclitaxel, Br. J. Cancer 92 (2005) 1240–1246.
[111] K. Kato, K. Chin, T. Yoshikawa, K. Yamaguchi, Y. Tsuji, T. Esaki, et al., Phase II study of NK105, a paclitaxel-incorporating micellar nanoparticle, for previously treated advanced or recurrent gastric cancer, Invest. New Drugs 30 (2012) 1621–1627.
[112] S.S. Wöhrer, M. Raderer, M. Hejna, Palliative chemotherapy for advanced gastric cancer, Ann. Oncol. 15 (2004) 1585–1595.
[113] M. Findlay, D. Cunningham, A. Norman, J. Mansi, M. Nicolson, T. Hickish, et al., A phase II study in advanced gastro-esophageal cancer using epirubicin and cisplatin in combination with continuous infusion 5-fluorouracil (ECF), Ann. Oncol. 5 (1994) 609–616.
[114] P. Ross, Prospective randomized trial comparing mitomycin, cisplatin, and protracted venous-infusion fluorouracil (PVI 5-FU) with epirubicin, cisplatin, and PVI 5-FU in advanced esophagogastric cancer, J. Clin. Oncol. 20 (2002) 1996–2004.
[115] A. Webb, D. Cunningham, J. Scarffe, P. Harper, A. Norman, J. Joffe, et al., Randomized trial comparing epirubicin, cisplatin, and fluorouracil versus fluorouracil, doxorubicin, and methotrexate in advanced esophagogastric cancer, J. Clin. Oncol. 15 (1997) 261–267.
[116] T. Eguchi, M. Fujii, K. Wakabayashi, K. Aisaki, Y. Tsuneda, M. Kochi, et al., Docetaxel plus 5-fluorouracil for terminal gastric cancer patients with peritoneal dissemination, Hepatogastroenterology 50 (2003) 1735–1738.
[117] S.C. Kim, D.W. Kim, Y.H. Shim, J.S. Bang, H.S. Oh, S.W. Kim, et al., *In vivo* evaluation of polymeric micellar paclitaxel formulation: toxicity and efficacy, J. Control. Release 72 (2001) 191–202.
[118] T.-Y. Kim, D.-W. Kim, J.-Y. Chung, S.G. Shin, S.-C. Kim, D.S. Heo, et al., Phase I and pharmacokinetic study of Genexol-PM, a cremophor-free, polymeric micelle-formulated paclitaxel, in patients with advanced malignancies, Clin. Cancer Res. 10 (2004) 3708–3716.
[119] S.Y. Lee, H.S. Park, K.Y. Lee, H.J. Kim, Y.J. Jeon, T.W. Jang, et al., Paclitaxel-loaded polymeric micelle (230 mg/m(2)) and cisplatin (60 mg/m(2)) *vs.* paclitaxel (175 mg/m(2)) and cisplatin (60 mg/m(2)) in advanced non-small-cell lung cancer: a multicenter randomized phase IIB trial, Clin. Lung Cancer 14 (2013) 275–282.
[120] C. Li, D.-F. Yu, R.A. Newman, F. Cabral, L.C. Stephens, N. Hunter, et al., Complete regression of well-established tumors using a novel water-soluble Poly(L-glutamic acid)-paclitaxel conjugate, Cancer Res. 58 (1998) 2404–2409.
[121] C. Li, J.E. Price, L. Milas, N.R. Hunter, S. Ke, D.-F. Yu, et al., Antitumor activity of Poly(L-glutamic acid)–paclitaxel on syngeneic and xenografted tumors, Clin. Cancer Res. 5 (1999) 891–897.
[122] M.E.R. O'Brien, M.A. Socinski, I.N. Popovich, Alexander Y. Bondarenko, A. Tomova, B.T. Bilynsky, Y.S. Hotko, et al., Randomized Phase III trial comparing single-agent gemcitabine or vinorelbine for the treatment of PS 2 patients with chemotherapy-naive advanced non-small cell lung cancer, J. Thorac. Oncol. 3 (2008) 728–734.
[123] P. Sabbatini, M.W. Sill, D. O'Malley, L. Adler, A.A. Secord, A phase II trial of paclitaxel poliglumex in recurrent or persistent ovarian or primary peritoneal cancer (EOC): a Gynecologic Oncology Group Study, Gynecol. Oncol. 111 (2008) 455–460.
[124] C.J. Langer, K.J. O'Byrne, M.A. Socinski, S.M. Mikhailov, K. Leśniewski-Kmak, M. Smakal, et al., Phase III trial comparing paclitaxel poliglumex (CT-2103, PPX) in combination with carboplatin versus standard paclitaxel and carboplatin in the treatment of PS 2 patients with chemotherapy-naive advanced non-small cell lung cancer, J. Thorac. Oncol. 3 (2008) 623–630.
[125] D.A. Richards, P. Richards, D. Bodkin, M.A. Neubauer, F. Oldham, Efficacy and safety of paclitaxel poliglumex as first-line chemotherapy in patients at high risk with advanced-stage non-small-cell lung cancer: results of a phase II study, Clin. Lung Cancer 7 (2005) 215–220.
[126] B. Rosenberg, L. VanCamp, T. Krigas, Inhibition of cell division in *Escherichia coli* by electrolysis products from a platinum electrode, Nature 205 (1965) 698–699.
[127] B. Rosenberg, L. VanCamp, E.B. Grimley, A.J. Thomson, The inhibition of growth or cell division in *Escherichia coli* by different ionic species of platinum(IV) complexes, J. Biol. Chem. 242 (1967) 1347–1352.
[128] B. Rosenberg, E. Renshaw, L. Vancamp, J. Hartwick, J. Drobnik, Platinum-induced filamentous growth in *Escherichia coli*, J. Bacteriol. 93 (1967) 716–721.
[129] B. Rosenberg, L. VanCamp, J.E. Trosko, V.H. Mansour, Platinum compounds: a new class of potent antitumour agents, Nature 222 (1969) 385–386.
[130] B. Rosenberg, L. VanCamp, The successful regression of large solid sarcoma 180 tumors by platinum compounds, Cancer Res. 30 (1970) 1799–1802.
[131] V. Cepeda, M.A. Fuertes, J. Castilla, C. Alonso, C. Quevedo, J.M. Pérez, Biochemical mechanisms of cisplatin cytotoxicity, Anticancer Agents Med. Chem. 7 (2007) 3–18.
[132] Cancer Drug Information - Cisplatin, *National Cancer Institute*, [Online]. Available at: http://www.cancer.gov/cancertopics/druginfo/cisplatin(Accessed: 08-Aug-2013).
[133] R.J. Kociba, S.D. Sleight, Acute toxicologic and pathologic effects of cis-diamminedichloroplatinum (NSC-119875) in the male rat, Cancer Chemother. Rep. 1 55 (1971) 1–8.
[134] X. Yao, K. Panichpisal, N. Kurtzman, K. Nugent, Cisplatin nephrotoxicity: a review, Am. J. Med. Sci. 334 (2007) 115–124.
[135] V. Pinzani, F. Bressolle, I.J. Haug, M. Galtier, J.P. Blayac, P. Balmès, Cisplatin-induced renal toxicity and toxicity-modulating strategies: a review, Cancer Chemother. Pharmacol. 35 (1994) 1–9.
[136] J.T. Hartmann, H.-P. Lipp, Toxicity of platinum compounds, Expert Opin. Pharmacother. 4 (2003) 889–901.
[137] L. Helson, E. Okonkwo, L. Anton, E. Cvitkovic, cis-Platinum ototoxicity, Clin. Toxicol. 13 (1978) 469–478.
[138] D. Ding, B.L. Allman, R. Salvi, Review: ototoxic characteristics of platinum antitumor drugs, Anat. Rec. (Hoboken) 295 (2012) 1851–1867.
[139] L.R. Kelland, S.Y. Sharp, Platinum compounds in cancer therapy, Current Opinion in Oncologic, Endocr. Metab. Investig. Drugs 1 (1999) 380–385.
[140] I. Judson, L.R. Kelland, New developments and approaches in the platinum arena, Drugs 59 (Suppl. 4) (2000) 29–36(discussion 37–8).
[141] S.Y. Sharp, C.F. O'Neill, P. Rogers, F.E. Boxall, L.R. Kelland, Retention of activity by the new generation platinum agent AMD0473 in four human tumour cell lines possessing acquired resistance to oxaliplatin, Eur. J. Cancer 38 (2002) 2309–2315.
[142] M. Kartalou, J.M. Essigmann, Mechanisms of resistance to cisplatin, Mutat. Res. 478 (2001) 23–43.
[143] M. Yokoyama, T. Okano, Y. Sakurai, S. Suwa, K. Kataoka, Introduction of cisplatin into polymeric micelle, J. Control. Release 39 (1996) 351–356.
[144] N. Nishiyama, M. Yokoyama, T. Aoyagi, T. Okano, Y. Sakurai, K. Kataoka, Preparation and characterization of self-assembled polymer – metal complex micelle from cis -Dichlorodiammineplatinum(II) and Poly(ethylene glycol) – Poly(α, β-aspartic acid) block copolymer in an aqueous medium, Langmuir 15 (1999) 377–383.
[145] N. Nishiyama, K. Kataoka, Preparation and characterization of size-controlled polymeric micelle containing cis-dichlorodiammineplatinum(II) in the core, J. Control Release 74 (2001) 83–94.
[146] N. Nishiyama, Y. Kato, Y. Sugiyama, K. Kataoka, Cisplatin-loaded polymer-metal complex micelle with time-modulated decaying property as a novel drug delivery system, Pharm. Res. 18 (2001) 1035–1041.
[147] N. Nishiyama, S. Okazaki, H. Cabral, M. Miyamoto, Y. Kato, Y. Sugiyama, et al., Novel cisplatin-incorporated polymeric micelles can eradicate solid tumors in mice, Cancer Res. 63 (2003) 8977–8983.
[148] H. Uchino, Y. Matsumura, T. Negishi, F. Koizumi, T. Hayashi, T. Honda, et al., Cisplatin-incorporating polymeric micelles (NC-6004) can reduce nephrotoxicity and neurotoxicity of cisplatin in rats, Br. J. Cancer 93 (2005) 678–687.
[149] Y. Matsumura, Poly (amino acid) micelle nanocarriers in preclinical and clinical studies, Adv. Drug Deliv. Rev. 60 (2008) 899–914.
[150] K. Endo, T. Ueno, S. Kondo, N. Wakisaka, S. Murono, M. Ito, et al., Tumor-targeted chemotherapy with the nanopolymer-based drug NC-6004 for oral squamous cell carcinoma, Cancer Sci. 104 (2013) 369–374.
[151] M. Baba, Y. Matsumoto, A. Kashio, H. Cabral, N. Nishiyama, K. Kataoka, et al., Micellization of cisplatin (NC-6004) reduces its ototoxicity in guinea pigs, J. Control Release 157 (2012) 112–117.
[152] R. Plummer, R.H. Wilson, H. Calvert, A.V. Boddy, M. Griffin, J. Sludden, et al., A Phase I clinical study of cisplatin-incorporated polymeric micelles (NC-6004) in patients with solid tumours, Br. J. Cancer 104 (2011) 593–598.
[153] K. Kitajima, M. Fukuoka, S. Kobayashi, Y. Kusunoki, M. Takada, S. Negoro, et al., [Studies on the appropriate administration of cisplatin based on pharmacokinetics and toxicity]., Gan to Kagaku Ryoho, Cancer Chemother. 14 (1987) 2517–2523.
[154] P.F. Bross, J. Beitz, G. Chen, X.H. Chen, E. Duffy, L. Kieffer, et al., Approval summary: gemtuzumab ozogamicin in relapsed acute myeloid leukemia, Clin. Cancer Res. 7 (2001) 1490–1496.
[155] R.A. Larson, M. Boogaerts, E. Estey, C. Karanes, E.A. Stadtmauer, E.L. Sievers, et al., Antibody-targeted chemotherapy of older patients with acute myeloid leukemia in first relapse using Mylotarg (gemtuzumab ozogamicin), Leukemia 16 (2002) 1627–1636.
[156] R.H.C. van der Jagt, C.C. Badger, F.R. Appelbaum, O.W. Press, D.C. Matthews, J.F. Eary, et al., Localization of radiolabeled antimyeloid antibodies in a human acute leukemia xenograft tumor model, Cancer Res. 52 (1992) 89–94.
[157] J.D. Griffin, D. Linch, K. Sabbath, P. Larcom, S.F. Schlossman, A monoclonal antibody reactive with normal and leukemic human myeloid progenitor cells, Leuk. Res. 8 (1984) 521–534.

[158] P.R. Hamann, L.M. Hinman, C.F. Beyer, D. Lindh, J. Upeslacis, D.A. Flowers, et al., An anti-CD33 antibody—Calicheamicin conjugate for treatment of acute myeloid leukemia. Choice of linker, Bioconjug. Chem. 13 (2002) 40–46.

[159] P.R. Hamann, L.M. Hinman, I. Hollander, C.F. Beyer, D. Lindh, R. Holcomb, et al., Gemtuzumab ozogamicin, a potent and selective anti-CD33 antibody—Calicheamicin conjugate for treatment of acute myeloid leukemia, Bioconjug. Chem. 13 (2002) 47–58.

[160] S. Petersdorf, K. Kopecky, R.K. Stuart, R.A. Larson, T.J. Nevill, L. Stenke, et al., Preliminary Results of Southwest Oncology Group Study S0106: An International Intergroup Phase 3 randomized trial comparing the addition of gemtuzumab ozogamicin to standard induction therapy versus standard induction therapy followed by a second randomiz, ASH Annu. Meet. Abstr. 114 (2009) 790.

[161] FDA-News-Release, 2010 - FDA: Pfizer Voluntarily Withdraws Cancer Treatment Mylotarg from U.S. Market, [Online]. Available at: http://www.fda.gov/NewsEvents/Newsroom/PressAnnouncements/2010/ucm216448.htm (Accessed: 09-May-2013).

[162] U. Brunnberg, M. Mohr, R. Noppeney, H.A. Dürk, M.C. Sauerland, C. Müller-Tidow, et al., Induction therapy of AML with ara-C plus daunorubicin versus ara-C plus gemtuzumab ozogamicin: a randomized phase II trial in elderly patients, Ann. Oncol. 23 (2012) 990–996.

[163] A.K. Burnett, R.K. Hills, D. Milligan, L. Kjeldsen, J. Kell, N.H. Russell, et al., Identification of patients with acute myeloblastic leukemia who benefit from the addition of gemtuzumab ozogamicin: results of the MRC AML15 trial, J. Clin. Oncol. 29 (2011) 369–377.

[164] P. Rajvanshi, Hepatic sinusoidal obstruction after gemtuzumab ozogamicin (Mylotarg) therapy, Blood 99 (2002) 2310–2314.

[165] L.W. Seymour, Hepatic drug targeting: Phase I evaluation of polymer-bound doxorubicin, J. Clin. Oncol. 20 (2002) 1668–1676.

[166] R. Duncan, L.C.W. Seymour, L. Scarlett, J.B. Lloyd, P. Rejmanová, J. Kopeček, Fate of N-(2-hydroxypropyl)methacrylamide copolymers with pendent galactosamine residues after intravenous administration to rats, Biochim. Biophys. Acta Gen. Subj. 880 (1986) 62–71.

[167] M.V. Pimm, A.C. Perkins, J. Strohalm, K. Ulbrich, R. Duncan, Gamma scintigraphy of a 123I-labelled N-(2-hydroxypropyl)methacrylamide copolymer–doxorubicin conjugate containing galactosamine following intravenous administration to nude mice bearing hepatic human colon carcinoma, J. Drug Target. 3 (1996) 385–390.

[168] P. Julyan, Preliminary clinical study of the distribution of HPMA copolymers bearing doxorubicin and galactosamine, J. Control. Release 57 (1999) 281–290.

[169] F. Alexis, E. Pridgen, L.K. Molnar, O.C. Farokhzad, Factors affecting the clearance and biodistribution of polymeric nanoparticles, Mol. Pharm. 5 (2008) 505–515.

[170] ClinicalTrials.gov. [Online], Available at: http://www.clinicaltrials.gov/(Accessed: 06-Aug-2013).

[171] UK Clinical Trials Gateway, [Online]. Available at: http://www.ukctg.nihr.ac.uk/ (Accessed: 06-Aug-2013).

[172] J.D. Heidel, T. Schluep, Cyclodextrin-containing polymers: versatile platforms of drug delivery materials, J. Drug Deliv. 2012 (2012) 262731.

[173] S. Mishra, J.D. Heidel, P. Webster, M.E. Davis, Imidazole groups on a linear, cyclodextrin-containing polycation produce enhanced gene delivery *via* multiple processes, J. Control Release 116 (2006) 179–191.

[174] K.C. Gatter, G. Brown, I.S. Trowbridge, R.E. Woolston, D.Y. Mason, Transferrin receptors in human tissues: their distribution and possible clinical relevance, J. Clin. Pathol. 36 (1983) 539–545.

[175] M.E. Davis, The first targeted delivery of siRNA in humans *via* a self-assembling, cyclodextrin polymer-based nanoparticle: from concept to clinic, Mol. Pharm. 6 (2009) 659–668.

[176] J.D. Heidel, J.Y.-C. Liu, Y. Yen, B. Zhou, B.S.E. Heale, J.J. Rossi, et al., Potent siRNA inhibitors of ribonucleotide reductase subunit RRM2 reduce cell proliferation *in vitro* and *in vivo*, Clin. Cancer Res. 13 (2007) 2207–2215.

[177] J.D. Heidel, Z. Yu, J.Y.-C. Liu, S.M. Rele, Y. Liang, R.K. Zeidan, et al., Administration in non-human primates of escalating intravenous doses of targeted nanoparticles containing ribonucleotide reductase subunit M2 siRNA, Proc. Natl. Acad. Sci. U. S. A. 104 (2007) 5715–5721.

[178] D.W. Bartlett, H. Su, I.J. Hildebrandt, W.A. Weber, M.E. Davis, Impact of tumor-specific targeting on the biodistribution and efficacy of siRNA nanoparticles measured by multimodality *in vivo* imaging, Proc. Natl. Acad. Sci. U. S. A. 104 (2007) 15549–15554.

[179] M.E. Davis, J.E. Zuckerman, C.H.J. Choi, D. Seligson, A. Tolcher, C.A. Alabi, et al., Evidence of RNAi in humans from systemically administered siRNA *via* targeted nanoparticles, Nature 464 (2010) 1067–1070.

[180] D.W. Bartlett, M.E. Davis, Impact of tumor-specific targeting and dosing schedule on tumor growth inhibition after intravenous administration of siRNA-containing nanoparticles, Biotechnol. Bioeng. 99 (2008) 975–985.

[181] A. Ribas, L. Kalinoski, J.D. Heidel, J. Peterkin, D.B. Seligson, J.E. Zuckerman, et al., Systemic delivery of siRNA *via* targeted nanoparticles in patients with cancer: results from a first-in-class phase I clinical trial, J. Clin. Oncol. 28 (2010)(abstract 3022).

[182] W.M. Association, World Medical Association Declaration of Helsinki: ethical principles for medical research involving human subjects, [Online]. Available at: http://www.wma.net/en/30publications/10policies/b3/index.html(Accessed: 01-Aug-2013).

[183] M. Marty, F. Cognetti, D. Maraninchi, R. Snyder, L. Mauriac, M. Tubiana-Hulin, et al., Randomized phase II trial of the efficacy and safety of trastuzumab combined with docetaxel in patients with human epidermal growth factor receptor 2-positive metastatic breast cancer administered as first-line treatment: the M77001 study group, J. Clin. Oncol. 23 (2005) 4265–4274.

[184] S. Chan, N. Davidson, E. Juozaityte, F. Erdkamp, A. Pluzanska, N. Azamia, et al., Phase III trial of liposomal doxorubicin and cyclophosphamide compared with epirubicin and cyclophosphamide as first-line therapy for metastatic breast cancer, Ann. Oncol. 15 (2004) 1527–1534.

[185] P. Gill, J. Wernz, D. Scadden, P. Cohen, G. Mukwaya, J. von Roenn, et al., Randomized phase III trial of liposomal daunorubicin versus doxorubicin, bleomycin, and vincristine in AIDS-related Kaposi's sarcoma, J. Clin. Oncol. 14 (1996) 2353–2364.

[186] Z.-M. Wang, J.X. Ho, J.R. Ruble, J. Rose, F. Ruker, M. Ellenburg, et al., Structural studies of several clinically important oncology drugs in complex with human serum albumin, Biochim. Biophys. Acta 1830 (12) (2013) 5356–5374.

[187] Y. Matsumura, Polymeric micellar delivery systems in oncology, Jpn. J. Clin. Oncol. 38 (2008) 793–802.

REFERENCES

[1] D. Peer, J. M. Karp, S. Hong, O. C. Farokhzad, R. Margalit, and R. Langer, "Nanocarriers as an emerging platform for cancer therapy." *Nature Nanotechnology*, vol. 2, no. 12, pp. 751–60, dec 2007. [Online]. Available: http://dx.doi.org/10.1038/nnano.2007.387

[2] D. L. Stirland, J. W. Nichols, S. Miura, and Y. H. Bae, "Mind the gap: A survey of how cancer drug carriers are susceptible to the gap between research and practice," *Journal of Controlled Release*, vol. 172, no. 3, pp. 1045–1064, dec 2013. [Online]. Available: http://www.sciencedirect.com/science/article/pii/S0168365913008146

[3] M. Yokoyama, S. Inoue, K. Kataoka, N. Yui, T. Okano, and Y. Sakurai, "Molecular design for missile drug: Synthesis of adriamycin conjugated with immunoglobulin G using poly(ethylene glycol)blockpoly(aspartic acid) as intermediate carrier," *Die Makromolekulare Chemie*, vol. 190, no. 9, pp. 2041–2054, sep 1989. [Online]. Available: http://onlinelibrary.wiley.com/doi/10.1002/macp.1989.021900904/abstract

[4] F. Danhier, O. Feron, and V. Préat, "To exploit the tumor microenvironment: Passive and active tumor targeting of nanocarriers for anti-cancer drug delivery." *Journal of Controlled Release*, vol. 148, no. 2, pp. 135–46, dec 2010. [Online]. Available: http://www.sciencedirect.com/science/article/pii/S0168365910007108

[5] P. Ehrlich, "Studies in Immunity," New York, 1906.

[6] K. Strebhardt and A. Ullrich, "Paul Ehrlich's magic bullet concept: 100 years of progress," *Nature Reviews Cancer*, vol. 8, no. 6, pp. 473–480, 2008.

[7] S. Boeckle and E. Wagner, "Optimizing targeted gene delivery: Chemical modification of viral vectors and synthesis of artificial virus vector systems," *The AAPS Journal*, vol. 8, no. 4, pp. E731–E742, dec 2006. [Online]. Available: http://dx.doi.org/10.1208/aapsj080483

[8] Y. Ren, S. M. Wong, and L. Y. Lim, "Application of plant viruses as nano drug delivery systems." *Pharmaceutical Research*, vol. 27, no. 11, pp. 2509–13, nov 2010. [Online]. Available: http://www.springerlink.com/content/0673qm41n3474811/

[9] H. Ringsdorf, "Structure and properties of pharmacologically active polymers," *Journal of Polymer Science: Polymer Symposia*, vol. 51, no. 1, pp. 135–153, 1975.

[10] A. Nori and J. Kopecek, "Intracellular targeting of polymer-bound drugs for cancer chemotherapy," *Advanced Drug Delivery Reviews*, vol. 57, no. 4, pp. 609–636, 2005.

[11] M. Wilchek, "Affinity therapy and polymer bound drugs," *Die Makromolekulare Chemie*, vol. 2, no. S19791, pp. 207–214, 1979. [Online]. Available: http://dx.doi.org/10.1002/macp.1979.020021979113

[12] M. Liscovitch and Y. Lavie, "Cancer multidrug resistance: a review of recent drug discovery research." *IDrugs*, vol. 5, no. 4, pp. 349–55, apr 2002. [Online]. Available: http://www.ncbi.nlm.nih.gov/pubmed/15565517

[13] R. Duncan, M. J. Vicent, F. Greco, and R. I. Nicholson, "Polymer-drug conjugates: towards a novel approach for the treatment of endrocine-related cancer," *Endocrine Related Cancer*, vol. 12, no. Supplement_1, pp. S189–S199, jul 2005. [Online]. Available: http://erc.endocrinology-journals.org/content/12/Supplement{_}1/S189.fullhttp://erc.endocrinology-journals.org/cgi/doi/10.1677/erc.1.01045

[14] R. Duncan, "Polymer conjugates as anticancer nanomedicines," *Nature Reviews Cancer*, vol. 6, no. 9, pp. 688–701, aug 2006. [Online]. Available: http://dx.doi.org/10.1038/nrc1958

[15] P. P. Adiseshaiah, J. B. Hall, and S. E. McNeil, "Nanomaterial standards for efficacy and toxicity assessment," *Wiley Interdisciplinary Reviews: Nanomedicine and Nanobiotechnology*, vol. 2, no. 1, pp. 99–112, 2009. [Online]. Available: http://www.ncbi.nlm.nih.gov/pubmed/20049834

[16] R. Duncan and M. J. Vicent, "Do HPMA copolymer conjugates have a future as clinically useful nanomedicines? A critical overview of current status and future opportunities," *Advanced Drug Delivery Reviews*, vol. 62, no. 2, pp. 272–282, 2010. [Online]. Available: http://www.sciencedirect.com/science/article/pii/S0169409X09003895

[17] R. Duncan and R. Gaspar, "Nanomedicine(s) under the microscope," *Molecular Pharmaceutics*, vol. 8, no. 6, pp. 2101–41, dec 2011. [Online]. Available: http://dx.doi.org/10.1021/mp200394t

[18] R. van der Meel, L. J. C. Vehmeijer, R. J. Kok, G. Storm, and E. V. B. van Gaal, "Ligand-targeted particulate nanomedicines undergoing clinical evaluation: current status." *Advanced Drug Delivery Reviews*, vol. 65, no. 10, pp. 1284–98, oct 2013. [Online]. Available: http://www.sciencedirect.com/science/article/pii/S0169409X13001956

[19] R. B. Weiss, R. C. Donehower, P. H. Wiernik, T. Ohnuma, R. J. Gralla, D. L. Trump, J. R. Baker, D. A. Van Echo, D. D. Von Hoff, and B. Leyland-Jones, "Hypersensitivity reactions from taxol." *Journal of Clinical Oncology*, vol. 8, no. 7, pp. 1263–1268, 1990.

[20] A. du Bois, M. Schlaich, H.-J. Lück, A. Mollenkopf, U. Wechsel, M. Rauchholz, T. Bauknecht, and H.-G. Meerpohl, "Evaluation of neurotoxicity induced by paclitaxel second-line chemotherapy," *Supportive Care in Cancer*, vol. 7, no. 5, pp. 354–361, aug 1999. [Online]. Available: http://dx.doi.org/10.1007/s005200050275

[21] D. Hanahan and R. A. Weinberg, "The hallmarks of cancer," *Cell*, vol. 100, no. 1, pp. 57–70, 2000.

[22] H. Maeda, J. Wu, T. Sawa, Y. Matsumura, and K. Hori, "Tumor vascular permeability and the EPR effect in macromolecular therapeutics: a review," *Journal of Controlled Release*, vol. 65, no. 1-2, pp. 271–284, 2000.

[23] H. Maeda, T. Sawa, and T. Konno, "Mechanism of tumor-targeted delivery of macromolecular drugs, including the EPR effect in solid tumor and clinical overview of the prototype polymeric drug SMANCS," *Journal of*

Controlled Release, vol. 74, no. 1-3, pp. 47–61, jul 2001. [Online]. Available: http://www.sciencedirect.com/science/article/pii/S0168365901003091

[24] A. J. Leu, D. A. Berk, A. Lymboussaki, K. Alitalo, and R. K. Jain, "Absence of functional lymphatics within a murine sarcoma: a molecular and functional evaluation," *Cancer Research*, vol. 60, no. 16, pp. 4324–4327, aug 2000. [Online]. Available: http://cancerres.aacrjournals.org/cgi/content/abstract/60/16/4324

[25] E. S. Lee, Z. Gao, D. Kim, K. Park, I. C. Kwon, Y. H. Bae, E. Seong, I. Chan, and Y. Han, "Super pH-sensitive multifunctional polymeric micelle for tumor pHe specific TAT exposure and multidrug resistance," *Journal of Controlled Release*, vol. 129, no. 3, pp. 228–236, 2008. [Online]. Available: http://www.pubmedcentral.nih.gov/articlerender.fcgi?artid=2603624{\&}tool=pmcentrez{\&}rendertype=abstract

[26] J. L. Wike-Hooley, J. Haveman, and H. S. Reinhold, "The relevance of tumour pH to the treatment of malignant disease." *Radiotherapy and Oncology*, vol. 2, no. 4, pp. 343–66, dec 1984. [Online]. Available: http://www.ncbi.nlm.nih.gov/pubmed/6097949

[27] I. F. Tannock and D. Rotin, "Acid pH in tumors and its potential for therapeutic exploitation," *Cancer Research*, vol. 49, no. 16, pp. 4373–4384, aug 1989. [Online]. Available: http://cancerres.aacrjournals.org/cgi/content/abstract/49/16/4373

[28] H. A. Kim, K. Kim, S. W. Kim, and M. Lee, "Transcriptional and post-translational regulatory system for hypoxia specific gene expression using the erythropoietin enhancer and the oxygen-dependent degradation domain." *Journal of Controlled Release*, vol. 121, no. 3, pp. 218–24, aug 2007. [Online]. Available: http://dx.doi.org/10.1016/j.jconrel.2007.05.036

[29] C. Wong, T. Stylianopoulos, J. Cui, J. Martin, V. P. Chauhan, W. Jiang, Z. Popović, R. K. Jain, M. G. Bawendi, and D. Fukumura, "Multistage nanoparticle delivery system for deep penetration into tumor tissue," *Proceedings of the National Academy of Sciences*, vol. 108, no. 6, pp. 2426–2431, 2011.

[30] S. D. Conner and S. L. Schmid, "Regulated portals of entry into the cell." *Nature*, vol. 422, no. 6927, pp. 37–44, mar 2003. [Online]. Available: http://dx.doi.org/10.1038/nature01451

[31] L. C. Hartmann, G. L. Keeney, W. L. Lingle, T. J. H. Christianson, B. Varghese, D. Hillman, A. L. Oberg, and P. S. Low, "Folate receptor overexpression is associated with poor outcome in breast cancer," *International Journal of Cancer*, vol. 121, no. 5, pp. 938–942, 2007.

[32] D. J. Slamon, G. M. Clark, S. G. Wong, W. J. Levin, A. Ullrich, and W. L. McGuire, "Human breast cancer: correlation of relapse and survival with amplification of the HER-2/neu oncogene," *Science*, vol. 235, no. 4785, pp. 177–182, 1987.

[33] K. R. Kalli, A. L. Oberg, G. L. Keeney, T. J. H. Christianson, P. S. Low, K. L. Knutson, and L. C. Hartmann, "Folate receptor alpha as a tumor target in epithelial ovarian cancer," *Gynecologic Oncology*, vol. 108, no. 3, pp. 619–626, 2008.

[34] M. N. Koopaei, R. Dinarvand, M. Amini, H. Rabbani, S. Emami, S. N. Ostad, and F. Atyabi, "Docetaxel immunonanocarriers as targeted delivery systems for HER 2-positive tumor cells: preparation, characterization, and cytotoxicity studies," *International Journal of Nanomedicine*, vol. 6, pp. 1903–1912, 2011.

[35] J. S. Ross and G. S. Gray, "Targeted therapy for cancer: the HER-2/neu and Herceptin story," *Clinical Leadership Management Review*, vol. 17, no. 6, pp. 333–340, 2003.

[36] D. R. Welch, "Biologic considerations for drug targeting in cancer patients," *Cancer Treatment Reviews*, vol. 14, no. 3-4, pp. 351–358, 1987.

[37] Y. H. Bae and K. Park, "Targeted drug delivery to tumors: myths, reality and possibility," *Journal of Controlled Release*, vol. 153, no. 3, pp. 198–205, 2011.

[38] R. A. Beckman, L. M. Weiner, and H. M. Davis, "Antibody constructs in cancer therapy: protein engineering strategies to improve exposure in solid tumors." *Cancer*, vol. 109, no. 2, pp. 170–9, jan 2007. [Online]. Available: http://www.ncbi.nlm.nih.gov/pubmed/17154393http://onlinelibrary.wiley.com/doi/10.1002/cncr.22402/full

[39] "Drugs@FDA: FDA Approved Drug Products." [Online]. Available: http://www.accessdata.fda.gov/Scripts/cder/drugsatfda/index.cfm

[40] A. E. Nel, L. Mädler, D. Velegol, T. Xia, E. M. V. Hoek, P. Somasundaran, F. Klaessig, V. Castranova, and M. Thompson, "Understanding biophysicochemical interactions at the nano-bio interface." *Nature Materials*, vol. 8, no. 7, pp. 543–57, jul 2009. [Online]. Available: http://www.ncbi.nlm.nih.gov/pubmed/19525947

[41] E. Blanco, H. Shen, and M. Ferrari, "Principles of nanoparticle design for overcoming biological barriers to drug delivery," *Nature Biotechnology*, vol. 33, no. 9, pp. 941–951, sep 2015. [Online]. Available: http://dx.doi.org/10.1038/nbt.3330

[42] T. M. Allen and P. R. Cullis, "Drug delivery systems: entering the mainstream." *Science (New York, N.Y.)*, vol. 303, no. 5665, pp. 1818–22, mar 2004. [Online]. Available: http://science.sciencemag.org/content/303/5665/1818.abstract

[43] H. Kobayashi, R. Watanabe, and P. L. Choyke, "Improving conventional enhanced permeability and retention (EPR) effects; what is the appropriate target?" *Theranostics*, vol. 4, no. 1, pp. 81–9, jan 2013. [Online]. Available: http://www.pubmedcentral.nih.gov/articlerender.fcgi?artid=3881228{\&}tool=pmcentrez{\&}rendertype=abstract

[44] E. Miele, G. P. Spinelli, E. Miele, F. Tomao, and S. Tomao, "Albumin-bound formulation of paclitaxel (Abraxane ABI-007) in the treatment of breast cancer," *International Journal of Nanomedicine*, vol. 4, pp. 99–105, jan 2009. [Online]. Available: http://www.pubmedcentral.nih.gov/articlerender.fcgi?artid=2720743{\&}tool=pmcentrez{\&}rendertype=abstract

[45] M. B. Fuertes, A. K. Kacha, J. Kline, S.-R. Woo, D. M. Kranz, K. M. Murphy, and T. F. Gajewski, "Host type I IFN signals are required for antitumor CD8+ T cell responses through CD8{alpha}+ dendritic cells." *The Journal of Experimental Medicine*, vol. 208, no. 10, pp. 2005–16, sep 2011. [Online]. Available: http://www.pubmedcentral.nih.gov/articlerender.fcgi?artid=3182064{\&}tool=pmcentrez{\&}rendertype=abstract

[46] "GSK to discontinue manufacture and sale of the BEXXAR® therapeutic regimen (tositumomab and iodine I 131 tositumomab) — GSK." [Online]. Available: https://us.gsk.com/en-us/media/press-releases/2013/gsk-to-discontinue-manufacture-and-sale-of-the-bexxar-therapeutic-regimen-tositumomab-and-iodine-i-131-tositumomab/

[47] "FDA Approval for Tositumomab and Iodine I 131 Tositumomab - National Cancer Institute." [Online]. Available: http://www.cancer.gov/about-cancer/treatment/drugs/fda-tositumomab-I131iodine-tositumomab

[48] P. F. Bross, J. Beitz, G. Chen, X. H. Chen, E. Duffy, L. Kieffer, S. Roy, R. Sridhara, A. Rahman, G. Williams, and R. Pazdur, "Approval summary: gemtuzumab ozogamicin in relapsed acute myeloid leukemia," *Clinical Cancer Research*, vol. 7, no. 6, pp. 1490–1496, jun 2001. [Online]. Available: http://clincancerres.aacrjournals.org/cgi/content/abstract/7/6/1490

[49] R. A. Larson, E. L. Sievers, E. A. Stadtmauer, B. Löwenberg, E. H. Estey, H. Dombret, M. Theobald, D. Voliotis, J. M. Bennett, M. Richie, L. H. Leopold, M. S. Berger, M. L. Sherman, M. R. Loken, J. J. M. van Dongen, I. D. Bernstein, and F. R. Appelbaum, "Final report of the efficacy and safety of gemtuzumab ozogamicin (Mylotarg) in patients with CD33-positive acute myeloid leukemia in first recurrence." *Cancer*, vol. 104, no. 7, pp. 1442–52, oct 2005. [Online]. Available: http://www.ncbi.nlm.nih.gov/pubmed/16116598

[50] K. E. Uhrich, S. M. Cannizzaro, R. S. Langer, and K. M. Shakesheff, "Polymeric systems for controlled drug release," *Chemical Reviews*, vol. 99, no. 11, pp. 3181–3198, nov 1999. [Online]. Available: http://dx.doi.org/10.1021/cr940351u

[51] F. Alexis, E. Pridgen, L. K. Molnar, and O. C. Farokhzad, "Factors affecting the clearance and biodistribution of polymeric nanoparticles." *Molecular Pharmaceutics*, vol. 5, no. 4, pp. 505–15, jan 2008. [Online]. Available: http://dx.doi.org/10.1021/mp800051m

[52] H. S. Choi, W. Liu, P. Misra, E. Tanaka, J. P. Zimmer, B. Itty Ipe, M. G. Bawendi, and J. V. Frangioni, "Renal clearance of quantum dots." *Nature Biotechnology*, vol. 25, no. 10, pp. 1165–70, oct 2007. [Online]. Available: http://dx.doi.org/10.1038/nbt1340

[53] B. H. Simon, H. Y. Ando, and P. K. Gupta, "Circulation time and body distribution of 14C-labeled amino-modified polystyrene nanoparticles in mice." *Journal of Pharmaceutical Sciences*, vol. 84, no. 10, pp. 1249–53, oct 1995. [Online]. Available: http://www.ncbi.nlm.nih.gov/pubmed/8801343http://linkinghub.elsevier.com/retrieve/pii/S0022354915499022

[54] Y. H. Bae and H. Yin, "Stability issues of polymeric micelles." *Journal of Controlled Release*, vol. 131, no. 1, pp. 2–4, oct 2008. [Online]. Available: http://dx.doi.org/10.1016/j.jconrel.2008.06.015

[55] W. G. Kreyling, A. M. Abdelmonem, Z. Ali, F. Alves, M. Geiser, N. Haberl, R. Hartmann, S. Hirn, D. J. de Aberasturi, K. Kantner, G. Khadem-Saba, J.-M. Montenegro, J. Rejman, T. Rojo, I. R. de Larramendi, R. Ufartes, A. Wenk, and W. J. Parak, "In vivo integrity of polymer-coated gold nanoparticles." *Nature Nanotechnology*, vol. 10, no. 7, pp. 619–23, jul 2015. [Online]. Available: http://dx.doi.org/10.1038/nnano.2015.111

[56] S. Dokka, D. Toledo, X. Shi, V. Castranova, and Y. Rojanasakul, "Oxygen radical-mediated pulmonary toxicity induced by some cationic liposomes," *Pharmaceutical Research*, vol. 17, no. 5, pp. 521–525, may 2000. [Online]. Available: http://dx.doi.org/10.1023/A:1007504613351

[57] R. Gref, A. Domb, P. Quellec, T. Blunk, R. Müller, J. Verbavatz, and R. Langer, "The controlled intravenous delivery of drugs using PEG-coated sterically stabilized nanospheres," *Advanced Drug Delivery Reviews*, vol. 16, no. 2-3, pp. 215–233, sep 1995. [Online]. Available: http://dx.doi.org/10.1016/0169-409X(95)00026-4

[58] G. Pasut and F. M. Veronese, "PEG conjugates in clinical development or use as anticancer agents: an overview," *Advanced Drug Delivery Reviews*, vol. 61, no. 13, pp. 1177–88, nov 2009. [Online]. Available: http://dx.doi.org/10.1016/j.addr.2009.02.010

[59] M. Morra, "Poly(ethylene oxide) coated surfaces," in *Water in Biomaterials Surface Science*, 2001, ch. 12, pp. 307–332.

[60] T. Ishida, X. Wang, T. Shimizu, K. Nawata, and H. Kiwada, "PEGylated liposomes elicit an anti-PEG IgM response in a T cell-independent manner," *Journal of Controlled Release*, vol. 122, no. 3, pp. 349–355, 2007. [Online]. Available: http://www.sciencedirect.com/science/article/pii/S0168365907002428

[61] A. L. Klibanov, K. Maruyama, V. P. Torchilin, and L. Huang, "Amphipathic polyethyleneglycols effectively prolong the circulation time of liposomes," *FEBS Letters*, vol. 268, no. 1, pp. 235–237, jul 1990. [Online]. Available: http://dx.doi.org/10.1016/0014-5793(90)81016-H

[62] M. K. Danquah, X. A. Zhang, and R. I. Mahato, "Extravasation of polymeric nanomedicines across tumor vasculature," *Advanced Drug Delivery Reviews*, vol. 63, no. 8, pp. 623–639, 2011.

[63] I. L. Medintz, A. R. Clapp, H. Mattoussi, E. R. Goldman, B. Fisher, and J. M. Mauro, "Self-assembled nanoscale biosensors based on quantum dot FRET donors." *Nature Materials*, vol. 2, no. 9, pp. 630–8, sep 2003. [Online]. Available: http://dx.doi.org/10.1038/nmat961

[64] S. Miura, H. Suzuki, and Y. H. Bae, "A multilayered cell culture model for transport study in solid tumors: evaluation of tissue penetration of polyethyleneimine based cationic micelles." *Nano Today*, vol. 9, no. 6, pp. 695–704, dec 2014. [Online]. Available: http://www.sciencedirect.com/science/article/pii/S1748013214001376

[65] T. Nomoto, Y. Matsumoto, K. Miyata, M. Oba, S. Fukushima, N. Nishiyama, T. Yamasoba, and K. Kataoka, "In situ quantitative monitoring of polyplexes and polyplex micelles in the blood circulation using intravital real-time confocal laser scanning microscopy," *Journal of Controlled Release*, vol. 151, no. 2, pp. 104–109, apr 2011. [Online]. Available: http://dx.doi.org/10.1016/j.jconrel.2011.02.011http://www.sciencedirect.com/science/article/pii/S0168365911000964

[66] K. Kim, J. H. Kim, H. Park, Y.-S. Kim, K. Park, H. Nam, S. Lee, J. H. Park, R.-W. Park, I.-S. Kim, K. Choi, S. Y. Kim, K. Park, and I. C. Kwon, "Tumor-homing multifunctional nanoparticles for cancer theragnosis: Simultaneous diagnosis, drug delivery, and therapeutic monitoring." *Journal of Controlled Release*, vol. 146, no. 2, pp. 219–27, sep 2010. [Online]. Available: http://www.sciencedirect.com/science/article/pii/S0168365910002580

[67] J. S. Y. Ma, J. Y. Kim, S. A. Kazane, S.-H. Choi, H. Y. Yun, M. S. Kim, D. T. Rodgers, H. M. Pugh, O. Singer, S. B. Sun, B. R. Fonslow, J. N. Kochenderfer, T. M. Wright, P. G. Schultz, T. S. Young, C. H. Kim, and Y. Cao, "Versatile strategy

for controlling the specificity and activity of engineered T cells." *Proceedings of the National Academy of Sciences*, vol. 113, no. 4, pp. E450–458, jan 2016. [Online]. Available: http://www.pnas.org/content/113/4/E450

[68] M. Brunelli, E. Manfrin, G. Martignoni, S. Bersani, A. Remo, D. Reghellin, M. Chilosi, and F. Bonetti, "HER-2/neu assessment in breast cancer using the original FDA and new ASCO/CAP guideline recommendations: impact on selecting patients for herceptin therapy." *American Journal of Clinical Pathology*, vol. 129, no. 6, pp. 907–911, 2008. [Online]. Available: http://www.ncbi.nlm.nih.gov/pubmed/18480007http://ajcp.ascpjournals.org/content/129/6/907.long

[69] K. F. Lee, H. Simon, H. Chen, B. Bates, M. C. Hung, and C. Hauser, "Requirement for neuregulin receptor erbB2 in neural and cardiac development." *Nature*, vol. 378, no. 6555, pp. 394–8, nov 1995. [Online]. Available: http://dx.doi.org/10.1038/378394a0

[70] A. Negro, "Essential roles of Her2/erbB2 in cardiac development and function," *Recent Progress in Hormone Research*, vol. 59, no. 1, pp. 1–12, jan 2004. [Online]. Available: http://rphr.endojournals.org/cgi/content/abstract/59/1/1

[71] E. A. Perez and R. Rodeheffer, "Clinical cardiac tolerability of trastuzumab." *Journal of Clinical Oncology*, vol. 22, no. 2, pp. 322–9, jan 2004. [Online]. Available: http://jco.ascopubs.org/content/22/2/322.full

[72] D. B. Kirpotin, D. C. Drummond, Y. Shao, M. R. Shalaby, K. Hong, U. B. Nielsen, J. D. Marks, C. C. Benz, and J. W. Park, "Antibody targeting of long-circulating lipidic nanoparticles does not increase tumor localization but does increase internalization in animal models." *Cancer Research*, vol. 66, no. 13, pp. 6732–40, jul 2006. [Online]. Available: http://cancerres.aacrjournals.org/cgi/content/abstract/66/13/6732

[73] H. Lee, H. Fonge, B. Hoang, R. M. Reilly, and C. Allen, "The effects of particle size and molecular targeting on the intratumoral and subcellular distribution of polymeric nanoparticles," *Molecular Pharmaceutics*, vol. 7, no. 4, pp. 1195–1208, 2010.

[74] K. N. Sugahara, T. Teesalu, P. P. Karmali, V. R. Kotamraju, L. Agemy, O. M. Girard, D. Hanahan, R. F. Mattrey, and E. Ruoslahti, "Tissue-penetrating delivery of compounds and nanoparticles into tumors," *Cancer Cell*, vol. 16, no. 6, pp. 510–520, dec 2009. [Online]. Available: http://linkinghub.elsevier.com/retrieve/pii/S1535610809003821

[75] J. S. Bennett, B. W. Berger, and P. C. Billings, "The structure and function of platelet integrins." *Journal of Thrombosis and Haemostasis*, vol. 7 Suppl 1, pp. 200–5, jul 2009. [Online]. Available: http://www.ncbi.nlm.nih.gov/pubmed/19630800

[76] M. Silhol, M. Tyagi, M. Giacca, B. Lebleu, and E. Vivès, "Different mechanisms for cellular internalization of the HIV-1 Tat-derived cell penetrating peptide and recombinant proteinsfused to Tat," *European Journal of Biochemistry*, vol. 269, no. 2, pp. 494–501, jan 2002. [Online]. Available: http://doi.wiley.com/10.1046/j.0014-2956.2001.02671.x

[77] C. Ciobanasu, E. Harms, G. Tunnemann, M. C. Cardoso, and U. Kubitscheck, "Cell-penetrating HIV1 TAT peptides float on model lipid bilayers," *Biochemistry*, vol. 48, no. 22, pp. 4728–4737, 2009.

[78] C. C. Gyenge, O. Tenstad, and H. Wiig, "In vivo determination of steric and electrostatic exclusion of albumin in rat skin and skeletal muscle." *The Journal of Physiology*, vol. 552, no. Pt 3, pp. 907–16, nov 2003. [Online]. Available: http://www.pubmedcentral.nih.gov/articlerender.fcgi?artid=2343468{\&}tool=pmcentrez{\&}rendertype=abstract

[79] S. E. A. Gratton, P. A. Ropp, P. D. Pohlhaus, J. C. Luft, V. J. Madden, M. E. Napier, and J. M. DeSimone, "The effect of particle design on cellular internalization pathways." *Proceedings of the National Academy of Sciences*, vol. 105, no. 33, pp. 11 613–8, aug 2008. [Online]. Available: http://www.pnas.org/content/105/33/11613.full

[80] H. Herd, N. Daum, A. T. Jones, H. Huwer, H. Ghandehari, and C.-M. Lehr, "Nanoparticle geometry and surface orientation influence mode of cellular uptake," *ACS Nano*, vol. 7, no. 3, pp. 1961–73, mar 2013. [Online]. Available: http://dx.doi.org/10.1021/nn304439f

[81] H. H. Gustafson, D. Holt-Casper, D. W. Grainger, and H. Ghandehari, "Nanoparticle uptake: the phagocyte problem," *Nano Today*, vol. 10, no. 4, pp. 487–510, aug 2015. [Online]. Available: http://www.sciencedirect.com/science/article/pii/S1748013215000766

[82] J. W. Nichols and Y. H. Bae, "EPR: evidence and fallacy," *Journal of Controlled Release*, vol. 190, pp. 451–464, sep 2014. [Online]. Available: http://www.sciencedirect.com/science/article/pii/S0168365914002685http://linkinghub.elsevier.com/retrieve/pii/S0168365914002685

[83] U. Prabhakar, H. Maeda, R. K. Jain, E. M. Sevick-Muraca, W. Zamboni, O. C. Farokhzad, S. T. Barry, A. Gabizon, P. Grodzinski, and D. C. Blakey, "Challenges and key considerations of the enhanced permeability and retention effect for nanomedicine drug delivery in oncology," *Cancer Research*, vol. 73, no. 8, pp. 2412–7, apr 2013. [Online]. Available: http://cancerres.aacrjournals.org/content/73/8/2412.short

[84] H. Holback and Y. Yeo, "Intratumoral drug delivery with nanoparticulate carriers," *Pharmaceutical Research*, vol. 28, no. 8, pp. 1819–1830, 2011.

[85] E. S. Lee, Z. Gao, and Y. H. Bae, "Recent progress in tumor pH targeting nanotechnology," *Journal of Controlled Release*, vol. 132, no. 3, pp. 164–170, 2008.

[86] F. Yuan, M. Leunig, S. K. Huang, D. A. Berk, D. Papahadjopoulos, and R. K. Jain, "Microvascular permeability and interstitial penetration of sterically stabilized (stealth) liposomes in a human tumor xenograft," *Cancer Research*, vol. 54, no. 13, pp. 3352–3356, 1994.

[87] A. J. Primeau, A. Rendon, D. Hedley, L. Lilge, and I. F. Tannock, "The distribution of the anticancer drug doxorubicin in relation to blood vessels in solid tumors," *Clinical Cancer Research*, vol. 11, no. 24 Pt 1, pp. 8782–8, dec 2005. [Online]. Available: http://clincancerres.aacrjournals.org/cgi/content/abstract/11/24/8782http://www.ncbi.nlm.nih.gov/pubmed/16361566

[88] E. Smith, J. Breznik, and B. D. Lichty, "Strategies to enhance viral penetration of solid tumors," *Human Gene Therapy*, vol. 1060, no. September, pp. 1053–1060, may 2011. [Online]. Available: http://www.ncbi.nlm.nih.gov/pubmed/21443415

[89] S. Paget, "The distribution of secondary growths in cancer of the breast," *The Lancet*, vol. 133, no. 3421, pp. 571–573, mar 1889. [Online]. Available: http://www.sciencedirect.com/science/article/pii/S0140673600499150

[90] L. a. Liotta and C. N. Rao, "Role of the extracellular matrix in cancer," *Annals of the New York Academy of Sciences*, vol. 460, no. 1 Biology, Chem, pp. 333–344, dec 1985. [Online]. Available: http://doi.wiley.com/10.1111/j.1749-6632.1985.tb51180.x

[91] F. G. Giancotti and R. Erkki, "Integrin signaling," *Science*, vol. 285, no. 5430, pp. 1028–1033, aug 1999. [Online]. Available: http://www.sciencemag.org/content/285/5430/1028.abstracthttp://www.sciencemag.org/cgi/doi/10.1126/science.285.5430.1028

[92] G. A. McQuibban, "Inflammation dampened by gelatinase a cleavage of monocyte chemoattractant protein-3," *Science*, vol. 289, no. 5482, pp. 1202–1206, aug 2000. [Online]. Available: http://www.sciencemag.org/content/289/5482/1202.abstract

[93] D. Barkan, J. E. Green, and A. F. Chambers, "Extracellular matrix: a gatekeeper in the transition from dormancy to metastatic growth," *European Journal of Cancer*, vol. 46, no. 7, pp. 1181–1188, may 2010. [Online]. Available: http://www.sciencedirect.com/science/article/pii/S0959804910001541http://www.pubmedcentral.nih.gov/articlerender.fcgi?artid=2856784{\&}tool=pmcentrez{\&}rendertype=abstract

[94] K. R. Levental, H. Yu, L. Kass, J. N. Lakins, M. Egeblad, J. T. Erler, S. F. T. Fong, K. Csiszar, A. Giaccia, W. Weninger, M. Yamauchi, D. L. Gasser, and V. M. Weaver, "Matrix crosslinking forces tumor progression by enhancing integrin signaling," *Cell*, vol. 139, no. 5, pp. 891–906, nov 2009. [Online]. Available: http://www.sciencedirect.com/science/article/pii/S0092867409013531http://www.pubmedcentral.nih.gov/articlerender.fcgi?artid=2788004{\&}tool=pmcentrez{\&}rendertype=abstract

[95] P. A. Netti, D. A. Berk, M. A. Swartz, A. J. Grodzinsky, and R. K. Jain, "Role of extracellular matrix assembly in interstitial transport in solid tumors," *Cancer Research*, vol. 60, no. 9, pp. 2497–2503, may 2000. [Online]. Available: http://cancerres.aacrjournals.org/cgi/content/abstract/60/9/2497

[96] M. Sarntinoranont, F. Rooney, and M. Ferrari, "Interstitial stress and fluid pressure within a growing tumor," *Annals of Biomedical Engineering*, vol. 31, no. 3, pp. 327–335, mar 2003. [Online]. Available: http://link.springer.com/10.1114/1.1554923

[97] R. K. Jain, "Transport of molecules in the tumor interstitium: a review," *Cancer Research*, vol. 47, no. 12, pp. 3039–3051, jun 1987. [Online]. Available: http://cancerres.aacrjournals.org/content/47/12/3039.short

[98] R. K. Jain and L. T. Baxter, "Mechanisms of heterogeneous distribution of monoclonal antibodies and other macromolecules in tumors: significance of elevated interstitial pressure," *Cancer Research*, vol. 48, no. 24_Part_1, pp. 7022–7032, dec 1988. [Online]. Available: http://cancerres.aacrjournals.org/cgi/content/abstract/48/24{_}Part{_}1/7022

[99] B. J. Meyer, A. Meyer, and A. C. Guyton, "Interstitial fluid pressure," *Circulation Research*, vol. 22, no. 2, pp. 263–271, feb 1968. [Online]. Available: http://circres.ahajournals.org/content/22/2/263.short

[100] H. P. Rutz, "A biophysical basis of enhanced interstitial fluid pressure in tumors." *Medical Hypotheses*, vol. 53, no. 6, pp. 526–9, dec 1999. [Online]. Available: http://www.sciencedirect.com/science/article/pii/S0306987799908058

[101] R. K. Jain and T. Stylianopoulos, "Delivering nanomedicine to solid tumors," *Nature Reviews Clinical Oncology*, vol. 7, no. 11, pp. 653–64, nov 2010. [Online]. Available: http://dx.doi.org/10.1038/nrclinonc.2010.139

[102] H. Wiig and M. A. Swartz, "Interstitial fluid and lymph formation and transport: physiological regulation and roles in inflammation and cancer." *Physiological Reviews*, vol. 92, no. 3, pp. 1005–60, jul 2012. [Online]. Available: http://physrev.physiology.org/content/92/3/1005

[103] R. Gutmann, M. Leunig, J. Feyh, A. E. Goetz, K. Messmer, E. Kastenbauer, and R. K. Jain, "Interstitial hypertension in head and neck tumors in patients: correlation with tumor size," *Cancer Research*, vol. 52, no. 7, pp. 1993–1995, apr 1992. [Online]. Available: http://cancerres.aacrjournals.org/cgi/content/abstract/52/7/1993

[104] J. R. Less, M. C. Posner, Y. Boucher, D. Borochovitz, N. Wolmark, and R. K. Jain, "Interstitial hypertension in human breast and colorectal tumors," *Cancer Research*, vol. 52, no. 22, pp. 6371–6374, nov 1992. [Online]. Available: http://cancerres.aacrjournals.org/content/52/22/6371.abstract

[105] V. P. Chauhan, T. Stylianopoulos, Y. Boucher, and R. K. Jain, "Delivery of molecular and nanoscale medicine to tumors: transport barriers and strategies," *Annual Review of Chemical and Biomolecular Engineering*, vol. 2, no. 1, pp. 281–98, jan 2011. [Online]. Available: http://www.ncbi.nlm.nih.gov/pubmed/22432620

[106] Y. Boucher, L. T. Baxter, and R. K. Jain, "Interstitial pressure gradients in tissue-isolated and subcutaneous tumors: implications for therapy," *Cancer Research*, vol. 50, no. 15, pp. 4478–4484, aug 1990. [Online]. Available: http://cancerres.aacrjournals.org/content/50/15/4478.short

[107] C.-H. Heldin, K. Rubin, K. Pietras, and A. Östman, "High interstitial fluid pressure an obstacle in cancer therapy," *Nature Reviews Cancer*, vol. 4, no. 10, pp. 806–813, oct 2004. [Online]. Available: http://www.ncbi.nlm.nih.gov/pubmed/15510161http://www.nature.com/doifinder/10.1038/nrc1456

[108] Y. Li, J. Wang, M. G. Wientjes, and J. L.-S. Au, "Delivery of nanomedicines to extracellular and intracellular compartments of a solid tumor," *Advanced Drug Delivery Reviews*, vol. 64, no. 1, pp. 29–39, jan 2012. [Online]. Available: http://dx.doi.org/10.1016/j.addr.2011.04.006

[109] H. Hashizume, P. Baluk, S. Morikawa, J. W. McLean, G. Thurston, S. Roberge, R. K. Jain, and D. M. McDonald, "Openings between defective endothelial cells explain tumor vessel leakiness," *The American Journal of Pathology*, vol. 156, no. 4, pp. 1363–1380, 2000.

[110] G. R. DiResta, J. Lee, J. H. Healey, A. Levchenko, S. M. Larson, and E. Arbit, "Artificial lymphatic system: a new approach to reduce interstitial hypertension and increase blood flow, pH and pO2 in solid tumors," *Annals of Biomedical Engineering*, vol. 28, no. 5, pp. 543–555, may 2000. [Online]. Available: http://link.springer.com/10.1114/1.295

[111] R. K. Jain, R. T. Tong, and L. L. Munn, "Effect of vascular normalization by antiangiogenic therapy on interstitial hypertension, peritumor edema, and lymphatic metastasis: insights from a mathematical model." *Cancer Research*, vol. 67, no. 6, pp. 2729–35, mar 2007. [Online]. Available: http://cancerres.aacrjournals.org/content/67/6/2729.short

[112] B. Sylven and I. Bois, "Protein content and enzymatic assays of interstitial fluid from some normal tissues and transplanted mouse tumors," *Cancer Research*, vol. 20, no. 6, pp. 831–836, jul 1960. [Online]. Available: http://cancerres.aacrjournals.org/content/20/6/831.short

[113] J. R. Levick, "Flow through interstitium and other fibrous matrices," *Quarterly Journal of Experimental Physiology*, vol. 72, no. 4, pp. 409–437, oct 1987. [Online]. Available: http://ep.physoc.org/content/72/4/409.abstract

[114] S. P. Sutera and R. Skalak, "The history of Poiseuille's law," *Annual Review of Fluid Mechanics*, vol. 25, no. 1, pp. 1–20, 1993.

[115] A. C. Guyton, H. J. Granger, and A. E. Taylor, "Interstitial fluid pressure," *Physiological Reviews*, vol. 51, no. 3, pp. 527–563, jul 1971. [Online]. Available: http://physrev.physiology.org/content/51/3/527.full-text.pdf+html

[116] R. A. Brace and A. C. Guyton, "Interstitial fluid pressure: capsule, free fluid, gel fluid, and gel absorption pressure in subcutaneous tissue," *Microvascular Research*, vol. 18, no. 2, pp. 217–228, sep 1979. [Online]. Available: http://www.sciencedirect.com/science/article/pii/002628627990030X

[117] T. E. Woodcock and T. M. Woodcock, "Revised Starling equation and the glycocalyx model of transvascular fluid exchange: an improved paradigm for prescribing intravenous fluid therapy." *British Journal of Anaesthesia*, vol. 108, no. 3, pp. 384–94, mar 2012. [Online]. Available: http://bja.oxfordjournals.org/content/early/2012/01/29/bja.aer515.short

[118] A. C. Guyton and A. W. Lindsey, "Effect of elevated left atrial pressure and decreased plasma protein concentration on the development of pulmonary edema," *Circulation Research*, vol. 7, no. 4, pp. 649–657, jul 1959. [Online]. Available: http://circres.ahajournals.org/content/7/4/649.short

[119] A. C. Guyton and J. E. Hall, *Textbook of Medical Physiology*, 11th ed. Saunders, 2005.

[120] G. Miserocchi, D. Negrini, A. Passi, and G. De Luca, "Development of lung edema: interstitial fluid dynamics and molecular structure," *News in Physiological Science*, vol. 16, no. 2, pp. 66–71, apr 2001. [Online]. Available: http://physiologyonline.physiology.org/content/16/2/66

[121] P. Pelosi, P. R. Rocco, D. Negrini, and A. Passi, "The extracellular matrix of the lung and its role in edema formation," *Anais da Academia Brasileira de Ciências*, vol. 79, no. 2, pp. 285–297, jun 2007. [Online]. Available: http://www.scielo.br/scielo.php?script=sci{_}arttext{\&}pid=S0001-37652007000200010{\&}lng=en{\&}nrm=iso{\&}tlng=en

[122] G. Gabbiani, "The myofibroblast in wound healing and fibrocontractive diseases." *The Journal of Pathology*, vol. 200, no. 4, pp. 500–3, jul 2003. [Online]. Available: http://www.ncbi.nlm.nih.gov/pubmed/12845617

[123] R. A. Clark, J. M. Folkvord, C. E. Hart, M. J. Murray, and J. M. McPherson, "Platelet isoforms of platelet-derived growth factor stimulate fibroblasts to contract collagen matrices," *The Journal of Clinical Investigation*, vol. 84, no. 3, pp. 1036–1040, 1989.

[124] M. Egeblad, E. S. Nakasone, and Z. Werb, "Tumors as organs: complex tissues that interface with the entire organism," *Developmental Cell*, vol. 18, no. 6, pp. 884–901, jun 2010. [Online]. Available: http://www.pubmedcentral.nih.gov/articlerender.fcgi?artid=2905377{\&}tool=pmcentrez{\&}rendertype=abstract

[125] R. Montesano and L. Orci, "Transforming growth factor beta stimulates collagen-matrix contraction by fibroblasts: implications for wound healing," *Proceedings of the National Academy of Sciences*, vol. 85, no. 13, pp. 4894–7, jul 1988. [Online]. Available: http://www.pubmedcentral.nih.gov/articlerender.fcgi?artid=280543{\&}tool=pmcentrez{\&}rendertype=abstract

[126] K. J. Pienta, N. McGregor, R. Axelrod, and D. E. Axelrod, "Ecological therapy for cancer: defining tumors using an ecosystem paradigm suggests new opportunities for novel cancer treatments." *Translational Oncology*, vol. 1, no. 4, pp. 158–64, dec 2008. [Online]. Available: http://www.pubmedcentral.nih.gov/articlerender.fcgi?artid=2582164{\&}tool=pmcentrez{\&}rendertype=abstract

[127] T. W. Yen, N. P. Aardal, M. P. Bronner, D. R. Thorning, C. E. Savard, S. P. Lee, and R. H. Bell, "Myofibroblasts are responsible for the desmoplastic reaction surrounding human pancreatic carcinomas," *Surgery*, vol. 131, no. 2, pp. 129–134, feb 2002. [Online]. Available: http://www.sciencedirect.com/science/article/pii/S0039606002290455

[128] H. Yu, J. K. Mouw, and V. M. Weaver, "Forcing form and function: biomechanical regulation of tumor evolution." *Trends in Cell Biology*, vol. 21, no. 1, pp. 47–56, jan 2011. [Online]. Available: http://www.sciencedirect.com/science/article/pii/S0962892410001832

[129] M. F. Flessner, J. Choi, K. Credit, R. Deverkadra, and K. Henderson, "Resistance of tumor interstitial pressure to the penetration of intraperitoneally delivered antibodies into metastatic ovarian tumors," *Clinical Cancer Research*, vol. 11, no. 8, pp. 3117–3125, apr 2005. [Online]. Available: http://www.ncbi.nlm.nih.gov/pubmed/15837768http://clincancerres.aacrjournals.org/cgi/doi/10.1158/1078-0432.CCR-04-2332

[130] H. Wiig and O. Tenstad, "Interstitial exclusion of positively and negatively charged IgG in rat skin and muscle," *American Journal of Physiology. Heart and Circulatory Physiology*, vol. 280, no. 4, pp. H1505–1512, apr 2001. [Online]. Available: http://ajpheart.physiology.org/content/280/4/H1505.long

[131] Q. Hogan, "Distribution of solution in the epidural space: examination by cryomicrotome section," *Regional Anesthesia and Pain Medicine*, vol. 27, no. 2, pp. 150–156, 2002. [Online]. Available: http://journals.lww.com/rapm/Fulltext/2002/03000/Distribution{_}of{_}Solution{_}in{_}the{_}Epidural{_}Space{_}.7.aspx

[132] D. J. Chaplin and S. A. Hill, "Temporal heterogeneity in microregional erythrocyte flux in experimental solid tumours." *British Journal of Cancer*, vol. 71, no. 6, pp. 1210–3, jun 1995. [Online]. Available: http://www.pubmedcentral.nih.gov/articlerender.fcgi?artid=2033835{\&}tool=pmcentrez{\&}rendertype=abstract

[133] C. J. Eskey, A. P. Koretsky, M. M. Domach, and R. K. Jain, "2H-nuclear magnetic resonance imaging of tumor blood flow: spatial and temporal heterogeneity in a tissue-isolated mammary adenocarcinoma," *Cancer Research*, vol. 52, no. 21, pp. 6010–6019, nov 1992. [Online]. Available: http://cancerres.aacrjournals.org/content/52/21/6010

[134] F. Mollica, "A model for temporal heterogeneities of tumor blood flow," *Microvascular Research*, vol. 65, no. 1, pp. 56–60, jan 2003. [Online]. Available: http://www.sciencedirect.com/science/article/pii/S0026286202000122

[135] D. Fukumura and R. K. Jain, "Tumor microvasculature and microenvironment: targets for anti-angiogenesis and normalization." *Microvascular Research*, vol. 74, no. 2-3, pp. 72–84, 2007. [Online]. Available: http://www.pubmedcentral.nih.gov/articlerender.fcgi?artid=2100036{\&}tool=pmcentrez{\&}rendertype=abstract

[136] T. P. Padera, B. R. Stoll, J. B. Tooredman, D. Capen, E. di Tomaso, and R. K. Jain, "Pathology: cancer cells compress intratumour vessels," *Nature Communications*, vol. 427, no. 6976, p. 695, feb 2004.

[137] M. Köbel, S. E. Kalloger, N. Boyd, S. McKinney, E. Mehl, C. Palmer, S. Leung, N. J. Bowen, D. N. Ionescu, A. Rajput, L. M. Prentice, D. Miller, J. Santos, K. Swenerton, C. B. Gilks, and D. Huntsman, "Ovarian carcinoma subtypes are different diseases: implications for biomarker studies," *PLoS Medicine*, vol. 5, no. 12, p. e232, 2008.

[138] D. Louis, H. Ohgaki, O. Wiestler, W. Cavenee, P. Burger, A. Jouvet, B. Scheithauer, and P. Kleihues, "The 2007 WHO classification of tumours of the central nervous system," *Acta Neuropathologica*, vol. 114, no. 2, pp. 97–109, 2007.

[139] J. Liu, S. K. Lau, V. A. Varma, R. A. Moffitt, M. Caldwell, T. Liu, A. N. Young, J. A. Petros, A. O. Osunkoya, T. Krogstad, B. Leyland-Jones, M. D. Wang, and S. Nie, "Molecular mapping of tumor heterogeneity on clinical tissue specimens with multiplexed quantum dots," *ACS Nano*, vol. 4, no. 5, pp. 2755–2765, 2010.

[140] A. J. Thistlethwaite, G. A. Alexander, D. J. Moylan, and D. B. Leeper, "Modification of human tumor pH by elevation of blood glucose," *International Journal of Radiation Oncology, Biology, Physics*, vol. 13, no. 4, pp. 603–610, 1987.

[141] E. M. Sevick and R. K. Jain, "Blood flow and venous pH of tissue-isolated Walker 256 carcinoma during hyperglycemia," *Cancer Research*, vol. 48, no. 5, pp. 1201–7, mar 1988. [Online]. Available: http://www.ncbi.nlm.nih.gov/pubmed/3342400

[142] L. Xu, D. Fukumura, and R. K. Jain, "Acidic extracellular pH induces vascular endothelial growth factor (VEGF) in human glioblastoma cells via ERK1/2 MAPK signaling pathway: mechanism of low pH-induced VEGF," *The Journal of Biological Chemistry*, vol. 277, no. 13, pp. 11 368–74, mar 2002. [Online]. Available: http://www.ncbi.nlm.nih.gov/pubmed/11741977

[143] E. K. Rofstad, "Acidic extracellular pH promotes experimental metastasis of human melanoma cells in athymic nude mice," *Cancer Research*, vol. 66, no. 13, pp. 6699–6707, jul 2006. [Online]. Available: http://www.ncbi.nlm.nih.gov/pubmed/16818644

[144] D. Fukumura, F. Yuan, W. L. Monsky, Y. Chen, and R. K. Jain, "Effect of host microenvironment on the microcirculation of human colon adenocarcinoma," *American Journal of Pathology*, vol. 151, no. 3, pp. 679–688, 1997. [Online]. Available: http://www.ncbi.nlm.nih.gov/pmc/articles/PMC1857859/

[145] S. K. Hobbs, W. L. Monsky, F. Yuan, W. G. Roberts, L. Griffith, V. P. Torchilin, and R. K. Jain, "Regulation of transport pathways in tumor vessels: role of tumor type and microenvironment," *Proceedings of the National Academy of Sciences*, vol. 95, no. 8, pp. 4607–4612, 1998. [Online]. Available: http://www.pnas.org/content/95/8/4607.short

[146] F. Yuan, H. A. Salehi, Y. Boucher, U. S. Vasthare, R. F. Tuma, and R. K. Jain, "Vascular permeability and microcirculation of gliomas and mammary carcinomas transplanted in rat and mouse cranial windows," *Cancer Research*, vol. 54, no. 17, pp. 4564–4568, 1994. [Online]. Available: http://cancerres.aacrjournals.org/content/54/17/4564.full.pdf+html

[147] B. S. Kuszyk, F. M. Corl, F. N. Franano, D. A. Bluemke, L. V. Hofmann, B. J. Fortman, and E. K. Fishman, "Tumor transport physiology: implications for imaging and imaging-guided therapy," *American Journal of Roentgenology*, vol. 177, no. 4, pp. 747–753, oct 2001. [Online]. Available: http://www.ajronline.org

[148] Q. Yu and I. Stamenkovic, "Cell surface-localized matrix metalloproteinase-9 proteolytically activates TGF-beta and promotes tumor invasion and angiogenesis," *Genes & Development*, vol. 14, no. 2, pp. 163–176, 2000. [Online]. Available: http://genesdev.cshlp.org/cgi/content/abstract/14/2/163

[149] M. Al-Hajj, M. S. Wicha, A. Benito-Hernandez, S. J. Morrison, and M. F. Clarke, "Prospective identification of tumorigenic breast cancer cells," *Proceedings of the National Academy of Sciences*, vol. 100, no. 7, pp. 3983–8, apr 2003. [Online]. Available: http://www.pnas.org/cgi/content/abstract/100/7/3983

[150] S. Bao, Q. Wu, R. E. McLendon, Y. Hao, Q. Shi, A. B. Hjelmeland, M. W. Dewhirst, D. D. Bigner, and J. N. Rich, "Glioma stem cells promote radioresistance by preferential activation of the DNA damage response," *Nature*, vol. 444, no. 7120, pp. 756–60, dec 2006. [Online]. Available: http://dx.doi.org/10.1038/nature05236

[151] P. C. Hermann, S. L. Huber, T. Herrler, A. Aicher, J. W. Ellwart, M. Guba, C. J. Bruns, and C. Heeschen, "Distinct populations of cancer stem cells determine tumor growth and metastatic activity in human pancreatic cancer," *Cell Stem Cell*, vol. 1, no. 3, pp. 313–23, sep 2007. [Online]. Available: http://dx.doi.org/10.1016/j.stem.2007.06.002

[152] J. Zhou, J. Wulfkuhle, H. Zhang, P. Gu, Y. Yang, J. Deng, J. B. Margolick, L. A. Liotta, E. Petricoin, and Y. Zhang, "Activation of the PTEN/mTOR/STAT3 pathway in breast cancer stem-like cells is required for viability and maintenance," *Proceedings of the National Academy of Sciences*, vol. 104, no. 41, pp. 16 158–63, oct 2007. [Online]. Available: http://www.pnas.org/cgi/content/abstract/104/41/16158

[153] D. Iliopoulos, H. A. Hirsch, G. Wang, and K. Struhl, "Inducible formation of breast cancer stem cells and their dynamic equilibrium with non-stem cancer cells via IL6 secretion," *Proceedings of the National Academy of Sciences*, vol. 108, no. 4, pp. 1397–1402, 2011.

[154] H. Clevers, "The cancer stem cell: premises, promises and challenges," *Nature Medicine*, vol. 17, no. 3, pp. 313–9, mar 2011. [Online]. Available: http://dx.doi.org/10.1038/nm.2304

[155] B.-B. S. Zhou, H. Zhang, M. Damelin, K. G. Geles, J. C. Grindley, and P. B. Dirks, "Tumour-initiating cells: challenges and opportunities for anticancer drug discovery," *Nature Reviews Drug Discovery*, vol. 8, no. 10, pp. 806–23, oct 2009. [Online]. Available: http://dx.doi.org/10.1038/nrd2137

[156] D. Bonnet and J. E. Dick, "Human acute myeloid leukemia is organized as a hierarchy that originates from a primitive hematopoietic cell," *Nature Medicine*, vol. 3, no. 7, pp. 730–737, jul 1997. [Online]. Available: http://dx.doi.org/10.1038/nm0797-730

[157] L. Jin, K. J. Hope, Q. Zhai, F. Smadja-Joffe, and J. E. Dick, "Targeting of CD44 eradicates human acute myeloid leukemic stem cells," *Nature Medicine*, vol. 12, no. 10, pp. 1167–74, oct 2006. [Online]. Available: http://dx.doi.org/10.1038/nm1483

[158] B. L. Roth, D. J. Sheffler, and W. K. Kroeze, "Magic shotguns versus magic bullets: selectively non-selective drugs for mood disorders and schizophrenia," *Nature Reviews Drug Discovery*, vol. 3, no. 4, pp. 353–359, 2004. [Online]. Available: http://www.nature.com/nrd/journal/v3/n4/abs/nrd1346.html

[159] V. Tirino, V. Desiderio, F. Paino, A. De Rosa, F. Papaccio, M. La Noce, L. Laino, F. De Francesco, and G. Papaccio, "Cancer stem cells in solid tumors: an overview and new approaches for their isolation and characterization," *FASEB Journal*, vol. 27, no. 1, pp. 13–24, jan 2013. [Online]. Available: http://www.fasebj.org/content/27/1/13.full

[160] H. Kitano, "Cancer as a robust system: implications for anticancer therapy," *Nature Reviews Cancer*, vol. 4, no. 3, pp. 227–35, mar 2004. [Online]. Available: http://dx.doi.org/10.1038/nrc1300

[161] P. A. Jones and S. B. Baylin, "The fundamental role of epigenetic events in cancer." *Nature Reviews Genetics*, vol. 3, no. 6, pp. 415–28, jun 2002. [Online]. Available: http://dx.doi.org/10.1038/nrg816

[162] T. Tian, S. Olson, J. M. Whitacre, and A. Harding, "The origins of cancer robustness and evolvability," *Integrative Biology*, vol. 3, no. 1, pp. 17–30, 2011.

[163] E. S. Lee, K. Na, and Y. H. Bae, "Doxorubicin loaded pH-sensitive polymeric micelles for reversal of resistant MCF-7 tumor," *Journal of Controlled Release*, vol. 103, no. 2, pp. 405–18, mar 2005. [Online]. Available: http://dx.doi.org/10.1016/j.jconrel.2004.12.018

[164] T. Minko, P. Kopečková, and J. Kopeček, "Chronic exposure to HPMA copolymer-bound adriamycin does not induce multidrug resistance in a human ovarian carcinoma cell line," *Journal of Controlled Release*, vol. 59, no. 2, pp. 133–148, may 1999. [Online]. Available: http://dx.doi.org/10.1016/S0168-3659(98)00186-2

[165] M. M. Gottesman, "Mechanisms of cancer drug resistance," *Annual Review of Medicine*, vol. 53, no. 1, pp. 615–627, feb 2002. [Online]. Available: http://www.annualreviews.org/doi/full/10.1146/annurev.med.53.082901.103929http://www.annualreviews.org/doi/10.1146/annurev.med.53.082901.103929

[166] G. P. Dunn, L. J. Old, and R. D. Schreiber, "The immunobiology of cancer immunosurveillance and immunoediting," *Immunity*, vol. 21, no. 2, pp. 137–48, aug 2004. [Online]. Available: http://dx.doi.org/10.1016/j.immuni.2004.07.017

[167] G. P. Dunn, A. T. Bruce, H. Ikeda, L. J. Old, and R. D. Schreiber, "Cancer immunoediting: from immunosurveillance to tumor escape," *Nature Immunology*, vol. 3, no. 11, pp. 991–998, 2002. [Online]. Available: http://www.nature.com/ni/journal/v3/n11/full/ni1102-991.html

[168] R. D. Schreiber, L. J. Old, and M. J. Smyth, "Cancer immunoediting: integrating immunity's roles in cancer suppression and promotion," *Science*, vol. 331, no. 6024, pp. 1565–1570, 2011. [Online]. Available: http://www.sciencemag.org/content/331/6024/1565.full

[169] D. Hanahan and R. A. Weinberg, "Hallmarks of cancer: the next generation," *Cell*, vol. 144, no. 5, pp. 646–674, mar 2011. [Online]. Available: http://www.ncbi.nlm.nih.gov/pubmed/21376230

[170] V. Shankaran, H. Ikeda, A. T. Bruce, J. M. White, P. E. Swanson, L. J. Old, and R. D. Schreiber, "IFNgamma and lymphocytes prevent primary tumour development and shape tumour immunogenicity." *Nature*, vol. 410, no. 6832, pp. 1107–11, apr 2001. [Online]. Available: http://dx.doi.org/10.1038/35074122

[171] S. Yachida, S. Jones, I. Bozic, T. Antal, R. Leary, B. Fu, M. Kamiyama, R. H. Hruban, J. R. Eshleman, M. A. Nowak, V. E. Velculescu, K. W. Kinzler, B. Vogelstein, and C. A. Iacobuzio-Donahue, "Distant metastasis occurs late during the genetic evolution of pancreatic cancer." *Nature*, vol. 467, no. 7319, pp. 1114–7, oct 2010. [Online]. Available: http://www.nature.com/nature/journal/v467/n7319/full/nature09515.html{\#}/references

[172] J. Jonkers and A. Berns, "Conditional mouse models of sporadic cancer," *Nature Reviews Cancer*, vol. 2, no. 4, pp. 251–65, apr 2002. [Online]. Available: http://dx.doi.org/10.1038/nrc777

[173] C. K. Osborne, K. Hobbs, and G. M. Clark, "Effect of estrogens and antiestrogens on growth of human breast cancer cells in athymic nude mice," *Cancer Research*, vol. 45, no. 2, pp. 584–590, feb 1985. [Online]. Available: http://cancerres.aacrjournals.org/cgi/content/abstract/45/2/584

[174] M. N. Wente, J. Kleeff, M. W. Büchler, J. Wanders, P. Cheverton, S. Langman, and H. Friess, "DE-310, a macromolecular prodrug of the topoisomerase-I-inhibitor exatecan (DX-8951), in patients with operable solid tumors," *Investigational New Drugs*, vol. 23, no. 4, pp. 339–347, 2005. [Online]. Available: http://www.ncbi.nlm.nih.gov/pubmed/16012793http://www.springerlink.com/content/r146751535545354/

[175] K. J. Harrington, S. Mohammadtaghi, P. S. Uster, D. Glass, A. M. Peters, R. G. Vile, and J. S. W. Stewart, "Effective targeting of solid tumors in patients with locally advanced cancers by radiolabeled pegylated liposomes," *Clinical Cancer Research*, vol. 7, no. 2, pp. 243–254, feb 2001. [Online]. Available: http://clincancerres.aacrjournals.org/content/7/2/243.short

[176] M. Buyse, P. Thirion, R. W. Carlson, T. Burzykowski, G. Molenberghs, and P. Piedbois, "Relation between tumour response to first-line chemotherapy and survival in advanced colorectal cancer: a meta-analysis," *The Lancet*, vol. 356, no. 9227, pp. 373–378, jul 2000. [Online]. Available: http://www.sciencedirect.com/science/article/pii/S0140673600025289

[177] S. D. Peddada, S. K. Laughlin, K. Miner, J.-P. Guyon, K. Haneke, H. L. Vahdat, R. C. Semelka, A. Kowalik, D. Armao, B. Davis, and D. D. Baird, "Growth of uterine leiomyomata among premenopausal black and white women," *Proceedings of the National Academy of Sciences*, vol. 105, no. 50, pp. 19 887–19 892, dec 2008. [Online]. Available: http://www.pnas.org/content/105/50/19887

[178] G. E. P. Box and N. R. Draper, *Empirical Model-Building and Response Surfaces*, ser. Wiley series in probability and mathematical statistics: Applied probability and statistics. Wiley, 1987.

[179] O. J. Becher and E. C. Holland, "Genetically engineered models have advantages over xenografts for preclinical studies," *Cancer Research*, vol. 66, no. 7, pp. 3355–3359, apr 2006. [Online]. Available: http://cancerres.aacrjournals.org/content/66/7/3355.abstracthttp://www.ncbi.nlm.nih.gov/pubmed/16585152

[180] Y. Matsumoto, J. W. Nichols, K. Toh, T. Nomoto, H. Cabral, Y. Miura, R. J. Christie, N. Yamada, T. Ogura, M. R. Kano, Y. Matsumura, N. Nishiyama, T. Yamasoba, Y. H. Bae, and K. Kataoka, "Vascular bursts enhance permeability of tumour blood vessels and improve nanoparticle delivery," *Nature Nanotechnology*, vol. advance on, feb 2016. [Online]. Available: http://dx.doi.org/10.1038/nnano.2015.342

[181] G. Kong, R. D. Braun, and M. W. Dewhirst, "Characterization of the effect of hyperthermia on nanoparticle extravasation from tumor vasculature," *Cancer Research*, vol. 61, no. 7, pp. 3027–3032, apr 2001. [Online]. Available: http://cancerres.aacrjournals.org/cgi/content/abstract/61/7/3027

[182] J. Eckes, O. Schmah, J. W. Siebers, U. Groh, S. Zschiedrich, B. Rautenberg, A. Hasenburg, M. Jansen, M. J. Hug, K. Winkler, and G. Pütz, "Kinetic targeting of pegylated liposomal doxorubicin: a new approach to reduce toxicity during chemotherapy (CARL-trial)," *BMC Cancer*, vol. 11, no. 1, p. 337, jan 2011. [Online]. Available: http://www.biomedcentral.com/1471-2407/11/337

[183] A. Gabizon, D. Tzemach, L. Mak, M. Bronstein, and A. T. Horowitz, "Dose dependency of pharmacokinetics and therapeutic efficacy of pegylated liposomal doxorubicin (DOXIL) in murine models," *Journal of Drug Targeting*, vol. 10, no. 7, pp. 539–48, nov 2002. [Online]. Available: http://www.tandfonline.com/doi/abs/10.1080/1061186021000072447

[184] A. Gabizon, R. Isacson, O. Rosengarten, D. Tzemach, H. Shmeeda, and R. Sapir, "An open-label study to evaluate dose and cycle dependence of the pharmacokinetics of pegylated liposomal doxorubicin," *Cancer Chemotherapy and Pharmacology*, vol. 61, no. 4, pp. 695–702, apr 2008. [Online]. Available: http://www.ncbi.nlm.nih.gov/pubmed/17549475

[185] P. Baluk, H. Hashizume, and D. M. McDonald, "Cellular abnormalities of blood vessels as targets in cancer," *Current Opinion in Genetics & Development*, vol. 15, no. 1, pp. 102–11, feb 2005. [Online]. Available: http://www.sciencedirect.com/science/article/pii/S0959437X04001911

[186] Arnida, M. M. Janát-Amsbury, A. Ray, C. M. Peterson, and H. Ghandehari, "Geometry and surface characteristics of gold nanoparticles influence their biodistribution and uptake by macrophages," *European Journal of Pharmaceutics and Biopharmaceutics*, vol. 77, no. 3, pp. 417–23, apr 2011. [Online]. Available: http://dx.doi.org/10.1016/j.ejpb.2010.11.010

[187] B. R. Smith, P. Kempen, D. Bouley, A. Xu, Z. Liu, N. Melosh, H. Dai, R. Sinclair, and S. S. Gambhir, "Shape matters: intravital microscopy reveals surprising geometrical dependence for nanoparticles in tumor models of extravasation," *Nano Letters*, vol. 12, no. 7, pp. 3369–77, jul 2012. [Online]. Available: http://dx.doi.org/10.1021/nl204175thttp://pubs.acs.org/doi/full/10.1021/nl204175t

[188] L. Eikenes, M. Tari, I. Tufto, O. S. Bruland, and C. de Lange Davies, "Hyaluronidase induces a transcapillary pressure gradient and improves the distribution and uptake of liposomal doxorubicin (Caelyx) in human osteosarcoma xenografts," *British Journal of Cancer*, vol. 93, no. 1, pp. 81–8, jul 2005. [Online]. Available: http://www.pubmedcentral.nih.gov/articlerender.fcgi?artid=2361478{\&}tool=pmcentrez{\&}rendertype=abstract

[189] L. Eikenes, Ø. S. Bruland, C. Brekken, and C. d. L. Davies, "Collagenase increases the transcapillary pressure gradient and improves the uptake and distribution of monoclonal antibodies in human osteosarcoma xenografts." *Cancer Research*, vol. 64, no. 14, pp. 4768–73, jul 2004. [Online]. Available: http://cancerres.aacrjournals.org/cgi/content/abstract/64/14/4768

[190] K. N. Sugahara, T. Teesalu, P. P. Karmali, V. R. Kotamraju, L. Agemy, D. R. Greenwald, and E. Ruoslahti, "Coadministration of a tumor-penetrating peptide enhances the efficacy of cancer drugs," *Science*, vol. 328, no. 5981, pp. 1031–1035, 2010. [Online]. Available: http://www.sciencemag.org/content/328/5981/1031.full

[191] G. Kong, R. D. Braun, and M. W. Dewhirst, "Hyperthermia enables tumor-specific nanoparticle delivery: effect of particle size," *Cancer Research*, vol. 60, no. 16, pp. 4440–4445, aug 2000. [Online]. Available: http://cancerres.aacrjournals.org/cgi/content/abstract/60/16/4440

[192] C. Li, Y. Miyamoto, Y. Kojima, and H. Maeda, "Augmentation of tumour delivery of macromolecular drugs with reduced bone marrow delivery by elevating blood pressure," *British Journal of Cancer*, vol. 67, no. 5, pp. 975–980, may 1993. [Online]. Available: http://dx.doi.org/10.1038/bjc.1993.179

[193] D. Lu, M. G. Wientjes, Z. Lu, and J. L.-S. Au, "Tumor priming enhances delivery and efficacy of nanomedicines," *The Journal of Pharmacology and Experimental Therapeutics*, vol. 322, no. 1, pp. 80–8, jul 2007. [Online]. Available: http://www.ncbi.nlm.nih.gov/pubmed/17420296http://jpet.aspetjournals.org/content/322/1/80.long

[194] W. Stöber, A. Fink, and E. Bohn, "Controlled growth of monodisperse silica spheres in the micron size range," *Journal of Colloid and Interface Science*, vol. 26, no. 1, pp. 62–69, jan 1968. [Online]. Available: http://www.sciencedirect.com/science/article/pii/0021979768902725

[195] C.-P. Tsai, Y. Hung, Y.-H. Chou, D.-M. Huang, J.-K. Hsiao, C. Chang, Y.-C. Chen, and C.-Y. Mou, "High-contrast paramagnetic fluorescent mesoporous silica nanorods as a multifunctional cell-imaging probe," *Small*, vol. 4, no. 2, pp. 186–91,

mar 2008. [Online]. Available: http://www.ncbi.nlm.nih.gov/pubmed/18205156http://onlinelibrary.wiley.com/doi/10.1002/smll.200700457/full

[196] G. H. Heppner, "Tumor heterogeneity," *Cancer Research*, vol. 44, no. 6, pp. 2259–65, jun 1984. [Online]. Available: http://www.ncbi.nlm.nih.gov/pubmed/6372991

[197] P. A. Kenny, C. M. Nelson, and M. J. Bissell, "The ecology of tumors: by perturbing the microenvironment, wounds and infection may be key to tumor development," *Scientist*, vol. 20, no. 4, p. 30, apr 2006. [Online]. Available: http://www.pubmedcentral.nih.gov/articlerender.fcgi?artid=2995893{\&}tool=pmcentrez{\&}rendertype=abstract

[198] H. Maeda, Y. Noguchi, K. Sato, and T. Akaike, "Enhanced vascular permeability in solid tumor is mediated by nitric oxide and inhibited by both new nitric oxide scavenger and nitric oxide synthase inhibitor," *Cancer Science*, vol. 85, no. 4, pp. 331–334, apr 1994. [Online]. Available: http://doi.wiley.com/10.1111/j.1349-7006.1994.tb02362.x

[199] T. S. Kuhn, *The structure of scientific revolutions*. [Chicago]: University of Chicago Press, 1962. [Online]. Available: http://books.google.com/books?id=8NICAAAAIAAJ

[200] M. J. Vicent, H. Ringsdorf, and R. Duncan, "Polymer therapeutics: clinical applications and challenges for development," *Advanced Drug Delivery Reviews*, vol. 61, no. 13, pp. 1117–1120, nov 2009. [Online]. Available: http://www.ncbi.nlm.nih.gov/pubmed/19682516http://www.sciencedirect.com/science/article/pii/S0169409X09002348

[201] R. Gaspar and R. Duncan, "Polymeric carriers: preclinical safety and the regulatory implications for design and development of polymer therapeutics," *Advanced Drug Delivery Reviews*, vol. 61, no. 13, pp. 1220–31, nov 2009. [Online]. Available: http://www.sciencedirect.com/science/article/pii/S0169409X09002439

[202] M. Gnant, B. Mlineritsch, W. Schippinger, G. Luschin-Ebengreuth, S. Pöstlberger, C. Menzel, R. Jakesz, M. Seifert, M. Hubalek, V. Bjelic-Radisic, H. Samonigg, C. Tausch, H. Eidtmann, G. Steger, W. Kwasny, P. Dubsky, M. Fridrik, F. Fitzal, M. Stierer, E. Rücklinger, and R. Greil, "Endocrine therapy plus zoledronic acid in premenopausal breast cancer," *New England Journal of Medicine*, vol. 360, no. 7, pp. 679–691, feb 2009. [Online]. Available: http://dx.doi.org/10.1056/NEJMoa0806285

[203] G. von Maltzahn, J.-h. Park, K. Y. Lin, N. Singh, C. Schwöppe, R. Mesters, W. E. Berdel, E. Ruoslahti, M. J. Sailor, S. N. Bhatia, and G. V. Maltzahn, "Nanoparticles that communicate in vivo to amplify tumour targeting," *Nature Materials*, vol. 10, no. 7, pp. 545–552, jul 2011. [Online]. Available: http://dx.doi.org/10.1038/nmat3049http://www.nature.com/nmat/journal/v10/n7/abs/nmat3049.html{\#}supplementary-information

[204] D. T. Luttikhuizen, M. C. Harmsen, and M. J. A. Van Luyn, "Cellular and molecular dynamics in the foreign body reaction," *Tissue Engineering*, vol. 12, no. 7, pp. 1955–70, jul 2006. [Online]. Available: http://online.liebertpub.com/doi/abs/10.1089/ten.2006.12.1955

[205] Z. Qin, "Inhibition of methylcholanthrene-induced carcinogenesis by an interferon gamma receptor-dependent foreign body reaction," *Journal of Experimental Medicine*, vol. 195, no. 11, pp. 1479–1490, jun 2002. [Online]. Available: http://jem.rupress.org/cgi/content/abstract/195/11/1479

[206] P. Ehrlich, "Über den jetzigen stand der karzinomforschung," *Nederlands Tijdschrift voor Geneeskunde*, vol. 5, pp. 273–279, 1909. [Online]. Available: http://www.ntvg.nl/publicatie/ueber-den-jetzigen-stand-der-karzinomforschung

[207] K. L. Knutson, Y. Dang, H. Lu, J. Lukas, B. Almand, E. Gad, E. Azeke, and M. L. Disis, "IL-2 immunotoxin therapy modulates tumor-associated regulatory T cells and leads to lasting immune-mediated rejection of breast cancers in neu-transgenic mice," *Journal of Immunology*, vol. 177, no. 1, pp. 84–91, jul 2006. [Online]. Available: http://www.jimmunol.org/cgi/content/abstract/177/1/84

[208] S. Onizuka, I. Tawara, J. Shimizu, S. Sakaguchi, T. Fujita, and E. Nakayama, "Tumor rejection by in vivo administration of anti-CD25 (interleukin-2 receptor {{alpha}}) monoclonal antibody," *Cancer Research*, vol. 59, no. 13, pp. 3128–3133, jul 1999. [Online]. Available: http://cancerres.aacrjournals.org/cgi/content/abstract/59/13/3128

[209] D. F. Williams, "On the mechanisms of biocompatibility." *Biomaterials*, vol. 29, no. 20, pp. 2941–53, jul 2008. [Online]. Available: http://dx.doi.org/10.1016/j.biomaterials.2008.04.023

[210] J. A. Hubbell, S. N. Thomas, and M. A. Swartz, "Materials engineering for immunomodulation." *Nature*, vol. 462, no. 7272, pp. 449–60, nov 2009. [Online]. Available: http://dx.doi.org/10.1038/nature08604

[211] P. C. Tumeh, C. L. Harview, J. H. Yearley, I. P. Shintaku, E. J. M. Taylor, L. Robert, B. Chmielowski, M. Spasic, G. Henry, V. Ciobanu, A. N. West, M. Carmona, C. Kivork, E. Seja, G. Cherry, A. J. Gutierrez, T. R. Grogan, C. Mateus, G. Tomasic, J. A. Glaspy, R. O. Emerson, H. Robins, R. H. Pierce, D. A. Elashoff, C. Robert, and A. Ribas, "PD-1 blockade induces responses by inhibiting adaptive immune resistance," *Nature*, vol. 515, no. 7528, pp. 568–571, nov 2014. [Online]. Available: http://dx.doi.org/10.1038/nature13954

[212] M. A. Postow, M. K. Callahan, and J. D. Wolchok, "Immune checkpoint blockade in cancer therapy," *Journal of Clinical Oncology*, vol. 34, no. 18, pp. JCO.2014.59.4358–, jan 2015. [Online]. Available: http://jco.ascopubs.org/content/early/2015/01/20/JCO.2014.59.4358.full

[213] C. Robert, J. Schachter, G. V. Long, A. Arance, J. J. Grob, L. Mortier, A. Daud, M. S. Carlino, C. McNeil, M. Lotem, J. Larkin, P. Lorigan, B. Neyns, C. U. Blank, O. Hamid, C. Mateus, R. Shapira-Frommer, M. Kosh, H. Zhou, N. Ibrahim, S. Ebbinghaus, and A. Ribas, "Pembrolizumab versus ipilimumab in advanced melanoma," *New England Journal of Medicine*, vol. 372, no. 26, pp. 2521–2532, apr 2015. [Online]. Available: http://dx.doi.org/10.1056/NEJMoa1503093

[214] B. Ríhová, L. Kovár, M. Kovár, and O. Hovorka, "Cytotoxicity and immunostimulation: double attack on cancer cells with polymeric therapeutics," *Trends in Biotechnology*, vol. 27, no. 1, pp. 11–7, jan 2009. [Online]. Available: http://www.ncbi.nlm.nih.gov/pubmed/19022512http://www.sciencedirect.com/science/article/pii/S0167779908002692

[215] T. Mrkvan, M. Sirova, T. Etrych, P. Chytil, J. Strohalm, D. Plocova, K. Ulbrich, and B. Rihova, "Chemotherapy based on HPMA copolymer conjugates with pH-controlled release of doxorubicin triggers anti-tumor immunity," *Journal of Controlled Release*, vol. 110, no. 1, pp. 119–29, dec 2005. [Online]. Available: http://dx.doi.org/10.1016/j.jconrel.2005.09.028

[216] O. A. Ali, N. Huebsch, L. Cao, G. Dranoff, and D. J. Mooney, "Infection-mimicking materials to program dendritic cells in situ," *Nature Materials*, vol. 8, no. 2, pp. 151–8, feb 2009. [Online]. Available: http://dx.doi.org/10.1038/nmat2357

[217] Y. Krishnamachari, S. M. Geary, C. D. Lemke, and A. K. Salem, "Nanoparticle delivery systems in cancer vaccines," *Pharmaceutical Research*, vol. 28, no. 2, pp. 215–36, feb 2011. [Online]. Available: http://link.springer.com/article/10.1007/s11095-010-0241-4/fulltext.html

[218] S. M. Geary, Q. Hu, V. B. Joshi, N. B. Bowden, and A. K. Salem, "Diaminosulfide based polymer microparticles as cancer vaccine delivery systems," *Journal of Controlled Release*, vol. 220, no. Pt B, pp. 682–90, dec 2015. [Online]. Available: http://www.sciencedirect.com/science/article/pii/S016836591530105X

[219] X. Xia, J. Mai, R. Xu, J. E. T. Perez, M. L. Guevara, Q. Shen, C. Mu, H.-Y. Tung, D. B. Corry, S. E. Evans, X. Liu, M. Ferrari, Z. Zhang, X. C. Li, R.-F. Wang, and H. Shen, "Porous silicon microparticle potentiates anti-tumor immunity by enhancing cross-presentation and inducing type I interferon response," *Cell Reports*, vol. 11, no. 6, pp. 957–66, may 2015. [Online]. Available: http://www.cell.com/article/S2211124715003848/fulltext

[220] M. A. Dobrovolskaia, D. R. Germolec, and J. L. Weaver, "Evaluation of nanoparticle immunotoxicity," *Nature Nanotechnology*, vol. 4, no. 7, pp. 411–414, jun 2009. [Online]. Available: http://dx.doi.org/10.1038/nnano.2009.175

[221] A. N. Ilinskaya and M. A. Dobrovolskaia, "Immunosuppressive and anti-inflammatory properties of engineered nanomaterials," *British Journal of Pharmacology*, vol. 171, no. 17, pp. 3988–4000, sep 2014. [Online]. Available: http://www.pubmedcentral.nih.gov/articlerender.fcgi?artid=4243973{\&}tool=pmcentrez{\&}rendertype=abstract

[222] S. Moghimi, "Cancer nanomedicine and the complement system activation paradigm: anaphylaxis and tumour growth," *Journal of Controlled Release*, vol. 190, pp. 556–562, sep 2014. [Online]. Available: http://www.sciencedirect.com/science/article/pii/S016836591400217Xhttp://linkinghub.elsevier.com/retrieve/pii/S016836591400217X

[223] M. K. Sabnani, R. Rajan, B. Rowland, V. Mavinkurve, L. M. Wood, A. A. Gabizon, and N. M. La-Beck, "Liposome promotion of tumor growth is associated with angiogenesis and inhibition of antitumor immune responses," *Nanomedicine : Nanotechnology, Biology, and Medicine*, vol. 11, no. 2, pp. 259–62, feb 2015. [Online]. Available: http://www.sciencedirect.com/science/article/pii/S154996341400433X

[224] N. Carelle, E. Piotto, A. Bellanger, J. Germanaud, A. Thuillier, and D. Khayat, "Changing patient perceptions of the side effects of cancer chemotherapy." *Cancer*, vol. 95, no. 1, pp. 155–63, jul 2002. [Online]. Available: http://www.ncbi.nlm.nih.gov/pubmed/12115329

[225] A. Coates, S. Abraham, S. B. Kaye, T. Sowerbutts, C. Frewin, R. M. Fox, and M. H. Tattersall, "On the receiving end–patient perception of the side-effects of cancer chemotherapy," *European Journal of Cancer & Clinical Oncology*, vol. 19, no. 2, pp. 203–8, feb 1983. [Online]. Available: http://www.ncbi.nlm.nih.gov/pubmed/6681766

[226] D. M. Barrett, N. Singh, D. L. Porter, S. A. Grupp, and C. H. June, "Chimeric antigen receptor therapy for cancer," *Annual Review of Medicine*, vol. 65, pp. 333–47, jan 2014. [Online]. Available: http://www.pubmedcentral.nih.gov/articlerender.fcgi?artid=4120077{\&}tool=pmcentrez{\&}rendertype=abstract

[227] M. L. Davila, I. Riviere, X. Wang, S. Bartido, J. Park, K. Curran, S. S. Chung, J. Stefanski, O. Borquez-Ojeda, M. Olszewska, J. Qu, T. Wasielewska, Q. He, M. Fink, H. Shinglot, M. Youssif, M. Satter, Y. Wang, J. Hosey, H. Quintanilla, E. Halton, Y. Bernal, D. C. G. Bouhassira, M. E. Arcila, M. Gonen, G. J. Roboz, P. Maslak, D. Douer, M. G. Frattini, S. Giralt, M. Sadelain, and R. Brentjens, "Efficacy and toxicity management of 19-28z CAR T cell therapy in B cell acute lymphoblastic leukemia," *Science Translational Medicine*, vol. 6, no. 224, p. 224ra25, feb 2014. [Online]. Available: http://www.pubmedcentral.nih.gov/articlerender.fcgi?artid=4684949{\&}tool=pmcentrez{\&}rendertype=abstract1.Davila,M.L.etal.Efficacyandtoxicitymanagementof19-28zCARTcelltherapyinBcellacutelymphoblasticleukemia.Sci.Transl.Med.6,224ra25

[228] R. Chen, N. R. Desai, J. S. Ross, W. Zhang, K. H. Chau, B. Wayda, K. Murugiah, D. Y. Lu, A. Mittal, and H. M. Krumholz, "Publication and reporting of clinical trial results: cross sectional analysis across academic medical centers," *The BMJ*, vol. 352, no. feb17_8, p. i637, feb 2016. [Online]. Available: http://www.bmj.com/content/352/bmj.i637